

Dissertation zur Erlangung des Doktorgrades
der Fakultät für Chemie und Pharmazie
der Ludwig-Maximilians-Universität München

Interaction of macrophages and diseased cells

Laura Maria Lindenthal

aus

München, Deutschland

2021

Erklärung

Diese Dissertation wurde im Sinne von § 7 der Promotionsordnung vom 28. November 2011 von Herrn Prof. Dr. Veit Hornung betreut.

Eidesstattliche Versicherung

Diese Dissertation wurde eigenständig und ohne unerlaubte Hilfe erarbeitet.

München, den 12.06.2021

.....
Laura Lindenthal

Dissertation eingereicht am 14.06.2021

1. Gutachter: Prof. Dr. Veit Hornung

2. Gutachter: Prof. Dr. Peter Murray

Mündliche Prüfung am 15.09.2021

Table of contents

Table of contents.....	I
List of Figures	V
List of tables	VII
Summary	1
Zusammenfassung.....	2
1 Introduction	4
1.1 Aging.....	4
1.1.1 The complexity of aging	4
1.1.2 The nine hallmarks of aging	4
1.1.3 The immune system ages and synergizes with the aging of other organ systems	5
1.2 Cellular senescence	6
1.2.1 The Hayflick limit.....	7
1.2.2 Cellular functions associated with senescence	7
1.2.3 Defining senescence at the molecular level.....	8
1.2.4 Senescence involves altered cell morphology and metabolism	13
1.2.5 The morphology of senescent cells.....	14
1.2.6 Senescent cell accrual in tissues.....	14
1.3 The senescence-associated secretory phenotype (SASP)	15
1.3.1 Classification of SASP molecules	15
1.3.2 Regulation of the SASP	17
1.3.3 Effects of the SASP	18
1.4 Targeting senescent cells	19
1.4.1 Non-pharmacological interventions.....	20
1.4.2 Drugs aiming for SASP reduction	21
1.4.3 Senotherapeutics: senolytics and senostatics.....	21
1.5 The interaction of senescent cells with immune cells	23
1.6 The role of macrophages for the immune system	24
1.6.1 Development and circulation	25
1.6.2 Plasticity and polarization	25
1.6.3 Antigen presentation	28
1.6.4 Removal of dead cells - efferocytosis.....	29
1.7 Efferocytosis signaling.....	31

Table of contents

1.7.1	“Eat-me” signals	31
1.7.2	“Don't eat-me” signals	32
1.7.3	“Come-get-me” signals.....	33
1.8	Aging and neurodegenerative disease.....	34
1.8.1	Clinical features of neurodegenerative diseases	35
1.8.2	Aggregation and pathogenesis of Huntington’s disease.....	35
2	Objectives.....	38
3	Materials	40
3.1	Frequently used reagents and plastics.....	40
3.2	Commercially available antibodies	42
3.3	Utilized plasmids	43
3.3.1	Maps of newly generated plasmids	44
3.4	Restriction enzymes	47
3.5	DNA and qRT-PCR primer	47
3.6	Technical equipment.....	48
3.7	Software	48
3.8	Buffers	49
4	Methods	50
4.1	Mice strains	50
4.1.1	DNA extraction and Genotyping	50
4.2	Cell lines	51
4.3	Isolation of primary cells.....	51
4.3.1	Isolation of bone marrow-derived macrophages.....	51
4.3.2	Isolation of peritoneal macrophages	52
4.3.3	Isolation of multinucleated giant macrophages	52
4.3.4	Isolation of bone marrow derived eosinophils	53
4.3.5	Isolation of primary mouse embryonic fibroblasts.....	53
4.3.6	Isolation of mixed glia cells	53
4.3.7	Isolation of primary neurons.....	54
4.4	Genetic manipulation of cell lines.....	54
4.4.1	Transient transfection of fibroblasts with Lipofectamine.....	54
4.4.2	Lentiviral transduction of primary neurons (Kerstin Voelkl).....	55
4.5	Generation of stable cell lines.....	55

4.5.1	Cloning strategy designing the Flp-in system.....	55
4.5.2	Generating of fluorescent reporter cell lines using the Flp-in system.....	55
4.5.3	Generating of a inducible aggregate expressing cell line using the piggy-bac system 56	
4.5.4	Generating of knock-out cell lines using the CRSPR-Cas9 sytem	56
4.6	RNA isolation and analysis	56
4.7	Induction of senescence.....	58
4.7.1	Induction of senescence in by γ -irradiation	58
4.7.2	Induction of senescence by X-ray.....	58
4.7.3	Induction of senescence in MEF cells by passaging stress	59
4.7.4	Induction of senescence by Palbociclib.....	59
4.7.5	Senescence-associated β -galactosidase assay	59
4.8	Cellular staining.....	59
4.8.1	General membrane staining of immortalized 3T3 cells	59
4.8.2	Staining for Flow Cytometry.....	59
4.8.3	Induction of apoptosis and fluorescent labeling of Jurkat cells and BMDEs	59
4.9	Imaging.....	60
4.9.1	Immunofluorescence of senescent cells	60
4.9.2	Live Cell imaging.....	60
4.10	Functionality assays.....	60
4.10.1	Phagocytosis assays.....	60
4.10.2	Seahorse bioenergetic measurements.....	62
1.1.1	LDH Cytotoxicity Assay	62
5	Results	63
5.1	Interaction of macrophages with senescent cells: overview of the experimental design and hypotheses	63
5.1.1	Senescence models: induction and quantification	64
5.1.2	Macrophages interact with, but do not engulf, senescent cells	66
5.1.3	Set-up of an <i>in vitro</i> efferocytosis assay to assess macrophage functionality.....	67
5.1.4	Senescent cells do not impair macrophage functionality by soluble molecules	71
5.1.5	Senescent cells express increased CD47	72
5.1.6	CD47 expression is responsible for the impairment effect of senescent cells	75
5.1.7	Efferocytosis impairment is independent of macrophage phenotype and target ...	78
5.1.8	The impairment effect of senescent cells is dominated by CD47	80

Table of contents

5.1.9	CD47 signaling can be followed downstream to macrophage SIRP α signaling	83
5.2	Multinucleated giant macrophages as cell type to remove senescent cells.....	87
5.2.1	Polykaryons can engulf senescent cells	87
5.3	A model system to analyze pathogenic aggregate removal by macrophages.....	90
5.3.1	Macrophages trigger aggregate elimination from fibroblasts	91
5.3.2	Studying aggregate removal in neuronal systems	95
5.3.3	Manipulation of aggregate formation conditions.....	97
5.3.4	Aggregate removal requires direct cell contact between macrophages and fibroblasts.....	99
5.3.5	Use of bystander cells to analyze aggregate removal.....	100
5.3.6	Aggregate removal is not mediated by the cell intrinsic apoptosis pathway or LAP 103	
5.3.7	Macrophages do not seem to kill fibroblasts upon aggregate removal	106
5.3.8	Macrophages do not induce lytic cell death to facilitate aggregate removal.....	109
5.3.9	Visualization of the aggregate removal by high resolution microscopy	111
6	Discussion.....	115
6.1	Interaction of macrophages with senescent cells.....	115
6.1.1	Analysis of macrophage functionality in the presence of senescent cells.....	116
6.1.2	Dispensable effects of SASP for macrophage functionality	117
6.1.3	CD47 as decisive factor for paralysis of macrophage function	118
6.1.4	CD47 mediates a transient paralysis effect on macrophage functionality	120
6.1.5	Potential for future therapeutic development	121
6.1.6	Giant macrophages provide the potential to remove senescent cells	122
6.2	A novel system to study the removal of Huntington aggregates.....	124
6.2.1	Analysis of pathogenic aggregate removal by macrophages.....	125
6.2.2	Deciphering the underlying mechanisms of aggregate removal	126
6.2.3	Transferring the cell culture model to a neuronal system holds several caveats... 130	
6.2.4	Potential mechanism and future perspectives	131
7	Literature.....	134
8	Appendix	i
8.1	Interaction of macrophages and senescent cells.....	i
8.2	A model system to analyze pathogenic aggregate removal by macrophages.....	iii
9	List of Abbreviations.....	v
10	Acknowledgements.....	ix

List of Figures

Figure 1-1: The p16 ^{INK4a} /Rb pathway.....	9
Figure 1-2: The p19 ^{ARF} /p53/p21 ^{Cip1} pathway.....	11
Figure 1-3: The PTEN/p27 ^{Kip1} pathway.	12
Figure 1-4: The Ras oncogene and its effects on senescence.....	13
Figure 1-5: Overview of therapeutic strategies to counter the effects of senescent cells.....	20
Figure 1-6: Overview of different stimuli, secreted cytokines, and biological functions between M1 and M2 macrophages.....	27
Figure 3-1: Plasmid map of pcDNA5_FRT-mCherry	44
Figure 3-2: Plasmid map of pcDNA5_FRT-mTagBFP2	45
Figure 3-3: Plasmid map of pEF5-FRT-TagRFP-T-IFT88-mCherry	46
Figure 3-4: Plasmid map of pEF5-FRT-TagRFP-T-IFT88-mTagBFP2	47
Figure 5-1: Induction and read out of a senescent phenotype.....	65
Figure 5-2: Macrophages interact with, but do not engulf senescent cells.....	67
Figure 5-3: Senescent cells impair macrophage functionality during efferocytosis independent of the means of senescence induction.....	70
Figure 5-4: Soluble factors released by senescent cells do not impair macrophage efferocytosis. .	72
Figure 5-5: Senescent cells express increased CD47.....	74
Figure 5-6 : The impairment of the efferocytosis capacity of macrophages by senescent cells is dependent on CD47 and reversible over time.....	77
Figure 5-7: The impairment of macrophage efferocytosis by senescent cells is independent of macrophage polarization or the phagocytosis target.....	79
Figure 5-8: CD47 KO cells do not show increased expression of CD22.....	81
Figure 5-9: CD47 KO cells do not show increased expression of CD24.....	82
Figure 5-10: Senescent cells impair efferocytosis by signaling via SIRP α and SHP-1 on the macrophages.	85
Figure 5-11: Polykaryons engulf senescent cells.....	89
Figure 5-12: Macrophages trigger aggregate elimination from fibroblasts.....	94
Figure 5-13: Microglia enhance aggregate stability in cortical neurons.....	96
Figure 5-14: Time-dependent induction of aggregate formation by a Tet-ON system.	98
Figure 5-15: Direct contact is required for macrophage-mediated aggregate removal.....	100
Figure 5-16: Macrophages target aggregate bearing cells in the presence of a “neutral” bystander cell.....	102
Figure 5-17: Aggregates in cells lacking the intrinsic mitochondrial apoptosis pathway are removed by macrophages, while LC3 mediated phagocytosis in macrophages is not required.	105
Figure 5-18: Macrophages do not appear to kill aggregate bearing cells.....	108
Figure 5-19: Quantification of lytic cell death by LDH release.....	110
Figure 5-20: Macrophages do not kill aggregate bearing cells upon aggregate removal.....	114
Figure 6-1: Proposed model of how senescent cells impair macrophage functionality.....	116
Figure 6-2: Membrane encapsulation of Htt aggregates	132
Figure 8-1: Peritoneal macrophages do not engulf senescent cells.	i
Figure 8-2: Data for single efferocytosis can be obtained from double efferocytosis samples.....	i

List of Figures

Figure 8-3: SIRP α treatment recovers efferocytosis in a titratable manner.....	ii
Figure 8-4: Proliferating cells do not impair macrophage functionality.	ii
Figure 8-5: Macrophages trigger aggregate elimination from fibroblasts.....	iii
Figure 8-6: All types of microglia enhance aggregate stability in neurons.	iv

List of tables

Table 3-1: Generally utilized reagents.	40
Table 3-2: Generally used plastics.....	41
Table 3-3: Commercially available primary antibodies.....	42
Table 3-4: Commercially available secondary antibodies.....	42
Table 3-5: Commercially available FACS antibodies.	42
Table 3-6: Commercially available and generated plasmids.....	43
Table 3-7: Restriction enzymes.	47
Table 3-8: DNA primer.....	47
Table 3-9: qRT-PCR primer.	48
Table 3-10: Technical gear.	48
Table 3-11: Software.	48
Table 3-12: RBC lysis buffer.....	49
Table 3-13: Tail lysis buffer.	49
Table 4-1: Genotyping PCR protocol.	51
Table 4-2: Master mix for Lipofectamine transfection.	55
Table 4-3: Composition of cDNA master mix.	57
Table 4-4: Composition of reverse transcriptase master mix.....	57
Table 4-5: Master mix for housekeeper GAPDH.....	57
Table 4-6: Master mix for other primers (including CDKN2A).	57
Table 4-7: qRT-PCR protocol for TaqMan mix.....	58
Table 4-8: qRT-PCR protocol for Sybr Mix.....	58

Summary

Excessive accumulation of senescent cells and cells bearing pathogenic aggregates have central roles in driving aging and chronic diseases such as cancer and neurodegenerative diseases. Despite this link, the role of phagocytes, the chief cell type responsible for removal of foreign and unwanted materials, has not yet been accounted for in senescent and diseased cell surveillance and removal. This study aimed to elucidate the role of macrophages in the context of senescence-associated diseases namely cellular senescence itself and Huntington's disease *in vitro*. By developing new co-culture systems examining phagocytes and diseased cells, we found that senescent cells evaded phagocytosis by macrophages. Most significantly, senescent cells mediated a transient impairment on macrophages for the efferocytosis of bystander targets, such as efferocytic corpses, linking senescent cells to an alteration of macrophage function. Mechanistically, this effect was mediated by increased expression of the "don't eat-me" signal CD47 on the surface of the senescent cells, relative to normal cells and was transient in nature and mediated by direct cell contact rather than via the plethora of soluble factors made by senescent cells. Further, genetic analysis showed the efferocytosis impairment effect was dependent on CD47. Moreover, we were able to follow the signaling from CD47 on the senescent cells to interact with SIRP α on the macrophages: the transient inhibition was reflected by changes in the downstream phosphatase SHP-1. Collectively, senescent cells caused transient paralysis of macrophage efferocytosis, which may help explain why aged tissues are associated with prolonged and constitutive inflammation, a process often linked to inefficient corpse removal. We also established a different type of co-culture system to demonstrate that macrophages triggered specific aggregate removal from fibroblasts, while maintaining cell viability. In this novel biological concept, distinct from entosis, trogocytosis or phagocytosis, macrophages detected and removed single aggregates from fibroblasts in a process requiring direct cell contact. Using fibroblasts genetically inactivated for mitochondrial apoptosis (Bax Bak double knockout cells) and a unique three cell reporter culture system, we determined that macrophages did not induce any type of cell death to the aggregate-bearing cells. Taken together, we propose a trogocytosis-like mechanism by which macrophages trigger aggregate removal from fibroblasts, although the "target" aggregate is far larger than for conventional trogocytosis. Thus, we established unexpected connections between macrophages and senescent cells, as well as a novel approach to study the removal of aggregates in Huntington's disease. This may help to provide the basis for novel treatments of age-related diseases.

Zusammenfassung

Eine übermäßige Ansammlung von seneszenten Zellen und Zellen, die pathogene Aggregate tragen, spielen eine zentrale Rolle beim Altern und bei chronischen Krankheiten wie Krebs und neurodegenerativen Erkrankungen. Trotz dieses Zusammenhangs wurde die Rolle von Phagozyten, dem Hauptzelltyp, der für die Entfernung von fremden und unerwünschten Materialien verantwortlich ist, bisher nicht für die Überwachung und Entfernung von seneszenten und erkrankten Zellen berücksichtigt. Ziel dieser Studie war es, die Rolle der Makrophagen im Zusammenhang mit Seneszenz-assoziierten Krankheiten, nämlich der zellulären Seneszenz selbst und Chorea-Huntington, *in vitro* aufzuklären. Durch die Entwicklung neuer Co-Kultur-Systeme, in denen die Interaktion zwischen Fresszellen und erkrankte Zellen untersucht wurde, fanden wir heraus, dass seneszente Zellen sich der Phagozytose durch Makrophagen entziehen können. Bedeutsam war, dass seneszente Zellen eine vorübergehende Verminderung der Kapazität der Makrophagen für die Efferozytose von Bystander-Zielzellen, wie z.B. totem, efferozytischen Zellmaterial, vermittelten. Unsere Ergebnisse verknüpften seneszente Zellen mit einer Veränderung der Makrophagenfunktion. Mechanistisch wurde dieser Effekt durch eine im Vergleich zu normalen Zellen verstärkte Expression des „Don't-eat-me“-Signals CD47 auf der Oberfläche der seneszenten Zellen vermittelt. Darüber hinaus war der Minderungseffekt nur von vorübergehender Natur. Die Minderung wurde durch direkten Zellkontakt vermittelt und nicht durch die Fülle der von seneszenten Zellen gebildeten löslichen Faktoren. Weiterhin zeigte die genetische Analyse, dass der Effekt der Efferozytoseminderung von CD47 abhängig war. Darüber hinaus konnten wir die Signalgebung von CD47 auf den seneszenten Zellen verfolgen, die mit SIRP α auf den Makrophagen interagiert: Die vorübergehende Hemmung spiegelte sich in Veränderungen der nachgeschalteten Phosphatase SHP-1 wider. Insgesamt verursachten seneszente Zellen eine vorübergehende Lähmung der Makrophagen-Efferozytose. Unsere Resultate könnten helfen zu erklären, warum gealterte Gewebe mit einer anhaltenden und konstitutiven Entzündung in Verbindung gebracht werden, einem Prozess, der oft mit einer ineffizienten Beseitigung von totem Zellmaterial verbunden ist. Wir etablierten ein weiteres Co-Kultursystem, um zu zeigen, dass Makrophagen eine spezifische Aggregatentfernung aus Fibroblasten auslösen, während die Lebensfähigkeit der Zellen erhalten bleibt. In diesem neuartigen biologischen Konzept, das sich von Entose, Trogozytose oder Phagozytose unterscheidet, erkannten und entfernten Makrophagen einzelne Aggregate von Fibroblasten in einem Prozess, der direkten Zellkontakt erforderte. Unter Verwendung von Fibroblasten, die genetisch für mitochondriale Apoptose inaktiviert sind (Bax Bak Doppel-Knockout-

Zellen), und eines einzigartigen Drei-Zellen-Reporter-Co-Kultursystems konnten wir feststellen, dass Makrophagen keine Art von Zelltod bei den Aggregat-tragenden Zellen induzierten. Zusammenfassend schlagen wir einen Trogozytose-ähnlichen Mechanismus vor, durch den Makrophagen die Entfernung von Aggregaten aus Fibroblasten auslösen, obwohl das "Ziel"-Aggregat viel größer ist als bei der herkömmlichen Trogozytose. So haben wir unerwartete Verbindungen zwischen Makrophagen und seneszenten Zellen sowie einen neuartigen Ansatz zur Untersuchung des Abbaus von Aggregaten bei Chorea-Huntington etabliert. Dies könnte dazu beitragen, die Grundlage für neuartige Behandlungen von altersbedingten Krankheiten zu schaffen.

1 Introduction

1.1 Aging

Since the broad period approximately beginning with the cessation of the Napoleonic wars and the emergence and acceleration of the industrial revolution, many human populations increased their lifespan coincident with decreases in mortality [1, 2]. Relative to the 19th century, advanced societies have almost doubled life expectancy. Life spans were extended by advancing basic hygiene and advantages in social behavior and infrastructure like cleaner drinking water, better sanitation and improvements in housing, education and nutrition [3]. This was complemented by the progress in medical care and technology by widespread application of vaccines, antibiotics and further advances in disease diagnosis, preventive and therapeutic medicine [4]. In spite of all improvements, the aging process can still be further modulated, for example by altered life styles including moderate physical activity, healthy diets and disease awareness and surveillance [5]. Regardless of many positive elements associated with an increased life span, aging provides serious health and socioeconomic concerns for modern societies [6].

1.1.1 The complexity of aging

Due to its onset of time-dependent exhaustion at all levels of the body, the aging process is more complex than originally thought [7]. The organism is eventually unable to sustain the physiological and molecular functions and ultimately collapses. However, the convoluted interplay of aging is hierarchically organized and can therefore occur at multiple organizational levels from molecules to cells to tissues, to organisms and populations [3]. Understanding of the complexity of the aging process has led to the development of integrative approaches to elucidate the many changes that take place at different levels of physiology. Aging is controlled by genetic pathways and biochemical processes that can be classified into nine tentative hallmarks proposed by Lopez-Otin *et al.* in 2013 [8]. These can be grouped into three categories: primary, antagonistic and integrative hallmarks. All hallmarks of aging share three core criteria: first, they manifest during normal aging, second their exaggeration accelerates aging, and third their amelioration impedes the normal aging process.

1.1.2 The nine hallmarks of aging

The primary hallmarks are genomic instability, telomere attrition, epigenetic alteration and the loss of proteostasis. Combined, they all have detrimental effects on the human body. Therefore, they are hypothesized to serve as initiating triggers, whose damaging events progressively accumulate with time [9]. The antagonistic hallmarks are deregulated nutrient sensing, mitochondrial

dysfunction and cellular senescence. In principle they can also be beneficial and even protective for the organism (discussed later), but can also become dysregulated and synergize with the detrimental, primary effects. Senescence for example, protects the organism from cancer on one hand as it forces potentially dangerous cells to exit the cell cycle and eventually to die before becoming transformed by oncogenes. On the other hand, accrual of excess senescent cells promotes aging and is closely linked to all elements of the aging process [10]. The third category comprises the two integrative hallmarks, stem cell exhaustion and altered intercellular communication. They arise when the accumulated damage caused by the other hallmarks cannot be compensated by tissue homeostatic mechanisms. It is important to point out the interconnectedness of all of these hallmarks to enable the understanding of their contribution to aging. [8]. In this thesis, several of the hallmarks of aging will be dissected. The main focus will lie on the interaction of immune cells with senescent cells and cells bearing defects in proteostasis linked to neurodegenerative diseases.

No single gene or decline in a biochemical system accounts for all aspects of the complex multifactorial process of aging in a healthy person. An exception to this principle are individuals born with progeroid syndromes, families of genetic diseases with single gene recessive alleles such as Bloom's or Werner syndrome [11, 12], many of which affect DNA repair pathways, and have been important in advancing aging research at the molecular genetic level. The complexity and interdependence involved in aging means targeting one gene or by one single drug is unlikely to modify aging. To date, no known intervention slows, stops or reverses the aging process in humans [13]. It is now of scientific interest to identify the mechanistic drivers and the corresponding interactors of the aging process to build the main pillars of research in the biology of aging. This will help to reveal the mechanisms which determine the decline of immunological processes associated with aging.

1.1.3 The immune system ages and synergizes with the aging of other organ systems

The decline of immunological processes with age is termed immunosenescence and interacts substantially with the nine proposed hallmarks of aging [14, 15]. Immunosenescence affects both the adaptive and the innate immune system, interfering with the delicate balance of different cell numbers in tissues and their physiology [16, 17].

In the adaptive immune system, this involves the loss of naïve T and B cell populations resulting in diminished diversity of the T and B cell repertoire. This results in increased susceptibility to new infections, an altered memory response to previously encountered pathogens and also a decreased

response to vaccines [18]. In the innate immune system, neutrophil monocyte populations, which must be produced in vast numbers each day (e.g. a normal human makes $\sim 10^9$ neutrophils every day [19]), become altered in quantity and function. This affects intracellular killing, antigen presentation and leads to increased numbers of natural killer cells with reduced cytotoxic activity, eventually resulting in a diminished potential to remove virus-infected and cancerous cells [20]. Unsurprisingly, advancing adult age is therefore the major risk factor for age-related human pathologies including cancer, diabetes, cardiovascular disorders, neurodegenerative diseases [21] and especially infections, which we now see in “real time” with the age-associated mortality to SARS-CoV-2 [22]. Another aspect of immunosenescence, which is important for this thesis, is the immune surveillance of diseased cells such as senescent cells and cells with defects in proteostasis networks.

1.2 Cellular senescence

Cellular senescence (CS) is a programmed change in cell state associated with permanent growth inhibition. More specifically, CS is an irreversible state of cell cycle arrest of previously replication-competent cells. CS is associated with defined morphological changes to cell size, apoptosis resistance and a broad inflammatory secretory profile known as senescence-associated secretory phenotype (SASP) [23]. Senescent cells acquire new functions, which are described below.

The phenomenon of senescence differs from other non-dividing cell states, such as quiescence, transient exit from the cell cycle, or terminal differentiation. “Exhaustion”, for example of T cells chronically stimulated with antigen, is another non-dividing state distinct from senescence, as populations of these cells can re-acquire the ability to proliferate [24, 25]. Specifically, quiescence results from a lack of nutrition or mitogenic signals and is reversible once the previously missing growth conditions are restored [26]. The phenomena of quiescent T-cells is linked to transient nutrient depletion, enabling long-term survival of peripheral T cells without triggering inappropriate immune activation, which is critical to the maintenance of an effective immune repertoire [27]. Terminal differentiation defines the developmentally programmed process that enables undifferentiated precursor cells to generate specialized effector cells. This process is usually accompanied by permanent withdrawal from the cell cycle undergoing functional and morphological changes, losing their original cellular identity. Terminal differentiation has been extensively studied for example in effector T cells [28], neurons [29] and resident peritoneal macrophages [30] and is well defined in their developmental maturation [31]. Taken together, other forms of non-dividing cell states occur due to lack of nutrition and growth factors, whereas

senescence in general takes place due to severe harm caused by aging, serious DNA damages and other mutagens.

1.2.1 The Hayflick limit

The *in vitro* phenomenon of cellular senescence was first described and quantified in 1961 by Hayflick and Moorhead [32]. They observed a finite proliferative capacity in explanted human fibroblasts and were able to dissect the growth phases of the primary culture into three parts: Phase I was defined as early growth phase, in which the primary culture was formed. Phase II was characterized by a rapid and sustained cell division necessitating many sub-cultivations. In Phase III bizarre nuclear forms were seen, and mitotic activity progressively decreased until it eventually ended. Hayflick and Moorhead named this the 'phase III phenomenon', which we know now as the first description of cellular senescence. Moreover, the number of cell divisions before primary cells reach the end of their replicative lifespan has been termed as the Hayflick limit [33]. In the experimental work described in this thesis, cells at the Hayflick limit will be used as one type of experimental senescent cell, as the generation of permanently growth-arrested fibroblasts can be produced in large quantities with highly reproducible characteristics.

1.2.2 Cellular functions associated with senescence

Cellular senescence has a pleiotropic effect that depends on the trigger and the cell type involved. To date, three primary cellular senescence routes have been identified [34]: developmentally programmed senescence (DS), stress-induced premature senescence (SIPS) and replicative senescence (RS) [35]. DS is found in embryonic developmental structures of mammals, which have been shown to express senescent biomarkers like p21. However, compared to other types of senescence, DNA damage is not required for this response to occur. DS cells induce a secretory proteome promoting vascular remodeling and angiogenesis [36]. SIPS is initiated after an external stimulus triggers cell cycle arrest. The stressful external stimulus can come from physical or chemical agents inducing oxidative stress and DNA damage [37]. The term premature refers to the fact that the senescence causing stress occurs at earlier population doublings. SIPS has been shown to play an important role in physiological processes like wound closure in response to tissue damage [38]. Finally, replicative senescence, originally described by Hayflick [32], appears to be a fundamental feature of somatic cells and is induced by telomere shortening resulting from the absence of telomerase activity. With each round of DNA replication, telomeres are progressively shortened, eventually reaching a critical length and thereby their maximum number of population doublings which prevents further replication, thereby halting cell division [39].

1.2.3 Defining senescence at the molecular level

An overarching goal of senescence research over the past decade has been to apply a molecular definition to cells permanently in cell cycle arrest that avoids the relatively vague terminology outlined in 1.2.2 [40, 41]. Molecular criteria applied to senescent cells present two clear practical challenges. First, the cells cannot be expanded, meaning that experimental settings are always dealing with a terminal cell state. The second challenge is defining senescent cells *in vivo*, which requires robust and reproducible biomarkers and molecular probes [42]. Cyclin-dependent kinase inhibitors p16^{INK4a}, p21^{Cip1}, and p27^{Kip1} are regarded as key effectors of cellular senescence. The most studied four senescence-inducing pathways involving these inhibitors are the p16^{INK4a}/Rb pathway, the p19^{ARF}/p53/p21^{Cip1} pathway, the PTEN/p27^{Kip1} pathway and senescence induction by the oncogene Ras. All of these pathways involve the commonality of cell cycle inhibitor protein involvement in the senescence process [43]. This is unsurprising because increased expression of cell cycle inhibitors forces cells out of cycle and potentially into a senescent state. The opposite is true in cancer: loss or inhibition of cell cycle inhibitory proteins allows cells to stay in cycle and potentially accrue other oncogenic changes. Although this yin-yang appraisal is oversimplified, the concept remains useful for thinking about senescence versus oncogenesis.

1.2.3.1 The p16^{INK4a}/Rb pathway

The retinoblastoma tumor suppressor protein (Rb) is the main substrate of the CDK4 and CDK6 D-type cyclin dependent kinases. In its unphosphorylated or hypophosphorylated form, Rb associates to several transcription factors, silencing their transactivation functions. Among those are the E2F proteins, which activate the expression of important cell cycle proteins such as cyclins E and A. Phosphorylation of Rb by CDK4 and CDK6 leads to the release of Rb from its transcriptionally repressive complexes thereby facilitating S-phase progression. The tumor suppressor protein p16^{INK4a} functions as an inhibitor of CDK4 and CDK6. By that it has the capacity to arrest cells in G1 phase of the cell cycle and thus implements irreversible growth arrest in the cell [44, 45] (Figure 1-1). Among the four members of the INK4 family, p16^{INK4a} (encoded by *CDKN2A*) is an important tumor suppressor that is inactivated in a large proportion (>30%) of human tumors [46]. p16^{INK4a} binds and inhibits cyclin-dependent kinases and thereby normally contributes to cell cycle arrest. In the majority of human tumors, the p16^{INK4a}/CDK4/D1/Rb pathway is deregulated either by loss of the tumor suppressors p16^{INK4a} or Rb, or by activation of the oncogenes CDK4 or cyclin D1. The critical property that distinguishes p16^{INK4a} from the other members of the INK4 family seems to be its capacity to be transcriptionally upregulated in response to senescence and oncogenic stresses.

Consistent with the role of p16^{INK4a} in senescence, inactivation of the p16^{INK4a}/Rb pathway results in lifespan extension or immortalization. This is manifested by the elevated frequency of p16^{INK4a} gene inactivation in immortal cell lines [47]. In summary, *CDKN2A* seems to be a critical effector of senescence [43].

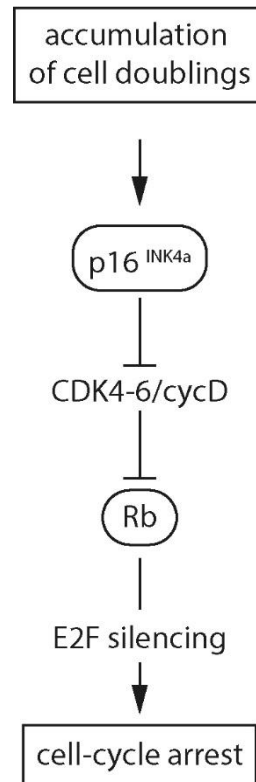


Figure 1-1: The p16^{INK4a}/Rb pathway (see text for details; adapted from Bringold *et al.* [43]).

1.2.3.2 The p19^{ARF}/p53/p21^{Cip1} pathway

The INK4a-ARF locus encodes two distinct tumor suppressors, p16^{INK4a} and p19^{ARF}. Whereas p16^{INK4a} restrains cell growth through preventing phosphorylation of the retinoblastoma protein, p19^{ARF} acts by attenuating Mdm2-mediated degradation of p53, thereby stabilizing p53. p53 activates p21^{Cip1}, which inhibits CDK1, causing cells to be arrested in the G2/M phase and decreasing the phosphorylation level of Rb by inhibiting the activity of CDK2 and CDK4. This prevents cells from entering the S phase, and ultimately leads to cell senescence. However, more severe stimuli lead instead to apoptosis [48, 49] (Figure 1-2). Concurring with the role of MDM2 as a repressor of p53 function, tumors overexpressing MDM2 have undetectable p53 levels but do not carry mutations in the p53 gene [48]. Consistent with its central role in the DNA damage response, which must involve cell cycle exit, p53 controls the expression of cell cycle inhibitors and especially of the CDK inhibitor

p21^{Cip1}. The protein amounts of p21^{Cip1} are elevated during senescence in several cellular systems [50]. Moreover, the *CDKN2A* locus contains an overlapping gene named ARF (Alternative Reading Frame) and encodes p19^{ARF}. Large homozygous deletions in the *CDKN2A* locus are common in human cancers with concomitant loss of both p19^{ARF} and p16^{INK4a} [46, 51]. The p19^{ARF} protein is an inhibitor of the p53-degrading activity of MDM2 [52]. Overexpression of p19^{ARF} thus results in stabilization of p53 and activation of its downstream targets. p16^{INK4a}/Rb and the p19^{ARF}/p53 pathways are probably used in a cell-type specific manner during the establishment of senescence. For example, the p19^{ARF} expression is transcriptionally upregulated during senescence in murine fibroblasts [53]. In summary, the *CDKN2A* locus encodes two key cell cycle inhibitory tumor suppressors, p16^{INK4a} and p19^{ARF}, that are transcriptionally activated by the accumulation of cell doublings. The induction of cell-cycle arrest by p19^{ARF} also requires the functional activity of p53, and p21^{Cip1}, being one of the most important targets of p53 [43]. Because of the central link between the *CDKN2A* and senescence, different groups have harnessed this locus as a molecular tool to “mark” senescent cells *in vivo*. The idea behind this approach is that senescent cells, having exited the cell cycle, express increased p16^{INK4a}. This is true at the mRNA and protein level as p16^{INK4a} expression is frequently used as a marker of senescence. Given this property, several groups developed reporter alleles where the murine *Cdk2na* locus was modified to report expression of p16^{INK4a} using luciferase or tdTomato [54, 55]. The results of these experiments were difficult to interpret as reporter activity did not necessarily associate with aging cells *in vivo*, and instead marked macrophages, which express high p16^{INK4a} amounts when they populate tissues. Thus, new reporter systems are needed to harness the usefulness of p16^{INK4a} as an *in vivo* marker of senescence.

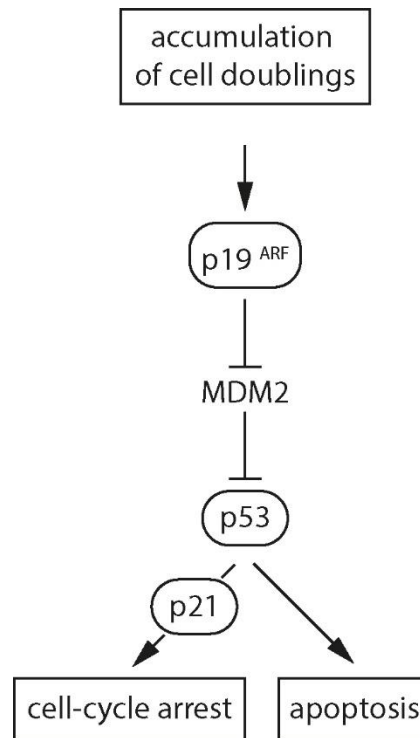


Figure 1-2: The p19^{ARF}/p53/p21^{Cip1} pathway (see text for details; adapted from Bringold *et al.* [43]).

1.2.3.3 The PTEN/p27^{Kip1} pathway

A new tumor suppressor pathway has begun to emerge quite recently, after the realization that the tumor suppressor PTEN, a lipid phosphatase, is the central negative regulator of the phosphatidylinositol-3-kinase (PI3K) signal transduction cascade. PI3K catalyzes the conversion of phosphatidylinositol 4,5-phosphate (PIP2) to phosphatidylinositol 3,4,5-phosphate (PIP3) and activates AKT kinase and other downstream effectors [56]. PTEN dephosphorylates PIP3 at the plasma membrane, thereby inhibiting PI3K-mediated signals for cell growth, proliferation, and survival [57]. This results in upregulation of the CDK inhibitor p27^{Kip1}, which either binds to cyclin D either alone, or in complex with its catalytic subunit CDK4. In doing so p27^{Kip1} inhibits the catalytic activity of CDK4, which means that it prevents CDK4 from adding phosphate residues to its principal substrate, the Rb protein. Increased levels of the p27^{Kip1} protein typically cause cells to arrest in the G1 phase of the cell cycle (Figure 1-3).

Loss of the tumor suppressor PTEN occurs in many human cancers and its inactivation may result as widespread as the inactivation of p53 or p16^{INK4a}/p19^{ARF}. PTEN's main target is an oncogene: the PI3K catalytic subunit p110 α is frequently amplified in ovarian cancers [58]. Treatment of human fibroblasts with PI3K inhibitors reduces the lifespan of cells accelerating the onset of senescence

[59]. Upregulation of the PI3K inhibitor p27^{Kip1} contributes to senescence. Moreover, the protein p27^{Kip1} accumulates in senescent murine and human fibroblasts. In the case of human tumors, p27^{Kip1} protein levels are often significantly diminished, particularly in their more advanced stages [60]. The downregulation of p27^{Kip1} in tumors occurs principally by protein destabilization, although it remains to be established whether this is a direct reflection of the balance between the activities of PTEN and PI3K [43].

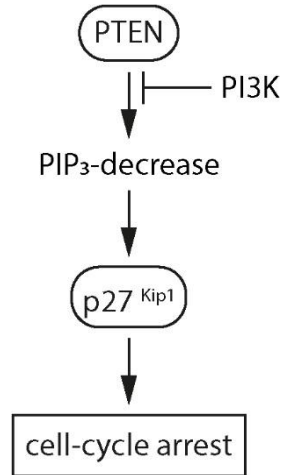


Figure 1-3: The PTEN/p27^{Kip1} pathway (see text for details; adapted from Bringold *et al.* [43]).

1.2.3.4 Mutated Ras induces senescence

Oncogenic Ras mutations are the most frequently observed oncogenic change in human tumors [61]. Ras activates a myriad of signaling routes that have been implicated in cellular proliferation, survival, generation of oxidative stress, and cytoskeletal changes [62]. In particular, the MAPK cascade formed by the kinases Raf/Mek/Erk is essential for proliferation, and another important Ras-activated target is PI3K. However, mutant Ras expression in normal cells induces a special type of senescence and forces cells to exit the cell cycle and eventually to die: this is termed oncogene-induced senescence. Among the various Ras-activated signaling effectors, the most important one for induction of senescence-like arrest is the Raf/Mek cascade, suggesting that Ras-driven proliferation is the relevant stimulus that triggers senescence [63]. Constitutive activation of Mek induces the accumulation of p16^{INK4A}, thereby the dephosphorylation of Rb, promoting cellular senescence [64]. Moreover, Ras-induced Raf has been shown to activate the MDM2 inhibitor p19^{Arf}, consequently inducing a p53-dependent cell cycle arrest [65] (Figure 1-4). In addition, Ras-induced oxidative stress has been proposed to be responsible for the induction of senescence [66]. The induction of senescence in response to a potent oncogene such as Ras indicates that senescence is

a programmed cellular response that can be triggered not only by the accumulation of cell doublings, but also by proliferative stresses. Therefore, cells have a way to detect the consequences of oncogene-induced stress, exit the cell cycle in a senescent state and die [67]. This new aspect further reinforces the anti-tumorigenic role of senescence. However, if mutant Ras is expressed in the absence of other guardians of the cell state (like p53) then transformation ensues. The entire cell cycle inhibitor and oncogenic stress network is therefore linked at many levels with senescence [43].

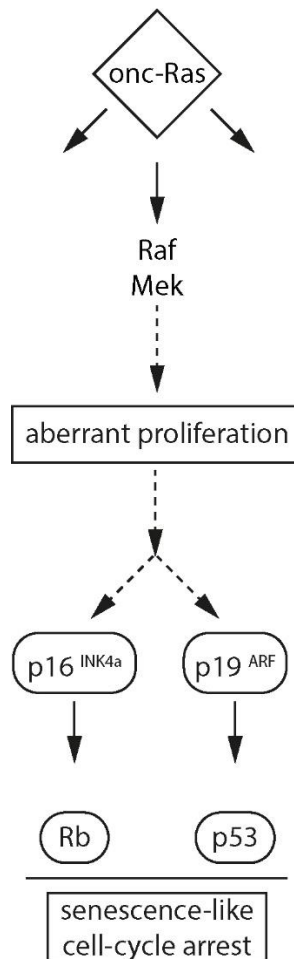


Figure 1-4: The Ras oncogene and its effects on senescence (see text for details; adapted from Bringold *et al.* [43]).

1.2.4 Senescence involves altered cell morphology and metabolism

Diverse signals induce senescence, such as repeated cell culture, telomere attrition, irradiation, oncogene activation, oxidative damage and the perturbation of mitochondrial homeostasis. Oxidative stress, in particular, contributes to DNA damage and telomere shortening [68]. Telomere shortening is one kind of DNA damage that triggers the DNA damage response (DDR), leading to

arrested cell cycle in an attempt to repair the perceived damage. Telomere shortening, which occurs at each cell division because of incomplete replication, could be one type of “counting” mechanism for the induction of replicative senescence [69]. Another inducer of senescence is the accumulation of unfolded or misfolded proteins in different cellular compartments. For example, prolonged and unresolved ER stress can cause senescence [70]. Overnutrition and metabolic stress may also lead to cellular senescence, because these stressors disrupt the cellular capacity to transport or process macronutrients [71]. For example, adipose tissue from obese mice shows enhanced activity of senescence-associated β -galactosidase (SA- β -Gal) and higher expression of p53, both associated with the senescent phenotype [72]. Senescent cells have been studied in mice to perform as major contributors to obesity-induced neurogenesis and alleviated anxiety-related behavior [73]. Moreover, hepatocyte senescence can result in fatty liver disease (hepatic steatosis) in mice and human patients [74], which is also linked to hepatocellular carcinoma. Obese individuals display increased production of reactive oxygen species (ROS) in the adipose tissue [75]. These increased ROS may in turn induce cell senescence by a process involving the DDR, epigenetic regulation and protein secretion patterns controlled by p53, p21 and Rb [76].

1.2.5 The morphology of senescent cells

Senescent cells have specific morphologies. They have an enlarged cytoplasm in culture [77], they are flattened [78], and vacuolated [79]. In some cases they become multinucleated as a consequence of corrupted cell division [80]. Causes of this altered appearance include cytoskeleton abnormalities and increased size and numbers of organelles [81], which may be linked to the production of the SASP (discussed below). The increased organelle mass is probably linked to preparation for cell division but due to cell cycle inhibition, results in organelle accumulation [81, 82]. Senescent cells are metabolically active, characterized by increased glycolysis relative to normal proliferating cells, decreased fatty acid oxidation and increased ROS generation [83]. They also activate pro-survival factors thereby becoming resistant to apoptosis [84, 85]. Although none of these markers is completely specific on its own or universal for all senescence types, there is ample consensus that senescent cells express most of them.

1.2.6 Senescent cell accrual in tissues

The organismal effects of senescence in specific contexts are pleiotropic. Senescent cells can activate both innate and adaptive immune response helping to maintain tissue homeostasis. Senescence contributes to wound healing, tissue repair, regeneration and the activation of host immunity necessary for these vital functions [86-88]. For example the size of atherosclerotic plaques

and resulting vessel obstruction can be limited by senescence [82]. However, a failure to eliminate senescent cells can contribute to their persistence in tissues resulting in anatomic lesions (e.g. as in an atherosclerotic plaque). The loss of replicative capacity of certain cell types (e.g. T cells, pancreatic β -cells) may lead to defects in tissue regeneration and result in immune suppression [89].

Thus, cellular senescence has both positive and negative roles [90]. Initially defined as a tumor suppressor program, cellular senescence was thought to restrict the propagation of damaged cells. However, these arrested cells, are metabolically active and secrete a variety of molecules to communicate with the tissue microenvironment and the neighboring cells (discussed below). These molecules attract immune cells, which can target and eliminate the senescent cells. In general, senescent cell clearance gives rise to beneficial outcomes, such as tumor suppression, tumor regression, tissue remodeling and embryonic development. In contrast, senescent cell accumulation tends to be associated with detrimental effects, such as cancer or aging. What factors determine the accumulation or disposal of senescent cells remains elusive [91]. One hypothesis is that depending on the trigger, the cell type and the cellular context, distinct senescence responses are unleashed and that could affect the recruitment and activity of immune cells [92]. Dissecting the mechanisms involved in senescent cell clearance in each individual scenario will be critical to better exploit cellular senescence with therapeutic purposes.

1.3 The senescence-associated secretory phenotype (SASP)

Even though senescent cells permanently exit the cell cycle, they remain metabolically active, which is highlighted by the secretion of a plethora of different SASP molecules. The heterogeneous composition of the SASP is dependent on the original cell type, the manner of senescence induction and the surrounding hormonal milieu.

1.3.1 Classification of SASP molecules

SASP components are broadly classified into the three following groups: (1) soluble signaling factors binding to a receptor such as cytokines and chemokines, (2) proteases like serine proteases and (3) regulatory proteins such as epidermal growth factor (EGF) [23]. Because of the breadth of different SASP components, along with their variable cell-to-cell expression, few studies have systematically attempted to define the contributions of one SASP component relative to the others. Such an experiment is complicated due to overlap between some SASP components (e.g. IL1- α and IL-1 β) and the challenge of generating a genetic system where only senescent cells lack the SASP component of interest. For these reasons, "SASP" is regarded as a generic phenomenon [39, 93].

The first group includes cytokines, chemokines and growth factors, of which the most studied are IL-6 and IL-1. IL-6 seems to play a fundamental role in the paracrine and autocrine maintenance of the SASP [94, 95]. It directly induces cell cycle arrest and acts as a pro-mitogenic factor in oncogene-induced senescence. IL-1 α has been demonstrated to act as “upstream” regulator of the SASP, being necessary and sufficient to induce specific SASP factor expression [96]. In particular, cell surface-bound IL-1 α is essential for signaling the senescence-associated secretion of IL-6 and IL-8, which are known to reinforce the senescence growth arrest [97]. This was demonstrated by the addition of neutralizing IL-1 α antibodies, and IL-1 α depletion by RNA interference resulting in reduced senescence-associated IL-6/IL-8 secretion. Furthermore, conditioned medium from IL-1 α -depleted senescent cells markedly reduced the IL-6/IL-8-dependent invasiveness of metastatic cancer cells, indicating that IL-1 α regulates the biological effects of these cytokines [97]

The most prominent group of chemokines that is overexpressed and secreted by senescent cells are CC and CXC chemokines such as monocyte chemoattractant proteins (MCP)-1, -2, -3, -4, macrophage inflammatory protein (MIP) 1a and 3a (CCL-3, -20), monotactin-1 (CCL-16), and IL-8 (CXCL-8) among others [23]. Furthermore, growth factors HGF, FGF, TGF β , GM-CSF, EGFR and IGFs can be assigned to this first group [98]. IGF-1 in particular has a dynamic effect on fibroblasts: acute exposition promotes cell proliferation while prolonged exposition promotes senescence [99]. The second group includes several extracellular enzymes like matrix metalloproteases MMP-1, MMP-10, MMP-3 and serine proteases. These factors are capable of cleaving membrane-bound proteins, thereby destroying signaling molecules and remodeling the extracellular matrix. This enables senescent cells to modify their microenvironment [100]. Moreover, small non-protein components, such as ROS and nitrogen species that damage neighboring cells, can be included in this group [101]. The third group includes regulatory factors without an own enzymatic activity. However, when factors like tissue inhibitors of metalloproteases (TIMP), the plasminogen activator inhibitor (PAI), and insulin-like growth factor binding proteins (IGFBP) bind to factors from the first and second group, they regulate their functioning. For example, TIMP inhibits the activity of most MMPs [102] and the function of IGFBP and IGF transport proteins [103]. Finally, extracellular vesicles, in particular vesicles associated with microRNAs [104] can affect neighboring cells and cells located at a considerable distance, both by initiating and suppressing cellular senescence, depending on the composition of microRNAs.

1.3.2 Regulation of the SASP

SASP production is thought to change as senescent cells persist. Superficially, this process can be subdivided into three phases [105]. The first phase is the initial SASP secretion (possibly as a defensive response to replicative failure) and begins immediately after a DNA damage event and lasts hours. However, this phase is not sufficient to initiate senescence [106]. The next phase is the “early” SASP phase, which continues for several days after the initiation of CS. During this period the most important SASP factors start to appear, among them IL-1 α . During the next 4–10 days, the secretion of most factors intensifies due to the autocrine effect of SASP, which ultimately leads to the formation of “mature” SASP [105]. The events that activate the SASP are still incompletely understood. However, it is known, that the SASP is regulated at multiple levels, including transcription, translation, mRNA stability, and secretion [107]. Furthermore, the SASP relies on autocrine and paracrine positive feedback loops that cause robust signal amplification [91].

The DNA damage response (DDR), is coupled to the SASP expression. The knockdown of DDR components such as ATM, Chk2, NBS1 and H2AX reduces the secretion of SASP factors, including IL-6 and IL-8 [108, 109]. However, the DDR cannot be the only regulator as transient DNA damage does not lead to senescence and expression of the SASP. Moreover, the activation of the DDR, but not the presence of DNA damage per se regulates the senescent states and the SASP [108, 110]. This hypothesis is supported by the fact, that the DDR is immediate, while the expression of the SASP takes several days. However, the cytosolic DNA sensor cGAS was found to link the DDR to SASP initiation. In response to the accumulation of cytoplasmic DNA, cGAS finally activates the adaptor protein STING, which is then activating NF- κ B. [111]. As a key player in the inflammatory response, NF- κ B has been shown to be of utmost importance in regulating the SASP expression on a global level [95, 112]. The activation of NF- κ B leads to the transcription of SASP related genes like IL-6. [113]. Another DDR-dependent mechanism of SASP regulation involves the transcription factor GATA4 [114]. Normally, GATA4 is degraded via p62-mediated autophagy, a process that is suppressed in senescent cells. This leads to GATA4 stabilization and accumulation, which facilitates the initiation and maintenance of NF- κ B activity [114]

The key player in DDR-independent SASP regulation is the stress kinase p38. It activates the p16^{INK4a}/Rb signaling pathway, which mediates cell cycle arrest in senescent cells [115]. The suppression of p38 has been demonstrated to prevent the secretion of most of the cytokines, chemokines and growth factors that built the SASP [116]. Furthermore, maintaining p38 in the active state over long time can initiate the SASP independent of any other stimuli that cause senescence

[115]. Another key player in SASP regulation is the mTOR protein. The role of mTOR in the regulation of SASP was identified via two regulatory mechanisms [117]. On the one hand, it has been shown that mTOR can control the translation of IL-1 α and thus regulate the SASP [118]. On the other hand, mTOR is able to prevent the degradation of the transcripts of a large number of SASP factors [117]. The plethora of SASP molecules, as well as the context dependent composition of the secreted factors, leads to an increase in the number of studies focused on detailing the molecular mechanisms of SASP regulation [119].

1.3.3 Effects of the SASP

The central difficulty in aging research deals with the secretion of bioactive SASP factors by senescent cells. The competing models propose both beneficial and detrimental effects of the SASP. The beneficial effects comprise the ability of the SASP to prevent the proliferation of damaged cells. Moreover, the SASP provides the communication of the senescent cells to immune cells *in vivo* [120]. This indicates the appearance of senescent cells in the body, recruiting immune cells to the site of damage. As a result, the mobilized natural killer (NK) cells, macrophages and T cells contribute to the removal of damaged or oncogene-expressing cells from the organism [121, 122].

On the other hand, the accumulation of senescent cells and the prolonged secretion of SASP show detrimental effects promoting the spread of premature senescence to neighboring cells [23, 92]. This can ultimately lead to disruption in the functioning of tissues, accelerate the development of aging and various age-associated diseases [123, 124]. Moreover, it has been demonstrated, that SASP components have the potential to promote proliferation, survival and metastasis in already committed precancerous cells [125, 126]. In a young healthy organism, the positive effect of the SASP is well regulated [119]. However, with age or in case of lesions, its effectiveness can be significantly impaired. This leads to the accumulation of senescent cells in the population and, consequently, to prolonged secretion of SASP factors [127, 128]. Therefore, the outcome of the influence of SASP components on the microenvironment may be defined by the balance between how long the senescent cells remain in the population and their rate of elimination by the cells of the immune system [12, 14–16]. The effects of SASP that are positive for the organism are due to the temporary presence of senescent cells, whereas its negative effects are associated with the accumulation of senescent cells and the emergence of a focus of chronic inflammation [119, 129–131]. Once the SASP molecules are released into the extracellular space, they impact adjacent normal cells via the auto/paracrine pathway. By that, the senescent cells initiate cell cycle arrest and stop proliferation in the neighboring cells. This greatly accelerates the development of CS in the

population [80, 83, 117]. It was shown, that the SASP can also induce paracrine senescence in normal cells both in culture and in human and mouse models in oncogene induced senescence (OIS). Multiple SASP components were identified to mediate paracrine senescence, including TGF- β family ligands, VEGF, CCL2 and CCL20. Cells undergoing OIS can transmit paracrine senescence to their neighbors thereby reinforcing senescence in the tissue [96].

The pleiotropic functions of cellular senescence can be both beneficial and detrimental, according to the situation. Moreover, the scope of secreted molecules is extremely broad, diversified and even context dependent. This results in contradictory interpretations about the role of the SASP in the pathophysiology of chronic diseases [132]. In sum, the SASP is a complex network of secreted factors that can have a positive or negative effect on cancer development and drug response.

1.4 Targeting senescent cells

A long-standing concept in aging research is that more senescent cells lead to more problems, for example, the more senescent cells present, the greater the chance for “escape” to an oncogenic state. Therefore, if less senescent cells are a desirable health objective, how can these cells be specifically targeted? A breakthrough in senescence research was achieved by van Deursen and colleagues who created genetically engineered mice where p21 positive cells could be exogenously depleted [133]. They showed that very old mice had improved health (“healthspan”) once senescent cells were depleted. Subsequently, strategies targeting senescence cells are classified into the following groups: (1) non-pharmacological interventions that prevent the accumulation of senescent cells, (2) broad pharmacological therapies aimed at reducing the amount of SASP molecules produced by already existing senescent cells, and (3) pharmacological therapies aimed at reducing the number of senescent cells in the organism (senolytics, senostatics and related approaches) (Figure 1-5).

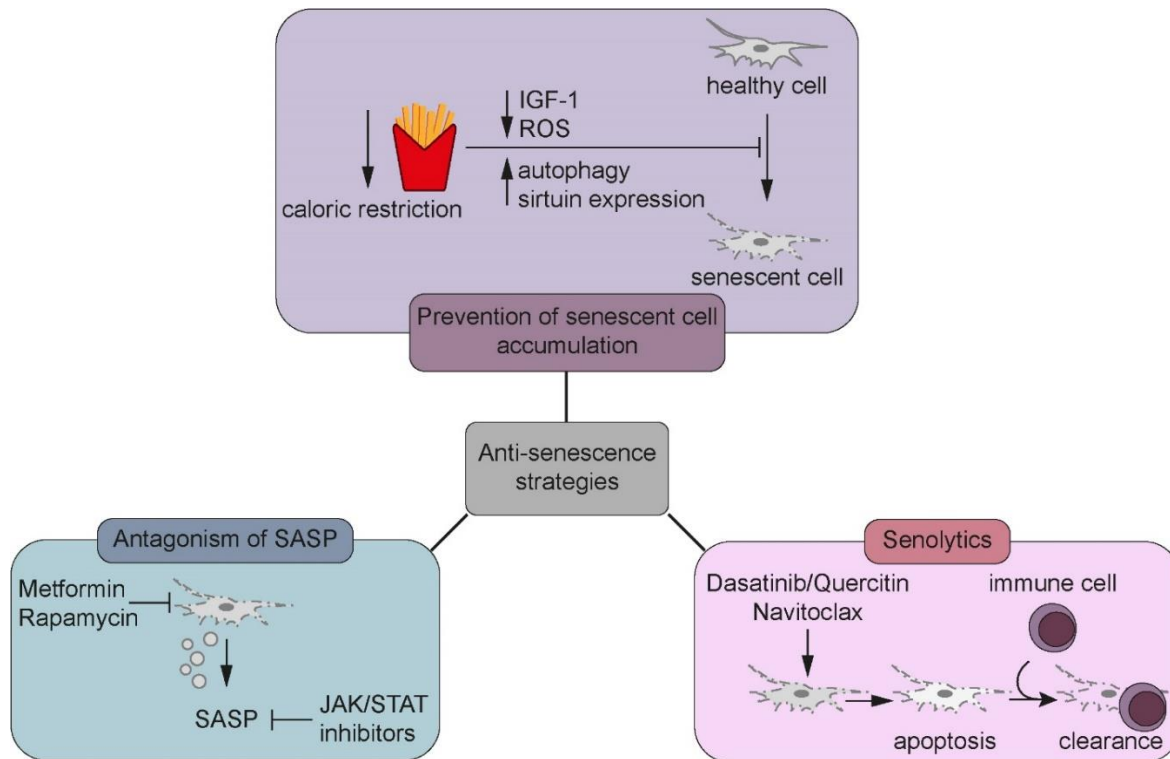


Figure 1-5: Overview of therapeutic strategies to counter the effects of senescent cells (adapted from Montoya *et. al* [134]).

1.4.1 Non-pharmacological interventions

Caloric restriction is the most prominent approach, especially with the general public. Caloric restriction reduces body weight, body fat and plasma insulin concentrations and extends lifespan [135]. In mice, a 26% calorically restricted diet for three months started in adulthood reduces the number of senescent cells in rapidly proliferating (intestinal) and slowly proliferating (hepatic) tissues [136]. Caloric restriction, even if started in adulthood, reduces fat deposition and the concomitant increase in telomere-associated DNA damage foci in hepatocytes [74]. A study of the human colonic mucosa showed that adults who had been voluntarily exposed to a 30% caloric restriction (with appropriate nutrition) for over 10 years had significantly reduced expression of $p16^{\text{INK4a}}$ and reduced local concentrations of IL-6 [137]. The underlying mechanisms included a reduction of ROS from nutrient metabolism, stimulation of autophagy, increased expression of sirtuins, and enhancement of normal DDR mechanisms [138]. At the organismal level, caloric restriction leads to reductions in bioavailable IGF-1 [139], a known inducer of cellular senescence [99]. Until now, research focused predominantly on the effects of individual nutrients and sometimes foods, but rarely on dietary patterns. It turned out that the populations of the so-called

“Blue Zones” have been able to increase life expectancy and to reduce obesity to result into the world’s longest-lived communities. However, diet operates irrespective and together with other factors as an appreciable contributor to survival, with a strength comparable to or greater than all other measured variables [140-142].

1.4.2 Drugs aiming for SASP reduction

This category of compounds contains mostly molecules approved for other indications that have demonstrated anti-senescence properties *in vitro*, in animal models, or in translational studies in humans. The challenge with an anti-SASP strategy lies in the ability to block the deleterious effects of SASP proteins, without interfering with their anti-oncogenic properties. The anti-diabetic drug metformin, which is able to block the SASP in transformed fibroblasts, is a candidate for those bispecific compounds [143]. Chronic metformin use is associated with extended life span and health span, independent of its antihyperglycemic efficacy [144]. Notably, the precise molecular target(s) of metformin remain unclear, despite it being the most prescribed drug in the world. Other anti-SASP molecules are the immunosuppressant rapamycin and related rapalogs like temsirolimus, which inhibit parts of the mTORC1 anabolic signaling pathway, and are often combined with other immunosuppressives to block organ rejection in transplantation. Rapalogs inhibit expression of several SASP members and increase autophagy in senescent cells [145]. Rapamycin has been demonstrated to extend maximal life-span in mammalian species. It is not clear, however, whether the drug slows down aging or if it has isolated effects on longevity by suppressing cancers or other effects [146]. Rapalogs can have serious side effects, such as nephrotoxicity, thrombocytopenia and, hyperdyslipidemia [147], which limit their use as an anti-aging approach. A third group of approved drugs with anti-SASP features are JAK-STAT inhibitors (also termed “Jakinibs”). The JAK-STAT (signal transducer and activator of transcription) pathway is an intracellular signaling cascade responsible for many pro-inflammatory responses. Inhibition of this pathway has an anti-SASP effect *in vitro* [148]. Since several JAK inhibitors are available for the treatment of autoimmune diseases [149], a natural extension would be to assess their potential against cell senescence in humans.

1.4.3 Senotherapeutics: senolytics and senostatics

Overall there is conflicting evidence, therefore, that broad anti-aging therapeutics such as Jakinibs or Rapalogs have the power to delay aging. An entirely different approach is the elimination of senescent cells themselves. These senotherapeutic strategies can be distinguished in two categories. The first category are pharmacological agents that eliminate senescent cells. Senolytics induce apoptosis in senescent cells allowing the remaining non-senescent population to preserve

or restore tissue function. The second category are senostatics and senomorphics, which interfere with specific pathways in order to restore the appropriate cellular function, preserve viability and prolong the lifespan.

Treating senescence is complicated in the traditional paradigm of “one drug, one target, one disease”. Senolytics are designed to be used in combination with other compounds and moreover intended to go after whole networks rather than a single target. Dasatinib (a kinase inhibitor that was originally developed to target BCR-ABL, but has a much broader target range) and quercetin (a flavonoid commonly found in dietary supplements) are first generation senolytics and induce apoptosis of certain types of senescent cells [150, 151]. More importantly, the combination of dasatinib and quercetin alleviates several senescence-associated phenotypes [150]. Another class of senolytics are BCL2 inhibitors such as navitoclax [152], which is clinically indicated for adult chronic lymphocytic leukemia. Problematic with all three agents was that they seemed to sensitize some, but not all types of senescent cells [150, 152]. Even though new senolytics have been developed in recent years, all of these reagents still show undesirable side effects. Therefore they cannot be used to target aging [124]. Moreover, senolytics appear to wipe out not only the detrimental, but also the beneficial effects of senescent cells.

In contrast to senolytics, senostatics do not kill senescent cells but inhibit their paracrine signaling and therefore block the spreading of senescence via the bystander effect. Two different strategies are applied for the development of senostatics: generalized agents, modulating the paracrine signaling network, and precision senostatics, inhibiting only particular components in the signaling composition. For generalized senostatics, several therapeutic targets have been emerged and examined, like for example NF- κ B. A potential problem for targeting such factors is that they have also important non-senescence related functions. For example NF- κ B plays an essential role in controlling acute inflammatory response and immune response [153]. Precision senostatics have not been seriously considered yet because the composition of the paracrine signaling of senescent cells is complex and heterogeneous, consisting of a plethora of different factors [23]. Moreover, it depends on the cell type, the stage of senescence and the type of senescence inducing stimuli [154-156]. As our current understanding of senotherapy is far from complete, many challenges are still to overcome for a successful drug development program [151, 157]. In future clinical trials focusing on the elimination of senescent cells, it will be important to determine when to initiate the treatments (age of the patients), the schedule (continuous, periodic and/or sporadic), as well as the specific markers to determine the efficacy of the therapy [158].

1.5 The interaction of senescent cells with immune cells

The SASP has been proposed to aid immune cell attraction. This is consistent with the composition of the SASP, which contains many chemokines. This immune activation may result in tumor clearance, suggesting, the senescence program being able to prevent cancer development [23, 159]. Furthermore, it is hypothesized that the induction of senescence, rather than cell death may provide a more effective strategy for targeting cancers [132]. Senescent cells are able to activate both innate and adaptive immune responses. Reactivation of endogenous p53 in p53-deficient tumours can produce complete tumor regression. This was shown using RNA interference (RNAi) to conditionally regulate endogenous p53 expression in a mosaic mouse model of liver carcinoma [160]. The primary response to p53 was not apoptosis, but instead involved the induction of a cellular senescence program that was associated with differentiation and the upregulation of inflammatory cytokines. The innate immune system was activated by increased expression of transcripts specific to natural killer (NK) cells, macrophages and neutrophils, infiltrating the tumors following p53 reactivation. This eventually resulted in tumor clearance [160].

Moreover, cells of the innate immune system such as NK cells, macrophages and neutrophils were found in the proximity of senescent cells in fibrotic livers. Senescent activated stellate cells generated during liver damage were shown to be preferentially killed by NK cells both *in vitro* and *in vivo*. In doing so, immune clearance of senescent cells yielded another benefit: the resolution of liver fibrosis following damage [161], which occurred when cells were unable to enter the senescent state. Whilst mechanistically NK cells have been the primary focus to date in regard to immune surveillance of senescent cells, also other innate immune cells appear to be important. A study demonstrated that p53-expressing senescent stellate cells release factors which promote macrophage polarization towards a tumor-inhibiting M1 state capable of targeting senescent cells in cultures [162]. M2 macrophages have high phagocytosis capacity [163] and thus may have the potential to also induce cell death in senescent cells [164]. Interestingly, macrophages may also promote induction of cell senescence in tumor cells as a possible anti-cancer mechanism. In 2011, it was demonstrated that pre-malignant senescent hepatocytes undergo immune-mediated clearance by CD4⁺ T cells [165]. The presence of major histocompatibility complex class II (MHC-II) molecules on senescent hepatocytes appeared to be important for direct killing, even though the presence of monocytes/macrophages was required. Whilst senescent cells may promote T cell recruitment for their clearance, T cells may also induce cellular senescence in cancer cells as a mechanism to limit cancer progression [166].

Macrophages, as the main phagocytic cell type in the mammalian organism, likely play a major role in the recognition and clearance of senescent cells. A key question is whether macrophage-mediated processes underlying the recognition of senescent cells are specific, as senescent cells are self. Furthermore, senescent cells do not seem to express key “identifiers” for immune recognition such as surface phosphatidyl serine (PtdSer) on apoptotic cells that signals their engulfment (see below). Thus, detection of senescent cells by phagocytes is an important concept that will be addressed in this thesis.

Macrophages are phagocytes: when they encounter a target, three distinct processes have to occur at the same time. First, a phagocyte evaluates the target for the absence of “don’t eat me” signals that prevent phagocytosis of normal cells. CD47 is an important “don’t eat me” signal and will be discussed throughout the thesis. Second, the size of the target has to be determined. Very little is known about target size discrimination by phagocytes but this has important implications for medical device failure (titanium rods, breast implants, etc. [167]) and large indigestible targets that drive phagocyte death and inflammation (asbestosis fibers, for example [168]). Third, most phagocytic targets express a “eat me” signal (discussed below). Senescent cells may also express specific cell surface antigens [169]. This would not only provide insights into the mechanisms mediating immune clearance, but would also provide means to specifically identify senescent cells in tissues. However, possession of specific molecules that provoke phagocytosis seem unlikely and such molecules are unsubstantiated in the literature [170]. Senescent cells display higher amounts of ROS, resulting in changes in cell metabolism and/or the presence of dysfunctional mitochondria, which can lead to the oxidation of phospholipids [171]. During apoptosis, oxidized lipids on the surface of cell membranes can function as pattern recognition ligands promoting macrophage recognition [172].

1.6 The role of macrophages for the immune system

Macrophages are differentiated cells of the myeloid lineage found in every tissue of the body. Although phagocytosis and microbial killing were the cardinal functions of macrophages to be described [173], they perform a broad range of important immunological functions during the innate response and also contribute to the maintenance of tissue homeostasis and tissue repair [174, 175]. On a cellular level, macrophages hold the following functions: (1) phagocytosis of pathogens, infected or dead cells and cellular debris, (2) antigen presentation by displaying processed antigens associated with major histocompatibility complex (MHC) molecules and (3)

production of trophic factors, immunological mediators and effector molecules, such as different types of cytokines, including IL-1, IL-6 and tumor necrosis factor- α (TNF- α) [176, 177].

1.6.1 Development and circulation

Macrophages originate from three types of progenitors. First, microglia (the macrophages of the brain) originate from the yolk sac and populate the developing nervous system very early in embryogenesis. Once the blood brain barrier is established, turnover of microglia is extraordinarily slow (in homeostasis) [178]. The second source of macrophages arises from myeloid-erythroid progenitors in the fetal liver; these cells populate all embryonic tissues and give rise to the alveolar macrophages and intestinal macrophages present at birth [179]. Fate tracking studies were used to define the turn-over of the myeloid-erythroid macrophages, which varies depending on the organ. In the case of the intestine, 100% of the myeloid-erythroid macrophages are replaced by one month with monocyte-derived macrophages, while alveolar macrophages are replaced over years (in mice) [180]. The third and predominant macrophage source are monocytes from bone marrow myeloid progenitors, which are produced continuously through life [181]. One of the most important concepts in macrophage research from the past few years is that different tissues confer “identity” to the specific macrophage type needed. Thus, transfer of peritoneal GATA6⁺ embryo-derived macrophages into the lung causes rapid (hours to days) conversion into a macrophage that is molecularly nearly identical to an alveolar macrophage [182]. The process of tissue “imprinting” makes sense in that seeding of organs from the monocyte pool must cause conversion to a macrophage type needed for specific tasks in that environment [183]. The entire process of macrophage seeding is also controlled by niche competition, which regulates the proportion of macrophages in a given tissue, for example, the regular spacing of Kupffer cells in the liver [184].

1.6.2 Plasticity and polarization

Macrophages are intrinsically heterogeneous and their phenotype and functions are regulated by the surrounding micro-environment. Macrophage polarization (or activation) is a process, by which macrophages phenotypically mount a specific phenotype and a functional response to the environmental stimuli and signals that encounter in each specific tissue and context [185]. Macrophages have the ability to change their activation states in response to growth factors (e.g., CSF-1 and GM-CSF) and external cues such as cytokines and microbial products, but also other modulators including nucleotide derivatives, antibody-Fc receptor stimulation, glucocorticoids, infection, phagocytosis and potentially any other entity capable of being recognized by macrophages [186]. The activation of macrophages has emerged as a key area of immunology,

tissue homeostasis, disease pathogenesis and in resolving and non-resolving inflammation [184, 187]. Monocytes and macrophages migrate to the sites of inflammation or injury to eliminate the primary inflammatory signals and finally contribute to wound healing and tissue repair [188]. This process is mainly initiated by pathogen associated molecular patterns (PAMPs), released from invading pathogens, and damage-associated molecular patterns (DAMPs), released from damaged or dead cells [189]. In addition, activation of tissue-resident memory T cells by antigens can trigger the recruitment of macrophages via secretion of various inflammatory cytokines and chemokines.

Two major macrophage activation states are commonly described: classically activated, or inflammatory (M1) and alternatively activated or anti-inflammatory (M2) macrophages (Figure 1-6). The phenomenon of the two different M1/M2 phenotypes is typically referred to the term “macrophage polarization” [190, 191]. While in practice, such a dichotomy does not exist except under specific (and largely laboratory conditions), the polarization paradigm is both useful and misused at the same time [186, 192]. Accordingly, herein, precision will be used to refer to macrophage polarization and caveats and limitations are noted where appropriate. An additional issue is species specificity in the gene and protein expression patterns of, for example, human versus rodent versus swine polarized macrophages, which are likely tailored depending on the immune response needed balanced with cost: high production of reactive free radicals in rodent macrophages may damage DNA but at a low cost due to reduced lifespan and increased reproductive fitness compared to (relatively) long-lived primates.

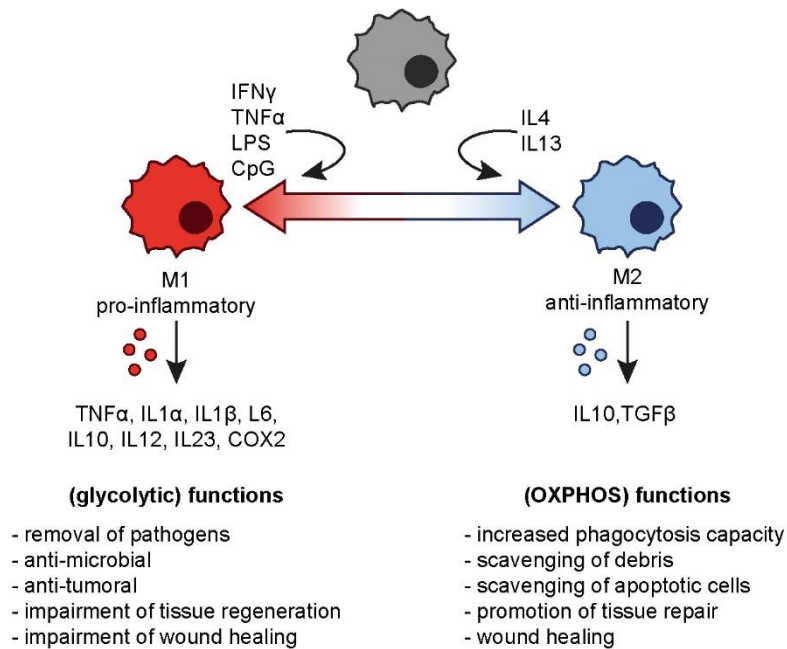


Figure 1-6: Overview of different stimuli, secreted cytokines, and biological functions between M1 and M2 macrophages.

M1 macrophages are induced by Th1 cytokines, such as IFN- γ and TNF- α , in combination with pathogen-derived molecules such as lipopolysaccharide (LPS) or bacterial cytidine-guanosine (CpG). These macrophages produce and secrete pro-inflammatory cytokines like TNF- α , IL-1 α , IL-1 β , IL-6, IL-12, IL-23, cyclooxygenase-2 (COX-2) and require autocrine-paracrine production of IL-10 to suppress (in part) their pro-inflammatory functions. At the functional level, M1 macrophages participate in the removal of pathogens during infection through activation of the nicotinamide adenine dinucleotide phosphate (NADPH) oxidase system, and subsequent generation of reactive oxygen species (ROS) and nitric oxide (NO) production. Therefore, M1 macrophages have antimicrobial and anti-tumoral activity, mediate ROS-induced tissue damage, and impair tissue regeneration and wound healing. To protect against such tissue damage, the chronic inflammatory response is inhibited by numerous regulatory mechanisms of which the immunoregulatory function of M2 macrophages is an important component [176, 185, 193].

M2 macrophages, which are in most cases anti-inflammatory, are polarized by Th2 cytokines IL-4 and IL-13 via activating STAT6. Beside IL-4 and IL-13 other cytokines such as IL-10 control M2 polarization via activating STAT3 [194] which, for example, induces increased sensitivity to IL-4 and IL-13 signaling [195]. M2 macrophages have an anti-inflammatory cytokine profile, which is characterized by low production of IL-12 and relatively high production of both IL-10 and TGF- β [196,

197]. Functionally, M2 macrophages have a relative increase in phagocytosis capacity (compared to M1 macrophages), scavenge debris and apoptotic cells, promote tissue repair and wound healing, and possess pro-angiogenic and pro-fibrotic properties [185, 193]. Therefore, in general, M2 cells take part in type 2 immune responses and have key roles in helminth clearance [198], dampening of inflammation, orchestrating the promotion of tissue remodeling [174], angiogenesis, immunoregulation and tumor formation and progression [199]. However, the M1/M2 phenotype does not reflect the different phenotypic subsets of macrophages [200]. Exposure of M2 macrophages to M1 signals, or vice versa, which induce “re-polarization” or “re-programing” of differentiated macrophages is another evidence of their high functional plasticity which can be potentially pursued for therapeutic goals [201].

Three broad pathways coordinate and contribute to macrophage polarization: (1) epigenetic and cell survival pathways that prolong or shorten macrophage development and viability in inflammatory environments; (2) factors specific to distinct tissue microenvironments and (3) extrinsic factors such as microbial products and cytokines released in inflammation that are the primary drivers in establishing the polarized state. Numerous intellectual and practical advances have provided a framework for rationally describing and manipulating macrophage polarization. However the phenotype of an activated macrophage within a given time and space does not necessarily signify its function [190].

1.6.3 Antigen presentation

Macrophages are antigen presenting cells (APCs) and thereby initiate and regulate the immune response. Capture, endocytosis and presentation of self or foreign antigen are important features of macrophage biology, which provide the link between innate and adaptive immunity [202]. Macrophages reside in all organs where they control the surrounding tissue for invading pathogens. They alert the immune system to the presence of pathogens by engulfing them, processing their antigens and presenting the peptide fragments bound to human leukocyte antigen (HLA) molecules on their surface. After antigen processing, macrophages migrate toward the T cells to prime and stimulate them [177]. Activated macrophages express high levels of co-stimulatory and antigen presenting molecules such as CD80, CD86, and MHC class I and II molecules on their surface. The precise and relative relationship between macrophages and other specialized migratory and tissue resident dendritic cells that perform specific antigen presentation functions (e.g. cross presentation of antigens – extracellular antigens processed for CD8+ T cell recognition on MHCI molecules - by BATF3-dependent cDC1) remains unclear and one the most controversial topics in immunology.

1.6.4 Removal of dead cells - efferocytosis

Cell death is a universal feature of infected and damaged tissues. Cell death can occur by unregulated, “accidental” means such as mechanical or osmotic lysis, particularly in the early stages of inflammation. Apoptosis is the most prominent mechanism of programmed cell death observed in inflamed tissues [203, 204]. The stimuli that trigger apoptosis within inflamed tissues vary widely depending on the type of inflammation and can be due to pathogen-derived, host-derived or iatrogenic stimuli. Unwanted cell clearance via the phenomenon of apoptosis is defined as efferocytosis and is dependent on mostly specialized phagocytes like macrophages.

The mechanisms of efferocytosis follow the execution of the three main efferocytosis signaling programs: (1) “find-me” signaling, the chemoattractant-mediated recruitment of macrophages to apoptotic cells, (2) “eat-me” signaling, the receptor-mediated recognition and engulfment of apoptotic cells, and (3) post-engulfment signaling, the signals related to the phagolysosomal processing of engulfed cellular material.

In order for macrophages to engulf their target, they first must find a cell undergoing apoptosis. This find-me stage of efferocytosis is mediated by the release of numerous soluble factors that attract macrophages to the site of cell death [205]. Key “find-me” signals include triphosphate nucleotides (ATP, UTP) [206], the chemokine CX3CL1 [207], and the signaling lipids lysophosphatidylcholine and sphingosine-1-phosphate (S1P) [208]. While all of these factors can stimulate macrophage migration to apoptotic cells, the relevance of individual “find-me” signals in efferocytosis depends on different factors including phagocyte and apoptotic cell type as well as the apoptotic stimulus and the stage of apoptosis being studied [209]. Also, some of these “find-me” signals function as key modulators of macrophage inflammatory responses.

The engulfment of apoptotic cell by macrophages results in the acquisition of excess cellular materials such as lipids, carbohydrates, proteins and nucleic acids. Macrophages can adjust to this increased metabolic load by activating degradation and efflux pathways [210]. In addition, engulfment of apoptotic cells engages multiple metabolic sensing pathways in macrophages. This plays an important role in controlling phagocytosis and immune signaling [211, 212]. Among these metabolite-sensing mechanisms, the nuclear receptor (NR) family of transcriptional regulators including LXR α , LXR β , PPAR γ , PPAR δ , RXR α [213], provides the best studied link between sensing ingested apoptotic cells and the macrophage efferocytosis machinery [214]. Further genetic studies have identified multiple NR family members as critical regulators of macrophage efferocytosis

in vitro and *in vivo*. NR activation can enhance the transcription of engulfment-related genes in macrophages [215]. This includes also PtdSer receptors modulating the activity of multiple NRs. The cellular source or precise molecular nature of the full range of NR-modulating ligands relevant for efferocytosis is to date not clear yet.

Phagocytosis is required for a broad range of physiological functions, from pathogen defense to tissue homeostasis, but the mechanisms required for phagocytosis of diverse substrates remain incompletely understood. For that reason recent studies use broad screening methods to reveal the complex structure of phagocytosis. One study using a CRISPR screen identified the previously poorly characterized gene NHLRC2 as a central inhibitory player in phagocytosis. The inhibitory effect on phagocytosis was further validated via sgRNA targeting and clonal knockout in RAW 264.7 and U937 cells and moreover in primary human macrophages. The study further exposed that NHLRC2 is enabling RhoA-Rac1 driven cytoskeletal rearrangement during initiation of phagocytosis and filopodia formation [216]. Another study characterized the transcriptional program of macrophages during phagocytosis via RNA sequencing. This revealed the specific modulation of solute carriers (SLCs) during efferocytosis. The different steps of phagocytosis, activate distinct and overlapping sets of SLCs and other molecules to promote glycolysis. Further, lactate, a natural by-product of aerobic glycolysis, was released via another SLC (SLC16A1) that was upregulated after corpse uptake. While glycolysis within phagocytes contributed to actin polymerization and the continued uptake of corpses, the lactate released via SLC16A1 influenced the establishment of an anti-inflammatory tissue environment. The study identified a previously unknown reliance on aerobic glycolysis during apoptotic cell uptake and showed that glycolytic byproducts of efferocytosis can influence surrounding cells [217].

Efferocytosis is not a simple “garbage disposal” process. Instead, it actively shapes the immunity, influencing tissue restorative programs. Macrophages, as main phagocytes involved in this process, have the ability to engage specific molecular pathways that control both phagocytosis and immune signaling, such as such as TLRs, interferons and the RIG-I-MAVS pathway [213]. This linkage supports the idea that the process of dead cell clearance is not simply an end unto itself. Quite the contrary, it suggests that the efferocytosis process provides key physiologic status information regarding cell death and tissue health to the immune system via macrophages (and other phagocytes).

1.7 Efferocytosis signaling

Efficient elimination of unnecessary and apoptotic cells is the purpose of homeostatic maintenance to promote tissue growth and enable the regulation of immune responses [218]. However, dying cells must be properly recognized and rapidly eliminated before the loss of membrane integrity leads to the leakage of potentially cytotoxic or antigenic contents.

1.7.1 “Eat-me” signals

The process of apoptotic cell corpse removal by professional phagocytes is complex and consists of two central elements: (1) recognition and (2) engulfment of the target. For the recognition by the phagocyte, the apoptotic cell displays different so-called “eat-me” signals on its cell surface. The most common and best characterized surface change on apoptotic cells is the loss of phospholipid asymmetry in the plasma membrane and the translocation of phosphatidylserine (PtdSer) from the inner to the outer leaflet of the lipid bilayer. The exposure of PtdSer occurs very early during the apoptotic process and is almost universally required for engulfment. Once at the apoptotic cell surface, PtdSer is recognized by different phagocyte receptors, of which the most prominent representative is the PtdSer receptor [219]. PtdSer binds to the PtdSer receptor indirectly via the bridging molecule Annexin I (AnxI), an intracellular protein, which translocates during apoptosis from the cytosol to the PtdSer-rich plaques in the outer leaflet of the plasma membrane [220]. Masking PtdSer on apoptotic cells, or preventing the PtdSer-exposure blocks *in vitro* and *in vivo* efferocytosis in peritoneal macrophages [221]. Whereas, when PtdSer is irreversibly exposed on the surface of healthy cells, they are engulfed alive by macrophages, indicating that PtdSer-exposure is necessary and sufficient for engulfment. Indirect “eat-me” signals can also appear through the specific interaction of serum proteins with the surface of apoptotic cells. These extracellular bridging molecules, make apoptotic cells more susceptible to phagocytosis by providing recognition sites for a greater number of phagocyte receptors, which include the vitronectin receptor ($\alpha_v\beta_3$ -integrin), the receptor-tyrosin kinase Mer, and the β_2 -glycoprotein-I (β_2 -GPI) receptor [222]. Moreover, bridging molecules such as milk-fat-globule-EGF-factor 8 (MFG-E8), growth-arrest-specific 6 (Gas6), or β_2 -glycoprotein-I (β_2 -GPI) [223] are also involved in efferocytosis. Another PtdSer binding bridging protein has recently been described with protein S (ProtS), which is known to bind to receptors of the Mer receptor-tyrosin kinase family [224]. Other extracellular bridging molecules known to facilitate engulfment have also been linked to the recognition of altered sugars. These include certain members of the collectin family, such as surfactant proteins-A and -D (SP-A and SP-D) and mannose-binding lectin (MBL), as well as the collectin-related first component of the classical

complement cascade, C1q. SP-A, SP-D, MBL and C1q bound to the surface of apoptotic cells are then recognized through the interaction of their collagenous tails with another soluble molecule, calreticulin (CRT). Lastly, thrombospondin-1 (TSP-1) is an extracellular matrix glycoprotein described to bind to apoptotic cells through an interaction with CD36 on the surface of apoptotic cells. TSP-1 is recognized by a cooperation between the integrin receptor $\alpha_v \beta_3$ and CD36 on phagocytes.

1.7.2 “Don't eat-me” signals

Living cells can also actively prevent their own engulfment by presenting “don't eat-me” signals to phagocytes. For example, CD31 on viable neutrophils mediates the disassociation from the phagocyte surface and thereby prevents their ingestion [225]. Defective CD31 signaling in apoptotic cells cancelled this effect and allowed engulfment [213, 226]. Moreover, CD31 interaction can discriminate between apoptotic and viable cells by selectively imparting ‘detachment’ signals to viable cells [225]. This mechanism prevents ingestion of viable self-cells by macrophages [218].

Probably the best-studied example of a self “don't eat-me” signal is the inhibitory molecule CD47. CD47 binds Signal Regulatory Protein or SIRP α (also called CD172a or SHPS-1) expressed on the phagocyte surface. When engaged by CD47, SIRP α recruits and activates SH2-containing protein tyrosine phosphatase (SHP)-1 or SHP-2 on its phosphorylated immunoreceptor tyrosine-based inhibitory motif (ITIM). The activated SHP-1 or SHP-2 subsequently blocks tyrosine-kinase mediated signal transduction, and especially signal transduction linked to phagocytosis. CD47 stimulation of SIRP α blocks, for example, IgG or complement-induced phagocytosis [227]. CD47 on red blood cells functions as a “don't eat-me” marker by representing a negative engulfment signal to splenic red pulp macrophages through the SIRP α receptor. In keeping with this “don't eat-me” effect, erythrocytes from CD47-deficient mice are rapidly eliminated from the blood stream of wild-type recipients *in vivo* and phagocytized by wild-type macrophages *in vitro* [228]. Similar to CD31, CD47 expression is reduced on many cell types during apoptosis. It is not known whether this down-regulation or redistribution is sufficient or whether additional, functional alterations also occur [229]. In any case, apoptotic cells (or *Cd47*^{-/-} viable cells) are no longer able to stimulate SIRP α and the downstream SHP-1. Viable cells or soluble CD47 constructs on the other hand are highly effectively stimulating SIRP α . Although CD47 appears to be a critical regulator, it is highly unlikely to be the only inhibitory signal preventing uptake of viable cells, which may have to be blocked to permit uptake of apoptotic cells [230]. Three examples are described below.

Manipulation of the CD47-SIRP α axis has practical consequences in experimental medicine. This includes: (1) human SIRP α is used in transgenic mice as a way to suppress mouse phagocyte-mediated engulfment of human hematopoietic cells engrafted with the intention of “humanizing” mice. Along with multiple human cytokines, SIRP α is one transgenic component of MISTRG mice developed by Flavell to facilitate human blood cell engraftment into immunodeficient mice [231]. (2) CD47 forms a keystone of xenotransplantation efforts. In this context, transplantation of for example an engineered pig heart into a human being, comes with the cost that the swine CD47 cannot suppress the human “eat-me” signals [232]. As such, along with the many other complications of xenotransplantation, host recognition and phagocytosis of engraft xeno-organs is a key element of new approaches to suppress graft rejection. Thus, pigs are being engineered to replace their own CD47 with human (or primate in the case of experimental transplantation) CD47 to suppress phagocytosis through the cognate SIRP α [233]. (3) CD47 potentially forms a barrier to tumor cell engulfment. In this setting, antibodies that block the CD47-SIRP α axis have been tested as a way to enhance recognition and clearance of “modified self” tumor cells [234]. From these and related experiments, several important facts about the biology of the CD47-SIRP α axis have come to light. First, CD47 is only one of possibly many anti-engulfment pathways, which are now known to include CD22, CD24 and Siglec-10 [235]. Second, genetic elimination of the CD47-SIRP α axis causes relatively minor phenotypes, suggesting other pathways are needed to suppress self-engulfment [236]. We need to keep in mind that organ and cell transplantation is an invention of the last century and entirely non-natural; no human physiological pathway evolved for organ swapping. Thus, the precise functions of pathways such as the CD47-SIRP α axis evolved to control phagocytosis. Strikingly, this thesis demonstrates that the expression of CD47 changes on senescent cells. Accordingly, the structure and interaction of and with CD47 will be important for the work described herein.

1.7.3 “Come-get-me” signals

Both “eat-me” and “don't eat-me” signals are crucial for the ability of phagocytes to recognize apoptotic cells. However, these signals can only apply when the phagocyte and apoptotic cell are proximal [237]. Therefore, attraction signals must exist to induce the migration of phagocytes to sites of apoptosis to facilitate the rapid removal of dying cells. Apart from the active display of “eat-me” signals, apoptotic cells lose the ability to present “don't eat-me” signals to the phagocyte. During apoptosis, the signaling of CD31 and CD47 is disabled such that the target apoptotic cell does not actively reject the phagocyte anymore. The lack of this repulsion signal together with the

interaction of the “eat-me” signals and their respective receptors causes the attachment of the apoptotic cell to the phagocyte, triggering the process of engulfment [225]. Moreover, apoptotic cells, but not non-apoptotic cells, secrete a chemotactic factor into the environment. Caspase-3-mediated activation of Ca^{2+} -independent phospholipase A2 (iPLA2) in apoptotic cells was linked to the release of the chemoattractant lysophosphatidylcholine (LPC) [237]. Supernatants of apoptotic cells or purified LPC could attract macrophages upon intraperitoneal or subcutaneous injection *in vivo*. One probable explanation is that most LPC exists in a form unavailable for receptor activation. In plasma, LPC mainly resides in complexes with hydrophobic serum proteins, such as albumin or lipoprotein complexes, which neutralize or inhibit LPC-mediated responses. Therefore, the phagocytes might be responding to a particular metabolite of LPC [238]. It is also possible that LPC is released by apoptotic cells in conjunction with an additional factor, which prevents the binding of inhibitory components. Other recruitment signals also exist. Apoptotic cells secrete increased levels of thrombospondin, which can recruit macrophages in a transwell chemotaxis assay [239]. A plethora of molecules that are involved in the recognition of unwanted and wanted cells has been identified. Since complete inhibition of uptake has never been demonstrated, even when multiple receptors are inhibited, phagocytic receptors seem to exist in extensive redundancy. However, mechanisms probably vary according to the phagocytic cell type and activation state, as well as the apoptotic cell type, apoptotic stage, apoptotic cue and/or the local environment of the apoptotic cell [218].

1.8 Aging and neurodegenerative disease

Cellular senescence is associated with the most common neurodegenerative diseases. Neurons in these neurodegenerative diseases express cellular senescence markers, including senescent microglia, senescent astrocytes, senescent neurons and several SASP factors [240]. Moreover, aging is known as the primary risk factor associated with most neurodegenerative diseases. As described before, cellular aging is defined as the slow decline in stress resistance and accumulation of damage over time. While different cells and tissues can age at different rates, the nine hallmarks of aging have emerged to better define the cellular aging process. Strikingly, many of these hallmarks of aging are also hallmarks of the etiology of several neurodegenerative disorders (NDs) like telomere shortening, persistently activated DNA damage response as well as increased production of SA- β -gal and increased p16^{INK4A} [241].

1.8.1 Clinical features of neurodegenerative diseases

Common neurodegenerative diseases such as Alzheimer's disease, Parkinson's disease, amyotrophic lateral sclerosis, and Huntington's disease (HD) are debilitating disorders with increasing prevalence in modern ageing societies. They are all characterized by progressive loss of selective populations of neurons. This results in an altered physiology of the brain and also of the innervated peripheral organs. As different neurodegenerative diseases target unique brain regions and have distinct disease pathologies and clinical symptoms they are generally regarded as separate clinical entities. Moreover, they are all associated with a broad spectrum of diverse clinical presentations. These include, amongst others, highly debilitating illnesses, cognitive decline, dementia and alterations in high order brain functions [242]. However, despite their wide range of different clinical manifestations, each disease shows commonalities, including their chronic and progressive nature, increase of prevalence with age, destruction of neurons in specific areas of the brain, and selective brain mass loss. Moreover, they share another common event: intracellular and extracellular protein aggregation. Presence of α -synuclein in Lewy bodies throughout the cortex is a primary feature of Dementia with Lewy Bodies, however, α -synuclein has also been demonstrated in the dopaminergic neurons in a subset of Parkinson's disease patients and in the amygdala in about 60% of diagnosed Alzheimer's disease patients [243-245]. Transactive response DNA binding protein 43 (TDP-43) inclusions are hallmarks of certain Frontotemporal Dementias and Amyotrophic Lateral Sclerosis [246], but have also now been demonstrated in several other types of mixed-dementia [247].

The disease-associated proteins involved in distinct NDs differ in terms of sequence, size, structure, expression level and function. However, the cellular and molecular mechanisms of protein misfolding, its intermediates, end-products and main features are remarkably similar. For most NDs, the associated protein(s) is often considered to be misfolded, evading both the protein folding proteostasis machinery and cellular degradation mechanisms, beginning to form aggregates that nucleate out into large fibrillar aggregates [248]. Evidence to date indicates that, although they differ in amino acid sequence, the various proteins involved in neurodegenerative diseases share common structures in their aggregate forms [249, 250].

1.8.2 Aggregation and pathogenesis of Huntington's disease

Huntington's disease is an autosomal dominant neurodegenerative genetic disorder. More precisely, HD is a hyperkinetic motor disorder with many linked physical impairments. As HD progresses, motor dysfunction increases [251]. It is defined in three stages, whereas the severity of

the symptoms increases with the progression of the disease. In early stage, individuals are largely functional, with subtle loss of coordination. In middle stage individuals have increasing difficulty with voluntary motor tasks in addition to light cognitive impairment. In late stage, individuals require assistance in all activities of daily living due to severe impairment of motility and furthermore show uncontrolled movement, mental instability and loss of cognitive function [252-254].

HD patients show many clinical symptoms, like cognitive impairment progresses, manifesting as the inability to control executive functions such as planning, inhibiting inappropriate behavior and abstract thinking. Further aspects are the loss of self and spatial awareness, depression, dementia, mood swings and anxiety. Mechanistically, HD is caused by mutations in the HTT gene, which encodes for huntingtin [252]. The N-terminal encoding region of HTT contains a trinucleotide repeat of cytosine-adenine-guanine (CAG), which encodes glutamine. The length of this trinucleotide repeat varies from individual to individual. In general, it is between 16 and 20 repeats but in mutant forms of huntingtin (mHTT), the length of CAG expands beyond 35 repeats. The excess polyglutamine residues at the N-terminus of the translated huntingtin protein leads to impaired protein folding resulting in cytosolic self-aggregation, and nuclear inclusion bodies. These inclusion bodies can lead to excitotoxicity, oxidative stress, impaired energy metabolism and apoptosis in neurons [255].

While several biological processes decline with age, they seem to decline more rapidly in patients with HD, suggesting a synergistic interplay. Animal models of HD and HD patients show markers of accelerated aging, further implicating the role of aging in HD pathogenesis. While mutant HTT is present ubiquitously throughout life, HD onset typically occurs in mid-life, suggesting that aging may play an active role in pathogenesis. There is a wide overlap between the hallmarks of aging and cellular alteration in HD, creating the hypothesis that delaying biological aging could delay onset or progression of HD symptoms. In healthy neurons, biological aging occurs over time, which eventually decreases stress resistance in cells. This decrease in stress resistance leads to an increase in unrepaired DNA damage, resulting in telomere attrition, finally leading to cellular senescence. In HD affected neurons, mutant HTT accelerates aging by intensifying particular hallmarks of aging. This may lead to the hyper-susceptibility of HD affected neurons to stress, thereby a further increase in DNA damage, and, as a result, accelerated telomere attrition. This increase in DNA damage could also lead to an increase in somatic instability, further increasing toxicity of mutant HTT. While it is important to point out the toxicity of mutant HTT on its own, in both aging and HD, many of these

'hallmarks' of cellular pathogenesis converge on common pathways and can synergistically cause cellular toxicity. Anti-aging therapies could be beneficial for multiple components of HD.

Increasing evidence suggests that ND pathogenesis is not restricted to the neuronal compartment but also involves immunological mechanisms. Microglia are the resident macrophage cells of the central nervous system (CNS) and act as the first and main form of CNS immune defense. Misfolded and aggregated proteins seem to bind to pattern recognition receptors on microglia and trigger an innate-type immune response involving the release of inflammatory mediators, which then drive disease progression and severity [256, 257]. Immune cell activation could potentially be one of the mechanisms by which protein aggregation contributes to neurodegeneration. Conversely, microglia have also been associated with a protective function in neurodegeneration. They cluster around protein plaques and can remove protein aggregates [258]. While there is increasing evidence that the immune system plays a pivotal role in the context of neurodegeneration, exactly how the immune response is modulated remains unclear. Understanding the interplay between immune cells and protein aggregates is therefore central to understanding the temporal process of neurodegeneration and may ultimately hold the key to prevent or delay the onset of neurodegenerative diseases. This major question will be tackled, in part, by the work in this thesis.

2 Objectives

Answering the question of why we age is a component of answering fundamental questions about life itself. There are innumerable theories existing about why and how we age, but, until recently, the definition of aging – senescence of cells and tissues – was uncertain [259]. Whether aging is an adaptive, regulated process, or merely a consequence arising from a stochastic accumulation of harmful events, is a universal question common to all societies. As the western/developed world moves towards an increasingly aged society, we will need novel scientific approaches as part of the challenge of mitigating aging [260]. Within this conceptual frame, little is known about how the immune system interacts with aged and diseased cells. Obviously, the immune system ages with the rest of the body. However, mechanisms must be in place to eliminate damaged and diseased cells. Our contention is that autonomous death of old and damaged cells (i.e. intrinsic apoptosis followed by corpse removal) is one of many ways the immune system interacts with, and eliminates unwanted cells. Therefore, the overall objective of this thesis was to decipher how macrophages, as the main phagocytes in the body [261], interact with age-related diseased cells.

Aim 1: Deciphering the interaction of macrophages and senescent cells

In general, the transient induction of senescence followed by senescent cell elimination promotes tissue remodeling and regeneration [86, 262]. However, long-term accumulation of senescent cells, drives persistent inflammation which ultimately impairs tissue function and can contribute to organ failure [263]. The fine balance between the accrual of senescent cells and their clearance within tissues remains unknown; senescent cells may outnumber the immune system rendering it unable to clear them, or attracted immune cells could become dysfunctional. Therefore, we wanted to decipher the specific mechanisms by which macrophages interact with senescent cells. By developing novel co-culture approaches, we sought to elucidate the interplay between macrophages and senescent cells. We hypothesized that macrophages are involved in the clearance of senescent cells. Therefore, the proposed interactions should be analyzed in a live-cell imaging approach, using fluorescent reporter cell lines which allows traceability of both cell types. Further, we hypothesized senescent cells are able to modulate macrophage functionality. We wanted to reveal whether, and how in particular, senescent cells could influence macrophages and decided to examine macrophage functionality during the process efferocytosis. The mechanisms determining the interactions between senescent cells and macrophages also in the context of efferocytosis should be further analyzed on a molecular level. We wanted to confine the important signaling

molecules both on the senescent cells and enclose their corresponding interaction partners on the macrophages. Moreover, we aimed to find a way to clear senescent cells by phagocytes. Establishing and in-depth understanding of the senescent cell-macrophage interplay may help to provide the basis for the development of novel therapeutic targets in various senescence-associated diseases.

Aim 2: Examination of the potential role of macrophages in age-related neurodegenerative diseases

Several approaches have shown the importance of macrophages for the removal of aggregates associated with age-related neurodegenerative diseases, such as in the removal of peptides associated with Alzheimer's disease [264], and alpha-synuclein [265]. This supports the importance to study macrophages in the context of aggregate removal. To date, no comparable study has been implemented to reveal the potential importance of macrophages for Huntington's disease (HD). Therefore, the second aim of the study was the development of a cellular model to examine the mechanisms involved in HD to gain an improved understanding of HD pathology in general. We aimed to establish an *in vitro* system between fibroblasts and macrophages using live-cell imaging, which enables precise tractability of the aggregate fate and the potential removal over time. We hypothesized macrophages are able to trigger aggregate removal in fibroblasts. We wanted to investigate the exact underlying mechanisms of the hypothesized aggregate removal, including the contribution of direct cell contact, bystander effects and involvement of cell death induction. We wanted to implement this by means of quantitative live-cell imaging and qualitative high-resolution microscopy. The study of Htt aggregates in fibroblasts can provide new insights in HD pathology. This eventually may help to convey findings from a cellular model to what occurs in the brain, providing the basis for the development of novel therapeutic strategies.

3 Materials

3.1 Frequently used reagents and plastics

Table 3-1: Generally utilized reagents.

Reagent	Source	Identifier
0.25 % Trypsin	Thermo Fisher	25200056
AmpliTaq Gold™ DNA Polymerase	Thermo Fisher	4311816
B-27™ Supplement (50x)	Thermo Fisher	17504-044
Bovine serum albumine (BSA)	Sigma	A2153
Cell dissociation media	Sigma	S-014-B
Chloroform	Fisher Chemical	C/4960/17
CSF-1 (Human)	Produced in insect cells by the MPI-Biochemistry protein production core	
CyQUANT™ LDH Cytotoxicity Assay Kit	Thermo Fisher	C20300
DMEM	Thermo Fisher	41966-029
DMSO	Sigma	D8418
DNAase	Sigma	DN25-10MG
Doxycycline	Sigma	D9891
EDTA	Carl Roth	6764.1
Ethanol	Sigma	32221
Fc block	Thermo Fisher	31880
Fetal bovine serum (FBS)	Biochrome	S0115
FLT3L	Peprtech	250-31L
GAPDH	Applied Biosystems	4352932E
GelRed	Biotium	41008
Glutaraldehyde	Sigma	340855-1L
GM-CSF	Peprtech	315-03
HBSS	Thermo Fisher	24020-091
HEPES	Biomol	05288.100
HEPES buffer	Biochrome	L1613
hygromycin	Thermo Fisher	10687010
IFN γ	Peprtech	315-05
IL-13	Peprtech	210-13
IL-4	Produced in insect cells by the MPI-Biochemistry protein production core	
IL-5	Peprtech	215-15
Isopropanol	Honeywell	33539-2.5L
KHCO ₃	Carl Roth	P748.1
L-Glutamine	Thermo Fisher	25030081
Lipofectamine3000	Thermo Fisher	L3000015
MgCl ₂	Carl Roth	KK36.2

Reagent	Source	Identifier
MgSO ₄	Sigma	M-2643
NaCl	Carl Roth	3957.1
Neurobasal medium	Thermo Fisher	21103-049
Nonessential amino acids	Thermo Fisher	11140050
Oligo(dT) primers	Invitrogen	N8080128
Opti-MEM transfection media	Thermo Fisher	31985062
P3000™ Transfection enhancer	Thermo Fisher	L3000015
Palbociclib	Selleckchem	S1116
Penicillin/Streptomycin	Lonza	17-745E
Percoll	Sigma	GE17-5445-02
PFA	Alfa Aesar	43368
phosphate-buffered saline (PBS)	Thermo Fisher	10010056
Poly-L-Lysine	R&D systems	3438-100-01
Proteinase K	Thermo Fisher	4333793
Quick-Load® DNA Ladder	NEB	N0551S/L
RPMI	Thermo Fisher	61870-010
SCF	Peptotech	250-03
Seahorse XF DMEM medium	Agilent	103575-100
Seahorse XFp Cell Mito Stress Test Kit	Agilent	103010-100
Senescence β-Galactosidase Staining Kit	Cell Signaling Technology	9860S
sodium pyruvate	Thermo Fisher	11360070
SuperScript IV reverse transcriptase	Invitrogen	18090050
SYBR™ Green Master Mix	Thermo Fisher	A25742
TaqMan™ Fast Advanced Master Mix	Thermo Fisher	4444557
Triton X-100	Sigma	X100-100ML
TRIzol	Invitrogen	15596018
Ultra-pure water	Thermo Fisher	10977-035
α-MEM medium	Thermo Fisher	32561-037
β-mercaptoethanol	Thermo Fisher	31350-010

Table 3-2: Generally used plastics

Plastic	Source	Identifier
10 cm dishes	Falcon	353003
12-well	Corning	3513
12-well Transwell® polycarbonate membrane cell culture inserts	Corning	CLS3401-48EA
48-well plates	Falcon	353078

Materials

Plastic	Source	Identifier
50 mL conical polypropylene tube	Greiner Bio-One	227261
6 cm dish	TPP	93060TPP
6-well plates	Greiner Bio-One	657160
8-chamber slides	ibidi	80826
96-well	Corning	3596
96 well HTS Transwell® permeable supports	Corning	CLS3381-1EA
microcentrifuge tube	eppendorf	0030120086
microreaction tube	Biozym	710970
syringe plunger	Henke Sass Wolf	5050-000V0
T175 flasks	Greiner Bio-One	660175
T75 flask	Greiner Bio-One	658175

3.2 Commercially available antibodies

Table 3-3: Commercially available primary antibodies.

Primary antibody	Isotype	Final concentration/dilution	Company	Identifier
Alexa Fluor® 594 anti-mouse CD24 Antibody	Rat IgG2b, κ	5 µg/mL	Biologend	101834
Alexa Fluor® 647 anti-mouse CD22 Antibody	Rat IgG1, κ	10 µg/mL	Biologend	126107
SHP-1 Polyclonal Antibody	Rabbit / IgG	1:200	Thermo Fisher	PA5-27803
CD47 Polyclonal Antibody	Rabbit / IgG	1:100	Thermo Fisher	PA5-116827

Table 3-4: Commercially available secondary antibodies.

Secondary antibody	Isotype	Final concentration/dilution	Company	Identifier
Rabbit IgG (H+L) Cross-Adsorbed Secondary Antibody	Goat / IgG	1:1000	Thermo Fisher	A-11008

Table 3-5: Commercially available FACS antibodies.

FACS antibody	Isotype	Company	Identifier
anti-mouse CD47 Antibody	Rat IgG2a, κ	Biologend	127507

FACS antibody	Isotype	Company	Identifier
anti-mouse F4/80 Antibody	Rat IgG2a, κ	Biolegend	123115
PE anti-mouse CD170 (Siglec-F) Antibody	Rat IgG2a, κ	Biolegend	155505

3.3 Utilized plasmids

Table 3-6: Commercially available and generated plasmids.

Vector	Insert	Backbone	Resistance	Source	Identifier
GFP control				[266]	
Htt27Q exon 1-GFP				[267]	
Htt97Q exon 1-GFP				[267]	
HttQ25-mCherry (Lentivirus)	mCherry	pFhSynW2	Amp	Klein Lab; MPI Neurobiology	
HttQ97-mCherry (Lentivirus)	mCherry	pFhSynW2	Amp	Klein Lab; MPI Neurobiology	
mcherry (Lentivirus)	mCherry	pFhSynW2	Amp	Klein Lab; MPI Neurobiology	
pCDNA_FRT_mCherry	mCherry	pcDNA™5/FRT	Amp	Griesbeck Lab; MPI Neurobiology	
pCDNA_FRT_mTagBFP 2	mTagBFP2	pcDNA™5/FRT	Amp	Griesbeck Lab; MPI Neurobiology	
pcDNA5/FRT				Thermo Fisher	K601002
pcDNA5-FRT/TO-GFP ABIN1				MRC PPU	DU32934
pCMV-hyPBbase				[268]	
pEF5-FRT-TagRFP-T-IFT88				Addgene	61684
pEF5-FRT-TagRFP-T-IFT88-mCherry	mCherry	pEF5-FRT-TagRFP-T-IFT88		unpublished	
pEF5-FRT-TagRFP-T-IFT88-mTagBFP2	mTagBFP2	pEF5-FRT-TagRFP-T-IFT88		unpublished	
pOG44				Thermo Fisher	K601002
pPB-CAG-rtTA-IRES-Hygro				Addgene	102423
pSpCas9(BB)-2A-GFP (PX458)				Addgene	48138
pTreTight-Htt94Q-CFP				Addgene	23966
TIA1 A381T-GFP				[269]	
WT TIA1-GFP				[269]	

Materials

3.3.1 Maps of newly generated plasmids

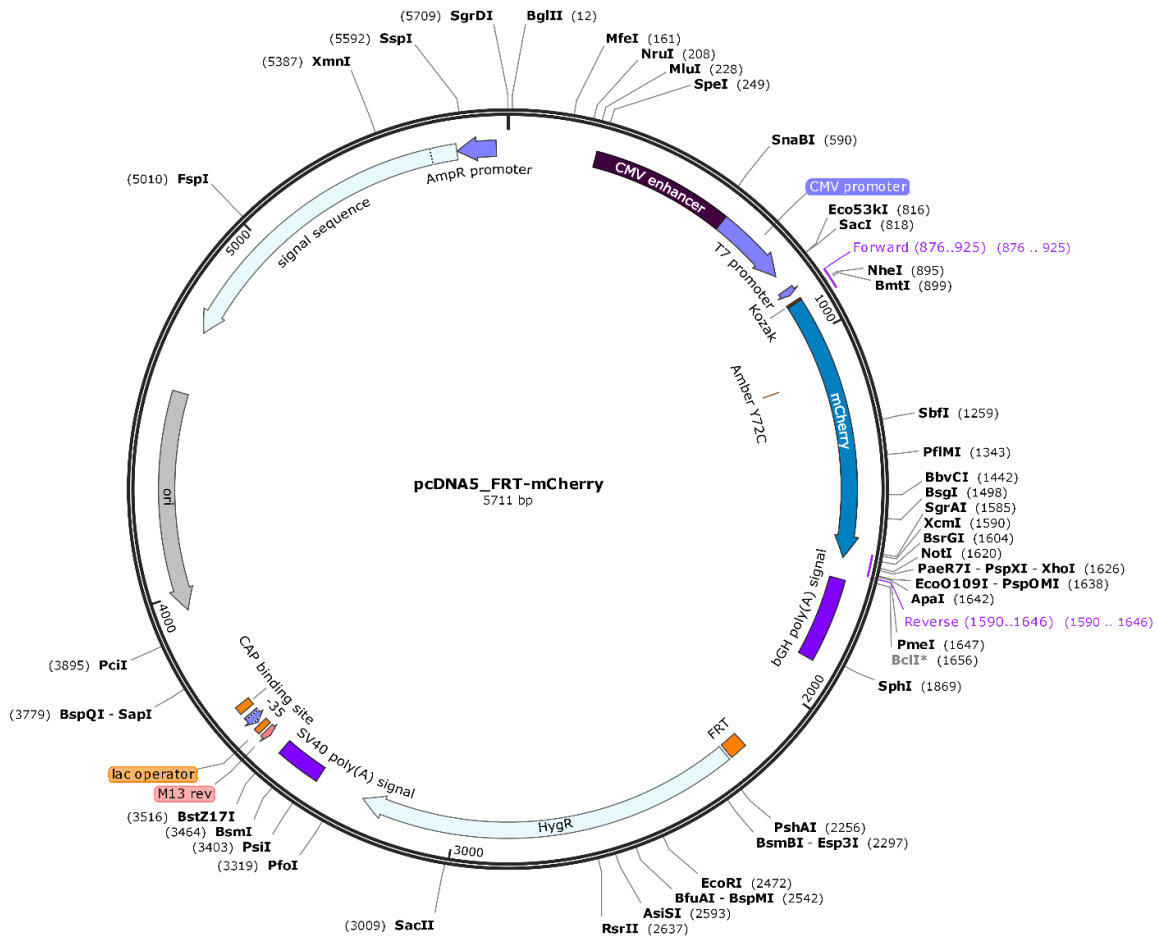


Figure 3-1: Plasmid map of pcDNA5_FRT-mCherry

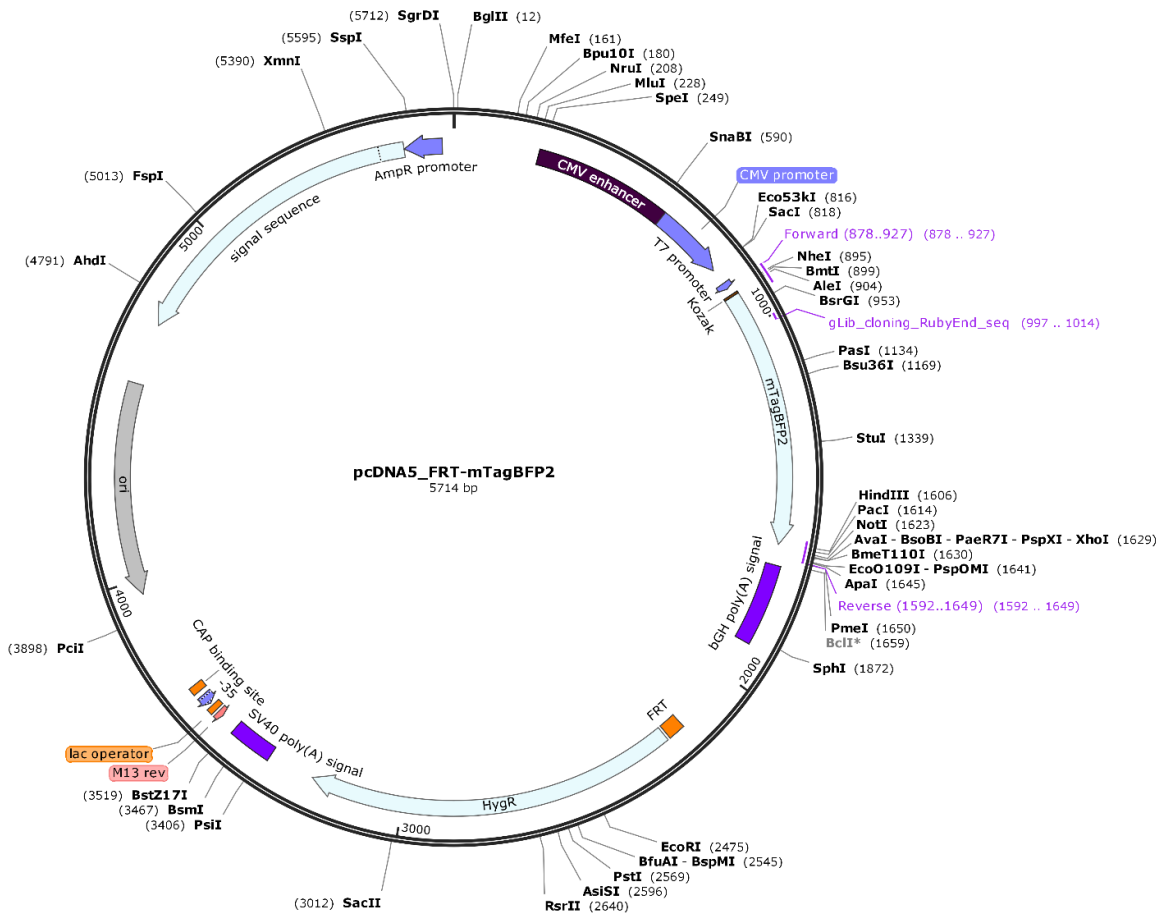


Figure 3-2: Plasmid map of pcDNA5_FRT-mTagBFP2

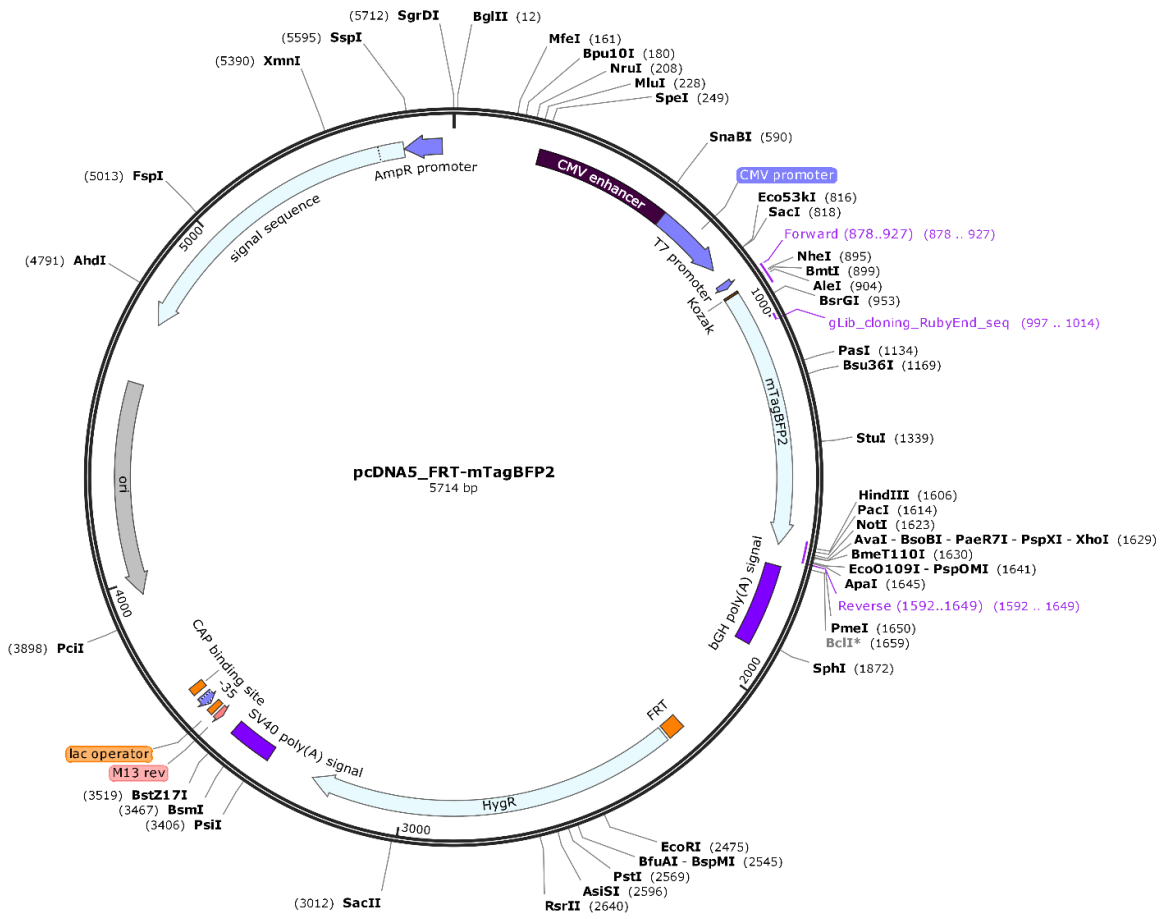


Figure 3-3: Plasmid map of pEF5-FRT-TagRFP-T-IFT88-mCherry

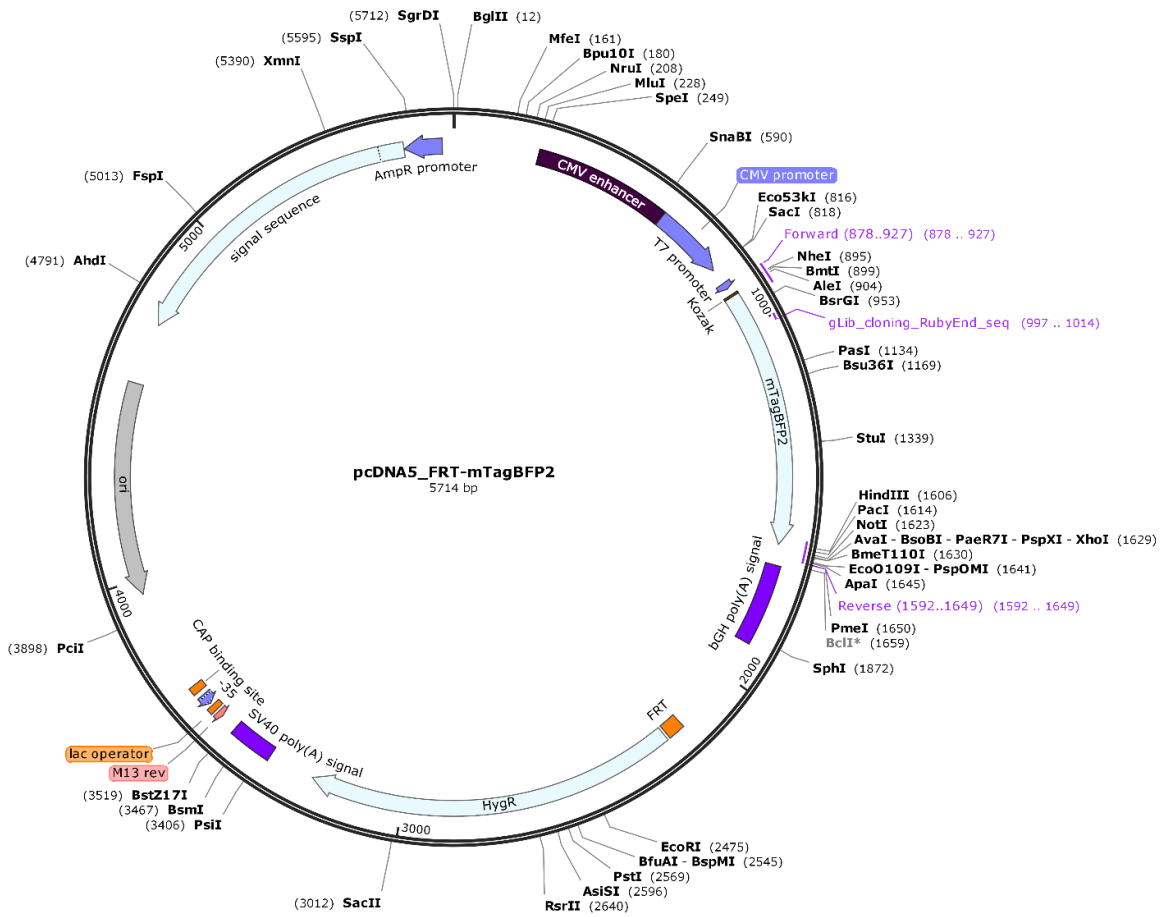


Figure 3-4: Plasmid map of pEF5-FRT-TagRFP-T-IFT88-mTagBFP2

3.4 Restriction enzymes

Table 3-7: Restriction enzymes.

Enzyme	Company	Identifier
NruI-HF	NEB	R3192S
NotI-HF	NEB	R3189S
Scal-HF	NEB	R3122S
BbsI-HF	NEB	R3539S

3.5 DNA and qRT-PCR primer

Table 3-8: DNA primer.

Target	Forward Primer	Reverse Primer
U6 primer	ACTATCATATGCTTACCGTAA	
CD47 CRISPR guide 1	CACCGCCACATTACGGACGATGCAA	AAACTTGCATCGTCCGTAATGTGGC
CD47 CRISPR guide 2	CACCGCACTTCATGCAATGAAACTG	AAACCAGTTTCATTGCATGAAGTGC

Materials

CD47 CRISPR guide 3	CACCGTCAGTCTCAGACTTAATCAA	AAACTTGATTAAGTCTGAGACTGAC
actinGFP 1	AAGTTCATCTGCACCACCG	TCCTTGAAGAAGATGGTGCG
actinGFP 2	GTAGGTGGAAATTCTAGCATCATCC	CTAGGCCACAGAATTGAAAGATCT
tdTomato	CTGTTCTGTACGGCATGG	GGCATTAAAGCAGCGTATCC
JAX universal control	AAGGGAGCTGCAGTGGAGTA	CCGAAAATCTGTGGGAAGTC

Table 3-9: qRT-PCR primer.

Target	Forward Primer	Reverse Primer
CDKN2A (p16 ^{INK4a})	GATTCAGGTGATGATGATGGGC	TGCACCGTAGTTGAGCAGAAG

3.6 Technical equipment

Table 3-10: Technical gear.

Instrument	Company
BD FACSAria™ III	Becton Dickinson
BD LSRFortessa™ Flow Cytometer	Becton Dickinson
Benchtop X-ray Irradiator	CellRad
C1000 Touch Thermal Cycler	BioRad
CFX96 Touch Deep Well Real-Time PCR System	BioRad
ChemiDoc	BioRad
Incucyte® S3 Live-Cell Analysis System	Sartorius
LSM780 Confocal Laser Scanning Microscope	Zeiss
Nano photometer NP80	Implen
Stratalinker	Stratagene
Tecan Spark	Tecan
XF HS Mini Analyzer	Agilent
ZEISS LSM980 WITH AIRYSCAN 2	Zeiss

3.7 Software

Table 3-11: Software.

Software	Company
Adobe Illustrator	Adobe
Arivis Vision 4D	Arivis
FlowJo	Beckton Dickinson
Graphpad Prism Version 7	GraphPad Software Inc.
GraphPad Software Inc.	BioRad
ImageJ	Wayne Rasband (NIH)
IncuCyte 2019B Rev2	Sartorius
Seahorse Analytics	Agilent
Snapgene	GSL Biotech LLC

3.8 Buffers

Table 3-12: RBC lysis buffer.

10x RBC lysis buffer
41.45 g NaCl
1 mL 0.5 M EDTA
5.45 g KHCO ₃
H ₂ O to final volume 500 mL

Table 3-13: Tail lysis buffer.

Tail lysis buffer
100 mM Tris
5 mM EDTA
5 % SDS
200 mM NaCl
in H ₂ O

4 Methods

4.1 Mice strains

All animal experimentation described in this thesis was performed at the Max Planck Institute of Biochemistry animal facility in accordance with approval from the “Regierung von Oberbayern” that covers the housing and breeding of mice without a phenotype (Animal Welfare Officer, Dr. Eva Hesse) that is additionally approved by the European Union. Euthanasia was performed by cervical dislocation following training by Dr. Corinna Mörth. All animals were documented using the Max Planck Society PyRat system, which is used for reporting animal usage yearly to government entities. Animal breeding was performed behind a barrier system that permits restricted access to approved users and incorporates a specific pathogen free hygiene system. In the case of the Murray group colony, these animals are maintained Helicobacter-free. Mice used herein were: (1) C57BL/6 “wild-type” mice sourced from the common breeding colony maintained by the animal facility. (2) “actinGFP” mice. These mice were a gift from Dr. Krishnamoorthy (MPI-Biochemistry) and constitutively express GFP under the control of the chicken beta-actin promoter. They were originally obtained from the Jackson Laboratories (Bar Harbor, ME) and (3) C57BL/6-Tg(CAG-EGFP)^{10sb/J}. tdTomato⁺ mice were a gift of Dr. Christian Meyer (MPI-Neurobiology). These animals are commonly called Ai14 and have tdTomato inserted into the *Rosa26* locus preceded by a loxP-STOP-LoxP cassette (B6.Cg-Gt(*ROSA*)26Sor^{tm14(CAG-tdTomato)Hze/J}). Two strategies were used to generate tdTomato⁺ cells. First, the Ai14 mice were crossed to Tie2-Cre mice (B6.Cg-Tg(Tek-cre)^{1Ywa/J}), which express Cre in all hematopoietic cells, permitting the isolation of tdTomato⁺ macrophages. In the second approach, we generated uniform tdTomato⁺ cells in all tissues by taking advantage of the female germline expression of Tie2-Cre to delete the LoxP-STOP-LoxP cassette when Tie2-Cre was kept in females and crossed to wild-type males.

4.1.1 DNA extraction and Genotyping

Biopsies obtained from tails were digested at 55° C overnight in 200 µL tail digestion buffer (Table 3-12), supplemented with 2.5 µL proteinase K (1.5 U/sample). The following day, samples were centrifuged at 18,000 x g at room temperature for 10 min and the supernatant was transferred to a new tube containing 500 µL isopropanol. Precipitated DNA samples were centrifuged at 18,000 x g at room temperature for 10 min and the supernatant was removed. Pellets were washed with 200 µL 70 % Ethanol and dissolved in 250 µL nuclease free water for 1 h at 37° C and either used directly for polymerase chain reaction (PCR) or stored at -20° C. For genotyping PCR, 1 µL of

extracted DNA solution was mixed with 22.2 μL nuclease free water, 3 μL 10x Gold Puffer, 0.1 μL of each forward and reverse primer (100 μM , Table 3-8) and 0.05 μL AmpliTaqGold. DNA was amplified according to the protocol on a PCR cycler (Table 4-1). 10 μL of the PCR product were applied on a 1 % agarose gel supplemented with Gel Red (1:25,000). All samples were run for 30 min at 120 V together with the Quick-Load[®] Purple 100 bp DNA Ladder. The gel was imaged under ultraviolet light using a Chemidoc Imaging System.

Table 4-1: Genotyping PCR protocol.

Temperature [°C]	Time [min]
1. 95	10:00
2. 95	00:30
3. 59	01:00
4. 72	01:00
5. Go to step 2. 32 times	
6. 72	05:00
7. 4	hold

4.2 Cell lines

Unless indicated otherwise, certified cell lines were purchased from the American Type Culture Collection (ATCC). Flp-In[™]-3T3 were purchased from Thermo Fisher. Bax^{-/-}Bak^{-/-} double deficient (DKO) immortalized 3T3 cells were provided by Dr. Joseph Opferman (St Jude Children's Research Hospital) [270]. All cell lines were tested to be free from Mycoplasma contamination by routine PCR screening approximately monthly. WT-NIH 3T3 (WT 3T3), Bax^{-/-}Bak^{-/-} 3T3 cells and Flp-In[™]-3T3 cells were grown in DMEM plus 10 % fetal bovine serum (FBS) and 1 % penicillin/streptomycin. Jurkat cells were grown in RPMI, plus 10 % FBS, 1 % penicillin/streptomycin and 0.1 % β -mercaptoethanol. All cell lines were grown in humidified tissue culture incubators at 37° C with 5 % CO₂.

4.3 Isolation of primary cells

4.3.1 Isolation of bone marrow-derived macrophages

Wild type mice were euthanized by cervical dislocation. Femurs and tibiae were excised and the bones were cleaned from remaining flesh and fibers. The clean bones were first disinfected in 70 % EtOH for two minutes, then washed in phosphate-buffered saline (PBS) once, and afterwards cut open at both ends. The bones were flushed with PBS through a 70 μM strainer into a 50 mL conical polypropylene tube using syringe and 26G needle. Cells were centrifuged for five minutes at 400 x g, the supernatant was discarded and the cell pellet resuspended with red blood cell (RBC)

Methods

lysis buffer for approximately two minutes. The RBC buffer was neutralized with 10 mL PBS. After pelleting the cells (400 x g, 5 min), cells were washed once with PBS (400 x g, 5 min). Cells from one mouse were seeded in each three 15 cm dishes containing 15 mL medium. BMDMs were grown in DMEM composed of 10 % fetal bovine serum (FBS), 1 % penicillin/streptomycin and 0.2 µg/mL human CSF-1 as described [271]. For polarization, BMDMs were stimulated with 2 ng/mL IFN γ or 10 ng/mL IL-4 and 10 ng/mL IL-13 for 24 hours prior to assay.

4.3.2 Isolation of peritoneal macrophages

Wild type mice were euthanized by cervical dislocation. The abdomen of the mouse was soaked with 70 % EtOH and a small incision was made along the midline with sterile scissors. The abdominal skin was retracted to expose the intact peritoneal wall. With the beveled end of a 26G needle facing inward, the needle was inserted through the peritoneal wall to inject 5 mL of cold PBS into the abdominal cavity. Using the same syringe and needle, the fluid was aspirated from the peritoneum. The injected PBS was dispensed into a 50 mL conical polypropylene tube that was kept on ice. The procedure was repeated additional two times and the peritoneal fluid of one mouse was collected in the same tube. The cells were centrifuged at 400 x g for 5 minutes. The supernatant was discarded and the cell pellet was resuspended in 1 mL of DMEM. Cells were counted and directly subjected to the corresponding assay [272].

4.3.3 Isolation of multinucleated giant macrophages

Macrophage progenitor cells were isolated as in the BMDM preparation described above. Cells of one mouse were plated on 4 10 cm dishes in complete α -MEM medium composed of 10 % FBS, 1 % penicillin/streptomycin and 0.2 µg/mL CSF-1. Three days after isolation, cells were scraped in PBS and counted. A volume of 4 mL cell suspension (1×10^6 cells/mL) was plated on each 1 permanox dish in the presence of 10 µg/mL of murine GM-CSF and 30 ng/mL murine IL-4 [273]. On day 7, the permanox plates were gently washed 3 times with PBS. Afterwards 5 mL of pre-warmed dissociation media (37 °C) were added and plates were incubated in the 37 °C cell incubator for 5 minutes. Cells were detached by gentle pipetting and finally dissociated by scraping. For separation of multinucleated giant macrophages (polykaryons), cells were centrifuged in a percoll gradient at 400 x g for 20 minutes at 18 °C. A 100 % percoll working solution was obtained by mixing percoll and 1.5 M NaCl (9:1 v/v). The working solution was further diluted with PBS to the desired densities. A volume of 12 mL 42 % percoll layer was added to the bottom of a 50 mL conical polypropylene tube, and a volume of 30 mL 12 % percoll layer, containing the scraped cells was layered on top. The

percoll gradient was covered by 10 mL complete α -MEM. After centrifugation, the percoll gradient was split into volumes of each 10 mL. The different layers were centrifuged and resuspended in 100 μ L DMEM. The cell numbers of the third layer (counted from the top) of the gradient was estimated.

4.3.4 Isolation of bone marrow derived eosinophils

Bone marrow cells were isolated as described for BMDM isolation and placed in eosinophil medium containing 20 % fetal bovine serum, 55 μ M β -mercaptoethanol, 10 mM nonessential amino acids, 1 mM sodium pyruvate, 1 % penicillin/streptomycin, 2 mM L-glutamine, and 25 mM N-2-hydroxyethylpiperazine-N'-2-ethanesulfonic acid (HEPES) buffer (Biochrome). Cells were stimulated with 100 ng/mL of stem cell factor (SCF) and 100 ng/mL of Fms-like tyrosine kinase 3 ligand (FLT3L) for 4 days at a density of 1×10^6 cells per mL in a T75 flask. From day 4 on, cells were kept in medium supplemented with 10 ng/mL of recombinant murine IL-5. At days 6, 8, 10 and 12, half of the culture medium was replaced by fresh medium. At day 8 the whole culture was subjected into a new flask. From day 10, cell density was monitored to keep the concentration at 1×10^6 cells per mL. At day 14, the cultures contained >90 % bone marrow derived eosinophils (BMDEs), indicated by high side scatter profile and expression of Siglec-F [274].

4.3.5 Isolation of primary mouse embryonic fibroblasts

Primary mouse embryonic fibroblasts (MEFs) were collected from sacrificed pregnant (E14-16) actin GFP mice, as described [275]. Intact uteri were removed, washed with cold PBS, and each embryo individually prepared by removing appendages including the head and internal organs. A surgical scalpel blade was used to finely mince the remaining tissue in 100 μ L of DNAase (1 mg/mL in H₂O) and 2 mL of 0.25 % trypsin. The suspension was then applied through a 5 mL serological pipette. Suspended cells derived from each embryo were cultured in DMEM composed of 10 % FBS, 1 % penicillin/streptomycin. Cells were further cultivated and cryopreserved in freezing medium at passage 4 (P4).

4.3.6 Isolation of mixed glia cells

Prior to the cell isolation, T75 flasks were coated with 6 mL Poly-L-Lysine for five minutes, followed by washing once with PBS and drying the flask for 20 minutes. Mixed glia cells were collected from newborn pups at the age of day 1 up to day 5 post birth. Heads were removed, disinfected in 70 % EtOH, cut open beginning at the spinal cord and the skull skin and bone were folded open so the whole brain could be removed gently. A surgical scalpel blade was used to finely mince the brain

Methods

tissue. The suspension was then applied through a 10 mL serological pipette and transferred to a 50 mL conical polypropylene tube and centrifuged at 400 x g for 5 minutes. The supernatant was discarded and the cells were resuspended in 10 mL 0.05 % Trypsin per 5-15 brains. The closed tube was placed in a cellular incubator (37 °C, 5 % CO₂) for 10 minutes. Afterwards the Trypsin was inactivated by the addition of 10 mL of DMEM composed of 10 % FBS, 1% penicillin/streptomycin and 2 % L-Glutamine. The suspension was filtered through a 70 µM strainer into a 50 mL conical polypropylene tube using a syringe plunger and the filtered cell suspension of each 4 brains was transferred to 1 coated T75 flask. The medium was changed one day and 4 days after seeding, cells were harvested with 0.05 % trypsin six days after seeding.

4.3.7 Isolation of primary neurons

Primary mouse neurons were collected from sacrificed pregnant wild-type mice at day 15 post-coitum, as described [276]. Intact uteri were removed, washed with cold PBS, and each embryo was individually prepared by decapitating in ice-cold dissection medium consisting of Hanks' balanced salt solution (HBSS) supplemented with 0.01 M HEPES, pH 7.4 (Biomol), 0.01 M MgSO₄, and 1 % penicillin/streptomycin. The skull was cut open and the cerebral hemispheres were separated from the rest of the brain. After removing the meninges, cortices were dissected and digested with prewarmed 0.25 % trypsin-EDTA supplemented with 0.75 % DNase for 15 min at 37 °C. Trypsin activity was quenched by washing in Neurobasal medium containing 5 % FBS and cells were dissociated in pre-warmed culture medium by gentle pipetting. Cells were centrifuged at 130 × g for 5 minutes, the supernatant was discarded and the pellet was resuspended in culture medium consisting of Neurobasal medium with 2 % B27 (17504-044; Thermo Fisher), 1 % L-Glutamine and 1 % penicillin/streptomycin. Cells were plated in 48-well plates at a density of 5x10⁴ cells per well, and 20 % fresh culture medium were added every 3-4 days.

4.4 Genetic manipulation of cell lines

4.4.1 Transient transfection of fibroblasts with Lipofectamine

Fibroblasts were seeded on the dish and attached overnight. Afterwards, two transfection mixes were prepared in separate 1.5 mL reaction tubes. Mix 1 contained Opti-MEM transfection media, P3000™ Transfection enhancer and respective plasmid DNA. Mix 2 contained Opti-MEM transfection media and Lipofectamine3000. Detailed volumes are depicted in Table 4-2. The two mixes were combined, mixed and incubated for 12 minutes at room temperature, then added drop wise to the well without further mixing.

Table 4-2: Master mix for Lipofectamine transfection.

Tube A
5 μ L Opti-MEM
0.1 μ g DNA
0.2 μ L P3000

Tube B
5 μ L Opti-MEM
0.3 μ L Lipofectamine

4.4.2 Lentiviral transduction of primary neurons (Kerstin Voelkl)

Virus was produced in HEK293T cells by Kerstin Voelkl (MPI of Neurobiology), as previously described [277]. Virus was thawed and immediately added to freshly prepared neuronal culture medium. 25 μ L of old neuronal culture medium were removed and 50 μ L of virus containing medium were added to the culture. Virus volume was individually adjusted according to virus titer and protein expression and usually transduced at 0.5 μ L/cm². After 7 days of virus exposure, optimal expression of Htt protein aggregates could be observed.

4.5 Generation of stable cell lines

4.5.1 Cloning strategy designing the Flp-in system

Sequences encoding for mCherry and mTagBFP2 were excised from pCDNA_FRT_mcherry and pCDNA_FRT_mTagBFP2 vectors via restriction enzyme digestion using NruI-HF and NotI-HF. Fluorescence inserts were ligated into the pEF5-FRT-TagRFP-T-IFT88 vector that was digested with the same enzymes. Correct insertion was verified by a test digestion using NruI-HF and NotI-HF, including an empty vector control.

4.5.2 Generating of fluorescent reporter cell lines using the Flp-in system

Flp-in 3T3 cells were seeded in 6-well plates at a density of 3×10^5 cells per well and attached overnight. After 24 hours, cells were transfected with 3 μ g total plasmid DNA, consisting of a 9:1 ratio of pOG44: pEF5-FRT-TagRFP-T-IFT88-mcherry or pOG44: pEF5-FRT-TagRFP-T-IFT88-mTagBFP2 plasmid DNA using Lipofectamine 3000. After 48 hours the transfection medium was replaced by fresh medium containing hygromycin (0.145 mg/mL final). After 6 days of treatment, hygromycin-resistant cells were expanded.

Methods

4.5.3 Generating of a inducible aggregate expressing cell line using the piggy-bac system

Bax^{-/-} Bax^{-/-} 3T3 cells were seeded in 6-well plates at a density of 3×10^5 cells per well and attached overnight. After 24 hours, cells were transfected with 1.8 µg total plasmid DNA, consisting of 0.15 µg pPB-CAG-rtTA-IRES-Hygro, 0.15 µg hypBase, and 1.5 µg pTreTight-Htt94Q-CFP using Lipofectamine. The vector pTreTight-Htt94Q-CFP was transfected linearized using Scal-HF. After 48 hours the transfection medium was replaced by fresh medium containing hygromycin (0.145 mg/mL final). After 6 days of treatment, six hygromycin-resistant foci were picked per well and the cells expanded. Expression of Htt94Q-CFP was induced by addition of 0.5 µM doxycycline. The first aggregates were observed after 16 h of induction by live cell imaging in the IncuCyte system.

4.5.4 Generating of knock-out cell lines using the CRSPR-Cas9 system

Primers for guide RNAs (gRNA) for CD47 were designed using web based tools from the Broad Institute (Cambridge, Mass). Phosphorylated primer oligomers were annealed and the product was ligated into pSpCas9(BB)-2A-GFP (PX458) that was previously digested with BbsI. The vector was checked for correct integration of the gRNA (U6 primer) and the correct plasmids were transfected into WT NIH-3T3 cells via Lipofectamine. The GFP positive subpopulation was separated from the bulk population by flow cytometry. The sorted bulk population was diluted to grow single cell clones. These clones were checked for gene loss by flow cytometry using a CD47 antibody.

4.6 RNA isolation and analysis

Cells of one well of a 12-well plate were lysed in 1 mL TRIzol. The suspension was transferred to a 1.5 mL microcentrifuge tube and 200 µL of chloroform were added for separation of DNA and RNA. The fusion was thoroughly mixed and centrifuged at 12 000 rpm at 4 °C for 10 minutes. 400 µL of the clear upper phase were transferred to a fresh 1.5 mL centrifuge tube containing 500 µL isopropanol for precipitation. The fusion was thoroughly mixed, incubated on ice for 10 minutes and centrifuged at 18,000 g at 4 °C for 10 minutes. The supernatant was discarded and the pellet was washed with 1 mL of 70 % EtOH, centrifuged at 18,000 g at 4 °C for 10 minutes. The supernatant was discarded, the pellet dried at room temperature for 5 minutes and 25 µL of distilled water were added. Extracted RNA was frozen at -20 °C for storage. RNA concentration was measured via nano photometer. cDNA was synthesized by incubating RNA in a fresh microreaction tube, together with oligo(dT) primers, random hexamers and water (Table 4-3). The mixture was incubated at 65 °C for 10 minutes followed by 10 minutes at 4 °C. Afterwards the mixture is reverse transcribed using SuperScript IV reverse transcriptase for 2 hours at 42 °C (Table 4-4). Further analysis by qRT-PCR was

performed using specific primers (see Table 3-9). qRT-PCR was run using corresponding protocols (Table 4-7; Table 4-8) on a real-time PCR system. Results were analyzed using the corresponding CFX Maestro Software. All values were normalized to GAPDH.

Table 4-3: Composition of cDNA master mix.

Component	Volume for 1x
dT oligos	0.40 μ L
random hexamer primers	0.06 μ L
H ₂ O (Millipore)	0.54 μ L

Table 4-4: Composition of reverse transcriptase master mix.

Component	Volume for 1x
5x first strand buffer	4 μ L
DTT	2 μ L
dNTPs	0.5 μ L
reverse transcriptase	0.25 μ L
H ₂ O (Millipore)	1.25 μ L

Table 4-5: Master mix for housekeeper GAPDH.

Component	Volume in μ L for 1x
20x Primer (=pre-mixed)	0.5
cDNA template	2
2xTaqMa	5
H ₂ O	2.5
Total	10 μ L

Table 4-6: Master mix for other primers (including *CDKN2A*).

Component	Volume in μ L for 1x
Primer fw	0.2
Primer rv	0.2
cDNA template	2
Sybr Green Mix	5
H ₂ O	2.6
Total	10 μ L

Table 4-7: qRT-PCR protocol for TaqMan mix.

Temperature [°C]	Time [min]
1. 50	02:00
2. 95	02:00
3. 95	00:30
4. 60	00:30
5. Plate read	
6. Go to 2. for 40 cycles	
7. END	

Table 4-8: qRT-PCR protocol for Sybr Mix.

Temperature [°C]	Time [min]
8. 95	00:30
9. 95	00:10
10. 60	00:30
11. Plate read	
12. Go to 2. for 40 cycles	
13. END	

4.7 Induction of senescence

4.7.1 Induction of senescence in by γ -irradiation

MEFs were cultured to 90 % confluence in T175 flasks. Two flasks containing the same embryo were harvested with 2 mL of 0.25 % trypsin and pooled in one 50 mL conical polypropylene tube. The tube was subjected to 10 Gy γ -irradiation using a calibrated Cesium-137 source (Gamma Cell 40, Atomic energy of Canada Limited). Primary cells were in DMEM composed of 10 % FBS and 1 % penicillin/streptomycin during irradiation. The irradiated cells were directly cryopreserved in freezing medium without further passaging.

4.7.2 Induction of senescence by X-ray

Fibroblasts were plated at a density of 5×10^4 cells per 12-well or 5×10^3 cells per 96-well. The same day, the plate was subjected to 15 Gy x-ray irradiation using a calibrated Benchtop X-ray Irradiator. The cells were kept in normal culture conditions for 7 days until a senescent phenotype could be observed.

4.7.3 Induction of senescence in MEF cells by passaging stress

MEFs were cultured according to the 3T3 protocol [275], which is referring to a 3-day transfer with an inoculum of 0.3×10^6 cells per 6 cm dish. As described after approximately eight passages (p8) depending on the embryo, cells reach the Hayflick limit and enter stable proliferative arrest, natural senescence.

4.7.4 Induction of senescence by Palbociclib

Fibroblasts were plated at a density of 5×10^4 cells per 12-well or 5×10^3 cells per 96-well. The day after, cells were treated with 5 μ M Palbociclib. The cells were kept in normal culture conditions for six days without further medium change until a senescent phenotype could be observed.

4.7.5 Senescence-associated β -galactosidase assay

Cellular senescence was assessed post irradiation by senescence-associated β -galactosidase (SA- β -gal) activity staining. Adherent cells were plated, and senescence was induced. Cells were fixed and stained according to manufacturer's instructions. SA- β -gal⁺ senescent cells stain an indigo blue dye that can be observed by light microscopy.

4.8 Cellular staining

4.8.1 General membrane staining of immortalized 3T3 cells

Immortalized fibroblasts were detached from the dish and rinsed once with serum-free DMEM. Following resuspension to a concentration of 2×10^7 cells/mL in Diluent C and incubation for 2 min with 4 mL of Diluent C containing concentrated PKH dyes. The reaction was stopped by the addition of an equal amount of FBS and the cells were then rinsed twice with DMEM containing 10 % FBS.

4.8.2 Staining for Flow Cytometry

Cells were suspended in FACS buffer (PBS containing 1 % FBS) and incubated with Fc block and cell surface markers for 30 minutes on ice in the dark. Afterwards cells were washed in FACS buffer and suspended for analysis on a flow cytometer. Data analysis was carried out using FlowJo software.

4.8.3 Induction of apoptosis and fluorescent labeling of Jurkat cells and BMDEs

Jurkat cells and BMDEs were irradiated in 10 cm dishes without lid, and subjected to UV irradiation for 3 min at 2400 - 200.000 μ J for 3 min, followed by incubation under normal cell culture conditions for 1 h. The apoptotic cells (ACs) were rinsed once with serum-free DMEM, resuspended to a concentration of 2×10^7 cells/mL in Diluent C, and incubated for 2 min with 4 mL of Diluent C containing concentrated PKH dyes. The reaction was stopped by the addition of an equal volume of

Methods

FBS and the cells were then rinsed twice with DMEM containing 10 % FBS and 1 % penicillin/streptomycin [278].

4.9 Imaging

4.9.1 Immunofluorescence of senescent cells

WT 3T3 fibroblasts were seeded at 8×10^3 cells per well in 8-chamber slides and directly treated with 5 μ M Palbociclib. Slides were kept in the incubator under normal cell culture conditions for 7 days. Cells were washed three times with PBS and fixed for 15 minutes with 4 % Paraformaldehyde (PFA). Afterwards they were washed again three times with PBS and blocked in blocking buffer (3 % BSA + 0.2 % Triton X-100 in PBS) for 1.5 hours. Blocking buffer was aspirated and primary antibody (dilution in 3 % BSA in PBS) was added over night at 4 °C. Cells were washed three times with PBS and secondary antibody dilution in 3 % BSA in PBS was added for 1 hour at RT in the dark, together with Phalloidin staining according to manufacturer's instructions. Cells were washed three times with PBS and kept in PBS at 4 °C until imaging, which was performed at a LSM780 Confocal Laser Scanning Microscope.

4.9.2 Live Cell imaging

Cells were plated in the desired format and subsequently monitored by live phase-contrast microscopy using the IncuCyte system with the 10X objective for 48 h. Confluency of cells, fluorescence intensities/area/object count were developed with the IncuCyte software. Further life cell imaging was performed in the ZEISS LSM980 WITH AIRYSCAN 2 using 63X objective for 24 h. All parameters for image acquisition and data extraction was performed with the Arivis Vision 4D software. Scans were selected manually according to image quality.

4.10 Functionality assays

4.10.1 Phagocytosis assays

4.10.1.1 *Single efferocytosis in the presence of senescent cells*

Senescent cells were plated at a density of 5×10^4 cells per well in 12-well plates as described before. After 24 h prior to the assay, the culture medium was changed. For co-culture conditions 1×10^5 BMDMs per well were added to the senescent cells. Senescent cells and macrophages were co-cultured for 6 and 24 h. PKH26-labeled apoptotic corpses (ACs) were incubated with the macrophages for 60 min at a 1:5 ratio (macrophages: AC) followed by washing three times with PBS to remove unbound ACs. The co-culture was analyzed by flow cytometry [278].

4.10.1.2 *Double efferocytosis in the presence of senescent cells*

The cells from the single efferocytosis assay were not harvested but further incubated with fresh medium for 2 h. ACs were irradiated and labeled with PKH67 as described before and added to the co-culture for 60 min. The co-culture was washed three times with PBS to remove unbound ACs [278]. Washed BMDMs were harvested by scraping in FACS buffer and the co-culture was analyzed by flow cytometry.

4.10.1.3 *In vitro engulfment assay of senescent cells*

Frozen irradiated MEFs cells were thawed and directly plated at a density of 5×10^3 senescent cells per well on 96-well plates. Immortalized fibroblasts were seeded at a density of 5×10^3 per well on 96-well and treated with 5 μ M Palbociclib for seven days as described before. BMDMs and multinucleated giant macrophages were added to the wells in ratios of 5:1, 10:1 and 20:1 (macrophages: senescent cells). The plates were immediately subjected to the IncuCyte device for live cell imaging.

4.10.1.4 *In vitro engulfment assay of protein aggregates from fibroblasts by BMDMs*

Fibroblasts were seeded at a density of 1×10^4 cells per 96-well and attached overnight. Lipofectamine was added as described before. After 24 hours, 70 % of aggregate expressing could be observed. The Lipofectamine containing medium was removed and replaced by fresh medium containing BMDMs in ratios of 5:1 and 10:1 (BMDMs: fibroblasts). The plates were immediately subjected to the IncuCyte system to be recorded for the 48 h. The change in the number of aggregates was quantified by detecting fluorescent object counts via the IncuCyte software.

4.10.1.5 *In vitro engulfment assay of protein aggregates from neurons by glia cells/BMDMs*

Cortical neurons were seeded in 48-well plates at a 5×10^3 cells per well, and 20 % fresh culture medium were added every 3-4 days. After one week of cultivation cells were transduced with lentivirus and incubated with the virus for another 7 days. The lentivirus containing medium was removed and replaced by fresh medium containing glia cells and BMDMs in ratios of 5:1 and 10:1 (BMDMs: neurons) or (glia cells: neurons). The plates were immediately subjected to the IncuCyte system to be recorded for the 48 h. The change in the number of aggregates was quantified by detecting fluorescent object counts via the IncuCyte software.

Methods

4.10.2 Seahorse bioenergetic measurements

Real-time oxygen consumption rate (OCR) and extracellular acidification rate (ECAR) measurements were conducted with a Seahorse XF HS Mini Analyzer. 4×10^4 BMDMs were plated into each well of Seahorse cell culture plates and pre-incubated at 37 °C in the absence of CO₂ in Seahorse XF DMEM medium supplemented with glutamine, glucose and pyruvate for a minimum of 45 min prior to the start of the assay. Injections of oligomycin (1.5 μM final), carbonyl cyanide-4 (trifluoromethoxy) phenylhydrazone (FCCP) (2 μM final), and rotenone/antimycin A (0.5 μM final) were diluted in the assay medium and loaded into ports A, B and C, respectively. The machine was calibrated according to manufacturer's instructions and the assay was performed using the glycolytic stress test assay protocol as suggested by the manufacturer. ECAR was measured under basal conditions followed by the sequential addition of oligomycin, FCCP and rotenone/antimycin A as adjusted in the default settings. Assay medium was injected as control. This allowed for an estimation of the contribution of individual parameters for basal respiration, ATP-linked respiration, H⁺ (Proton) Leak, Maximal Respiration, Spare Respiratory Capacity, and Non-mitochondrial respiration. The XF mito stress test report generator and the XF glycolysis stress test report generator automatically calculate the XF cell mito stress test and XF glycolysis stress test parameters from Wave data [279].

1.1.1 LDH Cytotoxicity Assay

The *in vitro* engulfment assay of protein aggregates from fibroblasts by BMDMs was set-up as described before. The addition of BMDMs was determined as starting point of the assay. Every 8 h from assay start sample medium was taken from the co-culture for a period of 48 h to determine cell death in the co-culture. For individual time points, 50 μL of culture medium were transferred to a 96-well plate and mixed with 50 μL of reaction mixture. The plate was incubated at room temperature for 30 min in the dark. Afterwards 50 μL of stop solution were added to each well and mixed by gentle tapping. The absorbance was measured at 490 nm and 680 nm in a plate reader and the % cytotoxicity was determined.

5 Results

5.1 Interaction of macrophages with senescent cells: overview of the experimental design and hypotheses

The overall goal of the first part of this thesis is to evaluate the interactions between macrophages and senescent cells using defined and tractable *in vitro* models. Excessive accumulation of senescent cells has central roles in driving aging [280] and chronic diseases [281]. The infiltration of tissues with senescent cells shortens healthy lifespans [282], drives organ aging [283] and promotes age-related organ deterioration/disorders [284] including cardiovascular diseases [285], cancer [286], neurodegenerative diseases [281] and osteoarthritis [287]. However, cellular senescence also plays a dual role during development and throughout tissue repair and regeneration [87, 262]. Senescence can also have beneficial effects like promoting the clearance of cell debris, reduction of fibrosis and can act as a potent barrier against tumorigenesis [288]. One concept is the timing and context at which the senescence program is activated determines the consequence. A transient induction of senescent cells pursued by rapid clearance at the early stages following injury promotes tissue repair [289], while the long-term accumulation of senescent cells impairs tissue function and can lead to organ failure [290]. From these observations, a central question concerns the mechanism of senescent cell removal in health as opposed to the situation in aging and disease, where senescent cell accrual is relentless.

The senescence-associated-secretory-phenotype (SASP) is one of the fundamental characteristics of senescent cells. As the SASP contains numerous cell recruitment chemokines and immune survival factors (e.g. CSF-1), a feasible hypothesis is that SASP triggers the recruitment of immune cells to the site of injury, resulting in subsequent elimination of senescent cells (by unknown mechanisms). Among these immune cells are macrophages which have regulatory roles in all stages of regeneration, repair and fibrosis. Macrophages are critical for the clearance of senescent cells during mouse embryogenesis. The absence of senescent cells can delay development and promote patterning defects, providing the first evidence that senescence-surveillance mechanisms operate during normal regeneration [291]. The clearance of senescent cells allows for repopulation by progenitor cells and regeneration of the damaged tissue, indicating that senescence-surveillance mechanisms operate during normal regeneration [87]. However, these studies did not distinguish between macrophage clearance of dead senescent cells, or whether an active macrophage-mediated pathway(s) was necessary to identify and then eliminate senescent cells [262]. In adults,

macrophages were shown to be important in the removal of senescent cells in models of liver injury, as well as for preventing excessive detrimental fibrosis and in resolving liver fibrosis [292]. Moreover, senescent hepatic stellate cells have been shown to secrete SASP molecules attracting macrophages [293]. Comparable to senescent cells, also the SASP has positive and negative effects. Besides the beneficial ability to recruit immune cells, SASP drives immune cell senescence and dysfunction, possibly leading to persistent and excessive accumulation of senescent cells [159].

The precise mechanism(s) underlying senescent cell accumulation within tissues remain unknown: either the senescent cells outnumber the immune system rendering it unable to clear them, or attracted immune cells become dysfunctional. Impaired clearance and regeneration in aged tissues as well as persistent damage may result from reduced macrophage recruitment, increased numbers of senescent cells or even damage to the macrophages themselves. If macrophages are depleted in the early stages of tissue repair in a number of organs, the inflammatory response is diminished [294], leading to defects in regeneration [295].

The specific mechanisms by which macrophages interact with senescent cells remain to be elucidated. The purpose of this thesis was to decipher, whether senescent cells are able to modulate macrophage functions eventually leading to a harmful accumulation of senescent cells throughout the aging process. Therefore, the experiments below were designed to evaluate the senescent cell-macrophage interplay.

5.1.1 Senescence models: induction and quantification

In initial experiments to determine the interaction between macrophages and senescent cells, we first generated senescent cells by defined and controllable *in vitro* approaches. In the experiments herein, murine fibroblasts were used as a workhorse that is tractable, convenient and reproducible. In general, passaging stress was applied to primary fibroblasts isolated from E14-15 embryos (MEFs) (4.3.5) to reach the Hayflick limit, which is defined as the number of times a normal cell population divides before the passaging stress forces them to entering the senescence phase [32]. These cells are referred to as Hayflick limit cells throughout this study. Alternatively, senescent cells were generated through chemicals e. g. Palbociclib, or radiation methods by γ -irradiation (Figure 5-1A). Irradiation leads to DNA damage, which eventually triggers cell cycle arrest [296]. Palbociclib is an FDA-approved selective cyclin-dependent kinase (CDK) 4/6 inhibitor, blocking cell cycle progression and thereby inducing senescence [297]. For the experiments that required the use of immortalized senescent 3T3 cells, senescence was induced by irradiation and Palbociclib, respectively. The

successful induction of senescence was quantified using several different readouts. First, we measured the expression of the cell cycle inhibitor p16 via qRT-PCR, which was significantly upregulated compared to proliferating fibroblasts and is a well-accepted marker of senescence (Figure 5-1B) [40]. Further, we used beta-galactosidase staining; compared to proliferating cells, senescent cells show high accumulation of lysosomal (beta)-galactosidase [298]. This converts x-gal into an indigo blue dye of which accumulation could be observed via light microscopy (Figure 5-1C). To underline the size difference and flat morphology of senescent cells [23], we also performed fluorescent microscopy of proliferating and senescent actinGFP MEFs. These Hayflick MEFs, highlight the characteristic cytoplasm expansion, which often reaches an order of magnitude larger compared to proliferating MEFs (Figure 5-1D). Taken together, this allows us to induce and readout senescence phenotypes in fibroblasts by different means.

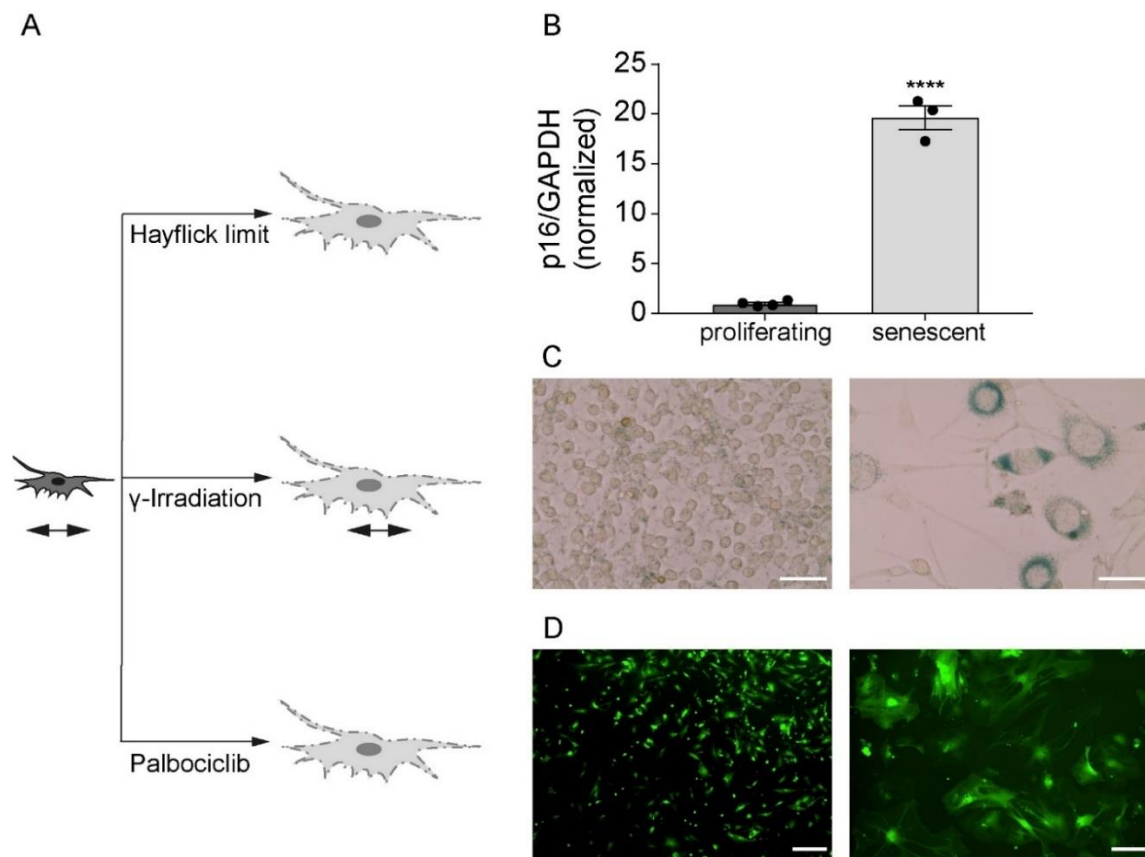


Figure 5-1: Induction and read out of a senescent phenotype.

A Schematic overview of senescence induction by passing stress until the Hayflick limit was reached, by γ -irradiation or by treatment with Palbociclib. **B** qRT-PCR quantification of p16^{INK4a} expression on the transcriptional level of proliferating and senescent cells (induced by Palbociclib). **C** β -galactosidase staining of proliferating (left) and senescent Hayflick limit (right) cells. Presence of lysosomal associated β -galactosidase converts the addition of x-gal to an indigo blue cell stain. **D** Fluorescence microscopy of proliferating (left) and senescent Hayflick limit (right) actinGFP MEFs, highlighting the morphological changes in terms of size difference and spread-out morphology. For **C** and **D** proliferating and senescent cells were recorded at the same magnification, scale bars indicate 50 μ m.

5.1.2 Macrophages interact with, but do not engulf, senescent cells

Timely clearance of senescent cells is required to maintain tissue and organismal homeostasis. Senescent cells recruit immune cells like macrophages for their eventual elimination. However, senescent cells have been shown to escape this process [299]. Investigating the specific modes of interaction between macrophages and senescent cells will help to prevent senescent cells from evading their clearance which will consequently prohibit the harmful accumulation of senescent cells in the tissue.

To measure the interaction between macrophages and senescent cells, we established a co-culture system with the two cell types. Senescence was induced in MEFs by applying passaging stress until the Hayflick limit, by γ -irradiation and by treatment with Palbociclib, respectively. The green fluorescent senescent actinGFP MEFs were imaged in co-culture with red fluorescent tdTomato⁺ macrophages. Using live cell imaging, the same cells were followed over time for up to 48 hours. The first important observation was senescent cells were motile to an extent and altered their shape across time; thus, despite their large size, they moved around within the culture. Moreover, macrophages interacted with the senescent cells (e.g. by crawling around and on top of the senescent cells), however, they were not able to phagocytose them (Figure 5-2A). Empirically, this property necessitated the quantification of each cell using shorter time increments of imaging. Using masking software supplied with the Incucyte imaging system, the cell area of the actinGFP MEFs was quantified over time in the absence and presence of macrophages. Independent of the number of applied macrophages, the quantified cell area of the senescent cells stayed constant over time (Figure 5-2B). Since senescent cells cannot divide (by definition), we therefore concluded that in this experimental setting, primary macrophages interacted with, but did not engulf or kill senescent cells. Otherwise, we would have observed time-dependent decline in the total green object area. This result gave the first clue that macrophages are not armed with a mechanism to kill or remove senescent cells by themselves.

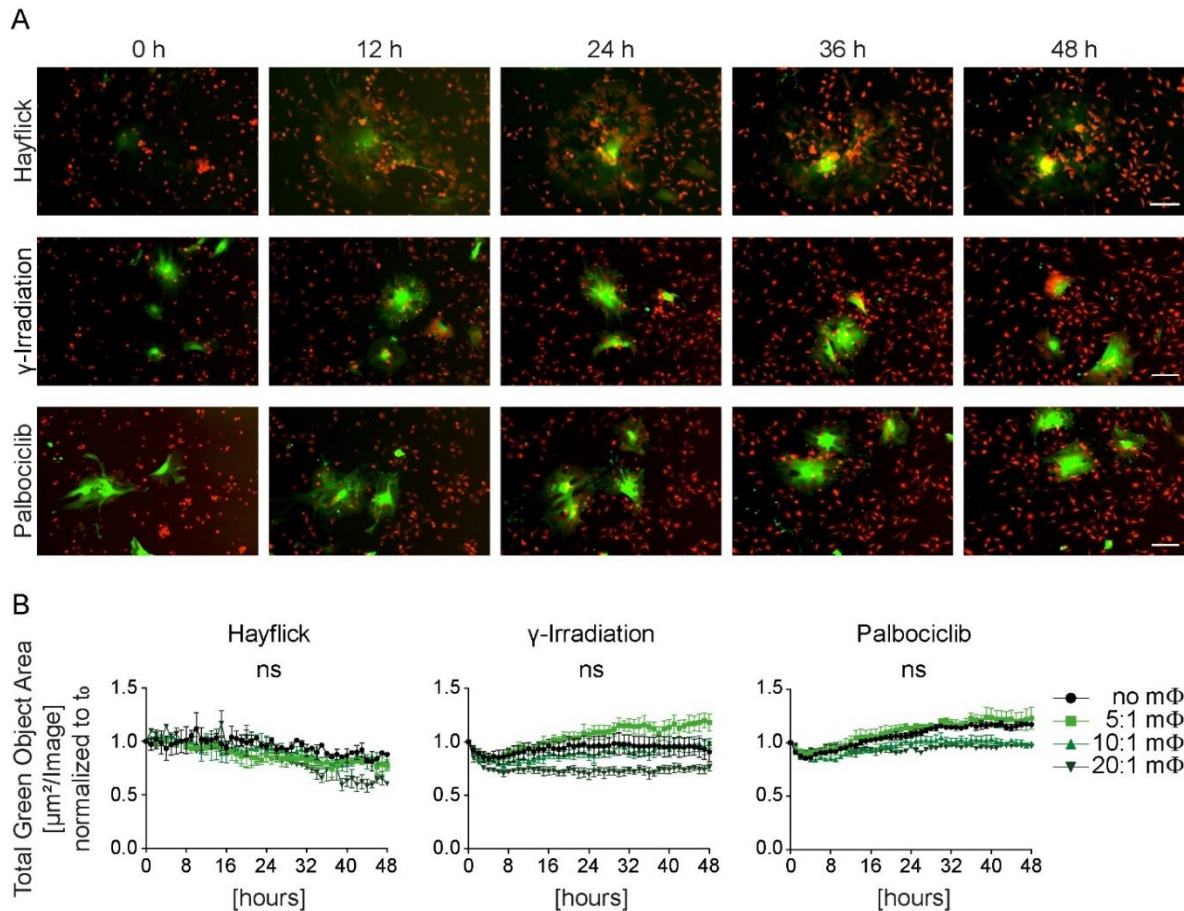


Figure 5-2: Macrophages interact with, but do not engulf senescent cells.

A Senescence was induced in actinGFP MEFs by passing stress until the Hayflick limit was reached, by γ -irradiation or by treatment with Palbociclib. Senescent MEFs were co-cultured with BMDMs, isolated from tdTomato⁺ mice, in a ratio of 10:1 BMDMs to senescent cells and imaged over 48 h. In each image group, the same field of view is shown across time. Data are representative of three independent experiments; scale bars indicate 100 μ m. **B** Quantification of green fluorescent area signal of senescent cells in the co-culture with different ratios of BMDMs. Data are representative of three independent experiments. All values are means \pm SEM. Statistically significant differences were determined by two-way ANOVA with Bonferroni correction.

5.1.3 Set-up of an *in vitro* efferocytosis assay to assess macrophage functionality

The previous co-culture experiments revealed senescent cells were able to escape or avoid any type of clearance mechanism by macrophages. Therefore, we next hypothesized senescent cells modulate macrophage functionality in different ways. In other words, an “active” pathway that macrophages use to detect and engulf living senescent cells seemed unlikely. Instead, living senescent cells should evade engulfment in the same way as all other living cells by deploying “don’t eat-me” signals. This hypothesis does not account for the accrual of senescent cells with age and disease, which argues other levels of interactions with macrophages occur. Therefore, the next step was to ask if senescent cells modulate a core macrophage function. We probed the effect of

Results

senescent cells on phagocytosis. Generally, macrophages ingest and degrade dead cells, debris, tumor cells, and foreign materials [261]. Moreover, they are the cell type primarily responsible for efferocytosis, the process of engulfing and eliminating apoptotic cells [300]. For these reasons we chose macrophage efferocytosis capacity as a readout for macrophage functionality for the following experiments. We developed and validated a series of novel efferocytosis assays to measure the influence of senescent cells on macrophage functionality.

A scheme of the overall assay procedure is shown in Figure 5-3A. When applied, Palbociclib was removed 24 hours prior to start of the co-culture to exclude potential harmful effects on macrophages, and thereby the overall assay readout. Macrophages were primed with senescent cells for 6 and 24 hours followed by the addition of PHK26 labelled apoptotic corpses (ACs) as the efferocytosis target for 1 hour. The macrophages were analyzed for the amount of engulfed ACs via flow cytometry. Therefore, we selected BMDMs for expression of the marker F4/80 [301]. The BMDMs were then further analyzed for the sub-population of macrophages having engulfed ACs (Figure 5-3B). Importantly, the interacting cell populations were extensively washed to remove efferocytic cells that “stick” but were not engulfed. Compared to other approaches examining efferocytosis as readout for macrophage functionality [278], our approach enables high-throughput screening of multiple conditions in parallel. It enabled us to study the interaction between macrophages and senescent cells with the quantifiable readout of engulfment of a third-party cell, where actively engulfing macrophages were expected to show higher granularity. In general, larger cells are more granular and show higher levels of fluorescence. This enables the detection of macrophages having engulfed a target. As an internal normalization control, we used macrophages and ACs alone, but in the absence of senescent cells (mΦ only). This control provides the maximum efferocytosis engulfment signal for the assay. We found all types of senescent cells significantly impaired macrophage efferocytosis compared to the control (Figure 5-3C). Our findings indicated that senescent cells impaired macrophage efferocytosis function independent of the means of senescence induction.

A key control in these experiments was to test the relative effect of senescent cells compared to proliferating, “normal” fibroblasts. In other words, is the inhibition of efferocytosis a property of senescent cells, or fibroblasts in general? To test this, macrophages were primed with proliferating, immortalized 3T3 fibroblasts instead of senescent fibroblasts, because MEF populations are very heterogeneous at the start and already contain senescent cells. 3T3 fibroblasts are also generated from MEFs [275], but cannot become senescent without applying any type of intervention (these

cells are immortalized but not transformed by definition). To induce the senescence phenotype, we seeded and treated 50.000 cells. Not all cells survive the senescence induction, leading to a decreased number of cells than originally plated as senescent cells in the well. To compare cell numbers of proliferating and senescent cells in our set-up we started with the same number of originally plated cells (50.000) for both conditions. Under these conditions, no effect of proliferating cells on macrophage efferocytosis could be observed (Figure 5-3D). This indicates the observed impairment effects results from senescent cells and not from fibroblasts in general.

The phagocytic target used for the overall efferocytosis assay were human Jurkat cells as these have been accepted as suitable target for other studies already [278]. However, mixing different species has been shown to cause xenotypic effects. Macrophages recognize and are activated by foreign molecular patterns [302]. To measure xenotypic effects resulting from the mixture of murine macrophages with human target cells, we added labelled primary bone marrow derived eosinophils that were verified by expression of Siglec-F [274] as phagocytic target to the assay (Figure 5-3E) instead of Jurkat cells. The assay procedure was conducted as described in 5.1.3. In our experimental setting no difference between Jurkat cells or eosinophils as efferocytosis target could be observed: additional presence of senescent cells significantly impaired macrophage efferocytosis function (Figure 5-3E).

In summary, we concluded senescent cells impaired macrophage functionality during efferocytosis independent of the means of senescence induction. The reduction in efferocytosis was specifically mediated by senescent cells and was shown to be independent of the species of the phagocytic target cell.

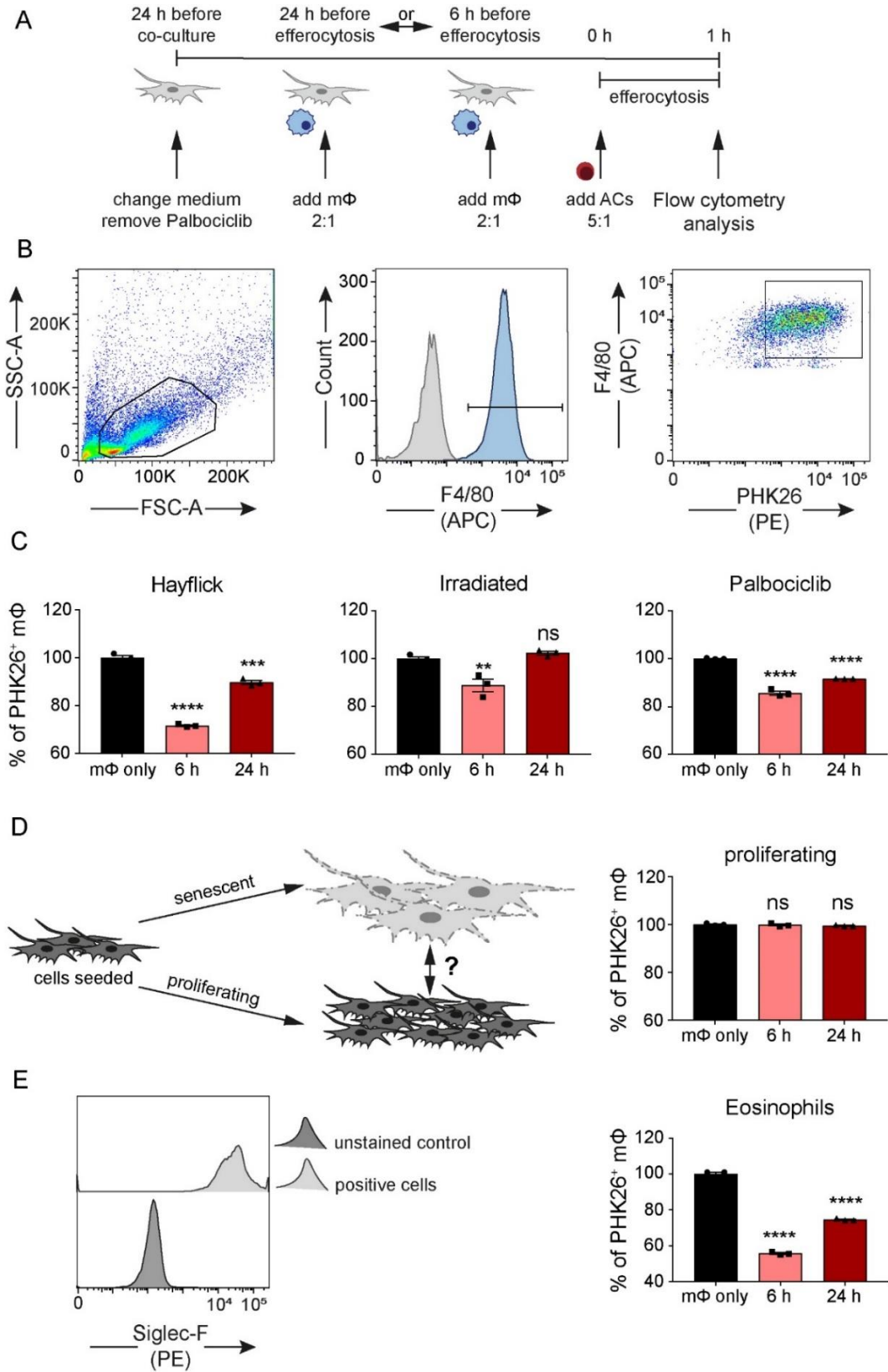


Figure 5-3: Senescent cells impair macrophage functionality during efferocytosis independent of the means of senescence induction.

A Schematic overview of the overall experimental design. BMDMs were primed with different types of senescent cells for 6 or 24 hours. ACs were labelled with PKH26 (red) and added to macrophages in a 5:1: ratio. Samples were subsequently analyzed by flow cytometry. **B** Gating strategy for efferocytosis assay. BMDMs were selected for expression of F4/80. The BMDM population was analyzed for the population of macrophages having engulfed ACs. **C** Quantification of efferocytosis of ACs by BMDMs in the presence of different types of senescent cells. **D** Schematic overview and results of efferocytosis of ACs by BMDMs in the presence of proliferating fibroblasts. **E** Selection of differentiated eosinophils by flow cytometry. **F** Results of efferocytosis of apoptotic eosinophils in the presence of senescent cells (induced by Palbociclib). All values in **C**, **D** and **F** are means \pm SEM; ** $p < 0.01$; *** $p < 0.001$; **** $p < 0.0001$. Statistically significant differences were determined by one-way ANOVA with Bonferroni correction; $n=3$ biological replicates.

5.1.4 Senescent cells do not impair macrophage functionality by soluble molecules

So far, we established senescent cells were able to impair macrophage efferocytosis. For the following experiments we wanted to confine the underlying mechanism(s) by which this impairment effect was manifested. Therefore, we determined whether the impairment effect required direct cell contact between the senescent cells and the macrophages or was mediated by soluble factors released from the senescent cells (e.g. factors in the SASP or other soluble factors that could suppress macrophage phagocytic functions). To test this, we performed two types of experiments. First, we performed a supernatant transfer assay. Senescent cells were cultured for 24 hours allowing soluble factors to be released into the media [303]. The conditioned media (CM) was transferred to the macrophages after removal of cell debris (Figure 5-4A). Macrophages were primed with total, undiluted CM for 6 and 24 hours and ACs were applied for 1 hour as described in 5.1.3. The amount of macrophages having engulfed ACs was measured by flow cytometry. Compared to the control, where no CM was applied, no significant change in efferocytosis capacity was observed. The efferocytosis capacity of macrophages was constantly independent of the presence or absence of CM (Figure 5-4B) and therefore, the SASP released by senescent cells did not impair macrophage phagocytic capacity. To substantiate these data, we conducted the efferocytosis assay in a transwell experiment. Macrophages were primed with senescent cells in the same well for 6 and 24 hours, however direct cell contact was disabled as the senescent cells were seeded onto the transwell insert (Figure 5-4C). Senescent cells were visually checked for viability and proper attachment to the transwell insert. ACs were added as efferocytosis target to the part of the well, containing previously seeded macrophages. Prohibited from direct cell contact, senescent cells were not able to significantly impair macrophage efferocytosis capacity. Compared to the control, where no senescent cells were present in the well, no significant change in efferocytosis capacity could be determined (Figure 5-4D). The soluble factors released by senescent cells that could pass the transwell insert did not obviously influence the phagocytic capacity of macrophages. The impairment seems to be rather regulated by direct cell contact.

Results

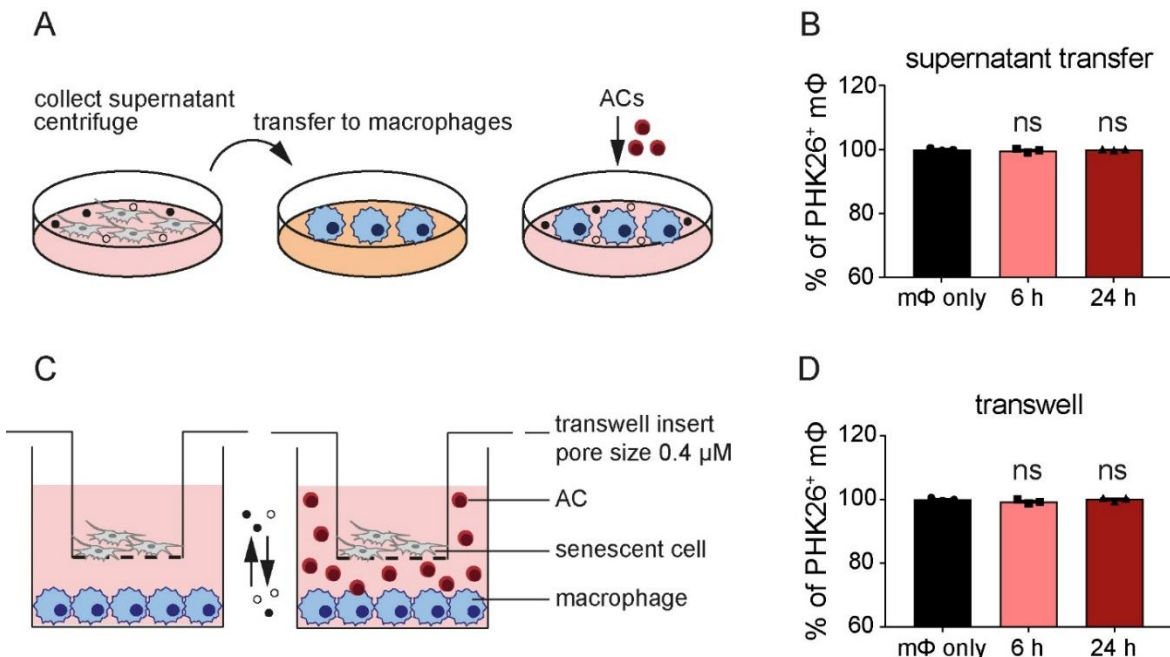


Figure 5-4: Soluble factors released by senescent cells do not impair macrophage efferocytosis.

A Schematic overview of supernatant transfer assay. Medium was conditioned by senescent cells (induced by Palbociclib) for 24 h. Conditioned medium was centrifuged and added to WT BMDMs for 6 or 24 hours. ACs were labelled with PKH26 and added in a 5:1: ratio. **B** Analysis of efferocytosis of ACs in the presence of the supernatant of senescent cells by flow cytometry. **C** Schematic overview of transwell assay. Senescent cells were seeded in a transwell insert, which was placed into a well containing BMDMs. ACs were labelled with PKH26 and added in a 5:1: ratio to the part of the well containing BMDMs. **D** Efferocytosis of ACs co-cultured with senescent cells in a transwell was analyzed by flow cytometry. Data in **B** and **D** are representative of three independent experiments. All values are means \pm SEM. Statistically significant differences were determined by one-way ANOVA with Bonferroni correction; n=3 biological replicates.

5.1.5 Senescent cells express increased CD47

Phagocytes recognize and respond to certain signals to orchestrate the selective and rapid removal of distinct cells. Such signals include direct and indirect “eat-me” markers for example on the apoptotic cell surface and the presence of “don't eat-me” markers normally found on living cells. Moreover, there are soluble “come-get-me” signals secreted by apoptotic cells to attract phagocytes to sites of apoptotic cell death. Once the target cells are identified, their uptake by phagocytes further depends on the molecular machinery [218]. As the impairment effect of senescent cells was mediated by direct cell contact, we hypothesized it could be mediated by the upregulation of “don't eat-me” molecules on the cellular membrane. While “don't eat-me” signals have naturally evolved to prevent immune destruction of “self” cells and thus to prevent autoimmunity, some cancer cells have co-opted and exploited this strategy to evade immune recognition and attack. The “don't eat-me” molecule CD47 is expressed on a high proportion of cancers and therefore has been extensively studied throughout the past years [218]. The

prototypical “don’t eat-me” signal is CD47. When CD47 is recognized by its receptor (SIRP α) on the surface of macrophages, these cells are no longer able to effectively engulf, or phagocytose, other cells and thus self-cells are not killed [304]. Therefore, inhibition of the CD47 pathway is the therapeutic vision in cancer therapy which could enforce the recognition and removal of malignant cells [305]. We first focused on CD47 expression, as its shown interaction with macrophages could be the basis for the impairment effect of senescent cells on macrophage functionality.

As a first step to investigating the CD47- SIRP α pathway, we examined senescent cells for their CD47 expression via immunofluorescence. To enable the visualization of the complete cells, we included a phalloidin staining, which stains the cytoskeleton by actin binding. As control, we included proliferating cells; these showed weak expression of CD47 located in the nucleus. By contrast, senescent cells showed comparatively high expression of CD47 located on the cell surface (Figure 5-5A). Our findings indicated that senescent cells express increased CD47 compared to proliferating cells. This high expression of CD47 may be responsible for the impairment effect of senescent cells on macrophage phagocytosis.

To examine, whether CD47 was indeed responsible for the impairment effect of senescent cells, the implementation of a loss-of-function experiment was essential. Therefore, we generated CD47 KO fibroblast cell lines, using CRISPR-Cas9 (4.5.4). We designed guide RNAs predicted to create a loss-of-function *Cd47* allele. After transfection, flow cytometry was used to isolate CD47-low, or -negative cells, which should enrich for CD47 knockout cells. After further single cell cloning, expansion, and validation by flow cytometry (our anti-CD47 antibodies perform poorly by immunoblotting), the KO cells were compared to proliferating and senescent WT fibroblasts for CD47 expression by immunofluorescence. Generated KO clones were validated by the absence of CD47 staining during immunofluorescence, which also indicated the overall specificity of the applied antibody (Figure 5-5A). The CD47 KO clones were further validated for their loss-of-function using flow cytometry, where also no CD47 expression could be detected (Figure 5-5B).

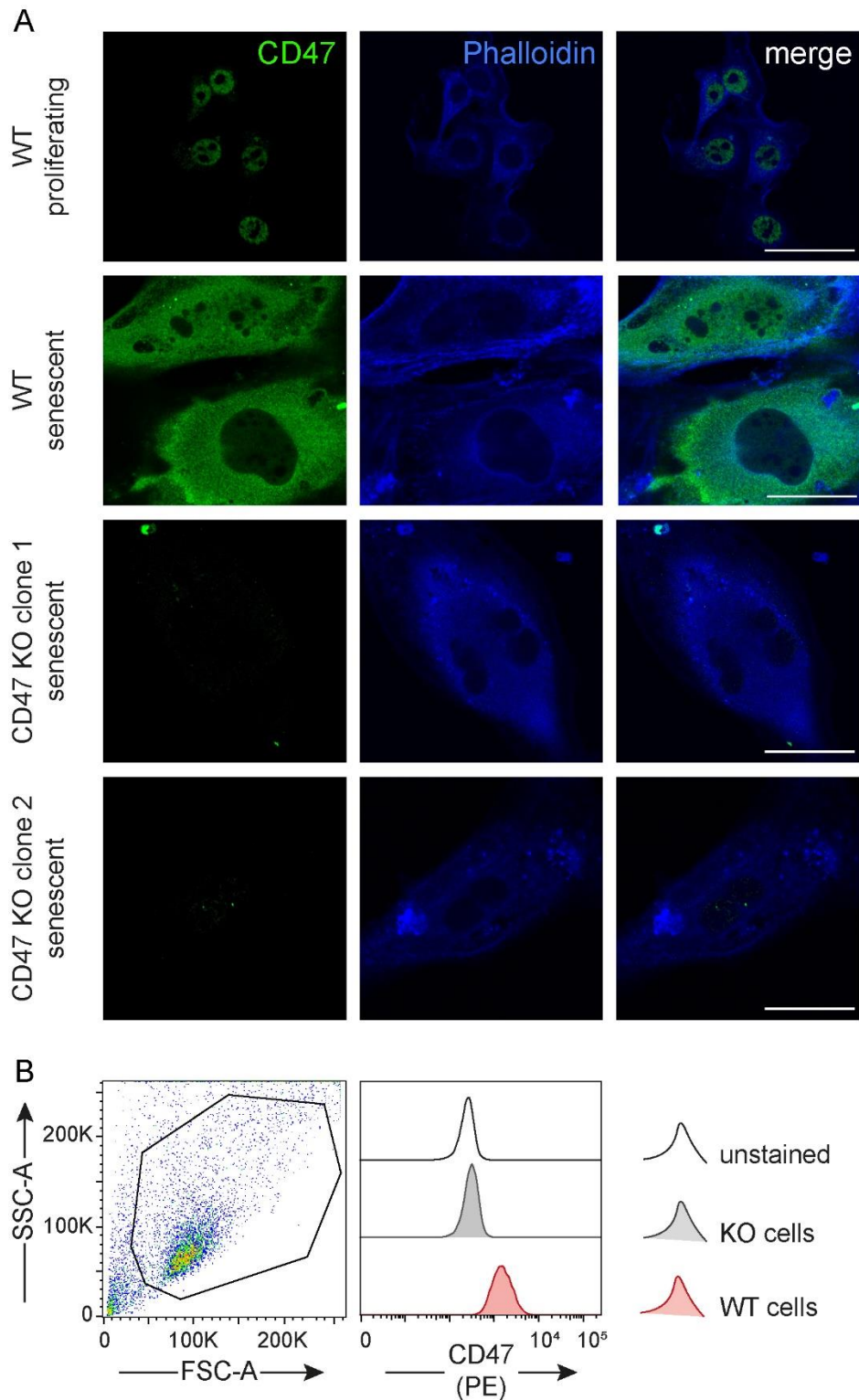


Figure 5-5: Senescent cells express increased CD47.

A Cells were fixed and stained with α -CD47 antibody (green) and Phalloidin (blue). Depicted are representative images of proliferating WT cells, senescent WT cells, senescent CD47 KO clone 1 and senescent CD47 KO clone 2 (senescence induced by Palbociclib). The CD47 KO clones indicate the overall specificity of the CD47 antibody; scale bars indicate 50 μ m. **B** CD47 KO cells were verified by CD47 staining in flow cytometry.

5.1.6 CD47 expression is responsible for the impairment effect of senescent cells

Using the CD47 knockout cells, we next went on to elucidate whether the increased CD47 expression on senescent cells (induced by Palbociclib) was the responsible factor for the impairment effect on macrophage efferocytosis capacity of senescent cells. Senescent CD47 KO cells were compared to senescent WT 3T3 cells in the efferocytosis assay as described in 5.1.3. The assay procedure is depicted in Figure 5-6A. Macrophages were primed with senescent cells for 6 and 24 hours followed by the addition of labelled ACs as efferocytosis target. The macrophages were analyzed for the amount of engulfed ACs via flow cytometry. In concordance with the preceding sections, the presence of WT senescent cells in the culture showed an impairment of efferocytosis as expected. However, both tested senescent CD47 KO clones failed to impair macrophage phagocytic capacity. No significant differences could be detected between the conditions in the presence and the absence of senescent CD47 KO cells compared to the control (Figure 5-6B). Consequently, we concluded the impairment effect of senescent cells on macrophage phagocytic capacity was critically dependent on CD47 expression on senescent cells.

Taking a closer look on the impairment effect of WT senescent cells on macrophage efferocytosis, the impairment was dependent on the duration of the preceding macrophage priming. Short priming for 6 hours resulted in a stronger inhibition of efferocytosis effect, compared to longer priming for 24 hours. Based on this experiment, we hypothesized, the impairment effect was likely to be both transient and reversible; in other words, senescent cells deliver a “paralysis” signal to neighboring macrophages (if such a signal was permanent, we would expect any macrophage *in vivo* that encountered a CD47⁺ cell to disable phagocytosis – this is clearly not the case). Therefore, we set-up a two-step efferocytosis approach: With the help of this two-step approach, a permanent impairment on macrophage efferocytosis should become more evident as it should persist even after “overfeeding” after the second efferocytosis. In case the impairment effect was only transient, we hypothesized it should not persist after the second efferocytosis (Figure 5-6C). After the first round of efferocytosis, the unbound ACs were removed and the cells were incubated without any efferocytosis target cell for two hours. This was followed by a second addition of labelled ACs as efferocytosis target. Then the macrophages were analyzed for the amount of engulfed ACs via flow cytometry. However, after the second efferocytosis, no significant impairment on macrophages efferocytosis in the presence of senescent cells could be detected anymore. This was independent of the genotype of the applied cells. Neither after preceding priming with WT senescent cells, nor after preceding priming with CD47 KO senescent cells a significant impairment on efferocytosis

Results

could be detected (Figure 5-6D). We therefore concluded the impairment effect on macrophage efferocytosis mediated by senescent cells was reversible.

In summary, our experiments indicated the impairment effect on macrophage efferocytosis, mediated by senescent cells was conveyed by the “don’t eat-me” molecule CD47. Further, the impairment seemed to be a reversible effect.

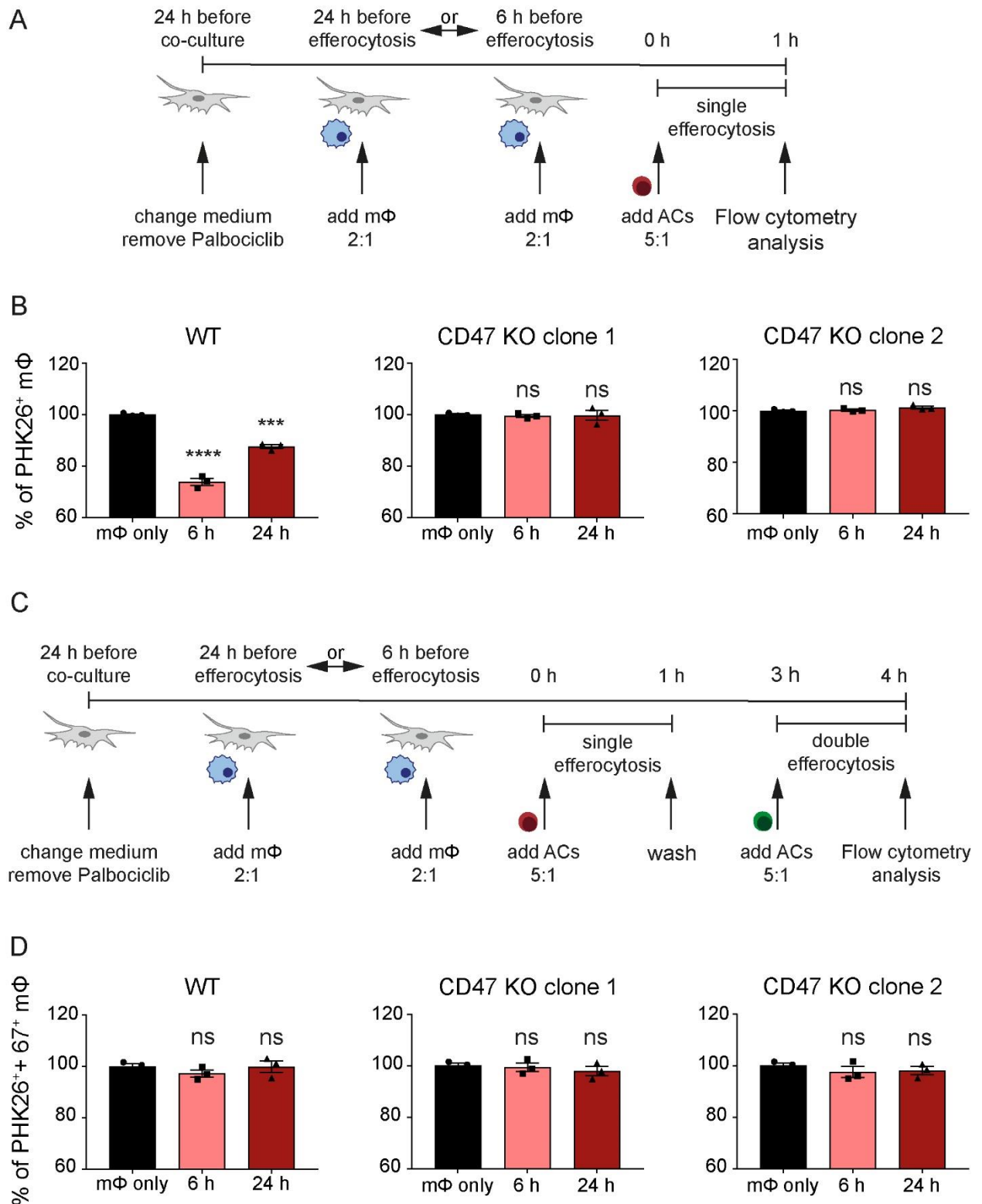


Figure 5-6 : The impairment of the efferocytosis capacity of macrophages by senescent cells is dependent on CD47 and reversible over time.

A Schematic overview of the overall experimental design for single efferocytosis. BMDMs were primed with different types of senescent cells for 6 or 24 h. ACs were labelled with PKH26 and added in a 5:1 ratio. Samples were analyzed by flow cytometry. **B** Single efferocytosis of ACs by BMDMs in the presence of senescent cells (induced by Palbociclib). **C** Schematic

Results

overview of the overall experimental design for double efferocytosis. BMDMs were primed with WT and CD47 KO senescent cells for 6 or 24 hours. ACs were labelled with PKH67 (first efferocytosis) and PKH26 (second efferocytosis) and added in a 5:1: ratio in a two-step (double) efferocytosis assay. Samples were analyzed by flow cytometry. **D** Double efferocytosis of ACs by BMDMs in the presence of senescent cells (induced by Palbociclib). For **B** and **D** data are representative of three independent experiments. All values are means \pm SEM; *** $p < 0.001$; **** $p < 0.0001$. Statistically significant differences were determined by one-way ANOVA with Bonferroni correction; $n=3$ biological replicates.

5.1.7 Efferocytosis impairment is independent of macrophage phenotype and target

Macrophages have diverse functions in homeostatic and immune responses. The broad spectrum of macrophage functions depends on both tissue environments and most importantly, the activation plasticity of the cells [191]. Plasticity in this setting means the ability of macrophages to change their functional profile rapidly through a process generally defined as polarization. Thereby macrophages respond to different stimuli coming from the local microenvironment and acquire a specific functional phenotype tailored to the functions needed (for example, recognition and killing intracellular pathogens). Although macrophage phenotypes should be seen as plastic and adaptable, they can be often simplified into two extremes for experimental purposes: a pro-inflammatory (M1-like) and an anti-inflammatory/pro-resolving (M2-like) profile [190]. Pro-inflammatory macrophages are induced by microbial products, such as the lipopolysaccharide (LPS) and by cytokines, such as interferon gamma (IFN- γ). Anti-inflammatory macrophages are induced by IL-4 and IL-13 secreted by innate and adaptive immune cells [306]. Based on this definition, M1-like macrophages are ignited and sustain inflammatory responses by secreting pro-inflammatory cytokines, activating endothelial cells and inducing the recruitment of other immune cells into the inflamed tissue. On the contrary, M2 macrophages promote the resolution of inflammation, phagocytose apoptotic cells, drive collagen deposition, coordinate tissue integrity, and release anti-inflammatory mediators [190] (Figure 5-7A). Importantly, this definition is generally restricted to highly defined experimental settings, whereas the situation *in vivo* is far more heterogeneous and complex [185]. Different types of macrophage phenotypes have previously been shown to be uniquely programmed to optimize efferocytosis [278]. Further, a recent study from our laboratory has shown macrophage polarization influences the efferocytosis capacity of macrophages [307]. Hence, we wanted to determine whether the impairment of macrophage efferocytosis, mediated by senescent cells, could be further manipulated by using macrophages with different activation states in our experimental set-up. Therefore, the efferocytosis assay described in 5.1.3 was repeated using unpolarized, M1-like and M2-like macrophages that were polarized for 24 hours in the co-culture with WT senescent fibroblasts. However, independent of the macrophage activation state, the phagocytic capacity was still significantly impaired (Figure 5-7B).

In addition, we wanted to reveal whether the impairment effect and its resolution in the CD47 KO cells could be manipulated by the application of different phagocytosis targets. Clearance of apoptotic cells is the final conclusion of the programmed cell death process [308]. Uncleared corpses can become secondarily necrotic, promoting inflammation and autoimmunity (for example, by released nucleic acids). Necrosis differs qualitatively from apoptosis in terms of cellular integrity and subsequent release of intracellular contents into the extracellular environment [309]. These differences result in drastically different means of clearance of the cell debris [310]. What distinguishes the phagocytosis of apoptotic cells from the phagocytosis of most bacteria or necrotic cells is the lack (or even suppression) of a pro-inflammatory immune response [311]. To explore whether the impairment effect of senescent cells was only restricted to a non-inflammatory setting, we applied apoptotic and necrotic corpses in addition to bacteria as phagocytic target. However, macrophage efferocytosis capacity was still impaired after priming with senescent WT cells, independent of the phagocytic target (Figure 5-7C). This effect was resolved in the co-culture with senescent CD47 KO cells, also independent of the target. In summary, the impairment of macrophage efferocytosis could not be altered by the application of macrophages in different activation states. Furthermore, the impairment of efferocytosis by senescent cells was independent of a pro- and non-inflammatory immune response. We concluded the impairment effect was globally mediated by CD47, as CD47 KO cells could not impair the efferocytosis anymore, independent of the target.

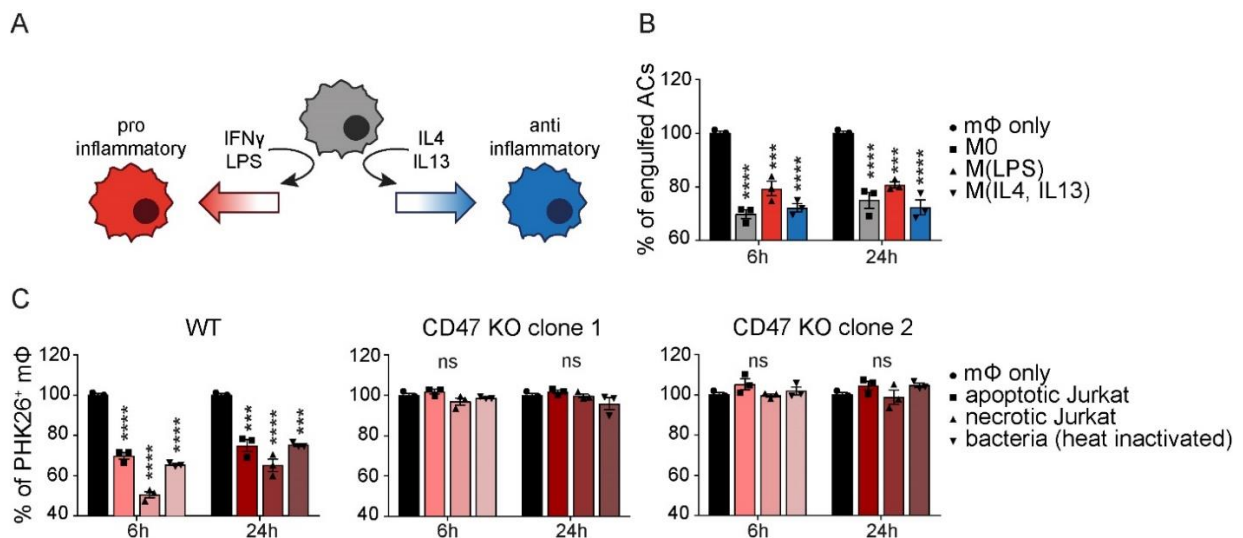


Figure 5-7: The impairment of macrophage efferocytosis by senescent cells is independent of macrophage polarization or the phagocytosis target.

Results

A Schematic overview of the overall experimental design to generate polarized activation states of macrophages. Unstimulated BMDMs can be polarized to a pro-inflammatory M1-like phenotype by the addition of IFN γ and LPS or to an anti-inflammatory M2-like phenotype by the addition of IL4 and IL13. **B** Efferocytosis of ACs by differently stimulated macrophages in the presence of senescent cells (induced by Palbociclib). **C** Phagocytosis of different targets by BMDMs in the presence of senescent cells (induced by Palbociclib). For **B** and **C** data are representative of three independent experiments. All values are means \pm SEM; *** $p < 0.001$; **** $p < 0.0001$. Statistically significant differences were determined by one-way ANOVA with Bonferroni correction; $n=3$ biological replicates.

5.1.8 The impairment effect of senescent cells is dominated by CD47

Monoclonal antibodies that antagonize the interaction of “don’t eat-me” signals with their macrophage-expressed receptors have therapeutic potential in cancer treatment [312]. However, variability in the magnitude and durability of the response to these agents has suggested the presence of additional, as yet unknown, “don’t eat-me” signals. Importantly, at least 135 ITIM-containing proteins exist and are expressed in cell-type specific ways [313]; conceivably, other ITIM receptors could work like CD47. Consequently, Barkal *et al.* suggested CD47 could not be the only “don’t eat-me” signal, but rather seems to operate in a complementary way with other molecules [314]. This led to the discovery of additional “don’t eat-me” signals associated with malignancy, including CD22 and CD24 [235, 315]. Further studies showed also CD24, similar to CD47, interacts with macrophages. However, CD24 signals through its receptor Siglec-10 [314]. At this stage in the development of this field, genetic evidence and observational studies in cancer models argue CD22 and CD24 are key complementary pathways to CD47 [314].

Accordingly, we performed an immunofluorescence analysis of the senescent cells and stained the cells with primary antibodies for CD47 and CD22 (Figure 5-8A) or CD47 and CD24 (Figure 5-9A). For visualization of the complete cells, a phalloidin staining was included. We compared proliferating and senescent WT cells. Unlike CD47, neither CD22 nor CD24 was upregulated in senescent cells compared to proliferating cells. This effect could also be quantified by measuring the fluorescence intensity signal for individual cells (Figure 5-8B and Figure 5-9B). Moreover, comparable to senescent WT cells, the senescent CD47 KO cells did not show upregulation of CD22 or CD24 (Figure 5-8A, Figure 5-9A). This effect was quantified (Figure 5-8B and 5-9B). No significant difference could be detected between senescent WT and senescent CD47 KO cells in the upregulation of CD22 or CD24. We therefore concluded CD47 KO cells did not compensate the loss of the “don’t eat-me” signal CD47 by upregulation of other “don’t eat-me” signals, but were dependent on CD47, as emphasized from the genetic experiments (Figure 5-6).

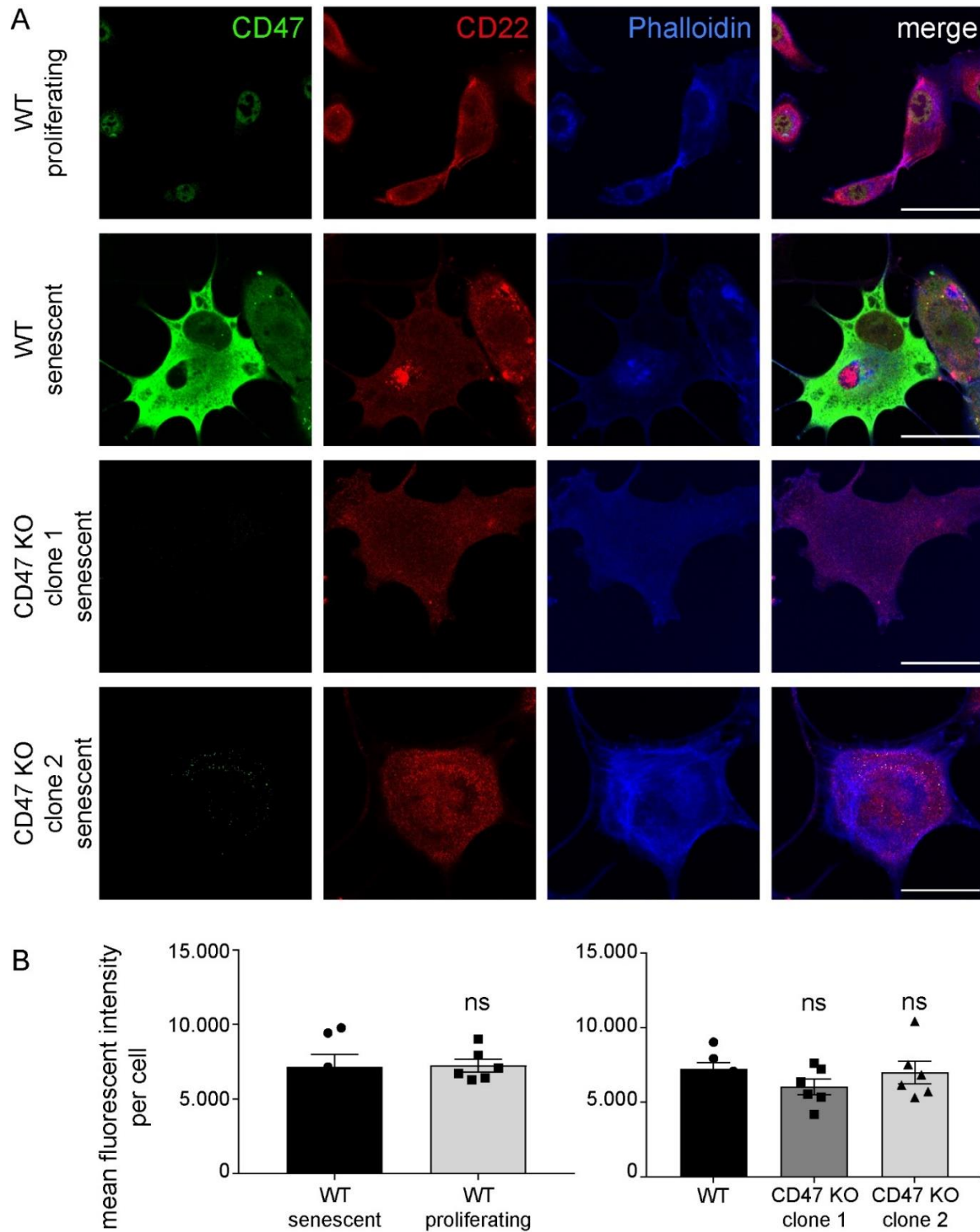


Figure 5-8: CD47 KO cells do not show increased expression of CD22

A Senescent or proliferating cells were fixed and stained with α -CD47 antibody (green), α -CD22 antibody (red) and Phalloidin (blue). Depicted are representative images of proliferating WT cells, senescent WT cells, CD47 KO clone 1 and CD47 KO clone 2. Scale bars indicate 50 μ m **B** Quantification of the CD22 signal in proliferating and senescent WT, senescent CD47 KO clone 1 and CD47 KO clone 2 (senescence was induced by Palbociclib). All values are means \pm SEM. Statistically significant differences were determined by one-way ANOVA with Bonferroni correction. n=6 biological replicates.

Results

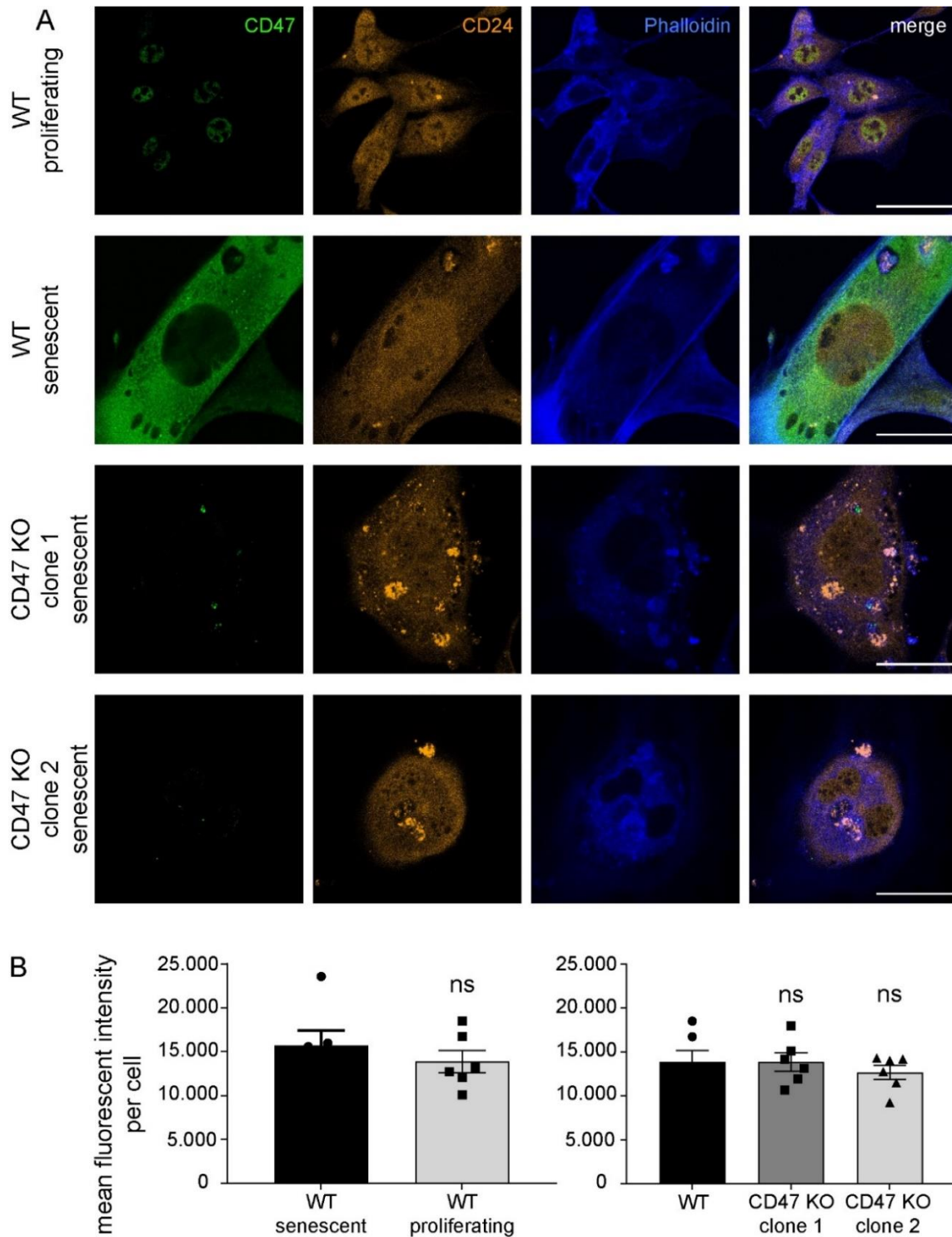


Figure 5-9: CD47 KO cells do not show increased expression of CD24

A Cells were fixed and stained with α -CD47 antibody (green), α -CD24 antibody (orange) and Phalloidin (blue). Depicted are representative images of proliferating WT cells, senescent WT cells, CD47 KO clone 1 and CD47 KO clone 2. Scale bars indicate 50 μ m. **B** Quantification of the CD24 signal in proliferating and senescent WT cells. Quantification of the CD24 signal in WT, CD47 KO clone 1 and CD47 KO clone 2 senescent cells (senescence was induced by Palbociclib). All values are means \pm SEM. Statistically significant differences were determined by one-way ANOVA with Bonferroni correction. n=6 biological replicates.

5.1.9 CD47 signaling can be followed downstream to macrophage SIRP α signaling

The experiments conducted throughout this study strongly suggest CD47 was the surface molecule solely responsible for the transient impairment effect of macrophage efferocytosis, mediated by senescent cells. Subsequently we wanted to decipher the crucial signal being processed further downstream in our system. The “don’t eat-me” signal CD47 inhibits cellular phagocytosis through its interaction with signal receptor protein-alpha (SIRP α), which is expressed on phagocytic cells, such as macrophages and dendritic cells. CD47 binding to SIRP α causes activation of the SHP-1 phosphatase [236]. SHP-1 is recruited to the cellular membrane and inhibits phagocytosis via dephosphorylation of downstream mediators required for the engulfment process [228]. We hypothesized SIRP α blocking antibodies would disrupt the CD47-SIRP α interaction, and consequently disable inhibitory signaling mediated by SIRP α [228] (Figure 5-10A).

We therefore conducted the efferocytosis assay in the presence of a SIRP α blocking antibody, which significantly alleviated the impairment effect on macrophage efferocytosis capacity mediated by senescent cells. We primed macrophages with senescent cells for 6 hours, since a stronger impairment effect could be observed for shorter priming in the preceding experiments (see 5.1.6). The presence of a SIRP α blocking antibody could significantly restore macrophage efferocytosis capacity compared to conditions without the blocking antibody (Figure 5-10B). This provided the first indication that CD47 expression on senescent cells signaled via SIRP α expressed on macrophages and also confirmed the primacy of the CD47- SIRP α axis in efferocytosis paralysis.

We next sought to follow the SIRP α signaling pathway further downstream. Therefore we tested if we could track SHP-1 recruitment to the cellular membrane of macrophages after priming with senescent cells. The SHP-1 recruitment was examined via immunofluorescence, using a primary antibody against SHP-1. After 6 hours of priming of macrophages with senescent WT fibroblasts, macrophages showed a ring-like accumulation of SHP-1 at the cellular membrane. This accumulation was less strong co-cultured with WT senescent cells for 24 hours. In the co-cultures with senescent CD47 KO cells, no accumulation but rather an even distribution of SHP-1 could be detected (Figure 5-10C). The fluorescence intensity accumulation upon binding of SHP-1 antibody was quantified for cellular cross-sections. The principle is shown in Figure 5-10D. The fluorescence intensity distribution was measured across each cell. Intensity profiles were quantified according to the measured distance in μm and the gray value (fluorescence) intensity. The intensity profiles of three exemplary macrophages from each co-culture condition were quantified (Figure 5-10E). Macrophages that were primed with WT senescent cells for 6 hours showed the highest

Results

fluorescence intensity at the outer borders of the intensity profile, reflecting the cellular membrane. Although SHP-1 was still detected at the cellular membrane in conditions where macrophages were primed with WT senescent cells for 24 hours, the intensity was reduced. No intensity differences in the profile, but rather an equal distribution could be detected after macrophages were primed with senescent CD47 KO cells.

In summary, the overall model that was refined throughout this thesis suggests that CD47 is upregulated on senescent cells and interacts with SIRP α on the macrophage surface. CD47 binding to SIRP α causes activation of the SHP-1 phosphatase. SHP-1 gets recruited to the cellular membrane and eventually inhibits phagocytosis via dephosphorylation of downstream mediators required for the engulfment process. Our data provides new insights in how senescent cells and macrophages act in concert. The value of these findings for the processes of tissue homeostasis and wound healing will be further conferred in the discussion section.

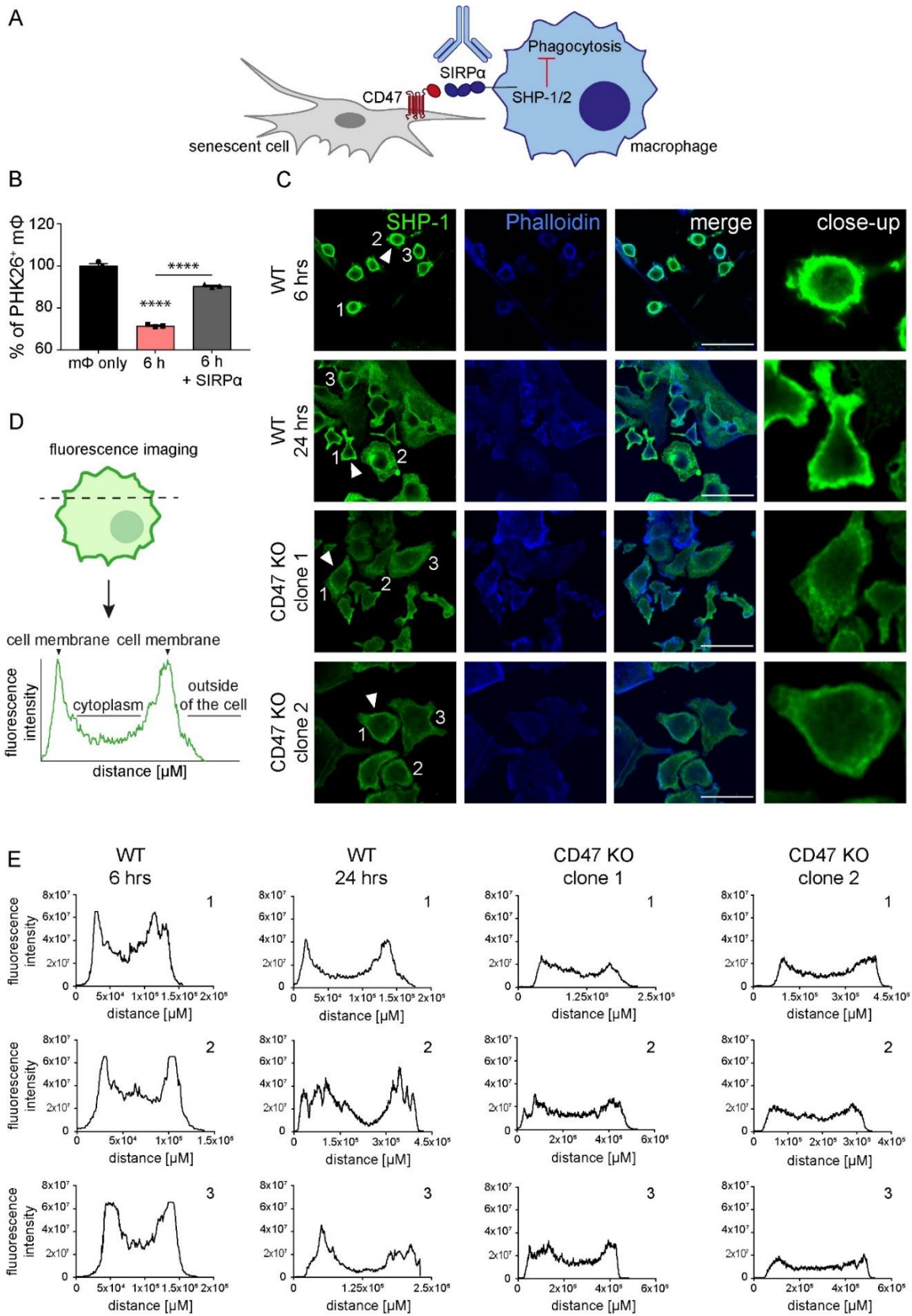


Figure 5-10: Senescent cells impair efferocytosis by signaling via SIRPα and SHP-1 on the macrophages.

Results

A Schematic overview of the overall experimental design to dissect CD47-SIRP α signaling. CD47 is expressed on senescent cells and interacts with SIRP α , an inhibitory receptor expressed on macrophages and other myeloid immune cells. When CD47 binds to SIRP α , it causes activation of the SHP-1 phosphatase that inhibits phagocytosis via dephosphorylation of downstream mediators required for the engulfment process. Antibodies that disrupt the CD47-SIRP α interaction, disable inhibitory signaling by SIRP α , thereby also disabling the impairment effect of senescent cells on the efferocytosis capacity of macrophages. **B** Efferocytosis in the presence of senescent cells (induced by Palbociclib) and a SIRP α blocking antibody. Data are representative of three independent experiments. All values are means \pm SEM. Statistically significant differences were determined by one-way ANOVA with Bonferroni correction; **** $p < 0.0001$. $n=3$ biological replicates. **C** The co-culture of BMDMs and senescent cells (induced by Palbociclib) was fixed and stained with α -SHP-1 antibody (green) and Phalloidin (blue). Depicted are representative images of the co-culture with WT cells for 6 h, WT cells for 24 h, CD47 KO clone 1 and CD47 KO clone 2 for 6 h. Senescent cells and macrophages were distinguished by size differences in the Phalloidin staining and specific binding of the SHP-1 antibody. Cells depicted in the close-up are indicated by an arrow, cells that were used for further quantification are numbered. Scale bars indicate 50 μ m. **D** Schematic overview of the intensity profile measurement of SHP-1 in BMDMs. Intensity was measured across the widest point of each cell. Intensity profiles were generated by measuring the distance in μ m and the gray value intensity. **E** Intensity measurements in BMDMs co-cultured with senescent cells. Three representative measurements are shown for the co-culture with senescent WT cells for 6 h, senescent WT cells for 24 h, senescent CD47 KO clone 1 and CD47 KO clone 2 for 6 h.

5.2 Multinucleated giant macrophages as cell type to remove senescent cells

Multinucleated giant cells (MGCs) were first observed in tuberculosis [316]. Giant cell formation results from fusion of mononuclear phagocytes which can contain from two to more than 200 nuclei [317]. Multinucleated giant macrophages are also called polykaryons. They are formed in response to the presence of alien indigestible particulates in tissues. Polykaryons are also present in diverse infectious and non-infectious chronic inflammatory conditions, including schistosomiasis, atherosclerosis, sarcoidosis and Langerhans cell histiocytosis [318, 319]. Moreover, they are often found under conditions where large and/or poorly degradable material is present. Polykaryons define the foreign body reaction to macroscopic organic and inorganic materials, such as uric acid crystals and surgical implants [318, 320]. Consequently, polykaryons are hypothesized to be specialized for uptake of large particles [321]. The role of MGCs in general and polykaryons in particular in disease is ambiguous. It remains unclear whether they are beneficial or detrimental to disease outcome. Moreover, fused macrophages seem to display different roles depending on the nature of the disease. Indeed, reduced [322, 323], increased [324, 325], or unchanged [326] phagocytic activity of MGCs compared to non-fused macrophages have all been reported. Since their first description in 1868, there have been few attempts to investigate the specific properties of polykaryons as well as their function. A recent study compared M2-activated macrophages and polykaryon cultures *in vitro*. Milde *et al.*, found polykaryons phagocytosed their target less avidly than unfused M2 macrophages [327]. However, polykaryons were remarkably more competent in the uptake of large particles [327]. In summary, there is strong evidence the main characteristic of polykaryons is the uptake of large particles which unfused macrophages are not capable of.

5.2.1 Polykaryons can engulf senescent cells

In the first part of this thesis, we were able to show how senescent cells impair macrophage functionality. However, we were not able to reveal how they could be removed by macrophages in an *in vitro* setting. As polykaryons have been shown to be able to engulf severely large targets, we hypothesized senescent cells as giant target would require a giant phagocyte to be removed from the tissue. Therefore, we suggested polykaryons may be able to engulf senescent cells. To examine, whether polykaryons would take up senescent cells we set-up a co-culture with the two cell types. Senescence was induced in MEFs treated with Palbociclib. The green fluorescent senescent actinGFP MEFs were imaged in co-culture with red fluorescent tdTomato⁺ polykaryons (Figure 5-11A). The same cell was followed over time for 48 hours. The co-culture showed giant macrophages were able to engulf senescent cells in a very slow process. This effect could be quantified by measuring the

Results

green fluorescent cell area over time. As an additional control, we included normal unfused BMDMs. BMDMs were not able to engulf senescent cells which has been shown earlier in this study (see 5.1.2). However, polykaryons were able to engulf senescent cells. The quantified cell area of the senescent cells significantly decreased over time whereas it stayed constant in the co-culture with BMDMs and the single culture of senescent cells alone (Figure 5-11B). These results indicate, BMDMs and polykaryons differ in their general phagocytic capacity to engulf cellular targets. To further assess the general phagocytic properties of polykaryons we set-up the co-culture with proliferating cells instead of senescent cells. Proliferating cells are no natural target for BMDMs [328]. Moreover, in our set-up BMDMs do not engulf proliferating cells. No significant difference in cell area could be detected between the single culture of proliferating cells, neither in the presence nor absence of macrophages. However, polykaryons were able to take up the proliferating cells. We could quantify a significant decrease of the cell area in the presence of polykaryons compared to the single culture control over time (Figure 5-11C). This indicated a strong global phagocytic capacity of polykaryons.

As polykaryons and BMDMs showed substantial differences in their general phagocytic capacity regarding timing and target specificity, we further evaluated the metabolic properties of polykaryons compared to BMDMs. An extracellular flux analysis should reveal potential differences in mitochondrial respiration. Polykaryons show a lower Oxygen Consumption Rate (OCR) (Figure 5-11D), suggesting their mitochondrial aerobic respiration was impaired. Further, we generated an energy profile of the two cell types. The relative utilization of the two energy pathways of the two populations was determined under both baseline and stressed conditions. The response to an induced energy demand resulted in their metabolic potential or energy profile. This energy profile indicated a rather quiescent phenotype for polykaryons and a more energetic phenotype for BMDMs (Figure 5-11E).

In summary, polykaryons showed the ability to engulf senescent cells. However, this process was comparably slow which was supported by the quiescent mitochondrial aerobic metabolism of polykaryons in general. A caveat of this system was that polykaryons did not seem to select a suitable target but rather had highly phagocytic properties under any circumstances. If these cells are suitable for therapeutic applications needs to be revealed by analyzing the phagocytic capacity of polykaryons in an *in vivo* system.

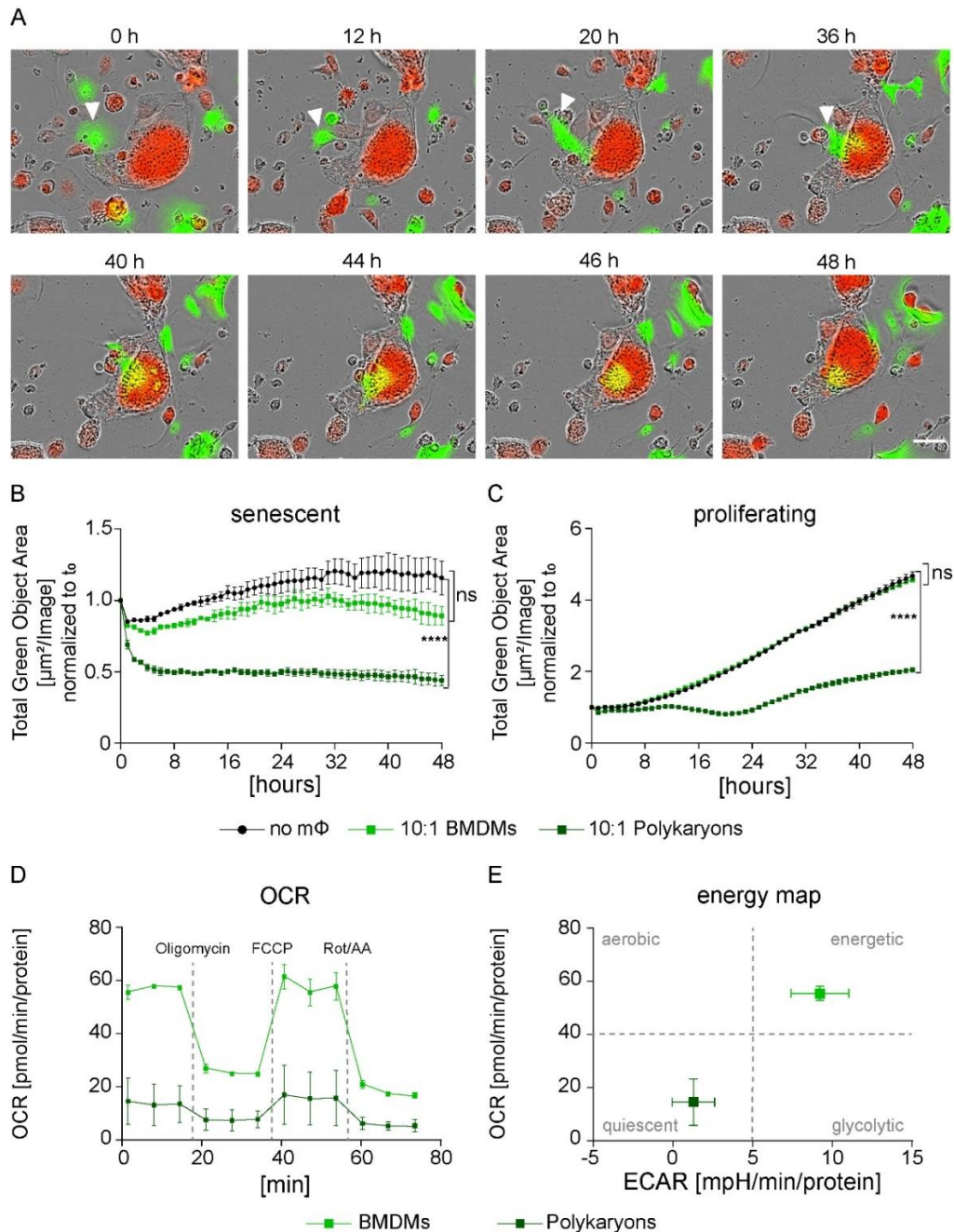


Figure 5-11: Polykaryons engulf senescent cells.

A Senescence was induced in actinGFP MEFs by treatment with Palbociclib. Senescent MEFs were co-cultured with polykaryons isolated from tdTomato⁺ mice in a ratio of 10:1 polykaryons to senescent cells and imaged over 48 hours. In each image group, the same field of view is shown across time. Data are representative of three independent experiments. The uptake of the senescent cell is indicated by a white arrow. The scale bar indicates 50 μm . **B** Quantification of the green fluorescent signal of senescent cells in the co-culture with BMDMs and polykaryons. Data are representative of three independent experiments. **C** Quantification of the green fluorescent signal of proliferating cells in the co-culture with BMDMs and polykaryons. **D** Measurement of mitochondrial aerobic respiration profile. The cells were sequentially treated with oligomycin, FCCP and rotenone/antimycin A (Rot/AA) and OCR was determined. **E** Energy phenotype profile. OCR and ECAR (extracellular acidification rate, not shown alone) are plotted together to generate an energy phenotype profile to compare BMDMs and polykaryons. Data in **B** and **C** are representative of three independent experiments. All values are means \pm SEM. Statistically significant differences were determined by two-way ANOVA with Bonferroni correction. For **B**, **C**, **D** and **E** $n=3$ biological replicates.

5.3 A model system to analyze pathogenic aggregate removal by macrophages

The overall goal of the second part of this thesis was to decipher the role of macrophages for the removal of mutant Huntingtin (Htt) aggregates in a defined and tractable cellular model. Htt aggregates were used as an example for how macrophages interact with aggregate-bearing cells. Thereby this thesis will help to acquire improved understanding of the features of Huntington's disease (HD) and potentially other neuropathologic aggregate-driven diseases.

Among the many risk factors for neurodegeneration, the aging process itself has by far the most influence. The pathogenesis of most neurodegenerative diseases is associated with the nine biological hallmarks of aging as outlined in the introduction. Moreover, senescent microglia, astrocytes and neurons as well as the occurrence of several cellular senescence markers such as telomere shortening, SASP factors, a persistently activated DNA damage response, increased SA- β -gal and increased p16^{INK4A}, have been reported in age-related neurodegenerative diseases [240].

Protein aggregation is a hallmark of many neurodegenerative disorders [329], including HD [330]. The *in situ* structure of protein aggregates inside cells has been investigated to gain insight into the role of inclusion bodies for their pathology and their deleterious cellular effects [267]. Although HD primarily affects the brain, Htt aggregates have been found in different peripheral cells and tissues. Also in other cell types they show detrimental effects, eventually leading to cell death [331], for example in the pancreas [332], in skeletal and heart muscle cells [333] and in fibroblasts [334]. Several therapeutic approaches aim to reduce the abundance of aggregates via immunotherapy. Efforts to develop evidence-based treatment strategies for neurodegenerative diseases are ongoing, but neither highly effective treatments nor potent protective approaches have yet been identified [240].

However, removal of protein aggregates associated with neurodegenerative diseases has not only been approached by pharmacological interventions [335, 336]. Assorted approaches have tried to clear the aggregates with the help of surrounding cells and several of these have shown the importance of macrophages for the aggregate removal process. For example, Fiala *et al.* showed macrophages originating from the blood can enter the brain and engulf amyloid peptides associated with Alzheimer's disease (AD) [264]. Intriguingly, macrophages isolated from the blood of AD patients are less effective at clearing amyloid peptides than those from unaffected individuals [337]. Macrophages have also been shown to be associated with alpha-synuclein (α -SYNC) clearance in the gastrointestinal tract. Phillips *et al.* suggested macrophages play an active role in removing α -SYNC

aggregates that accumulate with age in the neural circuitry of the gut. Their observations further indicated this housekeeping response does not clear the protein sufficiently to eliminate all synucleinopathies or their precursor aggregates from the healthy aging gastrointestinal tract [265]. However, none of these type of studies to date has been implemented to reveal the potential importance of macrophages for HD.

The development of cellular models to examine the mechanisms involved in HD disease will help to gain an improved understanding of HD pathology in general. The study of peripheral cells could provide new insights which help to convey HD pathology from a cellular model to what occurs in the brain. This could further aid to apply therapeutic strategies from peripheral systems to targeting the brain.

5.3.1 Macrophages trigger aggregate elimination from fibroblasts

In HD, mutant Htt is ubiquitously expressed throughout the body and has been shown to be associated with abnormalities in peripheral tissues which are important features of the pathophysiology of HD. Studying the interaction of Htt aggregates in such a peripheral cell type will likely enhance our general understanding of the pathogenesis of the disease [338].

To examine the process of aggregate removal in a reduced complexity cell biological approach, we set-up an *in vitro* system co-culturing fibroblasts and macrophages. As described above, macrophages have been shown to play a fundamental role in aggregate removal of other neurodegenerative diseases. Moreover, fibroblasts manifest cellular dysfunctions similar to neural HD cells [333, 335] and provide tractable, convenient and reproducible characteristics. For our study, we used three different types of aggregates. We applied two variants of the Htt protein, a variant with 27 glutamine repeats (Htt27Q) and a variant with 97 glutamine repeats (Htt97Q). The expansion of a polyQ stretch in the N-terminal region of Htt results in aggregation of the mutant protein and its length defines the onset and severity of the disease in humans. The expansion up to 35 repeats is considered normal, whereas an expanded CAG repeat of greater than 35 units causes characteristic neurological symptoms [339]. Accordingly, we are applying one variant not resulting in a disease phenotype (Htt27Q), whereas the other variant has been shown to cause severe HD in humans (Htt97Q) [340]. The Htt aggregates were complemented by an artificial aggregate, ABIN1. ABIN1 is a polyubiquitin binding protein, which is not disease related and has been shown to form aggregates when transfected into cells (Dr. A. Alpi, MPI-Biochemistry, unpublished). All protein aggregates are GFP-tagged. A GFP vector was included, as GFP is non-aggregating and therefore

Results

provides a key control for interpretation of the co-culture system. The basic assay platform is depicted in Figure 5-12A. Fibroblasts were seeded, followed by transfection with different types of aggregates and GFP-control. After the expression of green fluorescent aggregates was observed, macrophages were added to the culture in different ratios to the fibroblasts. Co-cultures were recorded via live-cell imaging and the number of green fluorescent aggregate objects was tracked over time. As described below, different variations of this culture system were used to further explore the interaction between macrophages and aggregate-bearing fibroblasts.

Representative images of WT fibroblasts, transfected with the different constructs are shown in Figure 5-12B. The upper panel shows the control: a single culture of aggregate-bearing fibroblasts at 48 hours post-transfection in the absence of macrophages. The lower panel shows a co-culture in the presence of macrophages. The GFP signal does not change over time independent of the presence or absence of macrophages in the culture. By contrast, for the different types of aggregates, fibroblasts co-cultured in the presence of macrophages showed a time-dependent reduction of green fluorescent objects, implicating an aggregate removal mechanism(s) mediated by the presence of macrophages.

Aggregate removal over time was quantified which is shown in Figure 5-12C. The number of aggregates in the conditions with Htt aggregates and artificial aggregates is significantly decreased in the co-cultures with macrophages over time. On the contrary, the number of aggregates in the single culture of transfected fibroblasts in the absence of macrophages stayed constant, indicating the fibroblasts alone were not able to eliminate the aggregates. Moreover, object numbers of the GFP-vector control in the presence of macrophages also stayed constant over time. At first glance, these results suggest the aggregate decline involves a macrophage-dependent trigger causing aggregate removal from fibroblasts. If this holds true, increasing the number of input macrophages should be approximately proportional to the rate of aggregate removal. In other words, more macrophages should lead to enhanced, and/or faster removal. Indeed, this was the case. Figure 5-12D shows the higher the macrophage number applied to the fibroblasts, the lower the aggregate count after 48 hours. However, a caveat of the system is the transient transfection of protein aggregates. This results in a variability in aggregate removal efficiency between the individual experiments (Figure 5-12C and Figure 5-12D). This correlation indicates the process of aggregate removal can be titrated using increasing numbers of macrophages.

In summary, the different aggregates used in this study were transiently expressed in fibroblasts over a time course of 48 hours. Macrophages specifically triggered aggregate elimination from fibroblasts in a quantifiable manner. However, as this approach is a simple cell biological model, the next step was to attempt a similar type of experiment in primary cortical neurons.

Results

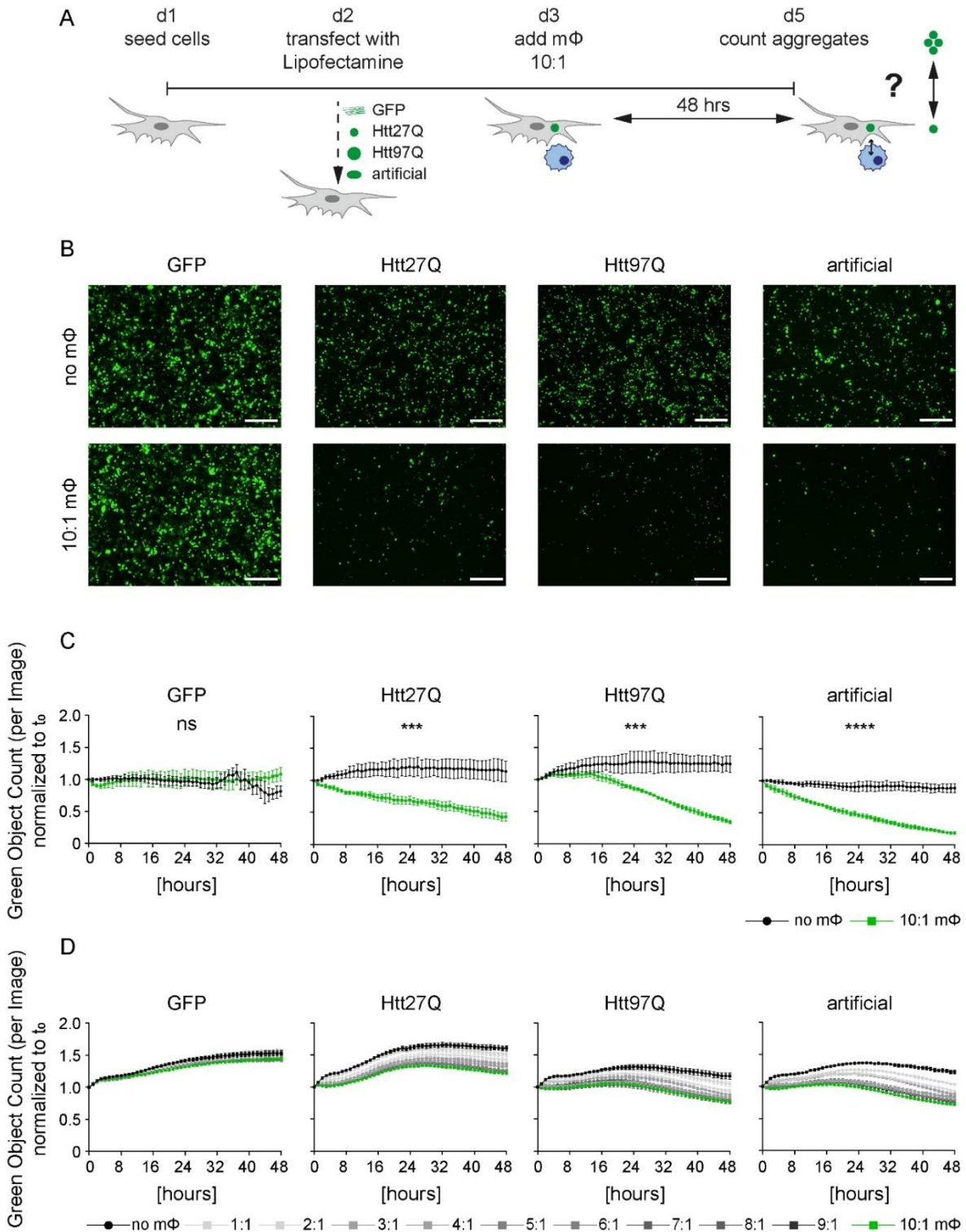


Figure 5-12: Macrophages trigger aggregate elimination from fibroblasts.

A Schematic overview of the overall experimental design. Fibroblasts were seeded 24 h prior to transfection. Cells were transfected with GFP (negative control, non-aggregating protein), Huntington aggregates Htt27Q and Htt97Q (Htt with 27 or 97 glutamine repeats fused to GFP) and artificial protein aggregates (ABIN1, artificially aggregating when transfected in cells). After 24 h, the cells expressed green fluorescent protein aggregates. BMDMs were added in a ratio of 10:1 and the co-culture was imaged once every hour for 48 h, in an IncuCyte live-cell imager. The number of green objects was

determined using the corresponding software. **B** Representative images of fibroblasts transfected with the different constructs in single culture and in co-culture with macrophages. Scale bars indicate 300 μm . **C** Quantification of green fluorescent object counts in transfected fibroblasts in single culture and in co-culture with macrophages. Data are representative of three independent experiments. **D** Quantification of green fluorescent object counts in transfected fibroblasts in single culture and in co-culture with different amounts of macrophages. Data are representative of two independent experiments. All values are means \pm SEM. Statistically significant differences were determined by two-way ANOVA with Bonferroni correction; *** $p < 0.001$; **** $p < 0.0001$; $n=3$ biological replicates.

5.3.2 Studying aggregate removal in neuronal systems

We next developed a similar experimental set-up with neurons, potentially providing a more relevant system for HD in the nervous system. In collaboration with Kerstin Voelkl (MPI Neurobiology), we isolated primary cortical neurons from E14 embryos and introduced mCherry-tagged aggregating Htt (Htt25Q, Htt97Q) via lentiviral transduction. Primary microglia, isolated from newborn pups, were added to the neurons as phagocytic cell type. We hypothesized microglia, being the main phagocytic cell in the brain, could also remove the aggregates from neurons. The experimental set-up is depicted in Figure 5-13A. Representative images of the transduced neurons in single culture and co-cultures are shown in Figure 5-13B. The upper panel displays neurons transduced with the different aggregates at the beginning of the experiment. The panel in the middle shows the transduced neurons after 48 hours. For all transduced constructs, we observed significant death of neurons in the single culture after 48 hours. These images indicate neurons could not tolerate Htt aggregates and the mCherry control. However, the presence of microglia seemed to stabilize all transduced constructs in the co-culture which is shown in the lower panel. This stabilizing effect of microglia over time was quantified and is depicted in Figure 5-13C. Although microglia are physiologically the phagocytic cells of the central nervous system, we did not observe the effect of aggregate removal in our experimental set-up, but rather an unexpected stabilization effect of microglia for aggregates in neurons. To further investigate the process of aggregate removal in a neuronal system, we replaced microglia with BMDMs, the macrophage type we used at the beginning (Figure 5-13D) [341] which showed the ability to remove aggregates in the preceding assay (see 5.3.1). BMDMs significantly engulfed neurons over time. However, although aggregate numbers decreased over time at the same rate in the absence and the presence of macrophages, this is a consequence of the overall effect of the macrophages eliminating neurons and their contents. BMDMs seemed to attack neurons in all conditions including the mCherry control. Thus, the co-culture scenario to study Htt aggregate removal in primary neurons turned out to be unsuitable for the purposes of determining the mechanisms of aggregate removal. We

therefore decided to continue to examine aggregate removal as a cell biological phenomenon in a co-culture system with fibroblasts and BMDMs throughout this thesis.

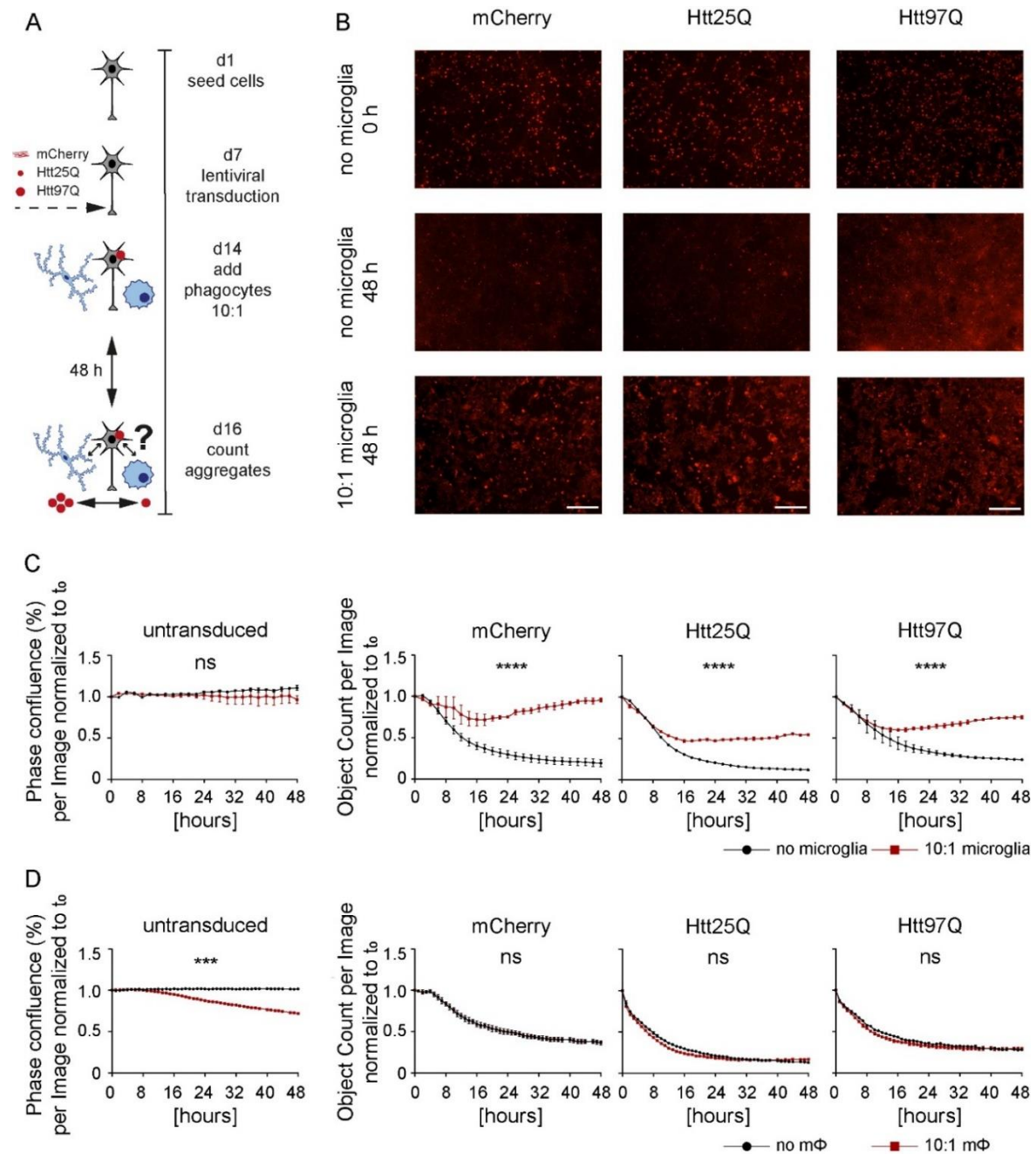


Figure 5-13: Microglia enhance aggregate stability in cortical neurons.

A Schematic overview of the experimental design. Cortical neurons were seeded and differentiated for 7 days. Cells were transduced with lentivirus encoding mCherry or the Huntington aggregates Htt25Q and Htt97Q (Htt with 25 or 97 glutamine repeats fused to mCherry). After 7 additional days the cells expressed fluorescent protein aggregates. Microglia and BMDMs were added in a ratio of 10:1 and the co-culture was imaged once every hour for 48 h in an IncuCyte live-cell imager. The number of red objects was determined using the corresponding software. **B** Representative images of neurons transduced with the different constructs in single culture and in co-culture with primary microglia. Scale bars indicate 300

μm . **C** Quantification of the red fluorescent object counts of transduced neurons with and without microglia. **D** Quantification of the red fluorescent object counts of transduced neurons with and without macrophages. For **C** and **D** data are representative of three independent experiments. All values are means \pm SEM. Statistically significant differences were determined by two-way ANOVA with Bonferroni correction; **** $p < 0.0001$; $n=3$ biological replicates.

5.3.3 Manipulation of aggregate formation conditions

Up to this point, the experiments showing aggregate removal by macrophages relied on a transient transfection approach; in this case with Lipofectamine. Given that liposome-mediated transfection can influence cell physiology [342], we sought an alternative approach to analyze the aggregate removal process. Thus, we developed a tetracycline (Tet) regulated system to induce Htt aggregate formation. Using the piggyBac system [268], we generated a stable 3T3 line expressing an *HTT* version with 94 CAG repeats fused to CFP under control of the Tet-responsive promoter (4.5.3). Addition of doxycycline to the system initiates the transcription of *HTT*, resulting in the expression of Htt94Q aggregates in the cell (Figure 5-14A). We followed aggregate induction in fibroblasts over time by live-cell imaging. After 16 hours of doxycycline induction, the first aggregates were observed. The optimal expression rate of aggregates was observed after 32 hours (Figure 5-14B), therefore this time was set as starting point for the co-culture. The co-culture between aggregate-bearing fibroblasts and macrophages was repeated as described in 5.3.1. Representative images of the single culture of fibroblasts alone (left) and the co-culture with macrophages (right) after 48 hours are shown in Figure 5-14C. Comparable to Lipofectamine induced aggregates (see Figure 5-12), the doxycycline-induced aggregates remained constant in a single culture of fibroblasts over 48 hours. In the co-culture with macrophages, less aggregates were observed, indicating macrophages removed the aggregates. This effect was quantified by counting green fluorescent aggregates using life-cell imaging over a 48 hour time increment (Figure 5-14D). The cells were recorded by life-cell imaging for 48 hours and the green fluorescent aggregates were counted. The number of aggregates in the single culture of transfected fibroblasts alone was slightly increased with progression of time. On the contrary, the number of aggregates was significantly decreased in the co-culture with macrophages over time. Collectively, these experiments indicated aggregate removal from fibroblasts by macrophages is independent of the means of aggregate induction. Moreover, the removal of aggregates from transiently transfected fibroblasts was not overtly influenced or facilitated by Lipofectamine.

Results

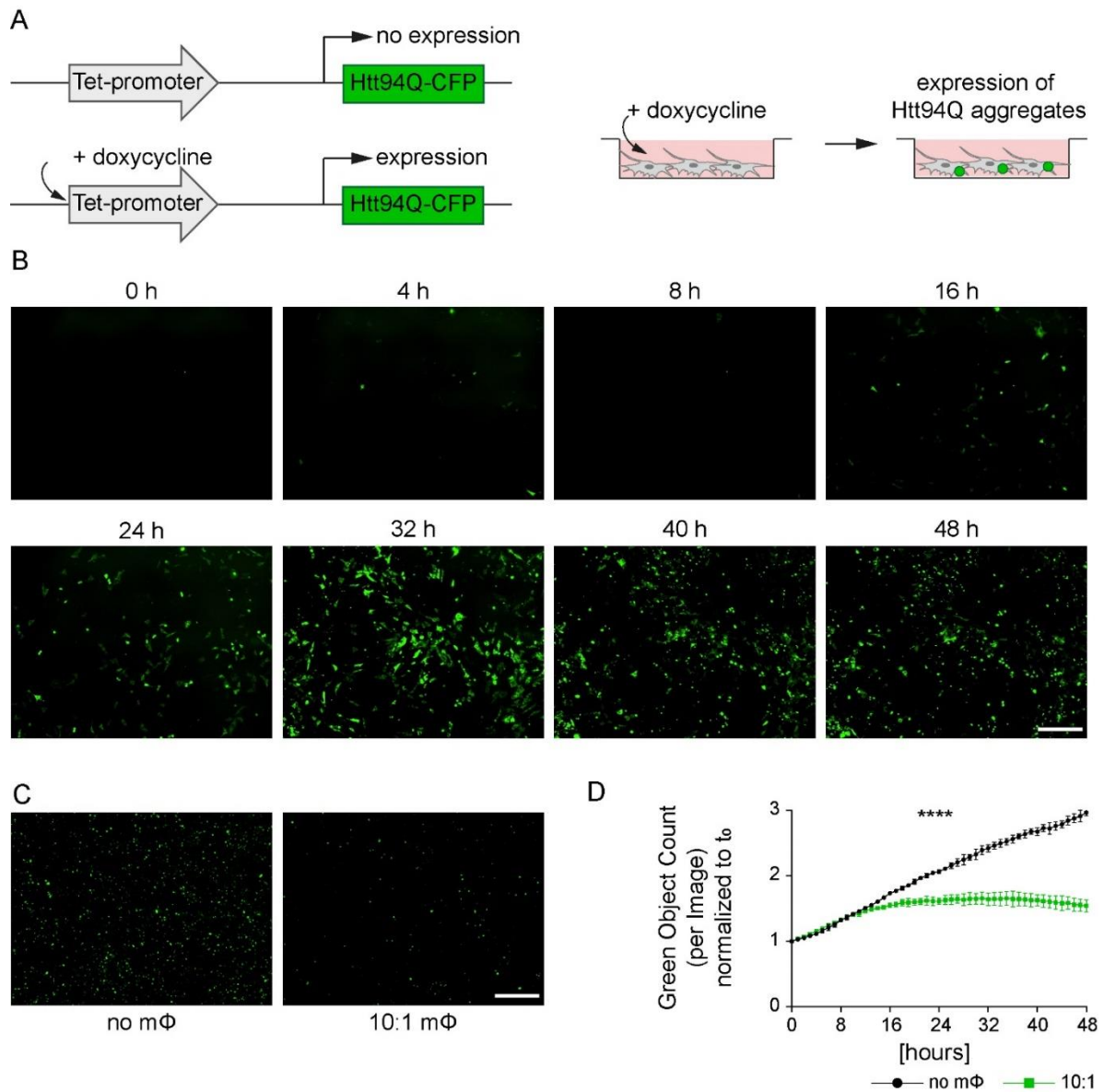


Figure 5-14: Time-dependent induction of aggregate formation by a Tet-ON system.

A CFP-tagged Htt version with 94 glutamine repeats (Htt94Q) is fused to a Tet-promoter. Upon addition of doxycycline, the Tet-promoter gets activated and drives the expression of the downstream positioned Htt94Q-CFP gene. **B** Representative images of time dependent induction of Huntington aggregates (Htt with 94 glutamine repeats fused to CFP) in fibroblast single cultures after treatment with doxycycline. **C** Representative images of fibroblasts after doxycycline induction in single culture and co-culture with macrophages. Macrophages were added 32 h after doxycycline induction. Scale bar indicates 300 μm . **D** Quantification of green fluorescent object counts of aggregate expressing fibroblasts in single culture and co-culture with macrophages. Data are representative of two independent experiments. All values are means \pm SEM. Statistically significant differences were determined by two-way ANOVA with Bonferroni correction; **** $p < 0.0001$; $n=3$ biological replicates.

5.3.4 Aggregate removal requires direct cell contact between macrophages and fibroblasts

Tissue macrophages recognize and engulf apoptotic cells in a 'silent' non-inflammatory fashion. These events require the display of "eat-me" signals on the apoptotic cell surface, the most fundamental of which is phosphatidylserine (PtdSer) [343]. Macrophages are recruited and migrate to apoptotic and injured cells in response to cues delivered by the apoptotic cells which release a set of so-called "find-me" signals [344]. Recent findings indicate macrophages do not always wait for cells to die before initiating a phagocytic attack. They may also engulf living cells if these expose sufficient levels of externalized PtdSer. In any case the engulfment of cells requires direct binding of the phospholipid and therefore direct cell contact [345]. We hypothesized, Htt aggregate removal requires direct contact between a macrophage and aggregate-bearing cell, as opposed to an indirect event. Indirect removal of aggregates could be a possibility in this system if macrophages consumed key metabolites in the cultures. Then stress response pathways would activate proteostasis pathways in the aggregate-bearing cells; in this case, the macrophage-mediated effect would be entirely indirect. We therefore performed co-cultures between aggregate-bearing fibroblasts and macrophages in a transwell approach. In this set-up, both cell types are present in the well, but direct cell contact is prohibited by the transwell insert. The fibroblasts were transfected with the aggregate constructs as described in 5.3.1 and the macrophages were seeded on a transwell insert that was subsequently added to the well (Figure 5-15A). Aggregate counts were captured via live-cell imaging over time and the number of green fluorescent objects was quantified. For all conditions the aggregate counts stayed constant over time independent of the presence or absence of macrophages (Figure 5-15B). This result indicates macrophages cannot trigger aggregate removal from fibroblasts via soluble factors. The aggregate removal from fibroblasts requires direct cell contact between fibroblasts and macrophages.

Results

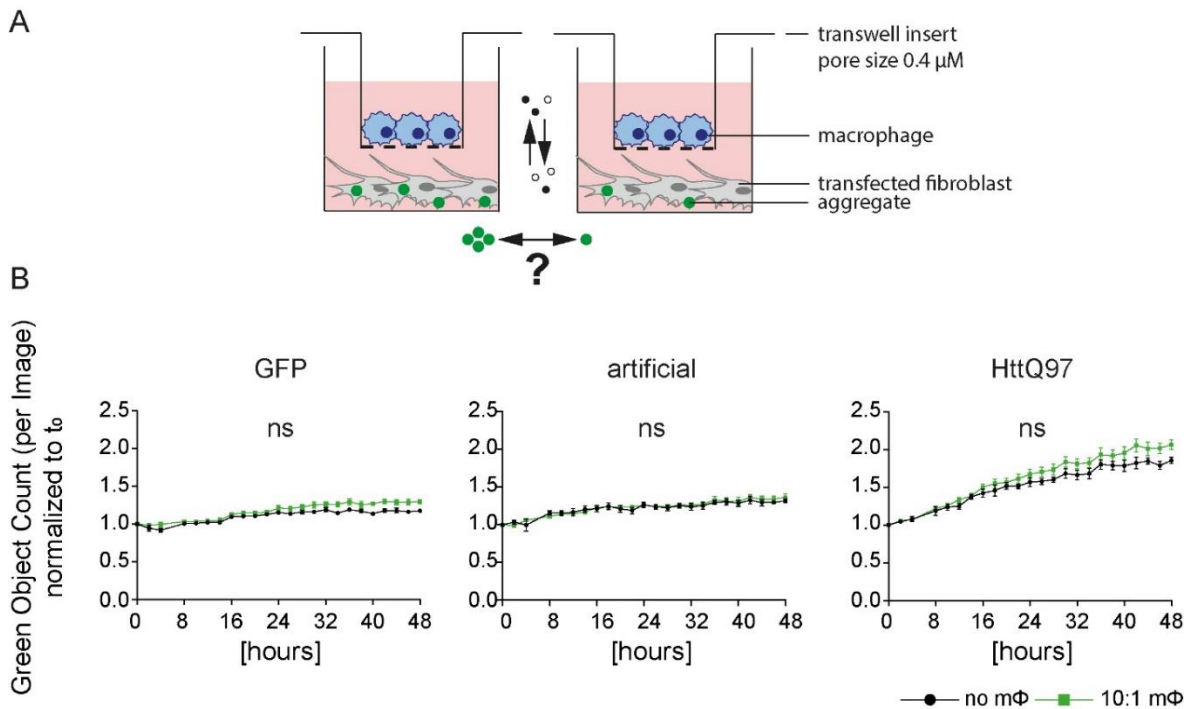


Figure 5-15: Direct contact is required for macrophage-mediated aggregate removal.

A Fibroblasts were seeded and transfected with the aggregate constructs. A transwell insert with the pore size of 0.4 μM containing BMDMs was placed into the well. **B** Quantification of the green fluorescent object counts of aggregate expressing WT 3T3 fibroblasts in single culture and co-culture with macrophages. Data are representative of three independent experiments. All values are means \pm SEM. Statistically significant differences were determined by two-way ANOVA with Bonferroni correction. $n=3$ biological replicates.

5.3.5 Use of bystander cells to analyze aggregate removal

So far, our experiments examined aggregate removal only between macrophages and the aggregate-bearing target cell. However, cell removal by macrophages in tissues causes bystander effects. For example, apoptotic tumor cells have been shown to trigger macrophage-mediated clearance of surrounding non-apoptotic bystander cells [346]. We wanted to decipher whether also the aggregate-bearing cells would have bystander effects on a third neutral cell line in our experimental set-up. We further wanted to see whether the efficiency of the aggregate removal could be disturbed by the presence of neutral cells in the culture. Therefore, we generated mCherry “calibrator” cell line using the Flp-in system (4.5.1). These cells constantly express mCherry, which is evenly distributed throughout the cell body. The general experimental set-up was performed as described in 5.3.1.

In this assay, the calibrator cells were added at the same time as the macrophages to the aggregate-bearing cells. The calibrator was red (mCherry) and the aggregate green (GFP), while the macrophages remained unlabeled. This system allowed coincident monitoring of the number of red

calibrator cells across time in comparison to the aggregates (Figure 5-16A). The number of aggregates in transfected fibroblasts in co-culture with calibrator cells but in the absence of macrophages slightly increased over time (Figure 5-16B). This indicates the calibrator cells did not interfere with aggregate stability in the transfected fibroblasts. Further, the number of aggregates significantly decreased over time in the co-culture with red calibrator cells in the presence of macrophages, whereas the GFP-vector control stayed constant. This suggested the removal of aggregates from fibroblasts is independent of the presence of a calibrator cell line.

The next question centered on the number of calibrator cells in the cultures. If macrophage and aggregate-bearing cells did not influence the calibrator (in any way), we would expect to find an increase in the number of dividing calibrator cells over time. Therefore, we quantified the red calibrator cell object count to reveal whether the aggregate bearing cells have bystander effects which trigger macrophages to also engulf or kill the calibrator cells. Over time, the number of red bystander cell objects slowly increased in either the presence or absence of macrophages. No significant differences could be quantified compared to controls (Figure 5-16C). These findings suggested the aggregate bearing cells did not trigger macrophages to remove a neutral cell from the culture. In summary, the neutral calibrator cells neither seemed to interfere with the aggregate stability in the fibroblasts, nor the aggregate removal process mediated by macrophages.

Results

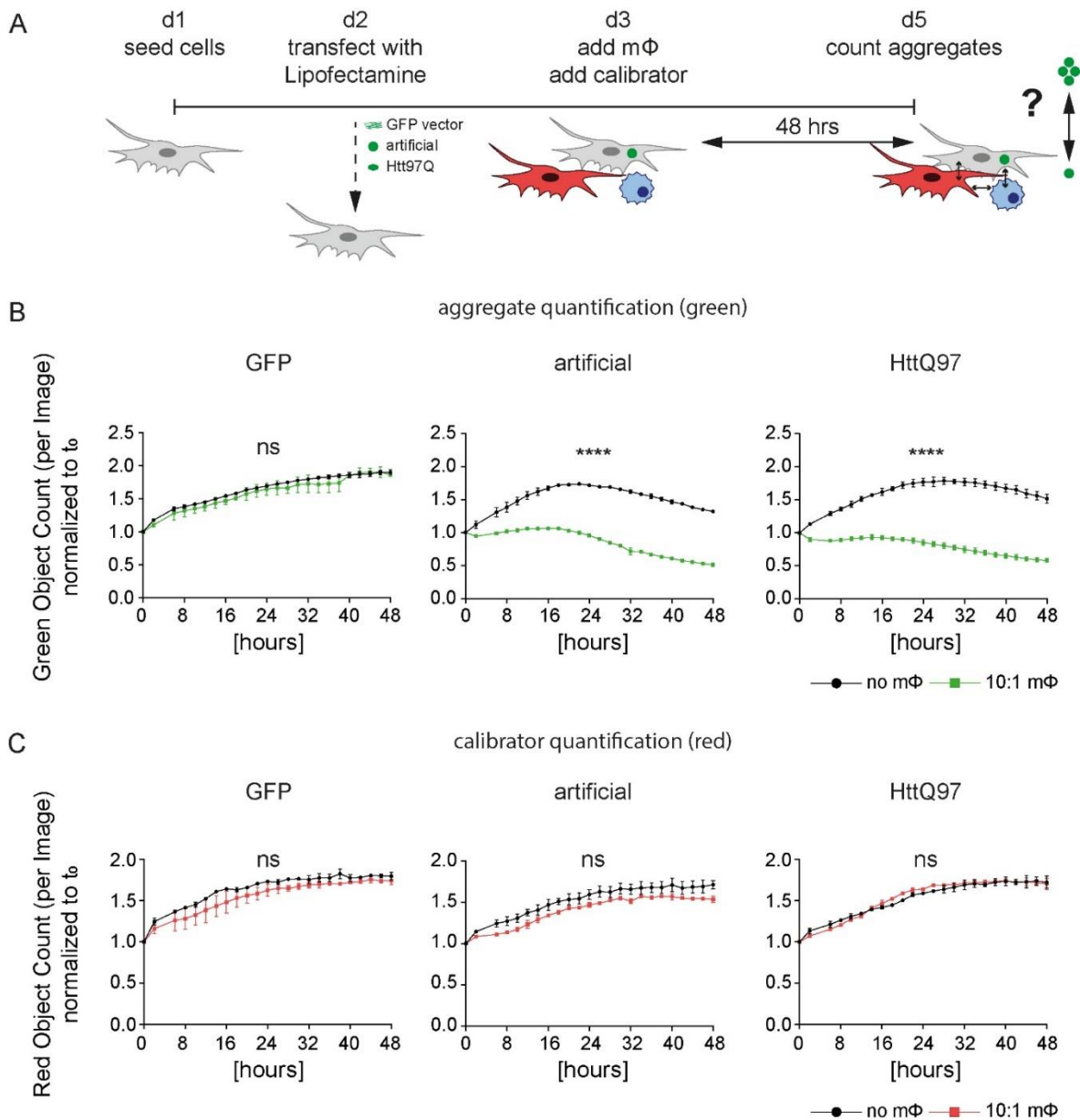


Figure 5-16: Macrophages target aggregate bearing cells in the presence of a “neutral” bystander cell.

A Schematic overview of the overall experimental design to using calibrator bystander cells to quantify aggregate removal. Fibroblasts were seeded 24 h prior to transfection. Cells were transfected with GFP, the Huntington aggregate Htt97Q or artificial protein aggregates. After 24 h, the cells expressed protein aggregates. At this point, BMDMs and mCherry Flp-in fibroblasts (calibrator) were added in parallel in a 10:1 ratio (macrophages:transfected fibroblasts) and 4:1 ratio (red calibrator: transfected fibroblasts) and the co-culture was imaged once every two hours for 48 h in an IncuCyte live cell imager. The number of green and red objects was determined using the corresponding software. **B** Quantification of the green fluorescent object counts of transfected fibroblasts in single culture and co-culture with macrophages. **C** Quantification of the red fluorescent cell object counts of mCherry Flp-in fibroblasts in co-culture with transfected fibroblasts and in culture with and without macrophages. For **B** and **C** data are representative of three independent experiments. All values are means \pm SEM. Statistically significant differences were determined by two-way ANOVA with Bonferroni correction; **** $p < 0.0001$; $n=3$ biological replicates.

5.3.6 Aggregate removal is not mediated by the cell intrinsic apoptosis pathway or LAP

We went on approaching further understanding of the mechanism by which macrophages trigger aggregate removal from fibroblasts. Therefore, we hypothesized one plausible pathway involved was the induction of the intrinsic apoptosis pathway in aggregate-bearing cells, triggering conventional efferocytosis (noting the decisive experiments showing direct cell to cell contact was required for aggregate removal). In this line of thinking, it is important to note that fibroblasts lack the molecular machinery for inflammasome-mediated caspase-1 activation and pyroptosis [347]. However, we rendered ferroptosis as an unlikely pathway as the cell culture media is replete with cysteine and no ferroptosis-inducing agents were present. Thus the apoptosis options for fibroblasts were largely centered on the intrinsic mitochondrial-mediated caspase pathway. We therefore disabled this pathway. We replaced the WT fibroblasts in our set-up by Bax Bak DKO fibroblasts being transfected with the protein aggregates. These cells cannot undergo intrinsic mitochondrial-mediated apoptosis [348] (Figure 5-17A). If macrophages triggered aggregate removal from fibroblasts by the induction of intrinsic apoptosis, it should be evident in our set-up. The co-culture assay was repeated as described in 5.3.1. In the single culture of aggregate bearing fibroblasts in the absence of macrophages the green object counts for all transfected constructs slightly increase over time. However, the object counts in the co-culture in the presence of macrophages showed a significant decrease in green fluorescent aggregates over time. The aggregate counts in the GFP-vector control slightly increased over time independent of the presence or absence of macrophages (Figure 5-17B). These results indicated that macrophages do not trigger the removal of protein aggregates by inducing intrinsic apoptosis to the fibroblasts.

A newly-described pathway for ingestion of large particulate structures is termed LC3-associated phagocytosis (LAP). LAP is mediated by the recognition of a variety of particulates, including protein aggregates [349] (Figure 5-17C). Engulfment of particulates via toll-like receptors (TLRs), phosphatidylserine (PtdSer), and Fc-receptor (FcR), respectively, triggers recruitment of the Rubicon-containing Class III PI3K complex to the cargo-containing phagosome. Rubicon also binds and stabilizes the NOX2 complex. Rubicon activity is required for recruitment of the downstream ubiquitin-like conjugation systems to generate LC3-II and localize it to the cargo-containing phagosome to form the LAPosome, where the target is eventually digested [350]. We therefore hypothesized the protein aggregates activate LAP in the macrophages, consequently triggering the removal of protein aggregates in fibroblasts. The co-culture assay described in 5.3.1 was repeated using macrophages lacking Rubicon. As Rubicon is essential for the formation of the PI3K complex

Results

and subsequent formation of the LAPosome, *Rbcn*^{-/-} macrophages would be disabled to trigger aggregate removal via LAP. However, the co-culture with *Rbcn*^{-/-} macrophages showed a significant decrease in green fluorescent aggregates over time. The aggregate counts were slightly increased in the single culture with transfected fibroblasts alone and also in the GFP-vector control (Figure 5-17D). Thus, macrophages did not trigger the removal of protein aggregates from fibroblasts via LAP.

The caveat of these experiments is that there are various options which could regulate the aggregate removal mediated by either of the two cell types in our system. Macrophages did not seem to induce cell death by the induction of intrinsic apoptosis to the fibroblasts and seemed to regulate aggregate removal in different ways than LAP. Particle internalization in general is initiated by the interaction of a diversity of receptors capable of stimulating phagocytosis. Moreover, most particles are recognized by more than one receptor and these receptors are capable of cross-talk and synergy which further complicates our understanding [351]. The possibilities to narrow down the potential underlying mechanisms enabling aggregate removal from fibroblasts by macrophages are limited by the availability of suitable cell lines and remain to be implemented into our experimental set-up.

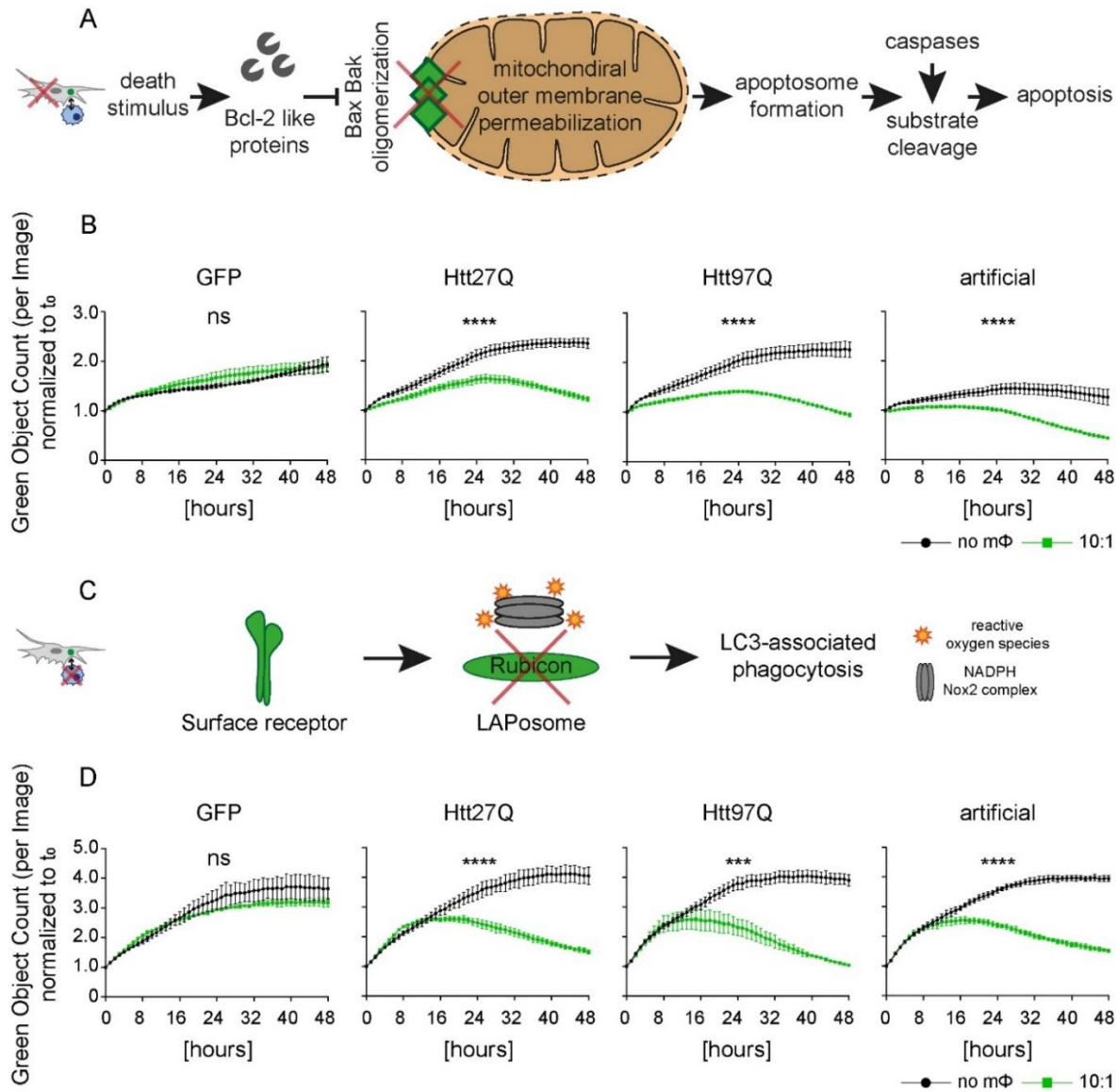


Figure 5-17: Aggregates in cells lacking the intrinsic mitochondrial apoptosis pathway are removed by macrophages, while LC3 mediated phagocytosis in macrophages is not required.

A Schematic overview of the mechanism targeted in the assay. In healthy cells, the BCL-2-like pro-survival proteins safeguard mitochondrial outer membrane integrity and cell survival by preventing the activation of Bax and Bak. Under conditions of stress, the BH3-only proteins are activated transcriptionally and/or posttranscriptionally to induce apoptosis by releasing Bax and Bak from inhibition by the BCL-2-like proteins. Once activated, Bax/Bak cause mitochondrial outer membrane permeabilization (MOMP) with consequent release of apoptogenic molecules, like cytochrome c. These are able to cause activation of the caspase cascade that eventually culminates in cellular demolition. This entire process is blocked in the Bax/Bak DKO fibroblasts used in the assay. **B** Quantification of the green fluorescent object counts of transfected Bax/Bak DKO fibroblasts in single culture and co-culture with macrophages. **C** Schematic overview of the mechanism targeted in the assay. LC3-associated phagocytosis (LAP) is a pathway for ingestion of particulate structures. After recognition of extracellular cargos by specific surface receptors, they are ingested into phagosomes. During LAP these are called LAPosomes. One of the components required specifically for LAP is Rubicon (encoded by *Rbcn*). The ingestion is terminated by the fusion with lysosomes by which extracellular particle is degraded. In the *Rbcn* KO macrophages, this process of LAP is prohibited. **D** Quantification of the green fluorescent object counts of transfected fibroblasts in single culture and co-culture with *Rbcn*^{-/-} macrophages. For **B** and **D** data are representative of three independent experiments. All values are means \pm SEM. Statistically significant differences were determined by two-way ANOVA with Bonferroni correction; *** $p < 0.001$; **** $p < 0.0001$; ns = not significant; n=3 biological replicates.

5.3.7 Macrophages do not seem to kill fibroblasts upon aggregate removal

During preceding experiments presented so far, we were able to exclude the induction of intrinsic apoptosis by macrophages to the aggregate-bearing cells and aggregate clearance via LAP as potential mechanisms. Moreover, we showed direct contact was required. There is a plethora of possible underlying mechanisms regarding different types of cell death and various types of phagocytosis but testing via candidate approaches (for example, individual knockouts in phagocytic receptors, of which there are ~100 [352]) is unfeasible. We decided to use a focused approach to ask the basic question of whether the aggregate bearing cells die at all upon aggregate removal; following which, the aggregate and cell debris would be eliminated.

To quantify cell death of aggregate bearing cells, we modified the basic structure of the calibrator bystander experiments. This time, we transfected the mCherry calibrator cell line with the aggregates or the GFP-vector control. Unlabeled macrophages were added, and the green fluorescent aggregate object count and the red fluorescent cell object count were recorded over time. The assay procedure is depicted in Figure 5-18A. In this way, we expected to detect the potential death of the aggregate carrying cells, which would be indicated by a decline in the red fluorescent cell object count matched with a decrease in the green object count. First, we verified the basic experimental set-up worked comparably to the other cell lines used herein. Therefore, we quantified the green fluorescent object count over time in the absence and presence of macrophages (Figure 5-18B). The number of green fluorescent aggregates slightly increased over time in the transfected calibrator cells in the absence of macrophages. This indicates, the calibrator cell line tolerated the protein aggregates in a corresponding way to the other fibroblast cell lines used throughout this study (see 5.3.1; 5.3.6). In the presence of macrophages, however, the number of aggregates significantly decreased over time. According to our previous findings, the number of green fluorescent objects for the GFP-vector control did not show any changes in green object numbers mediated by the presence or absence of macrophages. This indicates the assay worked as expected and the mCherry calibrator cells showed results comparable to the other used fibroblast cell lines throughout this study (see 5.3.1; 5.3.6). Next, we quantified the red fluorescent cell object count to quantify potential cell death overtime which did not significantly differ between the transfected fibroblasts in the presence or the absence of macrophages (Figure 5-18C). Therefore, macrophages did not cause a decrease in the number of aggregate bearing fibroblasts. The fact that the red signal slightly increased over time in all conditions was indicative of cell division of the mCherry⁺ cells, regardless of the presence or absence of macrophages.

One possible caveat of this experiment was the mixed culture of untransfected and transfected cells red calibrator cells all of which were exposed to the transient transfection with Lipofectamine. Therefore, not only aggregate bearing cells, but also healthy “normal” cells are present in the well. These have to be considered as additional population in the culture. We plausibly assume that the non-transfected cells may proliferate faster than the transfected cells. However, the quantification of the red cell objects cannot distinguish between these two populations. It is possible untransfected cells proliferate much faster and thereby compensate for the decrease in red cell objects triggered by macrophages. In our approach, we would therefore not be able to detect a decrease in red object counts resulting from macrophage induced cell death.

To account for the potential effect mediated by proliferating cells, we used an alternative approach to reveal whether the macrophages kill and subsequently phagocytose the aggregate carrying cells. In these experiments we analyzed the co-culture by flow cytometry after different time increments under co-culture conditions up to 48 hours to detect macrophage-mediated engulfment of red fibroblasts. If macrophages would engulf the aggregate bearing cells, this effect would be reflected in the macrophage populations analyzed via flow cytometry. The gating of the double positive macrophages is shown in Figure 5-18D. As assumed, we were able to show macrophages engulfing fibroblasts at the same rate, independent of the transfected construct. No significant difference could be detected between the cells transfected with the GFP vector control and the cells transfected with the protein aggregates (Figure 18-D). These findings indicated macrophages did not engulf the aggregate-bearing cells but only removed the protein aggregates from the cells.

In summary, we could show macrophages trigger the removal of protein aggregates independent of the aggregate bearing fibroblast cell line. Moreover, our results indicated the removal of aggregates triggered by macrophages was not mediated by the induction of cell death.

Results

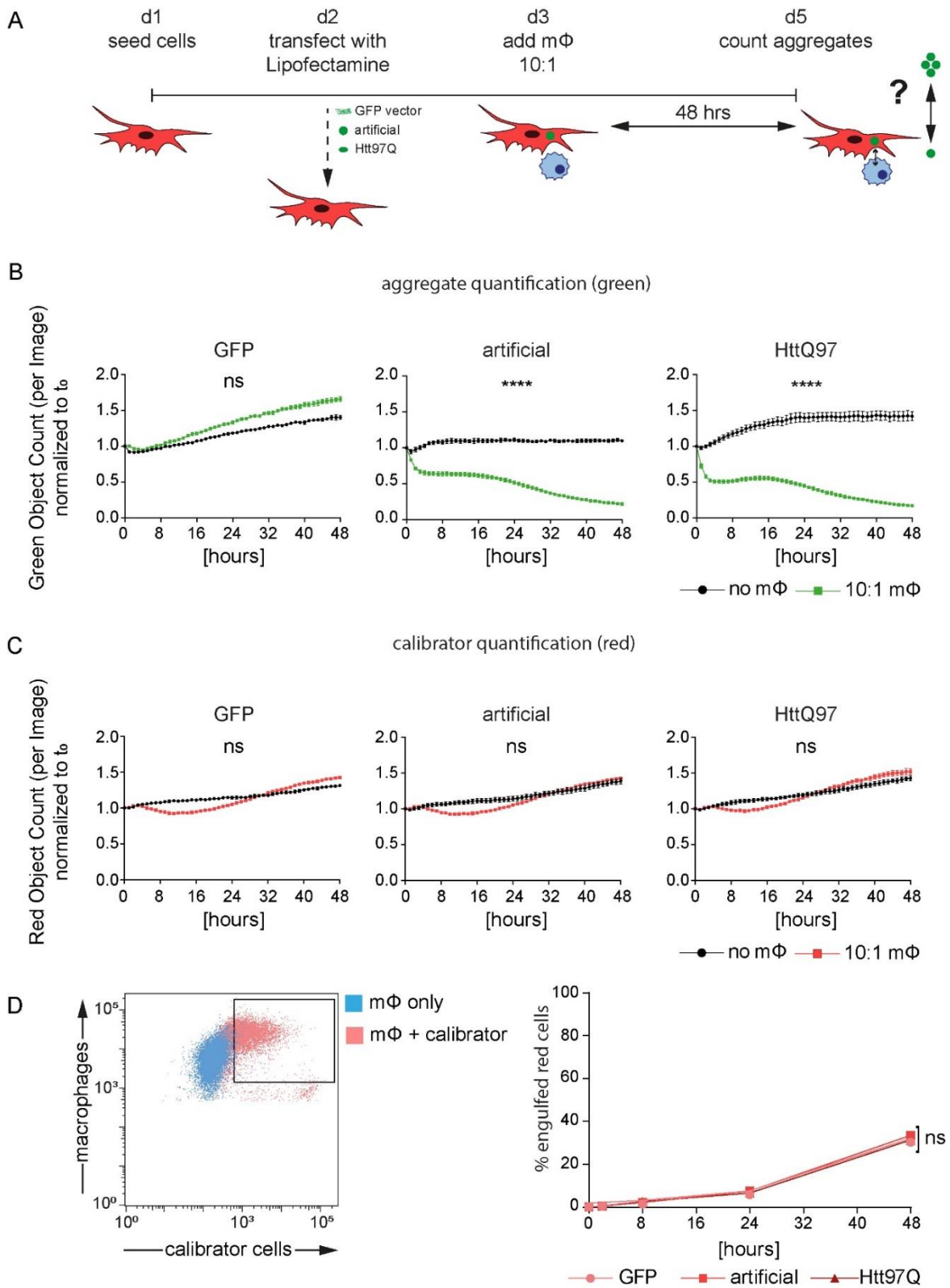


Figure 5-18: Macrophages do not appear to kill aggregate bearing cells.

A Schematic overview of the overall experimental design. Fibroblasts were seeded 24 h prior to transfection. Cells were transfected with GFP, the Huntington aggregate Htt97Q and artificial protein aggregates. After 24 h the cells expressed

protein aggregates. BMDMs were added in a ratio of 10:1 ratio and the co-culture was imaged once every two hours for 48 h in an IncuCyte live-cell imager. Green object counts and red cell object counts were recorded. The number of objects was determined using the corresponding software. **B** Quantification of the green fluorescent object counts of transfected fibroblasts in single culture and co-culture with macrophages. **C** Quantification of the red fluorescent cell object counts of transfected fibroblasts in single culture and co-culture with macrophages. **D** FACS analysis of engulfment of red Flp-in fibroblasts (and fibroblast-derived material) by macrophages. For **B**, **C** and **D** data are representative of three independent experiments. All values are means \pm SEM. Statistically significant differences were determined by two-way ANOVA with Bonferroni correction; **** $p < 0.0001$; $n=3$ biological replicates.

5.3.8 Macrophages do not induce lytic cell death to facilitate aggregate removal

The preceding experiments indicated macrophages did not trigger aggregate removal from fibroblasts by the induction of any obvious cell death pathway. To further validate these results with an independent approach we used a Lactate dehydrogenase (LDH) assay. This technique assesses the level of plasma membrane damage in a cell population. LDH is a stable enzyme, present in all cell types, which is rapidly released into the cell culture medium upon damage of the plasma membrane [353]. Measuring LDH levels in the well detects all forms of lytic cell death. We compared LDH levels in BaxBak DKO fibroblasts. These cells are disabled to undergo intrinsic apoptosis which is a non-lytic form of cell death and can therefore not be detected in an LDH assay. However, we already excluded intrinsic apoptosis as potential underlying mechanism for aggregate removal triggered by fibroblasts. Therefore, Bax Bak DKO fibroblasts are a suitable cell type to be used in an LDH assay.

To be able to compare cell death between individual conditions, we calculated the cytotoxicity compared to the positive control, provided with the assay. First, we compared potential toxicity of aggregates on fibroblasts in fibroblast single cultures in the absence of macrophages (Figure 5-19A). To determine the toxic effect of the transfection itself, we included untransfected cells as a control. The cytotoxicity in transfected fibroblasts was significantly higher compared to the untransfected cells. However, the cytotoxicity did not significantly differ between the GFP-vector control and the transfected protein aggregates. This indicated the transfection itself had a toxic effect on the cells. The transfection with vectors encoding for protein aggregates nonetheless did not increase the cytotoxicity effect compared to the transfected GFP vector control.

Moreover, we compared the co-cultures of aggregate-bearing cells and macrophages. As additional control, we added a macrophage single culture to track the LDH-release resulting only from the macrophages. The cytotoxicity did not significantly differ between the macrophage single culture control and the various co-cultures. Moreover, the cytotoxicity also did not significantly differ between the co-cultures in the presence of macrophages and fibroblasts transfected with

Results

aggregate constructs or GFP-vector control (Figure 5-19B). These results suggested macrophages do not induce lytic cell death to aggregate carrying fibroblasts.

Overall, these findings indicate protein aggregates are not significantly more toxic to fibroblasts than the GFP-vector control. Moreover, our results imply macrophages do not trigger aggregate removal from fibroblasts by the induction of lytic cell death. However, the LDH assay holds several caveats. Even though quantification of LDH is a widely used assay for the determination of cell viability, it has been shown to have low specificity and only diminished reproducibility [354, 355]. Moreover, it is limited to detect only lytic cell death, of which the best studied forms are pyroptosis, necroptosis and ferroptosis [356]. Apoptosis, as the best studied type of non-lytic cell death is not covered by this assay. The described experiment was performed in Bax Bak DKO fibroblasts, which are unable to undergo intrinsic apoptosis. However, extrinsic apoptosis mediated by death receptor activation (i.e. extrinsic apoptosis via the Caspase-8 pathway and death receptor activation) can still not be excluded as the underlying mechanism by which aggregates are removed from fibroblasts. Therefore our result provide evidence that macrophages do not induce cell death to fibroblasts.

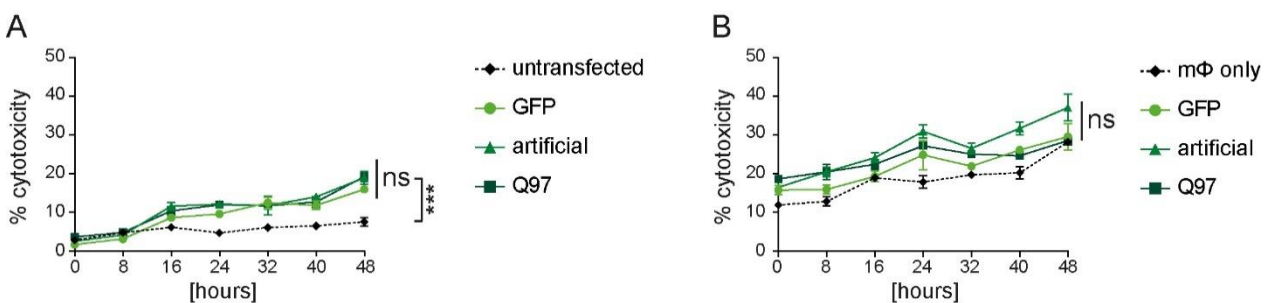
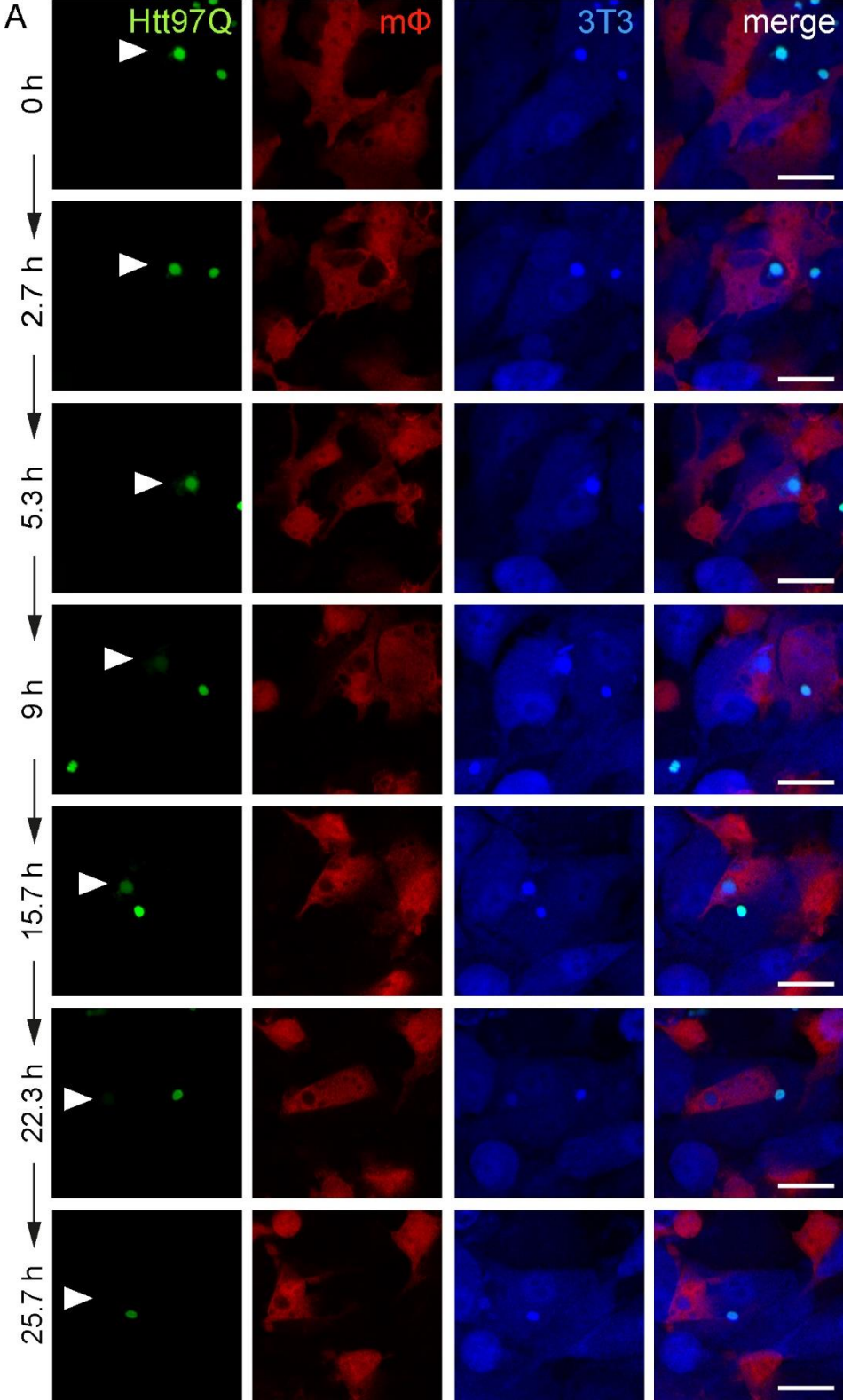


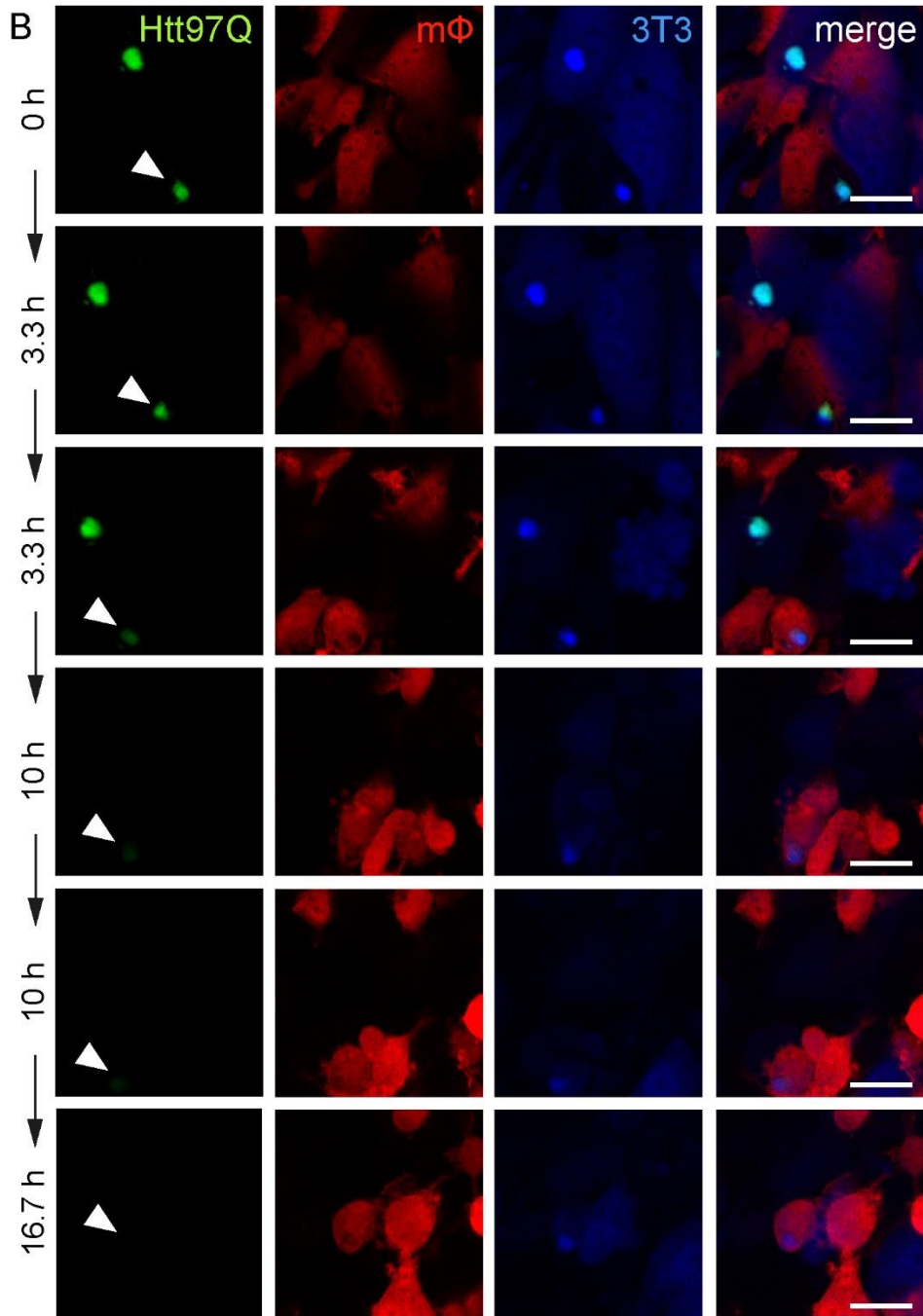
Figure 5-19: Quantification of lytic cell death by LDH release.

Supernatant of single and double culture was measured every 8 hours for a total time increment of 48 hours. The detected signal from the single culture of transfected fibroblasts and the co-culture with macrophages was determined as % cytotoxicity relative to a positive control. **A** LDH was measured in transfected Bax Bak DKO fibroblasts in single culture. **B** LDH was measured in transfected Bax Bak DKO fibroblasts in co-culture with macrophages in a ratio of 10:1 (macrophages:transfected cells). All values are means \pm SEM. Statistically significant differences were determined by two-way ANOVA with Bonferroni correction; *** $p < 0.001$; $n=3$ biological replicates.

5.3.9 Visualization of the aggregate removal by high resolution microscopy

The previous experiments pointed towards an active aggregate removal mechanism triggered by macrophages but without killing the aggregate bearing cells. However, all pursued approaches, hold certain caveats and therefore limit narrowing down the exact mechanism(s) responsible for the aggregate removal. Therefore, we wanted to visually follow this process at much higher resolution using laser scanning microscopy. To do so, we needed an additional labeled cell and generated a blue fluorescent reporter cell line using the Flp-in system (4.5.1). In the experimental set-up, these cells were used as aggregate-bearing cells. Further, we applied the green fluorescent Htt97Q aggregates used throughout the whole study, and tdTomato⁺ macrophages. Thus, we were able to track the fate of the aggregates (green), the aggregate bearing cells (blue) and the macrophages (red) over time. An issue we immediately noted in tracking these co-cultures via microscopy is that all cells in the co-culture were motile. Thereby exact tracking is lost as soon as cells move out of focus in Z-direction within the incubation period (26 h). Therefore, we recorded a Z-stack of 22 layers that was set to start at the very bottom and end at the very top of the cells for each time point. In total we captured the height of 11 μm . Merging all Z-stack images for each time point enabled us to follow the whole cells and aggregates over time, even if they changed the focusing plane. The figures below show representative individual aggregate removal events over time (Figure 5-20). These experiments indicated the following key features that were consistent with the overall results presented herein: (1) aggregates were removed from the fibroblasts by the macrophages over time as expected. In other words, aggregate removal was mediated by the macrophages. (2) Even after removal of the aggregate, the blue fluorescent cells did not disappear from the imaging frame, indicating the fibroblasts were not killed by the macrophages upon aggregate removal. Therefore, macrophages encountering an aggregate-bearing cell detect and remove it via a non-lytic process. To our knowledge, this phenomenon has not been described before. In several respects, aggregate removal is similar to trogocytosis, where one cell nibbles or bites another cell. Distinct from trogocytosis, however, is the scale involved: aggregates are massive compared to the small membrane pieces removed by trogocytosis. To reveal the exact mechanism, by which the aggregates are removed, further experiments are required and will be discussed in the discussion section.





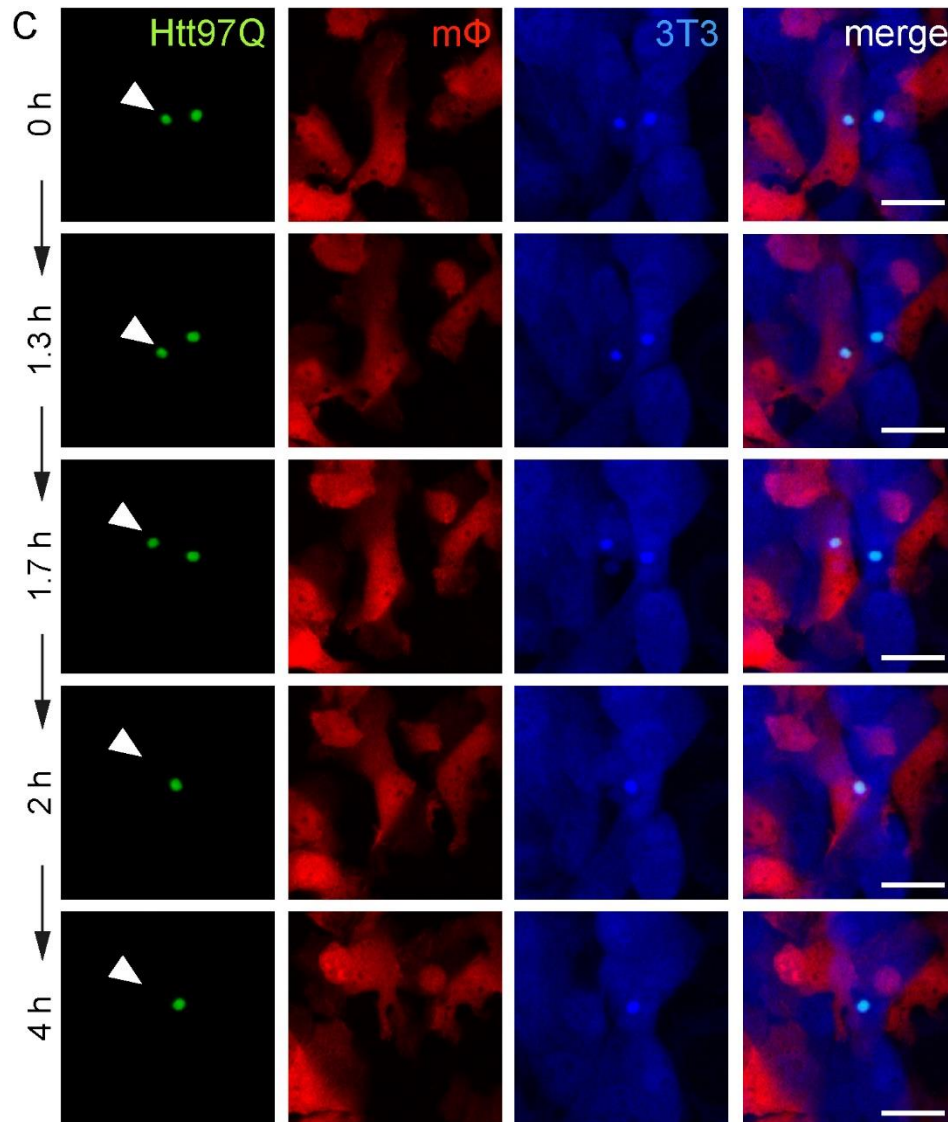


Figure 5-20: Macrophages do not kill aggregate bearing cells upon aggregate removal.

High resolution microscopy images of Flp-in-3T3-mTagBFP2 cells (blue), transfected with Htt97Q aggregates (green), co-cultured with tdTomato⁺ macrophages (red) in a ratio of 4:1 BMDMs:fibroblasts. The same imaging field was recorded over time in 22 Z-stacks of 500 nm distance from each other. Stacks were merged to generate a complete picture as cells are highly motile and therefore did not stay in the same Z-layer throughout the experiment. For all sub-figures **A**, **B**, and **C** the same cells in one imaging field were followed over time every 20 min for a total of 26 h. The aggregates that were removed by macrophages over time were highlighted by white arrows. Scale bars indicate 20 μ m.

6 Discussion

6.1 Interaction of macrophages with senescent cells

Aging is characterized by a gradual heterogeneous functional decline across multiple organ systems that eventually results in tissue dysfunction. Age is defined as a risk factor for the vast majority of diseases that carry a significant financial burden on healthcare systems [357], such as cardiovascular disease [358], osteoporosis, osteoarthritis [359], idiopathic pulmonary fibrosis (IPF) [360], cancer [361], and neurodegenerative diseases [362]. Cellular senescence has been recognized as a key biological process underlying normal aging [8, 41] and the excessive accumulation of senescent cells with time contributes to the pathogenesis of age-related and neurodegenerative diseases [363]. However, cellular senescence plays a dual role during development and throughout tissue repair and regeneration [87, 262]. The senescence response is widely recognized as a potent tumor suppressive mechanism because it forces potentially dangerous (i.e. oncogenically-transformed) cells out of the cell cycle [288]. Furthermore, senescence can have detrimental consequences when senescent cells develop altered secretion patterns. These include changes in the tissue microenvironment and promoting tumorigenesis [364]. One of the most pro-tumorigenic effects of the SASP is to promote the proliferation of epithelial cells, and thereby promoting, amongst others, breast cancer [365] and prostate cancer [366]. Moreover, senescent cells secrete factors that can create a gradient to promote cell migration and invasion. For example in breast cancer, high levels of IL-6 and IL-8 secreted by senescent fibroblasts are responsible for enhancing the invasiveness of a panel of cancer cell lines in cell-culture models [367].

Regarding senescent cell accrual in aging, both their protective versus detrimental consequences and their effect on tissue function have to be considered. The main questions that emerge are how senescent cells are physiologically removed in healthy tissue and why they do not get removed in aged or diseased organs. We considered two possibilities: (1) dead senescent cells are removed by macrophages (i.e. by corpse recognition). (2) Death of senescent cells could conceivably be induced by different cell intrinsic or extrinsic pathways. However, these pathways are broadly inconsistent with the fact that senescent cell numbers increase with aging. Second, as senescent cells are recognized as “self” (albeit, altered self) they should resist macrophage-mediated removal. To address these two major questions, we developed highly defined and robust *in vitro* co-culture systems to quantify the interplay between macrophages and senescent cells.

While senescent cells are refractory to any recognition/killing pathways possessed by macrophages, they alter the ability of macrophages to phagocytose bystander cell corpses. Thus, senescent cells reshape their local environment, and modify macrophage-mediated tissue remodeling pathways. We found the key

component involved in this process is the “don’t eat-me” protein, CD47. Its expression is increased on senescent cells and enforces transient suppression of macrophage efferocytosis. Aged tissues have defects in corpse clearance likely increasing with longevity and driving local inflammation. More specifically, we showed senescent cells transiently paralyze macrophage efferocytosis. This impairment effect was not mediated by an array of SASP molecules, but instead via direct cell contact by the surface receptor CD47 expressed on senescent cells. Genetic evaluation indicated CD47 as the driving factor for the impairment effect by signaling over the CD47 receptor SIRP α on macrophages and the phosphatase SHP-1, transiently reducing macrophage phagocytosis capacity (Figure 6-1).

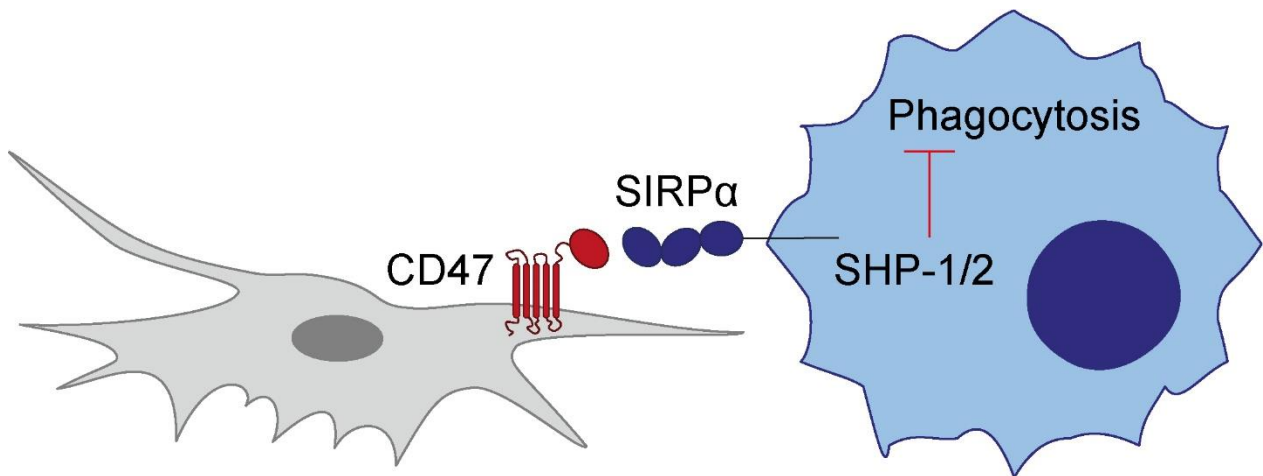


Figure 6-1: Proposed model of how senescent cells impair macrophage functionality.

Increased CD47 expression on senescent cells mediates interaction with SIRP α , an inhibitory receptor expressed on macrophages and other myeloid immune cells. When CD47 binds to SIRP α , it causes activation of the SHP-1 phosphatase that inhibits phagocytosis via dephosphorylation of downstream mediators required for the engulfment process.

6.1.1 Analysis of macrophage functionality in the presence of senescent cells

To evaluate, whether senescent cells can modulate macrophage functionality, we established a novel *in vitro* co-culture assay to examine the effect of senescent cells on macrophage phagocytosis capacity in its simplest form. Macrophages were only able to interact with senescent cells over time, but not capable of engulfing or killing them (Figure 5-2; Figure 8-1). During life-cell imaging, senescent cells were observed to be motile. They altered their shape across time; thus, despite their large size, they moved within the culture, which we were able to track using live cell imaging. Macrophages were observed to interact with the senescent cells (e.g. by crawling around and on top of the senescent cells), however, they were not able to phagocytose them (Figure 5-2A). Since senescent cells are much larger than macrophages (Figure 5-1), we added high numbers of macrophages to the senescent cells to see if this would induce killing or phagocytosis. Albeit increased ratios of 20 times more macrophages than senescent cells, no decreased

numbers of senescent cells were present in the culture at the end of the assay (Figure 5-2B). Thus, macrophages did not seem to be armed with a mechanism to kill or remove senescent cells alone but require an additional factor.

Due to the fact senescent cells could not be removed by macrophages, we wanted to decipher, whether senescent cells could escape their engulfment by altering macrophage functionality. Generally, macrophages are capable of dead cell degradation and ingestion. This further applies to cell debris, tumor cells and foreign materials [261]. Moreover, they are the cell type primarily responsible for efferocytosis, the process of engulfing and eliminating apoptotic cells [300]. Therefore, we chose to read out macrophage efferocytosis capacity to get an idea of the influence of senescent cells on macrophage functionality (Figure 5-3). Senescent cells were able to significantly impair macrophage efferocytosis capacity independent of the means of senescence induction, indicating a global overall impairment effect mediated by senescent cells (Figure 5-3C). The effect was restricted to the senescence phenotype and not mediated by fibroblasts in general (Figure 5-3D). Moreover, the impairment on efferocytosis was independent of the species of the apoptotic target (Figure 5-3E). The molecular mechanisms of senescent cell-mediated efferocytosis inhibition are discussed in depth below.

6.1.2 Dispensable effects of SASP for macrophage functionality

We found senescent cells to alter macrophage functionality by mediating an efferocytosis impairment. The SASP has been shown to mediate many of the cell-extrinsic functions of senescent cells [124]. Thus, we hypothesized that SASP components were responsible for this effect. The secretion of SASP factors which include numerous cell recruitment chemokines and immune survival factors [159], is one of the fundamental characteristics of senescent cells. SASP triggers recruitment of immune cells to the site of injury, a process implicated in the elimination of senescent cells [299]. However, it is clear that despite this beneficial function, SASP can also have detrimental consequences [368]. This includes mediating the “spreading” of senescence to normal neighboring cells thereby altering their cell state. In some instances, the SASP can also have immunosuppressive functions [369, 370] and may contribute to inflammation-linked aging [371]. Therefore, we first considered that an altered senescence secretome could be responsible for the impairment effect of senescent cells on macrophage efferocytosis. This did not turn out to be the case (Figure 5-4). In a twofold approach using conditioned media from senescent cells alone (Figure 5-4B) and separation of the cells using co-cultures via transwell methodologies, respectively (Figure 5-4D), we were able to show that soluble factors released from senescent cells did not impair macrophage efferocytosis. Consequently, we inferred that the impairment resulted from cell to cell contact, which has been shown as critical regulator of target engulfment by phagocytes [372]. Contrary to

the extended research in the field, where the SASP is held accountable for many effects linked with senescent cells, we found SASP did not influence macrophage efferocytosis.

6.1.3 CD47 as decisive factor for paralysis of macrophage function

The mechanisms by which phagocytes recognize targets is mostly mediated by direct cell contact [373]. This comprises surface molecule signaling consisting of direct and indirect “eat-me” markers for example on the apoptotic cell surface and “don’t eat-me” markers, normally found on living cells [218]. These signals include the coordinated activities of many molecular pathways in keeping with the key biological role of debris and dead cell removal as opposed to phagocytosis of normal living cells. Therefore, we examined senescent cells for the expression of different “don’t eat-me” molecules on the cellular membrane. The “don’t eat-me” molecule CD47 has been extensively studied throughout the past years [218]. Moreover, it has been shown to interact with macrophages via its binding partner SIRP α . When CD47 is recognized by SIRP α on the surface of macrophages, their ability to effectively engulf, or phagocytose other cells becomes substantially impaired, and thus the cell expressing CD47 is not killed [304]. This property of the CD47-SIRP α interaction is the basis for the development of anti-CD47 therapies, which are hypothesized to inhibit the “don’t eat-me” signals on malignant cells and facilitate their removal. We therefore hypothesized CD47 interaction with macrophages could provide a basis for the impairment effect of senescent cells on macrophage functionality. Indeed, senescent cells showed substantial upregulation of CD47 on the cellular membrane compared to proliferating cells (Figure 5-5; Figure 5-6). Subsequently, we generated CD47-deficient cells by Crispr-Cas9 engineering and induced senescence. By comparing WT and CD47 KO senescent cells in efferocytosis assays, we found the impairment of senescent cells was dependent on the upregulation of CD47 in the WT cells. CD47 KO cells were unable to impair macrophage efferocytosis (Figure 5-6B). Moreover, we observed a stronger impairment effect on macrophage efferocytosis capacity when macrophages were primed with senescent cells for a shorter time increment of 6 hours. This effect was diminished during longer priming for 24 hours (Figure 5-6D). We further evaluated whether the impairment effect of senescent cells on macrophage efferocytosis was permanent or reversible over time. Our two-step efferocytosis assay revealed the impairment effect could not be sustained during overfeeding in the second efferocytosis. These findings follow the hypothesis of a time-dependent impairment effect mediated by senescent cells. Our results suggest a transient paralysis effect on macrophage functionality mediated by increased CD47 expression on senescent cells (Figure 5-6; Figure 8-2).

As the impairment effect of senescent cells was affecting macrophage phagocytosis globally, we wanted to reveal whether it was also solely dependent on the increased CD47 expression on senescent cells.

During therapeutic use of monoclonal antibodies blocking CD47 in cancer therapy, it became clear that CD47 could not be the only “don’t eat-me” signal being highly expressed on cancer cells [314]. This led to the discovery of additional “don’t eat-me” signals associated with malignancy, including CD22 and CD24 [235, 315]. CD24, similar to CD47 interacts with macrophages, but via its receptor Siglec-10 [314]. Genetic evidence and observational studies in cancer models argued CD22 and CD24 are key complementary pathways to CD47 [314]. Accordingly, we examined senescent WT and CD47 KO cells for the potential upregulation of alternative “don’t eat me” signals (Figure 5-8, Figure 5-9). Interestingly, we were not able to detect any additionally upregulated “don’t eat-me” signal, neither in senescent WT nor CD47 KO cells. Taken together, our findings indicate senescent cells, contrary to tumor cells, are able to impair macrophage efferocytosis functionality solely by the upregulation of CD47 on the cellular surface.

Senescent cells have not only been shown to alter macrophage functionality by the release of SASP molecules, which could not be confirmed in our set-up. Senescent cells have furthermore been shown to alter macrophage phenotype via SASP factors. Different types of senescent cells have been demonstrated to stimulate macrophages towards altered phenotypes. Senescent cells produce IL-4 (and IL-13), causing macrophage polarization towards an anti-inflammatory M2-like phenotype [374] However, senescent cells have also been shown to release factors that skew macrophage polarization towards an inflammatory M1-like state [162]. We determined different efficiencies of the macrophage efferocytosis capacity in general, which seemed to be dependent on macrophage polarization [307]. This suggests that senescent cells can elicit phenotypic changes in macrophages, which can consequently affect macrophage functionality (Figure 5-7). Hence, we examined whether macrophage phenotype alterations would display different susceptibilities to the impairment effect mediated by senescent cells. This turned out not to be the case (Figure 5-7B), as senescent cells were able to impair macrophage efferocytosis independent of the macrophage phenotype. Despite previous studies showing that macrophage polarization could influence efferocytosis efficiency, the impairment effect mediated by senescent cells in our set-up was strong enough to overcome the polarization impact.

Next, we investigated whether the impairment effect of senescent cells was restricted to non-inflammatory efferocytosis. In general, the lack of a pro-inflammatory immune response distinguishes the phagocytosis of apoptotic cells from the phagocytosis of bacteria or necrotic cells [311]. Cell death is vital to the homeostasis of tissues [375]. It assures that cells triggered to die will cease to function and are cleared in an orderly manner. Many of these cells die in a cell autonomous manner and will subsequently be removed without inflammatory consequence [376]. In contrast, when bacteria and necrotic cells are recognized, they enhance proinflammatory responses of activated macrophages [377] through activation

of pattern-recognition receptors such as toll-like receptors (TLRs), NOD-like receptors (NLRs), and C-type lectins (CLECs), amongst others [309]. Recognition and subsequent engulfment of apoptotic and necrotic targets occurs by distinct and noncompeting mechanisms [310, 378]. We examined whether the impairment effect of senescent cells on macrophages would differ when targets, causing a pro-inflammatory response, were used as phagocytic prey. Therefore, we compared the influence of senescent cells on macrophage phagocytosis of apoptotic and necrotic corpses, as well as bacteria (Figure 5-7C). Perhaps surprisingly, the impairment effect of senescent cell seemed to be globally regulated and independent of the phagocytic target, thereby influencing both pro-, and non-inflammatory phagocytosis pathways. Moreover, the impairment effect was globally recovered in the senescent CD47 KO cells.

6.1.4 CD47 mediates a transient paralysis effect on macrophage functionality

We continued to follow the CD47 signaling pathway from the senescent cells to the macrophages (Figure 5-10). SIRP α is highly expressed on the surface of all myeloid lineage cells, including macrophages, granulocytes, monocytes and myeloid dendritic cells [234, 379, 380]. It inhibits their activation to perform phagocytosis. The intracellular domain of SIRP α contains immunoreceptor tyrosine-based inhibition motifs (ITIMs) [236], which confer its properties as an inhibitory receptor. Ligation of CD47 to SIRP α promotes phosphorylation of the intracellular ITIMs and activates the inhibitory phosphatases SHP-1 and SHP-2 [381]. The SHP phosphatases have a multifactorial role in negatively regulating immune cell activation, including dephosphorylation of proteins containing immunoreceptor tyrosine-based activation motifs (ITAMs) [381, 382]. This eventually results in the inhibition of phagocytosis via downstream mediators.

Impeding the interaction of macrophages and senescent cells via the CD47-SIRP α axis was successfully achieved by the addition of SIRP α blocking antibodies (Figure 5-10B). The impairment effect mediated by senescent cells on macrophages was restored upon addition of the blocking antibodies. These findings were consistent with the experiments in which CD47 KO cells were used. We next went on to track the signaling axis to a potential activation of the SHP phosphatases. We quantified SHP-1 recruitment to the macrophage cellular membrane as a consequence of the CD47-SIRP α interaction (Figure 5-10C; Figure 8-3). Co-culturing of macrophages with senescent WT cells resulted in a quantifiable accumulation of SHP-1 at the cellular membrane of the macrophages (Figure 5-10E). These findings confirmed the hypothesis that increased expression of CD47 on senescent cells lead to the impairment of macrophage efferocytosis capacity via signaling through SIRP α . We hypothesize that SIRP α further activated SHP-1 phosphatase also in our system, which eventually negatively regulated the phagocytosis capacity of macrophages. Moreover, we were able to confirm the previously suggested transient nature of the impairment effect mediated by senescent cells. The transient impairment was also displayed in SHP-1 accumulation in the

macrophages. The highest quantifiable SHP-1 accumulation could be detected after a shorter priming of macrophages with senescent cells for 6 hours. The accumulation was diminished after 24 hours, and no SHP-1 recruitment to the membrane was observed after priming with CD47 KO cells.

We therefore suggest this transient inhibition is a consequence of the binding properties of CD47 and SIRP α . Extensive biophysical characterization of the CD47-SIRP α interaction has been documented, including crystallographic analysis of the extracellular domain of SIRP α alone and in complex with CD47 [383, 384]. Because of the naturally occurring low affinity of SIRP α to CD47 in the sub-micromolar range [385] ($\sim 1 \mu\text{M}$ affinity [386]), WT SIRP α was characterized as a weak binding partner. This is consistent with the fact that phagocytosis cannot be inhibited strongly in a permanent manner [386, 387]. The low affinity of SIRP α for CD47 may contribute to the observed transient inhibition of efferocytosis mediated by senescent cells. The increased expression of CD47 documented here does not seem to sufficiently overcome the weak interaction between CD47 to SIRP α . The weak binding properties between the two molecules may explain why senescent cells were only able to strongly impair efferocytosis for a shorter time increment of 6 hours. We hypothesize the binding was already limited after a longer time increment of 24 hours, and therefore the observed impairment effect was consequently also diminished.

6.1.5 Potential for future therapeutic development

In future approaches, the properties of CD47/ SIRP α interactions between macrophages and senescent cells will be further characterized. This includes the analysis of proliferating fibroblasts, which should be added as additional control to reveal the role of CD47 for the transient impairment effect. Proliferating cells have been shown to impair macrophage efferocytosis at extremely high numbers (Figure 8-4). Whether this was due to nutrient limitation, or due to CD47 impairment resulting from accumulation effects of high cell numbers remains to be determined. However, this is technically challenging due to the differences in growth rates across experiments. Moreover, the accumulative effects of CD47 could be examined by adding high titrations of proliferating cells and further tracking SHP-1 accumulation on macrophages.

For CD47 being highly expressed not only on senescent but also on tumor cells, therapies targeting the CD47/SIRP α axis showed successes in preclinical tumor models and have advanced to clinical trials for both solid and hematologic malignancies including non-Hodgkin lymphoma, acute lymphocytic leukemia and multiple myeloma [388-390]. Consequently, the CD47-SIRP α axis has emerged as a new target for immune-oncology. CD47-SIRP α blocking peptides are also able to promote macrophage-mediated phagocytosis and immune response in cancer immunotherapy and have been proposed to synergistically

complement cancer immunotherapy by enhancing the effects of irradiation [391]. These peptides are being optimized to enhance anticancer effects [392]. Blocking the CD47/ SIRP α axis has been successfully applied to several other diseases. CD47 blocking antibodies have been shown to successfully restore phagocytosis and prevent atherosclerosis [393]. Moreover, CD47 blocking antibodies were shown to accelerate hematoma clearance and alleviate short- and long-term brain injury after intracerebral hemorrhage [394]. Anti-SIRP α antibodies benefit from more restricted expression of SIRP α in myeloid cells and could therefore have more favorable pharmacokinetic and toxicity profiles [395]. In addition, SIRP α blocking antibodies have been shown to induce phagocytosis of tumor cells [396]. The binding properties of both CD47 and SIRP α are modifiable [397], rendering them as suitable candidates for treating the impairment effect of senescent cells on macrophage efferocytosis.

It is remarkable that CD47 KO mice are viable and do not exhibit any strong phenotypes, such as massive accumulation of unwanted cells and autoimmunity [398]. In part, this could be due to redundant mechanisms to suppress phagocytosis; proteome-wide analysis identified more than 100 human ITIM-containing receptors [313]. Consequently, there are more ligands than just CD47, that upon binding lead to phosphorylation of an ITIM, which in turn leads to the recruitment of a protein tyrosine phosphatase and consequently results in the negative regulation of immune cell activation and phagocytosis, respectively [399]. The plethora of various signaling options, negatively regulating phagocytosis limits the potential usefulness of anti-CD47 drugs.

6.1.6 Giant macrophages provide the potential to remove senescent cells

Multinucleated giant cells of mononuclear phagocyte origin are called polykaryons and are seen in various pathologic states including infection, foreign body reactions, cancer, and other conditions of unknown causes such as sarcoidosis and rheumatoid arthritis [400, 401]. Moreover, they have been shown to accumulate in tissue surrounding total joint arthroplasties [402]. The factors involved in the formation of polykaryons are not completely understood and their function for various pathologic and physiologic settings is not known. A recent study found that polykaryons phagocytosed their target less avidly than unfused macrophages. However, polykaryons were remarkably more competent in the uptake of large particles [327]. There is strong evidence the main characteristic of polykaryons is the uptake of large particles, which unfused macrophages are not capable of. Thus, we wanted to reveal whether polykaryons would be able to phagocytose senescent cells, as these are notably larger than normal cells. This dramatic increase in size may be causing the lack of engulfment and thereby resulting accumulation of senescent cells within aging.

We were able to observe that polykaryons are indeed capable of phagocytosing senescent cells in a quantifiable manner (Figure 5-11A/B). However, the polykaryons used throughout our study did not seem to selectively determine a suitable target but appeared to have highly phagocytic properties under any circumstances (Figure 5-11C). This caveat of our *in vitro* system has to be considered for further approaches. Moreover, compared to the rapid process of efferocytosis [403], the engulfment of senescent cells was observed as a rather slow process, which may result from the comparatively quiescent metabolic activity of polykaryons (Figure 5-11D/E). Our data is in line with previous findings [327]. Giant multinucleated cells have been examined for their properties to contribute to remodeling in regards to fracture repair and disease [404]. However, whether polykaryons are suitable for therapeutic applications regarding tissue homeostasis and wound healing in the context of senescence needs to be revealed. Further, whether they can be induced in an organism to successfully remove senescent cells remains to be investigated and requires an analysis of the phagocytic capacity of polykaryons in an *in vivo* system.

Taken together, we have shown that senescent cells were able to escape the engulfment by unfused macrophages. Moreover, they were able to impair macrophage functionality, by diminishing macrophage efferocytosis capacity. The impairment effect was not mediated by the array of SASP molecules, but instead by direct cell contact with increased CD47 expression on senescent cells. Our genetic evaluation indicated that CD47 was the dominant factor for the impairment effect. Indeed, senescent cells were only able to transiently impair macrophage functionality. We could further track the transient paralysis on macrophages signaling in macrophages via SIPR α (the CD47 receptor) and the phosphatase SHP-1, which transiently reduced macrophage phagocytosis capacity. Furthermore, even though unfused macrophages were not able to engulf senescent cells, our findings indicated that due to the size differences giant senescent cells seemed to require a giant phagocyte to enable their engulfment. We were able to demonstrate that giant multinucleated macrophages (polykaryons) were able to engulf senescent cells. However, therapeutic applications to block the interactions between macrophages and senescent cells, as well as the removal of senescent cells by polykaryons require further *in vivo* studies.

6.2 A novel system to study the removal of Huntington aggregates

As described previously in this thesis, aging is associated with physical deterioration that leads to an increased risk of disease and death [405]. Moreover, it is the primary risk factor for most neurodegenerative diseases, including Huntington's disease (HD). Strikingly, many of the hallmarks of aging are also hallmarks of the pathology of HD and processes that decline during aging also decline at a more rapid rate in HD, further enhancing the role of aging in HD pathogenesis [406]. Few to no effective treatments are available for age related neurodegenerative diseases, which tend to progress in an irreversible manner and are associated with large socioeconomic and personal costs [240]. To develop successful interventions, it is important to consider the basic mechanisms of aging and their role in the onset and progression of neurodegenerative disease [240].

The accumulation of protein aggregates is a common pathological hallmark of many neurodegenerative disorders, including HD [330]. In case of HD, the protein aggregates are caused by a CAG triplet repeat expansion in the *huntingtin* (*HTT*) gene. *HTT* was first mapped to a specific chromosome in 1983 by James F. Gusella and colleagues, who determined an HD-associated restriction fragment length polymorphism [407]. This translates into a polyglutamine (polyQ) repeat, immediately following the first 17 amino acids of the huntingtin protein (Htt). PolyQ repeats in the disease range (> 37 repeats) yield Htt more susceptible to misfolding. Consequently, the formation of Htt aggregates in cells and neurons [408, 409], leads to dysfunction and death in the caudate and putamen, and the cerebral cortex [410]. To date, we do not fully understand the mechanisms underlying protein aggregation, how aggregates are cleared, or how other cellular proteins are involved in the formation and clearance processes [411]. Understanding how these aggregates form, and assessing their impact on neuronal function will contribute to the development of therapeutic targets to prevent disease progression.

The diagnosis of neurodegenerative disorders is problematic due to the fact that even though they can be broadly classified by their clinical presentations, few patients have "pure" syndromes. A vast majority presents mixed clinical features, with extrapyramidal and pyramidal movement disorders and cognitive or behavioral disorders being the most common [412]. The current diagnostic standard is neuropathological evaluation at autopsy, providing the key to understanding discrepancies between clinical and pathological diagnoses [413, 414]. However, the exact contribution of aggregate inclusions to pathology remains poorly characterized. To fully elucidate mechanisms of disease, it is essential that new and robust model systems are developed and verified, since the current ones are hold clear limitations [415]. While cell culture models have

pivotal roles in understanding pathways and interactions, animal models allow the study of neurodegenerative diseases in a systemic manner, although they are inaccurate representations of human pathology [416, 417]. In comparison to humans, the lifespan of rodents is limited and results in substantial practical, biological and cost limitations on the ability to study age-dependent effects. Furthermore, given the difference in brain size between rodents and primates, many rodent models are not ideal for studies involving medical device-delivered drugs [418]. The availability of newer, faster cell culture systems offers hope we will soon be able to closely mirror the disease in a petri dish. Advancing our understanding of the basic biology and pathobiology of protein aggregation [419, 420] will pave the way towards personalized medicine enhancing the probability of success of future clinical trials [421].

6.2.1 Analysis of pathogenic aggregate removal by macrophages

To this day, no drugs have been shown to efficiently treat any neurodegenerative disease, including several multi-billion euro failures [422, 423]. Even though removal of protein aggregates has not only been approached by pharmacological interventions. Previous studies attempt to use the potential of phagocytes to trigger aggregate removal. Macrophages were shown to play an active phagocytic role in removing alpha-synuclein (α -SYNC) aggregates that accumulate with age in the neural circuitry of the gut [265]. Macrophages adjacent to dystrophic terminal processes were swollen and contained vacuoles filled with insoluble α -SYNC, but they were not able to eliminate all aggregates or their precursors from the healthy aging gastrointestinal (GI) tract. This indicates that the phagocytic response of local macrophages was insufficient [265]. Another study demonstrated that clearance of amyloid- β peptide ($A\beta$) aggregates, associated with Alzheimer's disease (AD), is not solely the task of microglia. Macrophages recruited from the periphery also participate in removing these aggregates from the brain. Immunohistochemical studies of the frontal lobe and hippocampus of AD patients showed infiltration by blood-borne macrophages [337]. These contained intracellular $A\beta$, however, complete clearance of $A\beta$ deposits was not achieved. In contrast, control monocytes displayed excellent differentiation into macrophages followed by intracellular phagocytosis of $A\beta$ eventually resulting in $A\beta$ degradation [337]. Intriguingly, macrophages isolated from the blood of AD patients were less effective at clearing $A\beta$ than those from unaffected individuals [337].

None of these studies has been implemented to reveal the potential importance of macrophages for HD. Therefore, we aimed to develop a cellular model to examine the interplay between macrophages and Htt aggregate-bearing cells. Although HD primarily affects the brain, Htt

aggregates have been found to also cause detrimental effects in different peripheral cells and tissues [331]. Several peripheral organs are considerably affected and their peripheral symptoms may in fact manifest before those resulting from brain pathology [331]. Mutated *HTT* causes global accumulation of intracellular protein aggregates. This results in the impairment of energetic metabolism, transcriptional deregulation and hyper activation of programmed cell-death mechanisms [333], which have been extensively studied, in fibroblasts [332-334]. HD fibroblasts have been shown to manifest cellular dysfunctions similar to neural HD cells [424].

The study of peripheral cells may yield important insights that eventually shall help to convey HD pathology from a cellular model to what occurs in the brain. Therefore, we developed a novel cell culture approach to study the interaction between aggregate-bearing fibroblasts and macrophages (Figure 5-12). We found fibroblasts tolerated the aggregates and did not die in the culture period. Most significantly, macrophages triggered the aggregate removal from fibroblasts in a time dependent manner (Figure 5-12C, Figure 8-5). The decline in aggregates was proportional to the added number of macrophages; the higher the added number of macrophages, the greater the aggregate removal effect (Figure 5-12D). A limitation of the system was the transient induction and expression of protein aggregates in the fibroblasts.

In our initial experimental set-up, protein aggregates were induced via transient transfection using Lipofectamine. However, the use of Lipofectamine has been shown to cause stress in the transfected cells, which may result in gene expression changes and thereby may cause unpredictable bystander effects [425]. For this reason, we generated stable cell lines where protein aggregation was exogenously induced by doxycycline (Figure 5-14). The Htt inducible cell line showed expression of Htt aggregates over time and therefore enabled us to study the removal of protein aggregates triggered by macrophages in an alternative setting. Independent of the way protein aggregates were induced in fibroblasts, macrophages triggered their removal over time (Figure 5-14D). We concluded we had established a stable set-up to study the process of protein aggregate removal to reveal the underlying mechanisms.

6.2.2 Deciphering the underlying mechanisms of aggregate removal

The surface of phagocytes such as macrophages is equipped with a wide range of molecules for recognition and decoding of their cognate ligands. These ligands are expressed on the surface of the potential target to eventually trigger the engulfment of host-derived and foreign particles. Receptors either directly recognize the particle or recognize targets coated in opsonic molecules

[373]. This leads to clearance of the target either by phagocytosis or, for soluble molecules, by endocytosis [426]. Endocytosis is a cellular process in which substances are brought into the cell [427]. The material to be internalized is surrounded by an area of cell membrane, which then buds off inside the cell to form a vesicle containing the ingested material. In addition, endocytosis has been shown to require direct cell contact [428]. According to the literature, macrophages trigger aggregate removal by direct cell contact. Thus, we wanted to reveal whether this was also true for our system and we performed our assay in a transwell set-up (Figure 5-15), where direct cell contact was prohibited. Spatial separation of the two cell types resulted in a lack of aggregate removal, indicating that macrophages required direct cell contact to trigger aggregate removal from fibroblasts.

To better understand the mechanisms by which macrophages are able to trigger aggregate removal, we wanted to reveal, whether the aggregate-bearing cells would transmit bystander effects to a neutral cell in the system or whether macrophages would also recognize the non-aggregate-bearing cell via bystander effects. To do so, we added a third “calibrator” cell to the experimental set-up (Figure 5-16). Thereby we intended to reveal whether aggregate-bearing cells would show bystander properties like other diseased cells, for example in cancer models. Cancer cells have been demonstrated to release signals, which can influence nearby cells namely the bystander effect. The transmission of bystander effects among cancer cells involves the activation of inflammatory cytokines, death ligands, and reactive oxygen/nitrogen species [429]. Once they have been activated by contact with apoptotic tumor cells, macrophages have been shown to recognize and engulf non-apoptotic bystander tumor cells [346]. We therefore wanted to disclose, whether the aggregate-bearing cells would transmit bystander effects to the calibrator cells in our system and whether macrophages would also recognize these calibrator cells as target via bystander effects. Moreover, we wanted to reveal, whether the calibrator cells would impair the ability of macrophages to trigger aggregate removal. Surprisingly, neither the calibrator cells were able to influence the efficiency of aggregate removal from the aggregate-bearing cells (Figure 5-16B), nor did the aggregate-bearing cell induce bystander killing of the calibrator cells (Figure 5-16C). The process of aggregate removal triggered by macrophages was shown to occur in a very directed and specific way as it could not be manipulated by the addition of a calibrator cell line. We were not able to observe bystander effects mediated by any of the cell lines impairing the specific macrophage function. These findings suggested that macrophages target the aggregate-bearing cells in a very specific way.

A major function of macrophages is the remodeling of tissues, which can be pursued by the engulfment of apoptotic targets but also more actively through the induction of programmed cell death [430]. In order to decipher how macrophages trigger the aggregate removal from fibroblasts, a central question was whether macrophages triggered aggregate removal by active killing of the aggregate-bearing cell. Fibroblasts lack the molecular machinery for inflammasome-mediated caspase-1 activation and pyroptosis [347]. Active killing via ferroptosis was assumed to be unlikely as the cell culture media is replete with cysteine and no ferroptosis-inducing agents were present. Thus, we hypothesized the aggregate bearing-cells could be killed undergoing intrinsic mitochondrial-mediated apoptosis. We therefore used Bax Bak DKO fibroblasts as aggregate-bearing cells. These are disabled in undergoing intrinsic mitochondrial-mediated apoptosis [348] (Figure 5-17). However, as the efficiency of aggregate removal was not influenced in the set-up using Bax Bak DKO cells, we concluded that macrophages did not trigger aggregate removal by the induction of intrinsically mediated apoptosis (Figure 5-17B). Investigating other possible mechanisms by which macrophages could trigger aggregate removal, autophagy emerged as a major clearance pathway for toxic protein aggregates in recent literature. Autophagy receptors have been shown to play a critical role in aggregate clearance [431]. A newly-described pathway for ingestion of large particulate structures is termed LC3-associated phagocytosis (LAP) [213]. LAP provides a novel function for autophagy proteins and is a contributor to immune regulation and inflammatory responses across various cell and tissue types. Characterized by the conjugation of LC3 family proteins to phagosome membranes, LAP uses parts of the canonical autophagy machinery, following ligation of surface receptors that recognize a variety of cargos including pathogens, pathogen “shells” like zymosan, dying cells, soluble ligands and protein aggregates [349]. Engulfment of particulates via TLR, PtdSer, and FcR, respectively, triggers recruitment of the Rubicon-containing Class III PI3K complex to the cargo-containing LAP-engaged phagosome (“LAPosome”). Rubicon also binds and stabilizes the NOX2 complex to produce ROS [432] and is required for the formation of the LAPosome, where the target is eventually digested [350]. We therefore hypothesized that the protein aggregates activate LAP in the macrophages, consequently triggering the removal of protein aggregates in fibroblasts. Macrophages lacking Rubicon, are disabled in undergoing LAP and were added to the aggregate-bearing cells (Figure 5-17D). However, *Rbcn*^{-/-} KO macrophages were also still able to trigger aggregate removal from fibroblasts, indicating that aggregate removal is also not mediated by autophagocytosis or LAP in particular.

There is a plethora of possible underlying mechanisms regarding different types of cell death and various types of phagocytosis but testing them all, using candidate-selective approaches, is unfeasible. Instead, we decided to move on revealing, whether the aggregate-bearing cells die at all upon aggregate removal; following which, the aggregate and cell debris would be eliminated. By tracking the fate of the fibroblasts in parallel to the aggregates over time we wanted to disclose whether macrophages would kill the aggregate-bearing cells (Figure 5-18). We were able to show that the aggregate-bearing cells stayed the well, independent of the presence or absence of macrophages and independent of bearing aggregates or the vector control. Our data suggested, the aggregate-bearing cells would not be killed at all by macrophages. However, the experimental set-up had limitations, as it could not compensate for the influence of a non-transfected and therefore non-aggregate-bearing population in the set-up. To further validate these results with an independent approach, we performed an LDH assay (Figure 5-19). This technique assess the level of plasma membrane damage in a cell population. Lactate dehydrogenase (LDH) is a stable enzyme, present in all cell types, which is rapidly released into the cell culture medium upon damage of the plasma membrane [353]. Measuring LDH levels is limited to detect only lytic cell death, of which the best studied forms are pyroptosis, necroptosis and ferroptosis [356]. Apoptosis, as non-lytic cell death, is not covered by this assay. We compared LDH levels in BaxBak DKO fibroblasts to exclude non-lytic cell death in single culture and co-culture with macrophages (Figure 5-19B). No substantial differences in LDH release could be determined between the GFP-vector control, which is not engulfed, and the protein aggregates. Therefore, our findings suggest that macrophages did not trigger aggregate removal from fibroblasts by the induction of any form of lytic cell death. The LDH assay holds several caveats. Even though quantification of LDH is a widely accepted assay for the determination of cell viability, it has been shown to have low specificity, and only limited reproducibility [354, 355]. Extrinsic apoptosis mediated by death receptor activation (i.e. extrinsic apoptosis via the Caspase-8 pathway and death receptor activation) can still not be completely excluded as the underlying mechanism by which aggregates are removed from fibroblasts. Nevertheless, our results indicated that macrophages do not induce cell death to the aggregate-bearing cells.

Lastly, we decided to visually follow the process of aggregate removal by tracking the fate of the aggregate-bearing cell, the aggregates themselves and the macrophages via high resolution laser scanning microscopy (Figure 5-20). These experiments indicated the following key findings that were consistent with the overall results presented herein: (1) aggregates were removed from the

fibroblasts by the macrophages over time. Consequently, aggregate removal was mediated by the macrophages. (2) Even after removal of the aggregate, the blue fluorescent aggregate-bearing cells did not disappear from the imaging frame, indicating that the fibroblasts were not killed by the macrophages upon aggregate removal. These data were consistent with the absence of obvious cell death as discussed above. Therefore, we suggest that macrophages encounter an aggregate-bearing cell and eventually detect and remove the aggregate via a non-lytic process. To our knowledge, this phenomenon has not been described before. In several respects, aggregate removal seems to be similar to trophocytosis, where one cell “bites” another cell.

6.2.3 Transferring the cell culture model to a neuronal system holds several caveats

Even though we were able to develop a robust and highly reproducible cell culture model to study Htt aggregate removal, we wanted to transfer it to a neural setting to expand the scope of our study to a more natural scenario. As professional phagocytes in the CNS, microglia play important roles in synapse elimination and clearance of cellular debris during development and disease [178]. Moreover, they are capable of the internalization of protein aggregates [433]. Correspondingly, microglia adopt similar tasks as macrophages by performing phagocytic clearance following injury. For that reason, they are important for tissue repair and regeneration in the brain [434]. We directly conferred our cell biological set-up to a neural setting with cortical neurons as aggregate-bearing cells and microglia as phagocytes (Figure 5-13). Even though Htt aggregates have been associated with neuronal death, their general toxicity for neurons is controversially discussed in literature [435, 436]. The neurons in our *in vitro* setting, showed a lower capability of tolerating protein aggregates than fibroblasts (Figure 5-13B). Despite their phagocytic properties, in our setting microglia did not engulf the protein aggregates, but instead enhanced aggregate stability in neurons over time (Figure 5-13C; Figure 8-6). For some neurodegenerative diseases, macrophages have been shown to be more effective in the phagocytosis of protein aggregates than microglia [437]. Therefore, we applied macrophages as potential phagocytes to the neuronal setting. However, macrophages did not universally attack neurons, independent of the presence or absence of protein aggregates (Figure 5-13D). In summary, the set-up including primary neurons turned out to be unsuitable for the purpose of determining the mechanisms of Htt aggregate removal in a cell culture *in vitro* model. Despite the fact that our system was not applicable to a neuronal setting, we were able to gain more insights in the underlying mechanisms of aggregate removal in the co-culture system with fibroblasts and BMDMs.

6.2.4 Potential mechanism and future perspectives

One plausible mechanism, by which macrophages could trigger aggregate removal from fibroblasts is trogocytosis (from Greek *trogo*, meaning 'nibble') [438]. To our knowledge, this has not been approached in the context of aggregate removal so far. Trogocytosis was described as a process in which one cell physically extracts and ingests “bites” of cellular material from another cell. It has been documented in T, B and natural killer cells both *in vitro* and *in vivo*. Thus, this process may be important in the induction and regulation of immune responses, and possibly in the control of other cellular systems [439]. Macrophages are also able to interact with neighboring healthy cells via trogocytosis [439]. The purpose of trogocytosis is poorly understood, but it is thought to help the host to develop immune responses against microbes and tumors [440]. Trogocytosis occurs when two cells form a transient interaction during which the membranes appear to fuse. The cells eventually separate, with each participant cell having acquired plasma membrane components from the partner cell. The transferred membrane proteins retain their orientation and their function until they are recycled via normal membrane turnover [440]. In certain mouse tissues, more than half of the cells have undergone detectable trogocytosis at any given time [441]. In immune cells, trogocytosis leads to a variety of acquired functions that likely impact infection and immunity. For example, trogocytosis improves T cell signaling in response to antigens and enables activation of T cells by dendritic cells after acquiring antigens from neighboring cells [442, 443]. Trogocytosis has been implicated as a critical factor in several pathologies including cancer biology, tissue engraftment, and vaccination efficacy [444]. The process can occur without the transfer of cytosolic material [445], but it is unclear if the presumptive transient membrane fusion that occurs during certain types of cytosolic transfer also results in trogocytosis [440]. We were able to show, especially using high resolution microscopy, that the aggregate-bearing cells stayed intact and alive, even after the removal of the aggregates. Thus, we hypothesize the underlying mechanism varies from any form of death induction and subsequent phagocytosis of the cell debris [446]. Moreover, this excluded entosis, as non-apoptotic cell death mechanism. Entosis involves the invasion of one live cell into another, followed by the degradation of internalized cells by lysosomal enzymes. Thus, it could be excluded as potential mechanism [447].

We suggested macrophages trigger aggregate removal via a trogocytosis-like mechanism for the following reasons: Trogocytosis contrasts with phagocytosis, where one cell ingests another cell in its entirety [446]. Moreover, trogocytosis requires direct contact between living cells [448], which we could demonstrate in our transwell set-up. Trogocytosis has been described as a process for

the transfer of intact proteins [449]. The performed high resolution microscopy suggests macrophages take up the aggregates from fibroblasts, internalize them and subsequently digest them. Recent findings from other lab members also support this hypothesis. Sophia Mädler was able to confirm previously described membrane encapsulation of the protein aggregates [267] in our system (Figure 6-2). This encapsulation could facilitate the process of trogocytosis as it may present the aggregate to the macrophage.

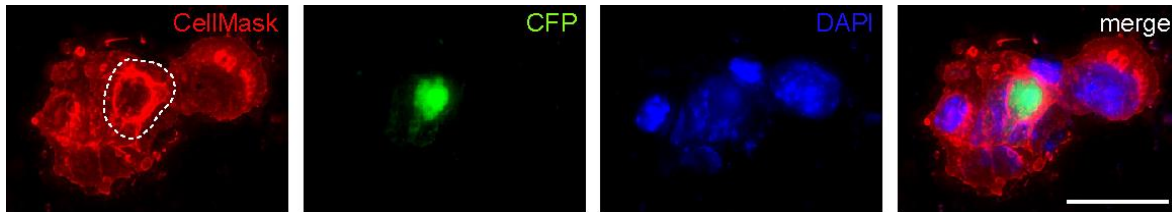


Figure 6-2: Membrane encapsulation of Htt aggregates

High resolution microscopy images of fixed tet-on Htt94Q-CFP fibroblasts. The same imaging field was recorded in 25 Z-stacks of 6.3 μm distance from each other. Stacks were merged to generate a complete picture. Cell membranes were stained with CellMask (red), aggregates are fused to CFP (green) and nuclei were stained with DAPI (blue). The membrane surrounding the Htt aggregate is highlighted with a dotted line. Scale bar indicates 25 μm . Unpublished data generated in collaboration with Sophia Mädler (MPI of Biochemistry).

Debatable, however, is the scale involved: aggregates are massively bigger compared to the small membrane pieces usually removed by trogocytosis [446]. To reveal the exact mechanism, by which the aggregates are removed, further experiments are required. Specific, global inhibition of trogocytosis, neither by genetic nor pharmacological approaches has been successful so far. Several approaches were aiming to inhibit trogocytosis in multiple cell types, including macrophages [445, 450, 451]. Effective inhibitor treatment may reveal, whether macrophages trigger aggregate removal via trogocytosis or a trogocytosis-like mechanism. Enhanced tractability of the fate of the aggregate could yield valuable information about the underlying mechanisms of the aggregate removal. Being able to track the aggregates also after engulfment by the macrophages via pH-sensitive fluorescent labelling [452] would help to reveal, whether macrophages eventually digest the aggregates in lysosomes.

Taken together, in this project we present a novel cell culture system to examine the removal of Htt aggregates from fibroblasts *in vitro*. We were able to demonstrate that macrophages specifically trigger the removal process. These findings were supported by the fact that no bystander effects could be detected. Specifically, neither did the aggregate-bearing cells trigger the additional clearance of neutral calibrator cells, nor did the calibrator cells interfere with the aggregate removal

efficiency. Moreover, our results indicate that macrophages do not trigger aggregate removal by killing the aggregate-bearing cells. In this sense, we hypothesize the aggregates are removed by a trogocytosis-like mechanism. However, this hypothesis remains to be confirmed by future experiments.

7 Literature

1. Oeppen, J. and J.W. Vaupel, *Demography. Broken limits to life expectancy*. Science, 2002. **296**(5570): p. 1029-31.
2. Nations, U., *Department of economic and social affairs, population division*. Trends in contraceptive use worldwide [Internet], 2015.
3. Fulop, T., et al., *Are We Ill Because We Age?* Front Physiol, 2019. **10**: p. 1508.
4. Kirkwood, T.B.L., *Why and how are we living longer?* Experimental Physiology, 2017. **102**(9): p. 1067-1074.
5. Rea, I.M., *Towards ageing well: Use it or lose it: Exercise, epigenetics and cognition*. Biogerontology, 2017. **18**(4): p. 679-691.
6. Berntsen, G., et al., *The Evidence Base for an Ideal Care Pathway for Frail Multimorbid Elderly: Combined Scoping and Systematic Intervention Review*. J Med Internet Res, 2019. **21**(4): p. e12517.
7. Rose, M.R., et al., *What is Aging?* Front Genet, 2012. **3**: p. 134.
8. López-Otín, C., et al., *The hallmarks of aging*. Cell, 2013. **153**(6): p. 1194-217.
9. Powers, E.T., et al., *Biological and chemical approaches to diseases of proteostasis deficiency*. Annu Rev Biochem, 2009. **78**: p. 959-91.
10. Lynch, M.D., *How does cellular senescence prevent cancer?* DNA Cell Biol, 2006. **25**(2): p. 69-78.
11. de Renty, C. and N.A. Ellis, *Bloom's syndrome: Why not premature aging?: A comparison of the BLM and WRN helicases*. Ageing Res Rev, 2017. **33**: p. 36-51.
12. Ozgenc, A. and L.A. Loeb, *Werner Syndrome, aging and cancer*. Genome Dyn, 2006. **1**: p. 206-217.
13. Lipsky, M.S. and M. King, *Biological theories of aging*. Disease-a-Month, 2015. **61**(11): p. 460-466.
14. Goronzy, J.J. and C.M. Weyand, *Understanding immunosenescence to improve responses to vaccines*. Nature Immunology, 2013. **14**(5): p. 428-436.
15. Sadighi Akha, A.A., *Ageing and the immune system: An overview*. Journal of Immunological Methods, 2018. **463**: p. 21-26.
16. Fülöp, T., A. Larbi, and G. Pawelec, *Human T cell aging and the impact of persistent viral infections*. Front Immunol, 2013. **4**: p. 271.
17. Solana, R., et al. *Innate immunosenescence: effect of aging on cells and receptors of the innate immune system in humans*. in *Seminars in immunology*. 2012. Elsevier.
18. Belkaid, Y. and B.T. Rouse, *Natural regulatory T cells in infectious disease*. Nat Immunol, 2005. **6**(4): p. 353-60.
19. Bekkering, S. and R. Torensma, *Another look at the life of a neutrophil*. World Journal of Hematology, 2013. **2**(2): p. 44-58.
20. Ray, D. and R. Yung, *Immune senescence, epigenetics and autoimmunity*. Clin Immunol, 2018. **196**: p. 59-63.
21. Partridge, L., J. Deelen, and P.E. Slagboom, *Facing up to the global challenges of ageing*. Nature, 2018. **561**(7721): p. 45-56.
22. O'Driscoll, M., et al., *Age-specific mortality and immunity patterns of SARS-CoV-2*. Nature, 2021. **590**(7844): p. 140-145.
23. Coppé, J.P., et al., *The senescence-associated secretory phenotype: the dark side of tumor suppression*. Annu Rev Pathol, 2010. **5**: p. 99-118.
24. Blank, C.U., et al., *Defining 'T cell exhaustion'*. Nature Reviews Immunology, 2019. **19**(11): p. 665-674.

25. McLane, L.M., M.S. Abdel-Hakeem, and E.J. Wherry, *CD8 T Cell Exhaustion During Chronic Viral Infection and Cancer*. *Annu Rev Immunol*, 2019. **37**: p. 457-495.
26. Tümpel, S. and K.L. Rudolph, *Quiescence: Good and Bad of Stem Cell Aging*. *Trends in Cell Biology*, 2019. **29**(8): p. 672-685.
27. Van de Velde, L.-A. and P.J. Murray, *Proliferating Helper T Cells Require Rictor/mTORC2 Complex to Integrate Signals from Limiting Environmental Amino Acids**. *Journal of Biological Chemistry*, 2016. **291**(50): p. 25815-25822.
28. Liu, B., et al., *A tale of terminal differentiation: IKKalpha, the master keratinocyte regulator*. *Cell cycle (Georgetown, Tex.)*, 2009. **8**(4): p. 527-531.
29. Wiedemann, C., *Terminal differentiation*. *Nature Reviews Neuroscience*, 2009. **10**(7): p. 469-469.
30. Iwama, A., et al., *Terminal differentiation of murine resident peritoneal macrophages is characterized by expression of the STK protein tyrosine kinase, a receptor for macrophage-stimulating protein*. *Blood*, 1995. **86**(9): p. 3394-403.
31. Matatall, K.A., et al., *Chronic Infection Depletes Hematopoietic Stem Cells through Stress-Induced Terminal Differentiation*. *Cell Reports*, 2016. **17**(10): p. 2584-2595.
32. Hayflick, L. and P.S. Moorhead, *The serial cultivation of human diploid cell strains*. *Exp Cell Res*, 1961. **25**: p. 585-621.
33. Shay, J.W. and W.E. Wright, *Hayflick, his limit, and cellular ageing*. *Nature Reviews Molecular Cell Biology*, 2000. **1**(1): p. 72-76.
34. von Kobbe, C., *Cellular senescence: a view throughout organismal life*. *Cellular and Molecular Life Sciences*, 2018. **75**(19): p. 3553-3567.
35. Lozano-Torres, B., et al., *The chemistry of senescence*. *Nature Reviews Chemistry*, 2019. **3**(7): p. 426-441.
36. Oubaha, M., et al., *Senescence-associated secretory phenotype contributes to pathological angiogenesis in retinopathy*. *Science Translational Medicine*, 2016. **8**(362): p. 362ra144-362ra144.
37. Toussaint, O., E.E. Medrano, and T. von Zglinicki, *Cellular and molecular mechanisms of stress-induced premature senescence (SIPS) of human diploid fibroblasts and melanocytes*. *Exp Gerontol*, 2000. **35**(8): p. 927-45.
38. Wang, Z. and C. Shi, *Cellular senescence is a promising target for chronic wounds: a comprehensive review*. *Burns & trauma*, 2020. **8**: p. tkaa021-tkaa021.
39. Campisi, J., *Replicative Senescence: An Old Lives' Tale?* *Cell*, 1996. **84**(4): p. 497-500.
40. He, S. and N.E. Sharpless, *Senescence in Health and Disease*. *Cell*, 2017. **169**(6): p. 1000-1011.
41. Gorgoulis, V., et al., *Cellular Senescence: Defining a Path Forward*. *Cell*, 2019. **179**(4): p. 813-827.
42. Di Micco, R., et al., *Cellular senescence in ageing: from mechanisms to therapeutic opportunities*. *Nature Reviews Molecular Cell Biology*, 2021. **22**(2): p. 75-95.
43. Bringold, F. and M. Serrano, *Tumor suppressors and oncogenes in cellular senescence*. *Exp Gerontol*, 2000. **35**(3): p. 317-29.
44. Kaelin Jr, W.G., *Functions of the retinoblastoma protein*. *Bioessays*, 1999. **21**(11): p. 950-958.
45. Ohtani, N., et al., *The p16INK4a-RB pathway: molecular link between cellular senescence and tumor suppression*. *J Med Invest*, 2004. **51**(3-4): p. 146-53.
46. Ruas, M. and G. Peters, *The p16INK4a/CDKN2A tumor suppressor and its relatives*. *Biochimica et biophysica acta*, 1998. **1378**(2): p. F115-77.

47. Brenner, A.J., M.R. Stampfer, and C.M. Aldaz, *Increased p16 expression with first senescence arrest in human mammary epithelial cells and extended growth capacity with p16 inactivation*. *Oncogene*, 1998. **17**(2): p. 199-205.
48. Momand, J., et al., *The MDM2 gene amplification database*. *Nucleic Acids Research*, 1998. **26**(15): p. 3453-3459.
49. Spallarossa, P., et al., *Doxorubicin induces senescence or apoptosis in rat neonatal cardiomyocytes by regulating the expression levels of the telomere binding factors 1 and 2*. *Am J Physiol Heart Circ Physiol*, 2009. **297**(6): p. H2169-81.
50. Tahara, H., et al., *Increase in expression level of p21(sdi1/cip1/waf1) with increasing division age in both normal and SV40-transformed human fibroblasts*. *Oncogene*, 1995. **10**(5): p. 835-840.
51. Quelle, D.E., et al., *Cancer-associated mutations at the INK4a locus cancel cell cycle arrest by p16INK4a but not by the alternative reading frame protein p19ARF*. *Proceedings of the National Academy of Sciences of the United States of America*, 1997. **94**(2): p. 669-673.
52. Sherr, C.J., *Tumor surveillance via the ARF-p53 pathway*. *Genes & development*, 1998. **12**(19): p. 2984-2991.
53. Kamijo, T., et al., *Tumor suppression at the mouse INK4a locus mediated by the alternative reading frame product p19 ARF*. *Cell*, 1997. **91**(5): p. 649-659.
54. Sorrentino, J.A., et al., *p16INK4a reporter mice reveal age-promoting effects of environmental toxicants*. *J Clin Invest*, 2014. **124**(1): p. 169-73.
55. Liu, J.-Y., et al., *Cells exhibiting strong p16^{INK4a} promoter activation in vivo display features of senescence*. *Proceedings of the National Academy of Sciences*, 2019. **116**(7): p. 2603-2611.
56. Engelman, J.A., J. Luo, and L.C. Cantley, *The evolution of phosphatidylinositol 3-kinases as regulators of growth and metabolism*. *Nat Rev Genet*, 2006. **7**(8): p. 606-19.
57. Sun, H., et al., *PTEN modulates cell cycle progression and cell survival by regulating phosphatidylinositol 3,4,5,-trisphosphate and Akt/protein kinase B signaling pathway*. *Proc Natl Acad Sci U S A*, 1999. **96**(11): p. 6199-204.
58. Shayesteh, L., et al., *PIK3CA is implicated as an oncogene in ovarian cancer*. *Nature genetics*, 1999. **21**(1): p. 99-102.
59. Tresini, M., et al., *A phosphatidylinositol 3-kinase inhibitor induces a senescent-like growth arrest in human diploid fibroblasts*. *Cancer research*, 1998. **58**(1): p. 1-4.
60. Lloyd, R.V., et al., *p27kip1: a multifunctional cyclin-dependent kinase inhibitor with prognostic significance in human cancers*. *The American journal of pathology*, 1999. **154**(2): p. 313-323.
61. Bos, J.L., *Ras oncogenes in human cancer: a review*. *Cancer research*, 1989. **49**(17): p. 4682-4689.
62. Malumbres, M. and A. Pellicer, *RAS pathways to cell cycle control and cell transformation*. *Front Biosci*, 1998. **3**(6): p. 887-912.
63. Lin, A.W., et al., *Premature senescence involving p53 and p16 is activated in response to constitutive MEK/MAPK mitogenic signaling*. *Genes & development*, 1998. **12**(19): p. 3008-3019.
64. Lin, T.Y., et al., *Loss of the candidate tumor suppressor BTG3 triggers acute cellular senescence via the ERK-JMJD3-p16(INK4a) signaling axis*. *Oncogene*, 2012. **31**(27): p. 3287-97.
65. Weber, J.D., et al., *p53-independent functions of the p19(ARF) tumor suppressor*. *Genes & development*, 2000. **14**(18): p. 2358-2365.

66. Lee, A.C., et al., *Ras proteins induce senescence by altering the intracellular levels of reactive oxygen species*. Journal of Biological Chemistry, 1999. **274**(12): p. 7936-7940.
67. David, G., *Regulation of oncogene-induced cell cycle exit and senescence by chromatin modifiers*. Cancer biology & therapy, 2012. **13**(11): p. 992-1000.
68. Passos, J.F., G. Saretzki, and T. von Zglinicki, *DNA damage in telomeres and mitochondria during cellular senescence: is there a connection?* Nucleic Acids Res, 2007. **35**(22): p. 7505-13.
69. Martin-Ruiz, C., et al., *Stochastic Variation in Telomere Shortening Rate Causes Heterogeneity of Human Fibroblast Replicative Life Span**. Journal of Biological Chemistry, 2004. **279**(17): p. 17826-17833.
70. Pluquet, O., A. Pourtier, and C. Abbadie, *The unfolded protein response and cellular senescence. A Review in the Theme: Cellular Mechanisms of Endoplasmic Reticulum Stress Signaling in Health and Disease*. American Journal of Physiology-Cell Physiology, 2015. **308**(6): p. C415-C425.
71. Burton, D.G.A. and R.G.A. Faragher, *Obesity and type-2 diabetes as inducers of premature cellular senescence and ageing*. Biogerontology, 2018. **19**(6): p. 447-459.
72. Minamino, T., et al., *A crucial role for adipose tissue p53 in the regulation of insulin resistance*. Nat Med, 2009. **15**(9): p. 1082-7.
73. Ogrodnik, M., et al., *Obesity-Induced Cellular Senescence Drives Anxiety and Impairs Neurogenesis*. Cell metabolism, 2019. **29**(5): p. 1061-1077.e8.
74. Ogrodnik, M., et al., *Cellular senescence drives age-dependent hepatic steatosis*. Nature Communications, 2017. **8**(1): p. 15691.
75. Higuchi, M., et al., *Differentiation of human adipose-derived stem cells into fat involves reactive oxygen species and Forkhead box O1 mediated upregulation of antioxidant enzymes*. Stem Cells Dev, 2013. **22**(6): p. 878-88.
76. Dodig, S., I. Čepelak, and I. Pavić, *Hallmarks of senescence and aging*. Biochemia medica, 2019. **29**(3): p. 030501-030501.
77. Neurohr, G.E., et al., *Excessive Cell Growth Causes Cytoplasm Dilution And Contributes to Senescence*. Cell, 2019. **176**(5): p. 1083-1097.e18.
78. Georgakopoulou, E.A., et al., *Specific lipofuscin staining as a novel biomarker to detect replicative and stress-induced senescence. A method applicable in cryo-preserved and archival tissues*. Aging, 2013. **5**(1): p. 37-50.
79. Aravinthan, A., et al., *Vacuolation in hepatocyte nuclei is a marker of senescence*. J Clin Pathol, 2012. **65**(6): p. 557-60.
80. Leikam, C., et al., *In vitro evidence for senescent multinucleated melanocytes as a source for tumor-initiating cells*. Cell Death & Disease, 2015. **6**(4): p. e1711-e1711.
81. Kwon, S.M., et al., *Metabolic features and regulation in cell senescence*. BMB reports, 2019. **52**(1): p. 5-12.
82. Machado-Oliveira, G., et al., *Cell Senescence, Multiple Organelle Dysfunction and Atherosclerosis*. Cells, 2020. **9**(10): p. 2146.
83. Ma, Y. and J. Li, *Metabolic shifts during aging and pathology*. Compr Physiol, 2015. **5**(2): p. 667-86.
84. Soto-Gamez, A., W.J. Quax, and M. Demaria, *Regulation of Survival Networks in Senescent Cells: From Mechanisms to Interventions*. Journal of Molecular Biology, 2019. **431**(15): p. 2629-2643.
85. Chen, W., et al., *p53-related apoptosis resistance and tumor suppression activity in UVB-induced premature senescent human skin fibroblasts*. Int J Mol Med, 2008. **21**(5): p. 645-53.

86. Serrano, M., *Senescence helps regeneration*. Dev Cell, 2014. **31**(6): p. 671-2.
87. Muñoz-Espín, D., et al., *Programmed Cell Senescence during Mammalian Embryonic Development*. Cell, 2013. **155**(5): p. 1104-1118.
88. Banito, A. and S.W. Lowe, *A new development in senescence*. Cell, 2013. **155**(5): p. 977-978.
89. Ye, J., et al., *Human regulatory T cells induce T-lymphocyte senescence*. Blood, 2012. **120**(10): p. 2021-2031.
90. Campisi, J. and F. d'Adda di Fagagna, *Cellular senescence: when bad things happen to good cells*. Nature Reviews Molecular Cell Biology, 2007. **8**(9): p. 729-740.
91. Lujambio, A., *To clear, or not to clear (senescent cells)? That is the question*. Bioessays, 2016. **38 Suppl 1**: p. S56-64.
92. van Deursen, J.M., *The role of senescent cells in ageing*. Nature, 2014. **509**(7501): p. 439-46.
93. Campisi, J., *Aging, Cellular Senescence, and Cancer*. Annual Review of Physiology, 2013. **75**(1): p. 685-705.
94. Gonzalez-Meljem, J.M., et al., *Paracrine roles of cellular senescence in promoting tumourigenesis*. British Journal of Cancer, 2018. **118**(10): p. 1283-1288.
95. Acosta, J.C., et al., *Chemokine Signaling via the CXCR2 Receptor Reinforces Senescence*. Cell, 2008. **133**(6): p. 1006-1018.
96. Acosta, J.C., et al., *A complex secretory program orchestrated by the inflammasome controls paracrine senescence*. Nature Cell Biology, 2013. **15**(8): p. 978-990.
97. Orjalo, A.V., et al., *Cell surface-bound IL-1 α is an upstream regulator of the senescence-associated IL-6/IL-8 cytokine network*. Proceedings of the National Academy of Sciences, 2009. **106**(40): p. 17031-17036.
98. Pollak, M., *The insulin and insulin-like growth factor receptor family in neoplasia: an update*. Nat Rev Cancer, 2012. **12**(3): p. 159-69.
99. Tran, D., et al., *Insulin-like growth factor-1 regulates the SIRT1-p53 pathway in cellular senescence*. Aging Cell, 2014. **13**(4): p. 669-78.
100. Rajagopalan, S. and E.O. Long, *Cellular senescence induced by CD158d reprograms natural killer cells to promote vascular remodeling*. Proc Natl Acad Sci U S A, 2012. **109**(50): p. 20596-601.
101. Karimian, A., Y. Ahmadi, and B. Yousefi, *Multiple functions of p21 in cell cycle, apoptosis and transcriptional regulation after DNA damage*. DNA Repair (Amst), 2016. **42**: p. 63-71.
102. Jun, J.I. and L.F. Lau, *The matricellular protein CCN1 induces fibroblast senescence and restricts fibrosis in cutaneous wound healing*. Nat Cell Biol, 2010. **12**(7): p. 676-85.
103. Childs, B.G., et al., *Senescent intimal foam cells are deleterious at all stages of atherosclerosis*. Science, 2016. **354**(6311): p. 472-477.
104. Terlecki-Zaniewicz, L., et al., *Small extracellular vesicles and their miRNA cargo are anti-apoptotic members of the senescence-associated secretory phenotype*. Aging (Albany NY), 2018. **10**(5): p. 1103-1132.
105. Terzi, M.Y., M. Izmirli, and B. Gogebakan, *The cell fate: senescence or quiescence*. Mol Biol Rep, 2016. **43**(11): p. 1213-1220.
106. Wang, W., et al., *Characterization of regulatory elements on the promoter region of p16(INK4a) that contribute to overexpression of p16 in senescent fibroblasts*. J Biol Chem, 2001. **276**(52): p. 48655-61.
107. Herranz, N. and J. Gil, *Mechanisms and functions of cellular senescence*. J Clin Invest, 2018. **128**(4): p. 1238-1246.

108. Rodier, F., et al., *Persistent DNA damage signalling triggers senescence-associated inflammatory cytokine secretion*. Nat Cell Biol, 2009. **11**(8): p. 973-9.
109. Rodier, F., et al., *DNA-SCARS: distinct nuclear structures that sustain damage-induced senescence growth arrest and inflammatory cytokine secretion*. J Cell Sci, 2011. **124**(Pt 1): p. 68-81.
110. Davalos, A.R., et al., *Senescent cells as a source of inflammatory factors for tumor progression*. Cancer Metastasis Rev, 2010. **29**(2): p. 273-83.
111. Yang, H., et al., *cGAS is essential for cellular senescence*. Proceedings of the National Academy of Sciences, 2017. **114**(23): p. E4612-E4620.
112. Kuilman, T., et al., *Oncogene-Induced Senescence Relayed by an Interleukin-Dependent Inflammatory Network*. Cell, 2008. **133**(6): p. 1019-1031.
113. McCool, K.W. and S. Miyamoto, *DNA damage-dependent NF- κ B activation: NEMO turns nuclear signaling inside out*. Immunol Rev, 2012. **246**(1): p. 311-26.
114. Kang, C., et al., *The DNA damage response induces inflammation and senescence by inhibiting autophagy of GATA4*. Science, 2015. **349**(6255): p. aaa5612.
115. Freund, A., C.K. Patil, and J. Campisi, *p38MAPK is a novel DNA damage response-independent regulator of the senescence-associated secretory phenotype*. The EMBO journal, 2011. **30**(8): p. 1536-1548.
116. Alspach, E., et al., *p38MAPK Plays a Crucial Role in Stromal-Mediated Tumorigenesis*. Cancer Discovery, 2014. **4**(6): p. 716-729.
117. Herranz, N., et al., *mTOR regulates MAPKAPK2 translation to control the senescence-associated secretory phenotype*. Nature Cell Biology, 2015. **17**(9): p. 1205-1217.
118. Laberge, R.M., et al., *MTOR regulates the pro-tumorigenic senescence-associated secretory phenotype by promoting IL1A translation*. Nat Cell Biol, 2015. **17**(8): p. 1049-61.
119. Borodkina, A.V., et al., *"Social Life" of Senescent Cells: What Is SASP and Why Study It?* Acta Naturae, 2018. **10**(1): p. 4-14.
120. Demaria, M., et al., *An Essential Role for Senescent Cells in Optimal Wound Healing through Secretion of PDGF-AA*. Developmental Cell, 2014. **31**(6): p. 722-733.
121. Fridlyanskaya, I., L. Alekseenko, and N. Nikolsky, *Senescence as a general cellular response to stress: A mini-review*. Experimental gerontology, 2015. **72**: p. 124-128.
122. Laberge, R.M., et al., *Mitochondrial DNA damage induces apoptosis in senescent cells*. Cell Death & Disease, 2013. **4**(7): p. e727-e727.
123. Li, Z., et al., *Aging and age-related diseases: from mechanisms to therapeutic strategies*. Biogerontology, 2021. **22**(2): p. 165-187.
124. McHugh, D. and J. Gil, *Senescence and aging: Causes, consequences, and therapeutic avenues*. J Cell Biol, 2018. **217**(1): p. 65-77.
125. Rao, S.G. and J.G. Jackson, *SASP: Tumor Suppressor or Promoter? Yes!* Trends Cancer, 2016. **2**(11): p. 676-687.
126. Pignolo, R.J., S.F. Law, and A. Chandra, *Bone aging, cellular senescence, and osteoporosis*. JBMR Plus. **n/a**(n/a): p. e10488.
127. Rodier, F. and J. Campisi, *Four faces of cellular senescence*. J Cell Biol, 2011. **192**(4): p. 547-56.
128. Malaquin, N., A. Martinez, and F. Rodier, *Keeping the senescence secretome under control: Molecular reins on the senescence-associated secretory phenotype*. Experimental Gerontology, 2016. **82**: p. 39-49.
129. Watanabe, S., et al., *Impact of senescence-associated secretory phenotype and its potential as a therapeutic target for senescence-associated diseases*. Cancer Science, 2017. **108**(4): p. 563-569.

130. Ritschka, B., et al., *The senescence-associated secretory phenotype induces cellular plasticity and tissue regeneration*. Genes Dev, 2017. **31**(2): p. 172-183.
131. Sun, Y., J.P. Coppé, and E.W. Lam, *Cellular Senescence: The Sought or the Unwanted?* Trends Mol Med, 2018. **24**(10): p. 871-885.
132. Wang, B., J. Kohli, and M. Demaria, *Senescent Cells in Cancer Therapy: Friends or Foes?* Trends Cancer, 2020. **6**(10): p. 838-857.
133. Baker, D.J., R.L. Weaver, and J.M. van Deursen, *p21 both attenuates and drives senescence and aging in BubR1 progeroid mice*. Cell reports, 2013. **3**(4): p. 1164-1174.
134. Amaya-Montoya, M., et al., *Cellular Senescence as a Therapeutic Target for Age-Related Diseases: A Review*. Advances in Therapy, 2020. **37**(4): p. 1407-1424.
135. Heilbronn, L.K., et al., *Alternate-day fasting in nonobese subjects: effects on body weight, body composition, and energy metabolism*. Am J Clin Nutr, 2005. **81**(1): p. 69-73.
136. Wang, C., et al., *Adult-onset, short-term dietary restriction reduces cell senescence in mice*. Aging (Albany NY), 2010. **2**(9): p. 555-66.
137. Fontana, L., et al., *The effects of graded caloric restriction: XII. Comparison of mouse to human impact on cellular senescence in the colon*. Aging Cell, 2018. **17**(3): p. e12746.
138. Fontana, L., J. Nehme, and M. Demaria, *Caloric restriction and cellular senescence*. Mech Ageing Dev, 2018. **176**: p. 19-23.
139. Fontana, L., et al., *Effects of 2-year calorie restriction on circulating levels of IGF-1, IGF-binding proteins and cortisol in nonobese men and women: a randomized clinical trial*. Aging Cell, 2016. **15**(1): p. 22-7.
140. Buettner, D. and S. Skemp, *Blue Zones: Lessons From the World's Longest Lived*. American journal of lifestyle medicine, 2016. **10**(5): p. 318-321.
141. Appel, L.J., *Dietary Patterns and Longevity*. Circulation, 2008. **118**(3): p. 214-215.
142. Wahlqvist, M.L., et al., *Does diet matter for survival in long-lived cultures?* Asia Pac J Clin Nutr, 2005. **14**(1): p. 2-6.
143. Moiseeva, O., et al., *Metformin inhibits the senescence-associated secretory phenotype by interfering with IKK/NF- κ B activation*. Aging Cell, 2013. **12**(3): p. 489-98.
144. Campbell, J.M., et al., *Metformin reduces all-cause mortality and diseases of ageing independent of its effect on diabetes control: A systematic review and meta-analysis*. Ageing Res Rev, 2017. **40**: p. 31-44.
145. Wang, R., et al., *Rapamycin inhibits the secretory phenotype of senescent cells by a Nrf2-independent mechanism*. Aging Cell, 2017. **16**(3): p. 564-574.
146. Harrison, D.E., et al., *Rapamycin fed late in life extends lifespan in genetically heterogeneous mice*. Nature, 2009. **460**(7253): p. 392-395.
147. Stallone, G., et al., *Management of Side Effects of Sirolimus Therapy*. Transplantation, 2009. **87**(8S): p. S23-S26.
148. Xu, M., et al., *JAK inhibition alleviates the cellular senescence-associated secretory phenotype and frailty in old age*. Proc Natl Acad Sci U S A, 2015. **112**(46): p. E6301-10.
149. Roskoski, R., Jr., *Janus kinase (JAK) inhibitors in the treatment of inflammatory and neoplastic diseases*. Pharmacol Res, 2016. **111**: p. 784-803.
150. Zhu, Y., et al., *The Achilles' heel of senescent cells: from transcriptome to senolytic drugs*. Aging Cell, 2015. **14**(4): p. 644-58.
151. Kang, C., *Senolytics and Senostatics: A Two-Pronged Approach to Target Cellular Senescence for Delaying Aging and Age-Related Diseases*. Mol Cells, 2019. **42**(12): p. 821-827.
152. Zhu, Y., et al., *Identification of a novel senolytic agent, navitoclax, targeting the Bcl-2 family of anti-apoptotic factors*. Aging Cell, 2016. **15**(3): p. 428-35.

153. Chien, Y., et al., *Control of the senescence-associated secretory phenotype by NF- κ B promotes senescence and enhances chemosensitivity*. *Genes Dev*, 2011. **25**(20): p. 2125-36.
154. De Cecco, M., et al., *L1 drives IFN in senescent cells and promotes age-associated inflammation*. *Nature*, 2019. **566**(7742): p. 73-78.
155. Hernandez-Segura, A., et al., *Unmasking Transcriptional Heterogeneity in Senescent Cells*. *Curr Biol*, 2017. **27**(17): p. 2652-2660.e4.
156. Wiley, C.D., et al., *Mitochondrial Dysfunction Induces Senescence with a Distinct Secretory Phenotype*. *Cell Metab*, 2016. **23**(2): p. 303-14.
157. Soto-Gamez, A. and M. Demaria, *Therapeutic interventions for aging: the case of cellular senescence*. *Drug Discovery Today*, 2017. **22**(5): p. 786-795.
158. von Kobbe, C., *Targeting senescent cells: approaches, opportunities, challenges*. *Aging*, 2019. **11**(24): p. 12844-12861.
159. Prata, L.G.P.L., et al., *Senescent cell clearance by the immune system: Emerging therapeutic opportunities*. *Seminars in immunology*, 2018. **40**: p. 101275-101275.
160. Xue, W., et al., *Senescence and tumour clearance is triggered by p53 restoration in murine liver carcinomas*. *Nature*, 2007. **445**(7128): p. 656-60.
161. Krizhanovsky, V., et al., *Senescence of activated stellate cells limits liver fibrosis*. *Cell*, 2008. **134**(4): p. 657-67.
162. Lujambio, A., et al., *Non-cell-autonomous tumor suppression by p53*. *Cell*, 2013. **153**(2): p. 449-60.
163. Rószter, T., *Understanding the Mysterious M2 Macrophage through Activation Markers and Effector Mechanisms*. *Mediators of inflammation*, 2015. **2015**: p. 816460-816460.
164. Hall, B.M., et al., *Aging of mice is associated with p16(*Ink4a*)- and β -galactosidase-positive macrophage accumulation that can be induced in young mice by senescent cells*. *Aging (Albany NY)*, 2016. **8**(7): p. 1294-315.
165. Kang, T.W., et al., *Senescence surveillance of pre-malignant hepatocytes limits liver cancer development*. *Nature*, 2011. **479**(7374): p. 547-51.
166. Braumüller, H., et al., *T-helper-1-cell cytokines drive cancer into senescence*. *Nature*, 2013. **494**(7437): p. 361-5.
167. Olmedo, D., et al., *Macrophages related to dental implant failure*. *Implant Dent*, 2003. **12**(1): p. 75-80.
168. Ishida, T., et al., *Live-cell imaging of macrophage phagocytosis of asbestos fibers under fluorescence microscopy*. *Genes and environment : the official journal of the Japanese Environmental Mutagen Society*, 2019. **41**: p. 14-14.
169. Burton, D.G.A. and A. Stolzing, *Cellular senescence: Immunosurveillance and future immunotherapy*. *Ageing Research Reviews*, 2018. **43**: p. 17-25.
170. Frescas, D., et al., *Senescent cells expose and secrete an oxidized form of membrane-bound vimentin as revealed by a natural polyreactive antibody*. *Proceedings of the National Academy of Sciences*, 2017: p. 201614661.
171. Ademowo, O.S., et al., *Lipid (per) oxidation in mitochondria: an emerging target in the ageing process?* *Biogerontology*, 2017. **18**(6): p. 859-879.
172. Canton, J., D. Neculai, and S. Grinstein, *Scavenger receptors in homeostasis and immunity*. *Nat Rev Immunol*, 2013. **13**(9): p. 621-34.
173. Tauber, A.I., *Metchnikoff and the phagocytosis theory*. *Nature Reviews Molecular Cell Biology*, 2003. **4**(11): p. 897-901.
174. Mantovani, A., et al., *Macrophage plasticity and polarization in tissue repair and remodelling*. *J Pathol*, 2013. **229**(2): p. 176-85.

175. Wynn, T.A. and K.M. Vannella, *Macrophages in Tissue Repair, Regeneration, and Fibrosis*. *Immunity*, 2016. **44**(3): p. 450-462.
176. Sica, A., et al., *Macrophage polarization in pathology*. *Cell Mol Life Sci*, 2015. **72**(21): p. 4111-26.
177. Wynn, T.A., A. Chawla, and J.W. Pollard, *Macrophage biology in development, homeostasis and disease*. *Nature*, 2013. **496**(7446): p. 445-55.
178. Li, Q. and B.A. Barres, *Microglia and macrophages in brain homeostasis and disease*. *Nature Reviews Immunology*, 2018. **18**(4): p. 225-242.
179. McGrath, K.E., J.M. Frame, and J. Palis, *Early hematopoiesis and macrophage development*. *Seminars in immunology*, 2015. **27**(6): p. 379-387.
180. Janssen, W.J., et al., *Myeloid Cell Turnover and Clearance*. *Microbiology spectrum*, 2016. **4**(6): p. 10.1128/microbiolspec.MCHD-0005-2015.
181. Lavine, K.J., et al., *Distinct macrophage lineages contribute to disparate patterns of cardiac recovery and remodeling in the neonatal and adult heart*. *Proc Natl Acad Sci U S A*, 2014. **111**(45): p. 16029-34.
182. Davies, L.C. and P.R. Taylor, *Tissue-resident macrophages: then and now*. *Immunology*, 2015. **144**(4): p. 541-548.
183. Guillems, M. and F.R. Svedberg, *Does tissue imprinting restrict macrophage plasticity?* *Nature Immunology*, 2021. **22**(2): p. 118-127.
184. Murray, P.J. and T.A. Wynn, *Protective and pathogenic functions of macrophage subsets*. *Nat Rev Immunol*, 2011. **11**(11): p. 723-37.
185. Sica, A. and A. Mantovani, *Macrophage plasticity and polarization: in vivo veritas*. *J Clin Invest*, 2012. **122**(3): p. 787-95.
186. Murray, P.J., et al., *Macrophage activation and polarization: nomenclature and experimental guidelines*. *Immunity*, 2014. **41**(1): p. 14-20.
187. Biswas, S.K. and A. Mantovani, *Macrophage plasticity and interaction with lymphocyte subsets: cancer as a paradigm*. *Nat Immunol*, 2010. **11**(10): p. 889-96.
188. Nourshargh, S. and R. Alon, *Leukocyte migration into inflamed tissues*. *Immunity*, 2014. **41**(5): p. 694-707.
189. Martinez, F.O., L. Helming, and S. Gordon, *Alternative activation of macrophages: an immunologic functional perspective*. *Annu Rev Immunol*, 2009. **27**: p. 451-83.
190. Murray, P.J., *Macrophage Polarization*. *Annual Review of Physiology*, 2017. **79**(1): p. 541-566.
191. Orecchioni, M., et al., *Macrophage Polarization: Different Gene Signatures in M1(LPS+) vs. Classically and M2(LPS-) vs. Alternatively Activated Macrophages*. *Frontiers in Immunology*, 2019. **10**(1084).
192. Martinez, F.O. and S. Gordon, *The M1 and M2 paradigm of macrophage activation: time for reassessment*. *F1000prime reports*, 2014. **6**: p. 13-13.
193. Murray, P.J. and T.A. Wynn, *Obstacles and opportunities for understanding macrophage polarization*. *Journal of Leukocyte Biology*, 2011. **89**(4): p. 557-563.
194. Wang, N., H. Liang, and K. Zen, *Molecular mechanisms that influence the macrophage m1-m2 polarization balance*. *Front Immunol*, 2014. **5**: p. 614.
195. Luzina, I.G., et al., *Regulation of inflammation by interleukin-4: a review of "alternatives"*. *Journal of leukocyte biology*, 2012. **92**(4): p. 753-764.
196. Zhang, F., et al., *TGF- β induces M2-like macrophage polarization via SNAIL-mediated suppression of a pro-inflammatory phenotype*. *Oncotarget*, 2016. **7**(32): p. 52294-52306.

197. Horibe, K., M. Hara, and H. Nakamura, *M2-like macrophage infiltration and transforming growth factor- β secretion during socket healing process in mice*. Archives of Oral Biology, 2021. **123**: p. 105042.
198. Chua, C.L., et al., *Monocytes and macrophages in malaria: protection or pathology?* Trends Parasitol, 2013. **29**(1): p. 26-34.
199. Belgiovine, C., et al., *Tumor-associated macrophages and anti-tumor therapies: complex links*. Cell Mol Life Sci, 2016. **73**(13): p. 2411-24.
200. Chistiakov, D.A., et al., *Macrophage phenotypic plasticity in atherosclerosis: The associated features and the peculiarities of the expression of inflammatory genes*. Int J Cardiol, 2015. **184**: p. 436-445.
201. Stout, R.D. and J. Suttles, *Functional plasticity of macrophages: reversible adaptation to changing microenvironments*. J Leukoc Biol, 2004. **76**(3): p. 509-13.
202. Fujiwara, N. and K. Kobayashi, *Macrophages in inflammation*. Curr Drug Targets Inflamm Allergy, 2005. **4**(3): p. 281-6.
203. Headland, S.E. and L.V. Norling, *The resolution of inflammation: Principles and challenges*. Semin Immunol, 2015. **27**(3): p. 149-60.
204. Rock, K.L. and H. Kono, *The inflammatory response to cell death*. Annu Rev Pathol, 2008. **3**: p. 99-126.
205. Medina, C.B. and K.S. Ravichandran, *Do not let death do us part: 'find-me' signals in communication between dying cells and the phagocytes*. Cell Death & Differentiation, 2016. **23**(6): p. 979-989.
206. Qu, Y., et al., *Pannexin-1 is required for ATP release during apoptosis but not for inflammasome activation*. J Immunol, 2011. **186**(11): p. 6553-61.
207. Truman, L.A., et al., *CX3CL1/fractalkine is released from apoptotic lymphocytes to stimulate macrophage chemotaxis*. Blood, 2008. **112**(13): p. 5026-36.
208. Gude, D.R., et al., *Apoptosis induces expression of sphingosine kinase 1 to release sphingosine-1-phosphate as a "come-and-get-me" signal*. Faseb j, 2008. **22**(8): p. 2629-38.
209. Elliott, M.R. and K.S. Ravichandran, *The Dynamics of Apoptotic Cell Clearance*. Dev Cell, 2016. **38**(2): p. 147-60.
210. Han, C.Z. and K.S. Ravichandran, *Metabolic connections during apoptotic cell engulfment*. Cell, 2011. **147**(7): p. 1442-5.
211. Kiss, R.S., et al., *Apoptotic cells induce a phosphatidylserine-dependent homeostatic response from phagocytes*. Curr Biol, 2006. **16**(22): p. 2252-8.
212. Fond, A.M., et al., *Apoptotic cells trigger a membrane-initiated pathway to increase ABCA1*. J Clin Invest, 2015. **125**(7): p. 2748-58.
213. Green, D.R., T.H. Oguin, and J. Martinez, *The clearance of dying cells: table for two*. Cell Death Differ, 2016. **23**(6): p. 915-26.
214. Elliott, M.R., K.M. Koster, and P.S. Murphy, *Efferocytosis Signaling in the Regulation of Macrophage Inflammatory Responses*. Journal of immunology (Baltimore, Md. : 1950), 2017. **198**(4): p. 1387-1394.
215. A-Gonzalez, N., et al., *Apoptotic cells promote their own clearance and immune tolerance through activation of the nuclear receptor LXR*. Immunity, 2009. **31**(2): p. 245-258.
216. Haney, M.S., et al., *Identification of phagocytosis regulators using magnetic genome-wide CRISPR screens*. Nature Genetics, 2018. **50**(12): p. 1716-1727.
217. Morioka, S., et al., *Efferocytosis induces a novel SLC program to promote glucose uptake and lactate release*. Nature, 2018. **563**(7733): p. 714-718.
218. Grimsley, C. and K.S. Ravichandran, *Cues for apoptotic cell engulfment: eat-me, don't eat-me and come-get-me signals*. Trends in Cell Biology, 2003. **13**(12): p. 648-656.

219. Lauber, K., et al., *Clearance of Apoptotic Cells: Getting Rid of the Corpses*. Molecular Cell, 2004. **14**(3): p. 277-287.
220. Arur, S., et al., *Annexin I is an endogenous ligand that mediates apoptotic cell engulfment*. Dev Cell, 2003. **4**(4): p. 587-98.
221. Asano, K., et al., *Masking of Phosphatidylserine Inhibits Apoptotic Cell Engulfment and Induces Autoantibody Production in Mice*. Journal of Experimental Medicine, 2004. **200**(4): p. 459-467.
222. Naeini, M.B., et al., *The role of phosphatidylserine recognition receptors in multiple biological functions*. Cellular & molecular biology letters, 2020. **25**: p. 23-23.
223. Hanayama, R., et al., *Identification of a factor that links apoptotic cells to phagocytes*. Nature, 2002. **417**(6885): p. 182-7.
224. Anderson, H.A., et al., *Serum-derived protein S binds to phosphatidylserine and stimulates the phagocytosis of apoptotic cells*. Nat Immunol, 2003. **4**(1): p. 87-91.
225. Brown, S., et al., *Apoptosis disables CD31-mediated cell detachment from phagocytes promoting binding and engulfment*. Nature, 2002. **418**(6894): p. 200-3.
226. Park, S.-Y. and I.-S. Kim, *Engulfment signals and the phagocytic machinery for apoptotic cell clearance*. Experimental & Molecular Medicine, 2017. **49**(5): p. e331-e331.
227. Oldenborg, P.A., H.D. Gresham, and F.P. Lindberg, *CD47-signal regulatory protein alpha (SIRPalpha) regulates Fcgamma and complement receptor-mediated phagocytosis*. J Exp Med, 2001. **193**(7): p. 855-62.
228. Oldenborg, P.A., et al., *Role of CD47 as a marker of self on red blood cells*. Science, 2000. **288**(5473): p. 2051-4.
229. Lv, Z., et al., *Loss of Cell Surface CD47 Clustering Formation and Binding Avidity to SIRPalpha Facilitate Apoptotic Cell Clearance by Macrophages*. Journal of immunology (Baltimore, Md. : 1950), 2015. **195**(2): p. 661-671.
230. Gardai, S.J., et al., *Recognition ligands on apoptotic cells: a perspective*. Journal of Leukocyte Biology, 2006. **79**(5): p. 896-903.
231. Rongvaux, A., et al., *Development and function of human innate immune cells in a humanized mouse model*. Nat Biotechnol, 2014. **32**(4): p. 364-72.
232. Boettcher, A.N., et al., *Porcine signal regulatory protein alpha binds to human CD47 to inhibit phagocytosis: Implications for human hematopoietic stem cell transplantation into severe combined immunodeficient pigs*. Xenotransplantation, 2019. **26**(2): p. e12466-e12466.
233. Navarro-Alvarez, N. and Y.-G. Yang, *CD47: a new player in phagocytosis and xenograft rejection*. Cellular & Molecular Immunology, 2011. **8**(4): p. 285-288.
234. Barclay, A.N., *Signal regulatory protein alpha (SIRPalpha)/CD47 interaction and function*. Current Opinion in Immunology, 2009. **21**(1): p. 47-52.
235. Yin, S.-S. and F.-H. Gao, *Molecular Mechanism of Tumor Cell Immune Escape Mediated by CD24/Siglec-10*. Frontiers in immunology, 2020. **11**: p. 1324-1324.
236. Weiskopf, K., *Cancer immunotherapy targeting the CD47/SIRPalpha axis*. European Journal of Cancer, 2017. **76**: p. 100-109.
237. Lauber, K., et al., *Apoptotic Cells Induce Migration of Phagocytes via Caspase-3-Mediated Release of a Lipid Attraction Signal*. Cell, 2003. **113**(6): p. 717-730.
238. Elliott, M.R., et al., *Nucleotides released by apoptotic cells act as a find-me signal to promote phagocytic clearance*. Nature, 2009. **461**(7261): p. 282-286.
239. Martin-Manso, G., et al., *Thrombospondin 1 promotes tumor macrophage recruitment and enhances tumor cell cytotoxicity of differentiated U937 cells*. Cancer research, 2008. **68**(17): p. 7090-7099.

240. Hou, Y., et al., *Ageing as a risk factor for neurodegenerative disease*. Nat Rev Neurol, 2019. **15**(10): p. 565-581.
241. Wyss-Coray, T., *Ageing, neurodegeneration and brain rejuvenation*. Nature, 2016. **539**(7628): p. 180-186.
242. Soto, C. and S. Pritzkow, *Protein misfolding, aggregation, and conformational strains in neurodegenerative diseases*. Nat Neurosci, 2018. **21**(10): p. 1332-1340.
243. Hamilton, R.L., *Lewy Bodies in Alzheimer's Disease: A Neuropathological Review of 145 Cases Using α -Synuclein Immunohistochemistry*. Brain Pathology, 2000. **10**(3): p. 378-384.
244. Spires-Jones, T.L., J. Attems, and D.R. Thal, *Interactions of pathological proteins in neurodegenerative diseases*. Acta Neuropathologica, 2017. **134**(2): p. 187-205.
245. Tofaris, G.K. and N.J. Buckley, *Convergent molecular defects underpin diverse neurodegenerative diseases*. Journal of Neurology, Neurosurgery & Psychiatry, 2018. **89**(9): p. 962-969.
246. Neumann, M., et al., *Ubiquitinated TDP-43 in Frontotemporal Lobar Degeneration and Amyotrophic Lateral Sclerosis*. Science, 2006. **314**(5796): p. 130-133.
247. Marsh, A.P., *Molecular mechanisms of proteinopathies across neurodegenerative disease: a review*. Neurological Research and Practice, 2019. **1**(1): p. 35.
248. Rochet, J.C. and P.T. Lansbury, Jr., *Amyloid fibrillogenesis: themes and variations*. Curr Opin Struct Biol, 2000. **10**(1): p. 60-8.
249. Kaye, R., et al., *Common structure of soluble amyloid oligomers implies common mechanism of pathogenesis*. Science, 2003. **300**(5618): p. 486-9.
250. Soto, C., *Unfolding the role of protein misfolding in neurodegenerative diseases*. Nat Rev Neurosci, 2003. **4**(1): p. 49-60.
251. Walker, F.O., *Huntington's disease*. Lancet, 2007. **369**(9557): p. 218-28.
252. Landles, C. and G.P. Bates, *Huntingtin and the molecular pathogenesis of Huntington's disease. Fourth in molecular medicine review series*. EMBO Rep, 2004. **5**(10): p. 958-63.
253. Moskowitz, C.B. and K. Marder, *Palliative care for people with late-stage huntington's disease*. Neurologic Clinics, 2001. **19**(4): p. 849-865.
254. Schindler, A., et al., *Fiberoptic endoscopic evaluation of swallowing in early-to-advanced stage Huntington's disease*. Sci Rep, 2020. **10**(1): p. 15242.
255. Labbadia, J. and R.I. Morimoto, *Huntington's disease: underlying molecular mechanisms and emerging concepts*. Trends Biochem Sci, 2013. **38**(8): p. 378-85.
256. Heneka, M.T., et al., *Neuroinflammation in Alzheimer's disease*. Lancet Neurol, 2015. **14**(4): p. 388-405.
257. Roy, E.R., et al., *Type I interferon response drives neuroinflammation and synapse loss in Alzheimer disease*. J Clin Invest, 2020. **130**(4): p. 1912-1930.
258. Weitz, T.M. and T. Town, *Microglia in Alzheimer's Disease: It's All About Context*. Int J Alzheimers Dis, 2012. **2012**: p. 314185.
259. da Costa, J.P., et al., *A synopsis on aging-Theories, mechanisms and future prospects*. Ageing Res Rev, 2016. **29**: p. 90-112.
260. Schmeer, C., et al., *Dissecting Aging and Senescence-Current Concepts and Open Lessons*. Cells, 2019. **8**(11): p. 1446.
261. Hirayama, D., T. Iida, and H. Nakase, *The Phagocytic Function of Macrophage-Enforcing Innate Immunity and Tissue Homeostasis*. International journal of molecular sciences, 2017. **19**(1): p. 92.
262. Muñoz-Espín, D. and M. Serrano, *Cellular senescence: from physiology to pathology*. Nat Rev Mol Cell Biol, 2014. **15**(7): p. 482-96.

263. Yousefzadeh, M.J., et al., *An aged immune system drives senescence and ageing of solid organs*. *Nature*, 2021. **594**(7861): p. 100-105.
264. Fiala, M., et al., *Cyclooxygenase-2-positive macrophages infiltrate the Alzheimer's disease brain and damage the blood-brain barrier*. *Eur J Clin Invest*, 2002. **32**(5): p. 360-71.
265. Phillips, R.J., C.N. Billingsley, and T.L. Powley, *Macrophages are unsuccessful in clearing aggregated alpha-synuclein from the gastrointestinal tract of healthy aged Fischer 344 rats*. *Anatomical record (Hoboken, N.J. : 2007)*, 2013. **296**(4): p. 654-669.
266. Leitman, J., F. Ulrich Hartl, and G.Z. Lederkremer, *Soluble forms of polyQ-expanded huntingtin rather than large aggregates cause endoplasmic reticulum stress*. *Nature Communications*, 2013. **4**(1): p. 2753.
267. Bäuerlein, F.J.B., et al., *In Situ Architecture and Cellular Interactions of PolyQ Inclusions*. *Cell*, 2017. **171**(1): p. 179-187.e10.
268. Yusa, K., et al., *A hyperactive piggyBac transposase for mammalian applications*. *Proceedings of the National Academy of Sciences of the United States of America*, 2011. **108**(4): p. 1531-1536.
269. Mackenzie, I.R., et al., *TIA1 Mutations in Amyotrophic Lateral Sclerosis and Frontotemporal Dementia Promote Phase Separation and Alter Stress Granule Dynamics*. *Neuron*, 2017. **95**(4): p. 808-816.e9.
270. Wei, M.C., et al., *Proapoptotic BAX and BAK: a requisite gateway to mitochondrial dysfunction and death*. *Science*, 2001. **292**(5517): p. 727-30.
271. Rutschman, R., et al., *Cutting Edge: Stat6-Dependent Substrate Depletion Regulates Nitric Oxide Production*. *The Journal of Immunology*, 2001. **166**(4): p. 2173-2177.
272. Zhang, X., R. Goncalves, and D.M. Mosser, *The isolation and characterization of murine macrophages*. *Curr Protoc Immunol*, 2008. **Chapter 14**: p. Unit 14.1.
273. Brunner, J.S., et al., *Environmental arginine controls multinuclear giant cell metabolism and formation*. *Nature Communications*, 2020. **11**(1): p. 431.
274. Schwartz, C., et al., *Eosinophil-specific deletion of I κ B α in mice reveals a critical role of NF- κ B-induced Bcl-xL for inhibition of apoptosis*. *Blood*, 2015. **125**(25): p. 3896-904.
275. Todaro, G.J. and H. Green, *Quantitative studies of the growth of mouse embryo cells in culture and their development into established lines*. *J Cell Biol*, 1963. **17**(2): p. 299-313.
276. Blumenstock, S., et al., *Novel proteostasis reporter mouse reveals different effects of cytoplasmic and nuclear aggregates on protein quality control in neurons*. *bioRxiv*, 2020: p. 2020.11.09.374231.
277. Riera-Tur, I., et al., *Amyloid-like aggregates cause lysosomal defects in neurons via gain-of-function toxicity*. *bioRxiv*, 2021: p. 2019.12.16.877431.
278. Yurdagul, A., Jr., et al., *Macrophage Metabolism of Apoptotic Cell-Derived Arginine Promotes Continual Efferocytosis and Resolution of Injury*. *Cell Metab*, 2020. **31**(3): p. 518-533.e10.
279. Tan, B., et al., *The profiles of mitochondrial respiration and glycolysis using extracellular flux analysis in porcine enterocyte IPEC-J2*. *Animal Nutrition*, 2015. **1**(3): p. 239-243.
280. Campisi, J., et al., *From discoveries in ageing research to therapeutics for healthy ageing*. *Nature*, 2019. **571**(7764): p. 183-192.
281. Bussian, T.J., et al., *Clearance of senescent glial cells prevents tau-dependent pathology and cognitive decline*. *Nature*, 2018. **562**(7728): p. 578-582.
282. Baker, D.J., et al., *Naturally occurring p16(Ink4a)-positive cells shorten healthy lifespan*. *Nature*, 2016. **530**(7589): p. 184-189.
283. Childs, B.G., et al., *Cellular senescence in aging and age-related disease: from mechanisms to therapy*. *Nature medicine*, 2015. **21**(12): p. 1424-1435.

284. Baker, D.J., et al., *Clearance of p16Ink4a-positive senescent cells delays ageing-associated disorders*. *Nature*, 2011. **479**(7372): p. 232-236.
285. Shakeri, H., et al., *Cellular senescence links aging and diabetes in cardiovascular disease*. *Am J Physiol Heart Circ Physiol*, 2018. **315**(3): p. H448-h462.
286. Milanovic, M., et al., *Senescence-associated reprogramming promotes cancer stemness*. *Nature*, 2018. **553**(7686): p. 96-100.
287. Jeon, O.H., et al., *Senescent cells and osteoarthritis: a painful connection*. *The Journal of clinical investigation*, 2018. **128**(4): p. 1229-1237.
288. Prieur, A. and D.S. Peeper, *Cellular senescence in vivo: a barrier to tumorigenesis*. *Current Opinion in Cell Biology*, 2008. **20**(2): p. 150-155.
289. Elder, S.S. and E. Emmerson, *Senescent cells and macrophages: key players for regeneration?* *Open biology*, 2020. **10**(12): p. 200309-200309.
290. Valentijn, F.A., et al., *Cellular senescence in the aging and diseased kidney*. *Journal of cell communication and signaling*, 2018. **12**(1): p. 69-82.
291. Yun, M.H., H. Davaapil, and J.P. Brookes, *Recurrent turnover of senescent cells during regeneration of a complex structure*. *eLife*, 2015. **4**: p. e05505.
292. Ovadya, Y., et al., *Impaired immune surveillance accelerates accumulation of senescent cells and aging*. *Nature Communications*, 2018. **9**(1): p. 5435.
293. Irvine, K.M., et al., *Senescent human hepatocytes express a unique secretory phenotype and promote macrophage migration*. *World J Gastroenterol*, 2014. **20**(47): p. 17851-62.
294. Duffield, J.S., et al., *Selective depletion of macrophages reveals distinct, opposing roles during liver injury and repair*. *J Clin Invest*, 2005. **115**(1): p. 56-65.
295. Lucas, T., et al., *Differential Roles of Macrophages in Diverse Phases of Skin Repair*. *The Journal of Immunology*, 2010. **184**(7): p. 3964-3977.
296. Tsai, K.K., et al., *Low-dose radiation-induced senescent stromal fibroblasts render nearby breast cancer cells radioresistant*. *Radiat Res*, 2009. **172**(3): p. 306-13.
297. Wagner, V. and J. Gil, *Senescence as a therapeutically relevant response to CDK4/6 inhibitors*. *Oncogene*, 2020. **39**(29): p. 5165-5176.
298. Kurz, D.J., et al., *Senescence-associated (beta)-galactosidase reflects an increase in lysosomal mass during replicative ageing of human endothelial cells*. *J Cell Sci*, 2000. **113** (Pt 20): p. 3613-22.
299. Kale, A., et al., *Role of immune cells in the removal of deleterious senescent cells*. *Immunity & Ageing*, 2020. **17**(1): p. 16.
300. Martin, C.J., K.N. Peters, and S.M. Behar, *Macrophages clean up: efferocytosis and microbial control*. *Current opinion in microbiology*, 2014. **17**: p. 17-23.
301. Waddell, L.A., et al., *ADGRE1 (EMR1, F4/80) Is a Rapidly-Evolving Gene Expressed in Mammalian Monocyte-Macrophages*. *Frontiers in Immunology*, 2018. **9**(2246).
302. Cadili, A. and N. Kneteman, *The Role of Macrophages in Xenograft Rejection*. *Transplantation Proceedings*, 2008. **40**(10): p. 3289-3293.
303. Neri, F., et al., *Quantitative Proteomic Analysis of the Senescence-Associated Secretory Phenotype by Data-Independent Acquisition*. *Current Protocols*, 2021. **1**(2): p. e32.
304. Chao, M.P., I.L. Weissman, and R. Majeti, *The CD47-SIRPα pathway in cancer immune evasion and potential therapeutic implications*. *Current Opinion in Immunology*, 2012. **24**(2): p. 225-232.
305. Huang, C.-Y., et al., *Regulation of CD47 expression in cancer cells*. *Translational Oncology*, 2020. **13**(12): p. 100862.
306. Viola, A., et al., *The Metabolic Signature of Macrophage Responses*. *Frontiers in Immunology*, 2019. **10**(1462).

307. S. Dichtl, L.L., L. Zeitler, K. Behnke, D. Schlösser, B. Strobl, J. Scheller, K. C. El Kasmi, P. J. Murray, *Lactate and IL6 define separable paths of inflammatory metabolic adaptation*. Science Advances, 2021. **7**(eabg3505).
308. Nagata, S. and K. Segawa, *Sensing and clearance of apoptotic cells*. Curr Opin Immunol, 2021. **68**: p. 1-8.
309. Westman, J., S. Grinstein, and P.E. Marques, *Phagocytosis of Necrotic Debris at Sites of Injury and Inflammation*. Frontiers in Immunology, 2020. **10**(3030).
310. Brouckaert, G., et al., *Phagocytosis of necrotic cells by macrophages is phosphatidylserine dependent and does not induce inflammatory cytokine production*. Molecular biology of the cell, 2004. **15**(3): p. 1089-1100.
311. Henson, P.M., *Dampening inflammation*. Nature Immunology, 2005. **6**(12): p. 1179-1181.
312. Advani, R., et al., *CD47 Blockade by Hu5F9-G4 and Rituximab in Non-Hodgkin's Lymphoma*. New England Journal of Medicine, 2018. **379**(18): p. 1711-1721.
313. Staub, E., A. Rosenthal, and B. Hinzmann, *Systematic identification of immunoreceptor tyrosine-based inhibitory motifs in the human proteome*. Cell Signal, 2004. **16**(4): p. 435-56.
314. Barkal, A.A., et al., *CD24 signalling through macrophage Siglec-10 is a target for cancer immunotherapy*. Nature, 2019. **572**(7769): p. 392-396.
315. Imbert, P.R.C., et al., *An Acquired and Endogenous Glycocalyx Forms a Bidirectional "Don't Eat" and "Don't Eat Me" Barrier to Phagocytosis*. Current Biology, 2021. **31**(1): p. 77-89.e5.
316. Langhans, T., *Ueber Riesenzellen mit wandständigen Kernen in Tuberkeln und die fibröse Form des Tuberkels*. Archiv für pathologische Anatomie und Physiologie und für Klinische Medicin, 1868. **42**(3): p. 382-404.
317. Mariano, M. and W.G. Spector, *The formation and properties of macrophage polykaryons (inflammatory giant cells)*. J Pathol, 1974. **113**(1): p. 1-19.
318. Helming, L. and S. Gordon, *Molecular mediators of macrophage fusion*. Trends in Cell Biology, 2009. **19**(10): p. 514-522.
319. Samokhin, A.O., et al., *Cholate-containing high-fat diet induces the formation of multinucleated giant cells in atherosclerotic plaques of apolipoprotein E-/- mice*. Arteriosclerosis, thrombosis, and vascular biology, 2010. **30**(6): p. 1166-1173.
320. Lai, S. and X. Zhou, *Inflammatory cells in tissues of gout patients and their correlations with comorbidities*. The open rheumatology journal, 2013. **7**: p. 26.
321. Anderson, J.M., A. Rodriguez, and D.T. Chang. *Foreign body reaction to biomaterials*. in *Seminars in immunology*. 2008. Elsevier.
322. Chambers, T., *Studies on the phagocytic capacity of macrophage polykaryons*. The Journal of pathology, 1977. **123**(2): p. 65-77.
323. Lay, G., et al., *Langhans giant cells from M. tuberculosis-induced human granulomas cannot mediate mycobacterial uptake*. The Journal of Pathology: A Journal of the Pathological Society of Great Britain and Ireland, 2007. **211**(1): p. 76-85.
324. Moreno, J.L., et al., *IL-4 promotes the formation of multinucleated giant cells from macrophage precursors by a STAT6-dependent, homotypic mechanism: contribution of E-cadherin*. Journal of leukocyte biology, 2007. **82**(6): p. 1542-1553.
325. Nakanishi-Matsui, M., et al., *Lipopolysaccharide induces multinuclear cell from RAW264. 7 line with increased phagocytosis activity*. Biochemical and biophysical research communications, 2012. **425**(2): p. 144-149.
326. Schlesinger, L., R. Musson, and R. Johnston Jr, *Functional and biochemical studies of multinucleated giant cells derived from the culture of human monocytes*. The Journal of experimental medicine, 1984. **159**(4): p. 1289-1294.

327. Milde, R., et al., *Multinucleated Giant Cells Are Specialized for Complement-Mediated Phagocytosis and Large Target Destruction*. Cell Reports, 2015. **13**(9): p. 1937-1948.
328. Ishidome, T., T. Yoshida, and R. Hanayama, *Induction of Live Cell Phagocytosis by a Specific Combination of Inflammatory Stimuli*. EBioMedicine, 2017. **22**: p. 89-99.
329. Chiti, F. and C.M. Dobson, *Protein Misfolding, Amyloid Formation, and Human Disease: A Summary of Progress Over the Last Decade*. Annu Rev Biochem, 2017. **86**: p. 27-68.
330. Hipp, M.S., S.H. Park, and F.U. Hartl, *Proteostasis impairment in protein-misfolding and -aggregation diseases*. Trends Cell Biol, 2014. **24**(9): p. 506-14.
331. Cisbani, G. and F. Cicchetti, *An in vitro perspective on the molecular mechanisms underlying mutant huntingtin protein toxicity*. Cell Death & Disease, 2012. **3**(8): p. e382-e382.
332. Smith, R., et al., *Mutant huntingtin interacts with {beta}-tubulin and disrupts vesicular transport and insulin secretion*. Hum Mol Genet, 2009. **18**(20): p. 3942-54.
333. Sassone, J., et al., *Huntington's disease: the current state of research with peripheral tissues*. Exp Neurol, 2009. **219**(2): p. 385-97.
334. Squitieri, F., et al., *Abnormal morphology of peripheral cell tissues from patients with Huntington disease*. J Neural Transm (Vienna), 2010. **117**(1): p. 77-83.
335. Pierzynowska, K., et al., *Genistein induces degradation of mutant huntingtin in fibroblasts from Huntington's disease patients*. Metabolic Brain Disease, 2019. **34**(3): p. 715-720.
336. Yang, W., et al., *Gedunin Degrades Aggregates of Mutant Huntingtin Protein and Intranuclear Inclusions via the Proteasomal Pathway in Neurons and Fibroblasts from Patients with Huntington's Disease*. Neurosci Bull, 2019. **35**(6): p. 1024-1034.
337. Fiala, M., et al., *Ineffective phagocytosis of amyloid-beta by macrophages of Alzheimer's disease patients*. J Alzheimers Dis, 2005. **7**(3): p. 221-32; discussion 255-62.
338. van der Burg, J.M.M., M. Björkqvist, and P. Brundin, *Beyond the brain: widespread pathology in Huntington's disease*. The Lancet Neurology, 2009. **8**(8): p. 765-774.
339. Kremer, B., et al., *A worldwide study of the huntington's disease mutation: The sensitivity and specificity of measuring CAG repeats*. New England Journal of Medicine, 1994. **330**(20): p. 1401-1406.
340. Myers, R.H., *Huntington's disease genetics*. NeuroRx : the journal of the American Society for Experimental NeuroTherapeutics, 2004. **1**(2): p. 255-262.
341. Murinello, S., et al., *Assessing Retinal Microglial Phagocytic Function In Vivo Using a Flow Cytometry-based Assay*. Journal of visualized experiments : JoVE, 2016(116): p. 54677.
342. Breunig, M., et al., *Breaking up the correlation between efficacy and toxicity for nonviral gene delivery*. Proceedings of the National Academy of Sciences of the United States of America, 2007. **104**(36): p. 14454-14459.
343. Segawa, K. and S. Nagata, *An Apoptotic 'Eat Me' Signal: Phosphatidylserine Exposure*. Trends Cell Biol, 2015. **25**(11): p. 639-650.
344. Ravichandran, K.S., *"Recruitment Signals" from Apoptotic Cells: Invitation to a Quiet Meal*. Cell, 2003. **113**(7): p. 817-820.
345. Lemke, G., *How macrophages deal with death*. Nature reviews. Immunology, 2019. **19**(9): p. 539-549.
346. Huang, Y., et al., *Macrophage-mediated Bystander Effect Triggered by Tumor Cell Apoptosis*. Molecular Therapy, 2007. **15**(3): p. 524-533.
347. Conos, S.A., L.M. Lindqvist, and J.E. Vince, *Simultaneous Detection of Cellular Viability and Interleukin-1 β Secretion from Single Cells by ELISpot*, in *Innate Immune Activation: Methods and Protocols*, D. De Nardo and C.M. De Nardo, Editors. 2018, Springer New York: New York, NY. p. 229-236.

348. Delbridge, A.R.D. and A. Strasser, *The BCL-2 protein family, BH3-mimetics and cancer therapy*. *Cell Death & Differentiation*, 2015. **22**(7): p. 1071-1080.
349. Heckmann, B.L. and D.R. Green, *LC3-associated phagocytosis at a glance*. *Journal of cell science*, 2019. **132**(5): p. jcs222984.
350. Martinez, J., *Detection of LC3-Associated Phagocytosis (LAP)*. *Current Protocols in Cell Biology*, 2020. **87**(1): p. e104.
351. and, A.A. and D.M. Underhill, *MECHANISMS OF PHAGOCYTOSIS IN MACROPHAGES*. *Annual Review of Immunology*, 1999. **17**(1): p. 593-623.
352. Rosales, C. and E. Uribe-Querol, *Phagocytosis: A Fundamental Process in Immunity*. *BioMed research international*, 2017. **2017**: p. 9042851-9042851.
353. Marc, A., et al., *POTENTIAL AND PITFALLS OF USING LDH RELEASE FOR THE EVALUATION OF ANIMAL CELL DEATH KINETICS*, in *Production of Biologicals from Animal Cells in Culture*, R.E. Spier, J.B. Griffiths, and B. Meignier, Editors. 1991, Butterworth-Heinemann. p. 569-575.
354. Forkasiewicz, A., et al., *The usefulness of lactate dehydrogenase measurements in current oncological practice*. *Cellular & Molecular Biology Letters*, 2020. **25**(1): p. 35.
355. Kaja, S., et al., *An optimized lactate dehydrogenase release assay for screening of drug candidates in neuroscience*. *Journal of pharmacological and toxicological methods*, 2015. **73**: p. 1-6.
356. Galluzzi, L., et al., *Molecular mechanisms of cell death: recommendations of the Nomenclature Committee on Cell Death 2018*. *Cell Death & Differentiation*, 2018. **25**(3): p. 486-541.
357. Niccoli, T. and L. Partridge, *Ageing as a risk factor for disease*. *Curr Biol*, 2012. **22**(17): p. R741-52.
358. North, B.J. and D.A. Sinclair, *The intersection between aging and cardiovascular disease*. *Circ Res*, 2012. **110**(8): p. 1097-108.
359. Raisz, L.G., *Local and systemic factors in the pathogenesis of osteoporosis*. *N Engl J Med*, 1988. **318**(13): p. 818-28.
360. Nalysnyk, L., et al., *Incidence and prevalence of idiopathic pulmonary fibrosis: review of the literature*. *Eur Respir Rev*, 2012. **21**(126): p. 355-61.
361. de Magalhães, J.P., *How ageing processes influence cancer*. *Nat Rev Cancer*, 2013. **13**(5): p. 357-65.
362. Querfurth, H.W. and F.M. LaFerla, *Alzheimer's disease*. *N Engl J Med*, 2010. **362**(4): p. 329-44.
363. Kritsilis, M., et al., *Ageing, cellular senescence and neurodegenerative disease*. *International journal of molecular sciences*, 2018. **19**(10): p. 2937.
364. Krtolica, A., et al., *Senescent fibroblasts promote epithelial cell growth and tumorigenesis: A link between cancer and aging*. *Proceedings of the National Academy of Sciences*, 2001. **98**(21): p. 12072-12077.
365. Parrinello, S., et al., *Stromal-epithelial interactions in aging and cancer: senescent fibroblasts alter epithelial cell differentiation*. *J Cell Sci*, 2005. **118**(Pt 3): p. 485-96.
366. Lehmann, B.D., et al., *Senescence-associated exosome release from human prostate cancer cells*. *Cancer Res*, 2008. **68**(19): p. 7864-71.
367. Coppé, J.P., et al., *Senescence-associated secretory phenotypes reveal cell-nonautonomous functions of oncogenic RAS and the p53 tumor suppressor*. *PLoS Biol*, 2008. **6**(12): p. 2853-68.
368. Behmoaras, J. and J. Gil, *Similarities and interplay between senescent cells and macrophages*. *Journal of Cell Biology*, 2020. **220**(2).

369. Di Mitri, D., et al., *Tumour-infiltrating Gr-1+ myeloid cells antagonize senescence in cancer*. Nature, 2014. **515**(7525): p. 134-137.
370. Eggert, T., et al., *Distinct functions of senescence-associated immune responses in liver tumor surveillance and tumor progression*. Cancer cell, 2016. **30**(4): p. 533-547.
371. Olivieri, F., et al., *Cellular Senescence and Inflammaging in Age-Related Diseases*. Mediators of inflammation, 2018. **2018**: p. 9076485-9076485.
372. Underhill, D.M. and H.S. Goodridge, *Information processing during phagocytosis*. Nature reviews. Immunology, 2012. **12**(7): p. 492-502.
373. Stuart, L.M. and R.A.B. Ezekowitz, *Phagocytosis: Elegant Complexity*. Immunity, 2005. **22**(5): p. 539-550.
374. Mazzoni, M., et al., *Senescent thyrocytes and thyroid tumor cells induce M2-like macrophage polarization of human monocytes via a PGE2-dependent mechanism*. Journal of Experimental & Clinical Cancer Research, 2019. **38**(1): p. 1-16.
375. Surh, C.D. and J. Sprent, *T-cell apoptosis detected in situ during positive and negative selection in the thymus*. Nature, 1994. **372**(6501): p. 100-103.
376. Kerr, J.F., A.H. Wyllie, and A.R. Currie, *Apoptosis: a basic biological phenomenon with wideranging implications in tissue kinetics*. British journal of cancer, 1972. **26**(4): p. 239-257.
377. Henson, P.M. and R.B. Johnston, Jr., *Tissue injury in inflammation. Oxidants, proteinases, and cationic proteins*. The Journal of Clinical Investigation, 1987. **79**(3): p. 669-674.
378. Cocco, R.E. and D.S. Ucker, *Distinct Modes of Macrophage Recognition for Apoptotic and Necrotic Cells Are Not Specified Exclusively by Phosphatidylserine Exposure*. Molecular Biology of the Cell, 2001. **12**(4): p. 919-930.
379. Kharitonov, A., et al., *A family of proteins that inhibit signalling through tyrosine kinase receptors*. Nature, 1997. **386**(6621): p. 181-186.
380. Barclay, A.N. and M.H. Brown, *The SIRP family of receptors and immune regulation*. Nature Reviews Immunology, 2006. **6**(6): p. 457-464.
381. Barclay, A.N. and T.K. Van den Berg, *The interaction between signal regulatory protein alpha (SIRP α) and CD47: structure, function, and therapeutic target*. Annual review of immunology, 2014. **32**: p. 25-50.
382. Liénard, H., et al., *Signal regulatory proteins negatively regulate immunoreceptor-dependent cell activation*. Journal of Biological Chemistry, 1999. **274**(45): p. 32493-32499.
383. Hatherley, D., et al., *The structure of the macrophage signal regulatory protein α (SIRP α) inhibitory receptor reveals a binding face reminiscent of that used by T cell receptors*. Journal of Biological Chemistry, 2007. **282**(19): p. 14567-14575.
384. Hatherley, D., et al., *Paired receptor specificity explained by structures of signal regulatory proteins alone and complexed with CD47*. Molecular cell, 2008. **31**(2): p. 266-277.
385. Subramanian, S., et al., *Species- and cell type-specific interactions between CD47 and human SIRP α* . Blood, 2006. **107**(6): p. 2548-56.
386. Weiskopf, K., et al., *Engineered SIRP α variants as immunotherapeutic adjuvants to anticancer antibodies*. Science (New York, N.Y.), 2013. **341**(6141): p. 88-91.
387. Brooke, G., et al., *Human Lymphocytes Interact Directly with CD47 through a Novel Member of the Signal Regulatory Protein (SIRP) Family*. The Journal of Immunology, 2004. **173**(4): p. 2562-2570.
388. Chao, M.P., et al., *Anti-CD47 Antibody Synergizes with Rituximab to Promote Phagocytosis and Eradicate Non-Hodgkin Lymphoma*. Cell, 2010. **142**(5): p. 699-713.
389. Chao, M.P., et al., *Therapeutic antibody targeting of CD47 eliminates human acute lymphoblastic leukemia*. Cancer Res, 2011. **71**(4): p. 1374-84.

390. Kim, D., et al., *Anti-CD47 antibodies promote phagocytosis and inhibit the growth of human myeloma cells*. *Leukemia*, 2012. **26**(12): p. 2538-45.
391. Wang, H., et al., *CD47/SIRP α blocking peptide identification and synergistic effect with irradiation for cancer immunotherapy*. *J Immunother Cancer*, 2020. **8**(2).
392. Lin, F., et al., *A Novel Blockade CD47 Antibody With Therapeutic Potential for Cancer*. *Front Oncol*, 2020. **10**: p. 615534.
393. Kojima, Y., et al., *CD47-blocking antibodies restore phagocytosis and prevent atherosclerosis*. *Nature*, 2016. **536**(7614): p. 86-90.
394. Tao, C., et al., *CD47 Blocking Antibody Accelerates Hematoma Clearance After Intracerebral Hemorrhage in Aged Rats*. *Translational Stroke Research*, 2020. **11**(3): p. 541-551.
395. Weiskopf, K., et al., *Direct SIRP α Blockade Augments Macrophage Responses to Therapeutic Anticancer Antibodies*. *Blood*, 2014. **124**(21): p. 2729-2729.
396. Andrejeva, G., et al., *Novel SIRP α Antibodies That Induce Single-Agent Phagocytosis of Tumor Cells while Preserving T Cells*. *The Journal of Immunology*, 2021: p. ji2001019.
397. Jalil, A.R., J.C. Andrechak, and D.E. Discher, *Macrophage checkpoint blockade: results from initial clinical trials, binding analyses, and CD47-SIRP α structure-function*. *Antibody therapeutics*, 2020. **3**(2): p. 80-94.
398. Fortin, G., et al., *A role for CD47 in the development of experimental colitis mediated by SIRP α +CD103⁻ dendritic cells*. *Journal of Experimental Medicine*, 2009. **206**(9): p. 1995-2011.
399. Kang, X., et al., *Inhibitory leukocyte immunoglobulin-like receptors: Immune checkpoint proteins and tumor sustaining factors*. *Cell Cycle*, 2016. **15**(1): p. 25-40.
400. Adams, D.O., *The granulomatous inflammatory response. A review*. *The American journal of pathology*, 1976. **84**(1): p. 164-192.
401. Papadimitriou, J., G. POSTE, and G. NICOLSON, *Membrane fusion*. 1978.
402. Prieto-Potin, I., et al., *Characterization of multinucleated giant cells in synovium and subchondral bone in knee osteoarthritis and rheumatoid arthritis*. *BMC Musculoskeletal Disorders*, 2015. **16**(1): p. 226.
403. Morioka, S., C. Maueröder, and K.S. Ravichandran, *Living on the Edge: Efferocytosis at the Interface of Homeostasis and Pathology*. *Immunity*, 2019. **50**(5): p. 1149-1162.
404. Odgren, P.R., H. Witwicka, and P. Reyes-Gutierrez, *The cast of clasts: catabolism and vascular invasion during bone growth, repair, and disease by osteoclasts, chondroclasts, and septoclasts*. *Connect Tissue Res*, 2016. **57**(3): p. 161-74.
405. Rose, M.R., *Adaptation, aging, and genomic information*. *Aging (Albany NY)*, 2009. **1**(5): p. 444.
406. Machiela, E. and A.L. Southwell, *Biological Aging and the Cellular Pathogenesis of Huntington's Disease*. *Journal of Huntington's disease*, 2020. **9**(2): p. 115-128.
407. Gusella, J.F., et al., *A polymorphic DNA marker genetically linked to Huntington's disease*. *Nature*, 1983. **306**(5940): p. 234-238.
408. Scherzinger, E., et al., *Self-assembly of polyglutamine-containing huntingtin fragments into amyloid-like fibrils: implications for Huntington's disease pathology*. *Proceedings of the National Academy of Sciences*, 1999. **96**(8): p. 4604-4609.
409. Daldin, M., et al., *Polyglutamine expansion affects huntingtin conformation in multiple Huntington's disease models*. *Scientific reports*, 2017. **7**(1): p. 1-15.
410. Bates, G.P., et al., *Huntington disease*. *Nat Rev Dis Primers*, 2015. **1**: p. 15005.
411. Tyedmers, J., A. Mogk, and B. Bukau, *Cellular strategies for controlling protein aggregation*. *Nature reviews Molecular cell biology*, 2010. **11**(11): p. 777-788.

412. Dugger, B.N. and D.W. Dickson, *Pathology of Neurodegenerative Diseases*. Cold Spring Harb Perspect Biol, 2017. **9**(7).
413. Hughes, A.J., et al., *Accuracy of clinical diagnosis of idiopathic Parkinson's disease: a clinico-pathological study of 100 cases*. Journal of neurology, neurosurgery & psychiatry, 1992. **55**(3): p. 181-184.
414. Adler, C.H., et al., *Low clinical diagnostic accuracy of early vs advanced Parkinson disease: clinicopathologic study*. Neurology, 2014. **83**(5): p. 406-412.
415. Slanzi, A., et al., *In vitro Models of Neurodegenerative Diseases*. Frontiers in Cell and Developmental Biology, 2020. **8**(328).
416. De Strooper, B., *Lessons from a failed γ -secretase Alzheimer trial*. Cell, 2014. **159**(4): p. 721-726.
417. Henley, D.B., et al., *Safety profile of semagacestat, a gamma-secretase inhibitor: IDENTITY trial findings*. Current medical research and opinion, 2014. **30**(10): p. 2021-2032.
418. Pouladi, M.A., A.J. Morton, and M.R. Hayden, *Choosing an animal model for the study of Huntington's disease*. Nature Reviews Neuroscience, 2013. **14**(10): p. 708-721.
419. Outeiro, T.F., et al., *Formation of toxic oligomeric α -synuclein species in living cells*. PLoS one, 2008. **3**(4): p. e1867.
420. Lázaro, D.F., et al., *Systematic comparison of the effects of alpha-synuclein mutations on its oligomerization and aggregation*. PLoS Genet, 2014. **10**(11): p. e1004741.
421. Hegde, R.N., et al., *TBK1 phosphorylates mutant Huntingtin and suppresses its aggregation and toxicity in Huntington's disease models*. The EMBO Journal, 2020. **39**(17): p. e104671.
422. Mehta, D., et al., *Why do trials for Alzheimer's disease drugs keep failing? A discontinued drug perspective for 2010-2015*. Expert opinion on investigational drugs, 2017. **26**(6): p. 735-739.
423. Cummings, J., C. Reiber, and P. Kumar, *The price of progress: Funding and financing Alzheimer's disease drug development*. Alzheimer's & dementia (New York, N. Y.), 2018. **4**: p. 330-343.
424. Marchina, E., et al., *Gene expression profile in fibroblasts of Huntington's disease patients and controls*. J Neurol Sci, 2014. **337**(1-2): p. 42-6.
425. Fiszer-Kierzkowska, A., et al., *Liposome-based DNA carriers may induce cellular stress response and change gene expression pattern in transfected cells*. BMC Molecular Biology, 2011. **12**(1): p. 27.
426. Gordon, S., *Phagocytosis: An Immunobiologic Process*. Immunity, 2016. **44**(3): p. 463-475.
427. Robinson, M.S., C. Watts, and M. Zerial, *Membrane Dynamics in Endocytosis*. Cell, 1996. **84**(1): p. 13-21.
428. Czekay, R.P., et al., *Direct binding of occupied urokinase receptor (uPAR) to LDL receptor-related protein is required for endocytosis of uPAR and regulation of cell surface urokinase activity*. Mol Biol Cell, 2001. **12**(5): p. 1467-79.
429. Wang, R., et al., *Molecular mechanism of bystander effects and related abscopal/cohort effects in cancer therapy*. Oncotarget, 2018. **9**(26): p. 18637-18647.
430. Diez-Roux, G. and R.A. Lang, *Macrophages induce apoptosis in normal cells in vivo*. Development, 1997. **124**(18): p. 3633-8.
431. Lim, J. and Z. Yue, *Neuronal Aggregates: Formation, Clearance, and Spreading*. Developmental Cell, 2015. **32**(4): p. 491-501.
432. Martinez, J., et al., *Molecular characterization of LC3-associated phagocytosis reveals distinct roles for Rubicon, NOX2 and autophagy proteins*. Nature cell biology, 2015. **17**(7): p. 893-906.

433. Paresce, D.M., R.N. Ghosh, and F.R. Maxfield, *Microglial Cells Internalize Aggregates of the Alzheimer's Disease Amyloid β -Protein Via a Scavenger Receptor*. *Neuron*, 1996. **17**(3): p. 553-565.
434. Neumann, H., M.R. Kotter, and R.J.M. Franklin, *Debris clearance by microglia: an essential link between degeneration and regeneration*. *Brain*, 2008. **132**(2): p. 288-295.
435. Kuemmerle, S., et al., *Huntington aggregates may not predict neuronal death in Huntington's disease*. *Ann Neurol*, 1999. **46**(6): p. 842-9.
436. Ross, C.A., *Intranuclear Neuronal Inclusions: A Common Pathogenic Mechanism for Glutamine-Repeat Neurodegenerative Diseases?* *Neuron*, 1997. **19**(6): p. 1147-1150.
437. Majerova, P., et al., *Microglia display modest phagocytic capacity for extracellular tau oligomers*. *Journal of Neuroinflammation*, 2014. **11**(1): p. 161.
438. Hudrisier, D. and E. Joly, *Plasma membrane nibbling: all lymphocytes do it, but why*. *ELSO Gaz*, 2002. **9**: p. 1-5.
439. Joly, E. and D. Hudrisier, *What is trogocytosis and what is its purpose?* *Nature Immunology*, 2003. **4**(9): p. 815-815.
440. Steele, S., et al., *Trogocytosis-associated cell to cell spread of intracellular bacterial pathogens*. *Elife*, 2016. **5**.
441. Yamanaka, N., et al., *Bone marrow transplantation results in human donor blood cells acquiring and displaying mouse recipient class I MHC and CD45 antigens on their surface*. *PLoS One*, 2009. **4**(12): p. e8489.
442. Osborne, D.G. and S.A. Wetzel, *Trogocytosis results in sustained intracellular signaling in CD4+ T cells*. *The Journal of Immunology*, 2012. **189**(10): p. 4728-4739.
443. Wakim, L.M. and M.J. Bevan, *Cross-dressed dendritic cells drive memory CD8+ T-cell activation after viral infection*. *Nature*, 2011. **471**(7340): p. 629-632.
444. Chung, B., et al., *Antigen-specific inhibition of high-avidity T cell target lysis by low-avidity T cells via trogocytosis*. *Cell reports*, 2014. **8**(3): p. 871-882.
445. Puaux, A.L., et al., *A very rapid and simple assay based on trogocytosis to detect and measure specific T and B cell reactivity by flow cytometry*. *European journal of immunology*, 2006. **36**(3): p. 779-788.
446. Bettadapur, A., H.W. Miller, and K.S. Ralston, *Biting Off What Can Be Chewed: Trogocytosis in Health, Infection, and Disease*. *Infection and Immunity*, 2020. **88**(7): p. e00930-19.
447. Overholtzer, M., et al., *A Nonapoptotic Cell Death Process, Entosis, that Occurs by Cell-in-Cell Invasion*. *Cell*, 2007. **131**(5): p. 966-979.
448. Batista, F.D., D. Iber, and M.S. Neuberger, *B cells acquire antigen from target cells after synapse formation*. *Nature*, 2001. **411**(6836): p. 489-494.
449. Wetzel, S.A., T.W. McKeithan, and D.C. Parker, *Peptide-specific intercellular transfer of MHC class II to CD4+ T cells directly from the immunological synapse upon cellular dissociation*. *The Journal of Immunology*, 2005. **174**(1): p. 80-89.
450. Pham, T., P. Mero, and J.W. Booth, *Dynamics of macrophage trogocytosis of rituximab-coated B cells*. *PLoS One*, 2011. **6**(1): p. e14498.
451. Miyake, K., et al., *Trogocytosis of peptide-MHC class II complexes from dendritic cells confers antigen-presenting ability on basophils*. *Proceedings of the National Academy of Sciences*, 2017. **114**(5): p. 1111-1116.
452. Burgstaller, S., et al., *pH-Lemon, a Fluorescent Protein-Based pH Reporter for Acidic Compartments*. *ACS Sensors*, 2019. **4**(4): p. 883-891.

8 Appendix

8.1 Interaction of macrophages and senescent cells

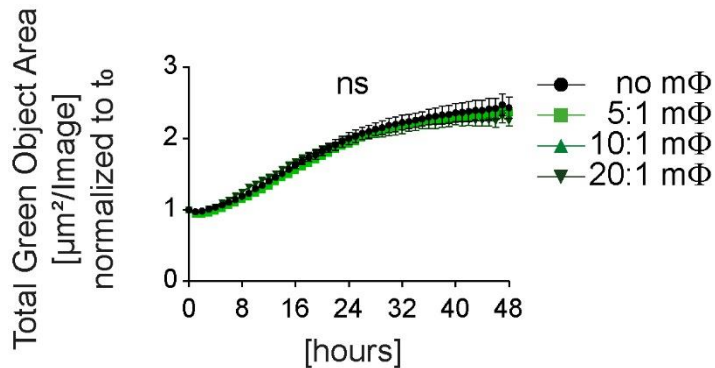


Figure 8-1: Peritoneal macrophages do not engulf senescent cells.

Senescent MEFs, isolated from actinGFP mice were co-cultured with peritoneal macrophages, isolated from tdTomato⁺ mice, in a ratio of 10:1 macrophages to senescent cells and imaged over 48 hours. Green fluorescent area signal of senescent cells was quantified in the co-culture with different ratios of macrophages. Data are representative of two independent experiments. All values are means \pm SEM. Statistically significant differences were determined by two-way ANOVA with Bonferroni correction. n=3 biological replicates

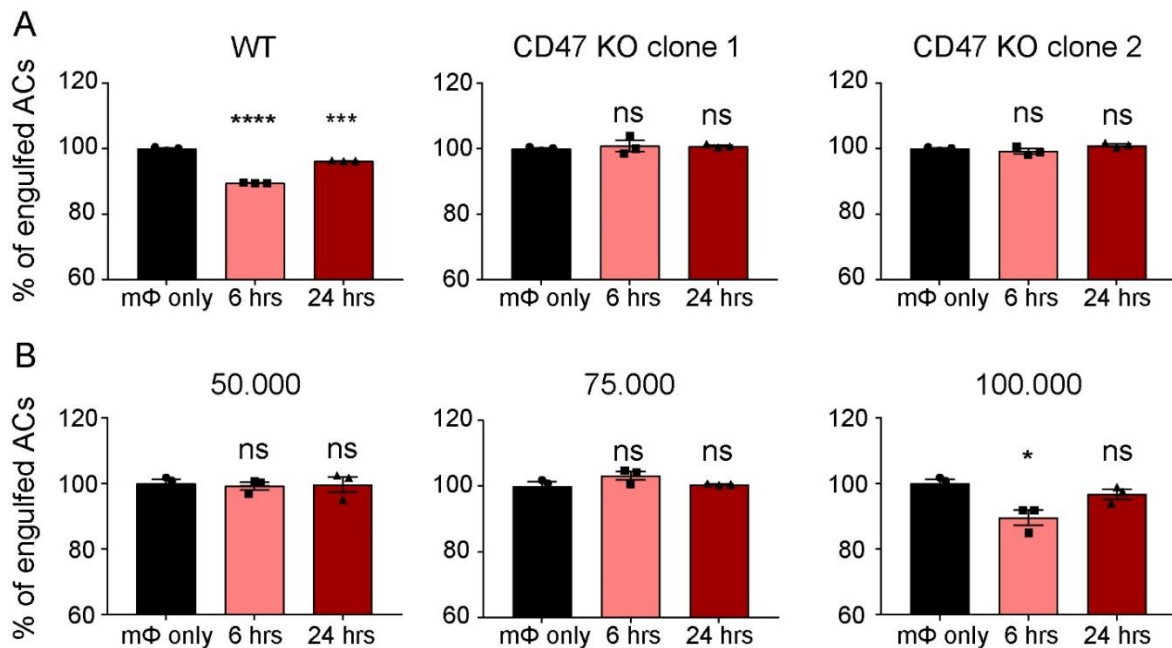


Figure 8-2: Data for single efferocytosis can be obtained from double efferocytosis samples.

BMDMs were primed with senescent and proliferating cells for 6 or 24 hours. ACs were labelled with PKH26 (red) and added to macrophages in a 5:1: ratio in a two-step (double) efferocytosis assay. Samples were subsequently analyzed by flow cytometry. BMDMs were selected for expression of F4/80. The BMDM population was analyzed for the population of macrophages having engulfed ACs. The data for the single efferocytosis, or the first step efferocytosis, was not obtained from individual samples, where only single efferocytosis was performed, but from the samples where double efferocytosis was performed. **A** Quantification of single efferocytosis of ACs by BMDMs in the presence of senescent WT and CD47 KO cells. **B** Quantification of single efferocytosis of ACs by BMDMs in the presence of different numbers of proliferating cells.

Appendix

Values are means \pm SEM; statistically significant differences were determined by one-way ANOVA with Bonferroni correction. n=3 biological replicates.

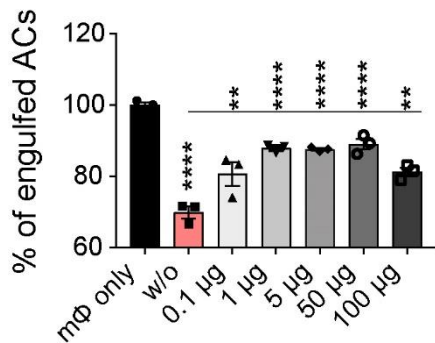


Figure 8-3: SIRTα treatment recovers efferocytosis in a titratable manner.

Efferocytosis in the presence of senescent cells (induced by Palbociclib) and a SIRTα blocking antibody. BMDMs were primed with senescent cells for 6 hours in all conditions, except mΦ only control. Blocking SIRTα antibody was added in different concentrations in parallel with BMDMs to the senescent cells. Samples were subsequently analyzed by flow cytometry. BMDMs were selected for expression of F4/80. The BMDM population was analyzed for the population of macrophages having engulfed ACs. Data are representative of three independent experiments. All values are means \pm SEM. Statistically significant differences were determined by one-way ANOVA with Bonferroni correction; ** p < 0.01 *** p < 0.001 **** p < 0.0001. n=3 biological replicates.

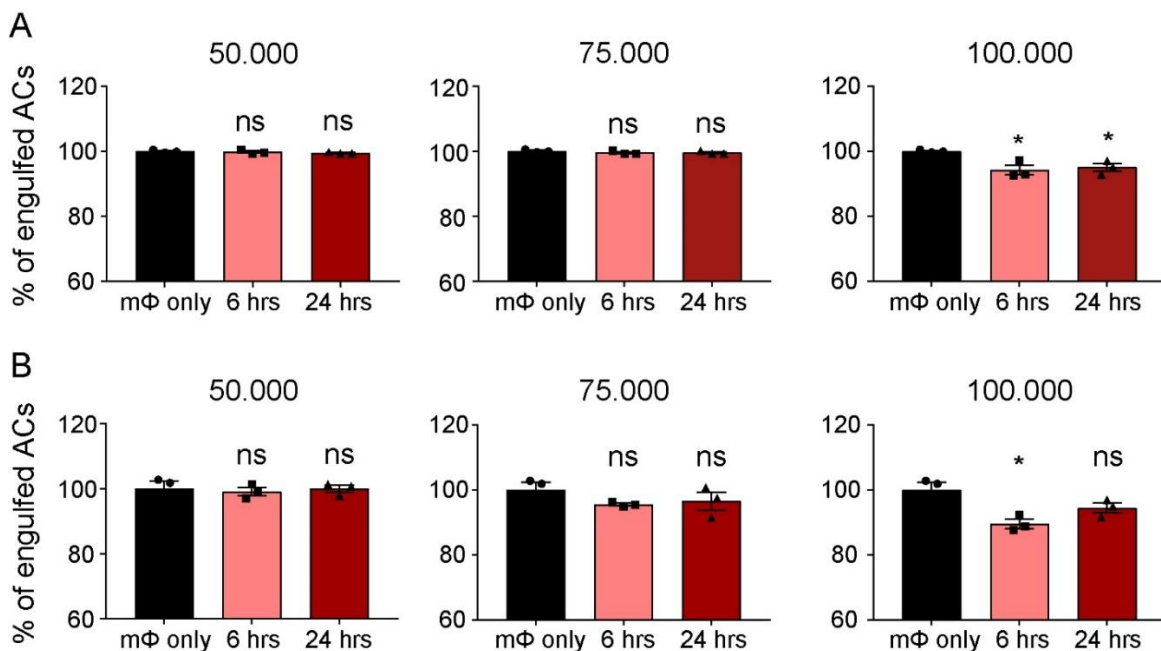


Figure 8-4: Proliferating cells do not impair macrophage functionality.

BMDMs were primed with different numbers of proliferating cells for 6 or 24 hours. ACs were labelled with PKH26 (red) and added to macrophages in a 5:1: ratio in a one-step (single) or two-step (double) efferocytosis assay. Samples were subsequently analyzed by flow cytometry. BMDMs were selected for expression of F4/80. The BMDM population was analyzed for the population of macrophages having engulfed ACs. A Quantification of single efferocytosis of ACs by BMDMs in the presence of different numbers of proliferating cells. B Quantification of double efferocytosis of ACs by BMDMs in the presence of different numbers of proliferating cells. Values are means \pm SEM; statistically significant differences were determined by one-way ANOVA with Bonferroni correction. n=3 biological replicates.

8.2 A model system to analyze pathogenic aggregate removal by macrophages

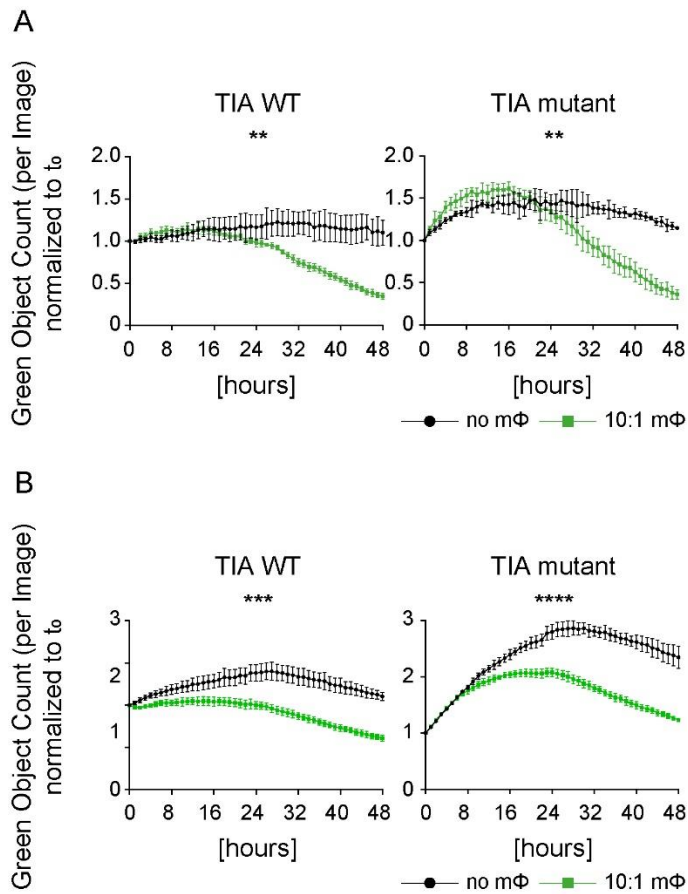


Figure 8-5: Macrophages trigger aggregate elimination from fibroblasts.

Fibroblasts were seeded and attached to the dish for 24 hours. Cells were transfected with plasmids containing T cell-restricted intracellular antigen-1 (TIA1 here TIA WT) and TIA1 A381T mutant (here TIA mutant) (all fused to GFP). After 24 hours, the cells expressed green fluorescent protein aggregates. BMDMs were added in a ratio of 10:1 and the co-culture was imaged for 48 hours, in an IncuCyte life cell imager, where green object counts were recorded once every hour. The number of green objects was determined using the corresponding software. **A** Quantification of green fluorescent object counts in transfected WT fibroblasts in single culture and in co-culture with macrophages. **B** Quantification of green fluorescent object counts in transfected WT fibroblasts in single culture and in co-culture with macrophages. Data are representative of three independent experiments performed under the exact conditions after 13 performed preliminary and titration experiments. All values are means \pm SEM. Statistically significant differences were determined by two-way ANOVA with Bonferroni correction. ** $p < 0.01$, *** $p < 0.001$, **** $p < 0.0001$. $n=3$ biological replicates.

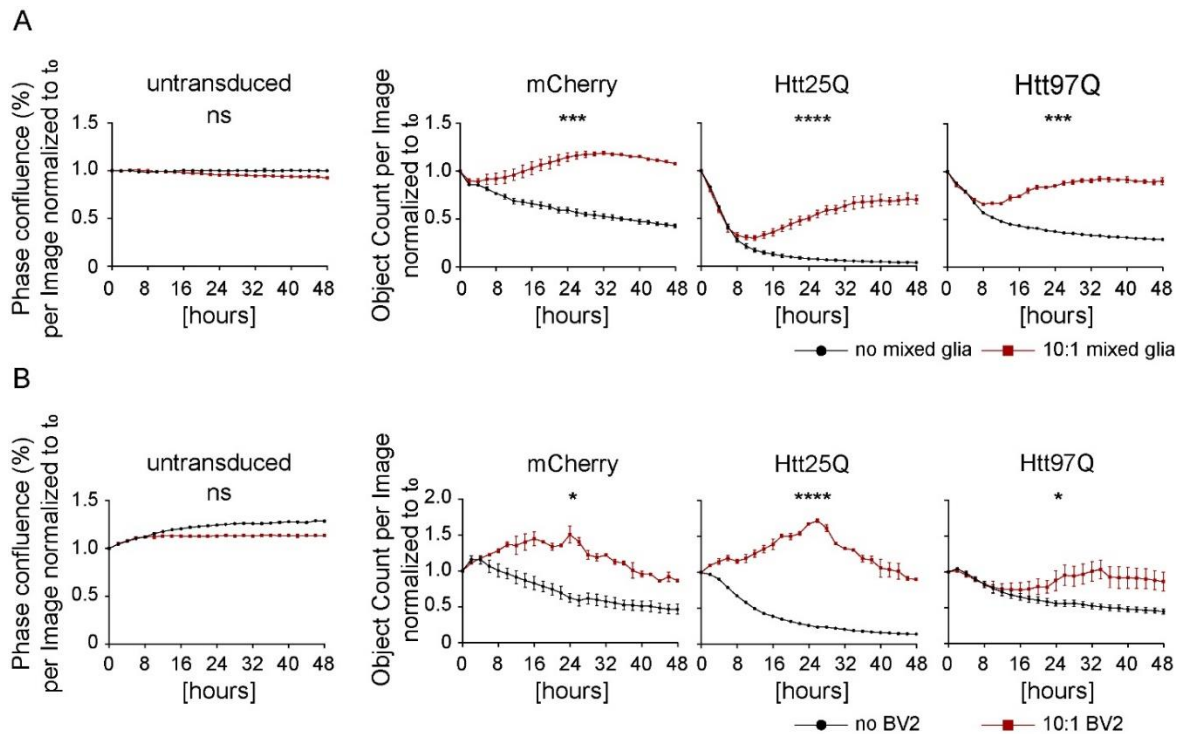


Figure 8-6: All types of microglia enhance aggregate stability in neurons.

Cortical neurons were seeded and differentiated over 7 days. Cells were transduced with lentiviruses encoding mCherry or the Huntington aggregates Htt25Q and Htt97Q (Htt with 25 or 97 glutamine repeats fused to mCherry). After 7 additional days the cells expressed fluorescent protein aggregates. Mixed glia cultures and BV2 cells were added in a ratio of 10:1 and the co-culture was imaged for 48 hours, in an IncuCyte life cell imager, where red object counts were recorded once every hour. The number of red objects was determined using the corresponding software. **A** Quantification of the red fluorescent object counts of transfected neurons with and without mixed glia cells. **B** Quantification of the red fluorescent object counts of transfected neurons with and without BV2 cells. Data are representative of two independent experiments. All values are means \pm SEM. Statistically significant differences were determined by two-way ANOVA with Bonferroni correction; * $p < 0.05$, *** $p < 0.001$, **** $p < 0.0001$; $n=3$ biological replicates.

9 List of Abbreviations

Acronym	Definition
AD	Alzheimer's disease
Anxl	Annexin I
APC	antigen presenting cell
ARF	Alternative Reading Frame
ATCC	American Type Culture Collection
ATM	Ataxia telangiectasia mutated
ATP	adenosine triphosphate
A β	amyloid- β peptide
Bak	Bcl-2 homologues antagonist/killer
BATF3	Basic Leucine Zipper ATF-Like Transcription Factor 3
Bax	Bcl-2-associated X protein
BCL2	B-cell lymphoma 2
BMDE	bone marrow derived eosinophil
BMDM	Bone marrow-derived macrophage
C1q	complement component 1q
CAG	cytosine-adenine-guanine
CCL2	CC-chemokine ligand 2
CCL20	C-C Motif Chemokine Ligand 20
CD	Cluster of differentiation
cDC1	conventional type 1 dendritic cells.
CDK1	Cyclin Dependent Kinase 1
CDK4	Cyclin Dependent Kinase 4
CDK6	Cyclin Dependent Kinase 6
CDKN2A	Cyclin Dependent Kinase Inhibitor 2A
cDNA	complementary DNA
cGAS	Cyclic GMP-AMP synthase
Chk2	Checkpoint kinase 2
CM	conditioned media
CNS	central nervous system
COX-2	cyclooxygenase-2
CpG	cytidine-guanosine
CRISPR	Clustered Regularly Interspaced Short Palindromic Repeats
CRT	calreticulin
CS	cellular senescence
CSF-1	colony stimulating factor 1
CX3CL1	C-X3-C Motif Chemokine Ligand 1
DAMPs	damage-associated molecular patterns
DDR	DNA damage response
DKO	Double knockout
DNA	deoxyribonucleic acid
DS	developmentally programmed senescence
ECAR	extracellular acidification rate
EDTA	Ethylenediaminetetraacetic acid

List of Abbreviations

Acronym	Definition
EGF	epidermal growth factor
EGFR	Epidermal Growth Factor Receptor
ER	endoplasmic reticulum
Erk	extracellular signal-regulated kinase
Fc	fragment crystallizable
FCCP	carbonyl cyanide-4 (trifluoromethoxy) phenylhydrazone
FcR	Fc-receptor
FDA	Food and Drug Administration
FGF	Fibroblast Growth Factor
FLT3	Fms-like tyrosine kinase 3 ligand
Gas6	growth-arrest-specific 6
GI	gastrointestinal
GM-CSF	granulocyte-macrophage colony-stimulating factor
H2AX	H2A histone family member X
HD	Huntington's disease
HEPES	N 2 hydroxyethylpiperazine-N'-2-ethanesulfonic acid
HGF	Hepatocyte Growth Factor
HLA	human leukocyte antigen
HTT	Huntingtin gene
Htt	Huntingtin protein
IFN- γ	Interferon-gamma
IGF	Insulin-like growth factor
IGFBP	growth factor binding proteins
IL	Interleukin
INK4	Inhibitor of Cyclin-Dependent Kinase
IPF	idiopathic pulmonary fibrosis
iPLA2	Ca ²⁺ independent PLA2
ITAM	immunoreceptor tyrosine-based activation motif
ITIM	immunoreceptor tyrosine-based inhibitory motif
JAK	Janus Kinase
KO	knockout
LAP	LC3-associated phagocytosis
LC3	Microtubule-associated protein 1A/1B-light chain 3
LDH	Lactate dehydrogenase
LPC	lysophosphatidylcholine
LPS	lipopolysaccharide
LXR α	liver X receptor α
LXR β	liver X receptor β
MAVS	mitochondrial antiviral signaling protein
MBL	mannose-binding lectin
MBL	Mannose-binding lectin
MCP	monocyte chemoattractant proteins
MDM2	Mouse double minute 2 homolog
MEF	Mouse embryonic fibroblasts
Mek	Mitogen-activated protein kinase kinase

Acronym	Definition
MFG-E8	milk-fat-globule-EGF-factor 8
MGCs	multinucleated giant cells
MHC-II	major histocompatibility complex class II
MIP	macrophage inflammatory protein
MMP	Matrix metalloproteinases
MTN-1	monotactin-1
mTOR	mechanistic Target of Rapamycin
mTORC1	mammalian target of rapamycin complex 1
NADPH	nicotinamide adenine dinucleotide phosphate
NBS1	Nijmegen Breakage Syndrome 1
ND	neurodegenerative disorders
NF- κ B	nuclear factor 'kappa-light-chain-enhancer' of activated B-cells
NHLRC2	NHL Repeat Containing 2
NK	Natural killer
NO	nitric oxide
NOX	NADPH oxidase
NOX2	NADPH oxidase 2
NR	nuclear receptor
OCR	oxygen consumption rate
OIS	oncogene induced senescence
OXPPOS	oxidative phosphorylation
PAMPs	pathogen associated molecular patterns
PBS	phosphate-buffered saline
PFA	Paraformaldehyde
PI3K	phosphatidylinositol-3-kinase
PIP2	phosphatidylinositol 4,5-phosphate
PIP3	phosphatidylinositol 3,4,5-phosphate
PPAR γ	peroxisome proliferator-activated receptor γ
PPAR δ	peroxisome proliferator-activated receptor δ
PtdSer	phosphatidyl serine
PTEN	Phosphatase and Tensin homolog
p-value	Probability value
Rac1	Ras-related C3 botulinum toxin substrate 1
Raf	rapidly accelerated fibrosarcoma
Ras	Rat sarcoma
Rb	retinoblastoma protein
RhoA	Ras homolog family member A
RIG-I	retinoic acid inducible gene I
RNA	Ribonucleic acid
ROS	reactive oxygen species
ROS	reactive oxygen species
RS	replicative senescence
RXR α	Retinoid X receptor alpha
S1P	sphingosine-1-phosphate
SARS-CoV-2	Severe acute respiratory syndrome coronavirus type 2

List of Abbreviations

Acronym	Definition
SASP	senescence-associated secretory phenotype
SA- β -Gal	senescence-associated β -galactosidase
SCF	stem cell factor
sgRNA	single guide RNA
SHP	Src homology 2 domain phosphatase-1
Siglec-F	Sialic acid-binding immunoglobulin-type lectin F
SIPS	stress-induced premature senescence
SIRP α	Signal Regulatory Protein α
SLC	solute carrier
SP-A	surfactant proteins-A
SP-D	surfactant proteins-D
STAT	Signal Transducer and Activator of Transcription
STING	Stimulator of interferon genes
TDP-43	Transactive response DNA binding protein 43
TGF β	Transforming growth factor beta
TGF- β	Transforming Growth Factor β
Th1	T helper cell type 1
TIMP	tissue inhibitors of metalloproteases
TLR	toll-like receptor
TNF- α	tumor necrosis factor- α
TSP-1	thrombospondin-1
UTP	Uridine triphosphate
VEGF	Vascular Endothelial Growth Factor
x-gal	5-Brom-4-chlor-3-indoxyl- β -D-galactopyranosid
α -	anti-
α -SYNC	alpha-synuclein
β 2-GPI	the β 2-glycoprotein-I
β 2-GPI	β 2-glycoprotein-I

10 Acknowledgements

I would like to express my gratitude towards my supervisor Peter Murray for giving me the opportunity to conduct this thesis in his laboratory. He was constantly available for feedback, advice and ideas. I am thankful for his patience, providing me a lot of freedom in performing experiments and his trust. His passion for science and his will to lead research projects to success have always been an inspiration for me to move on, especially during challenging phases of the project. Without his exceptional guidance and contribution, this project would not have been realized.

Thanks a lot to my official doctor father Veit Hornung, who stepped in when bureaucracy was about to bar in the way of science. In this line, I want to thank my TAC committee, Veit Hornung, Anne Krug and Barbara Walzog for their great feedback throughout the past four years. Thanks for taking this responsibility seriously, providing useful advice to solve the caveats of the project and taking a lot of time to answer all my questions.

I am grateful for having amazing colleagues by my side. Special thanks to Steffi, who does not only share my passion for hard workouts and the appreciation for “Illusionists”, but was always there for the minor and major problems challenging my professional and everyday life. Many thanks to Alessandra for her regular FACS support, Alex for his supportive hands-on assistance whenever required, Annette for many hours shared in front of the microscope, Johanna for keeping up with me from the first day to the end, Leonie for fruitful project discussions and assistance in image quantification, Marion for helpful feed-back at any time, Maria for her helpfulness with bureaucracy, Nina for caring about mice and general organization and Sophia for the great collaboration on the “blobs”. Thank you all for your support and your willingness to help at any time.

Many thanks to my collaborators along the way: Karim el Kasmi and Daniela Schlösser at Boehringer Ingelheim, who teamed up in with us to look into the human senescence system, thereby greatly enhancing the project outcome. Thanks to Kerstin Voelkl, who enabled my digression into neurobiology. Without her help, and the help of Tobias Beyer, I could not have realized my interdisciplinary project plans.

Further, I would like to give credit to Martin Spitaler, Markus Oster, Giovanni Cardone and Jochen Rech, the present and past members of the MPI Core Facility. Thanks for taking the time to teach me the use of complicated instruments and helping me to set-up complex screens.

Acknowledgements

Thanks to IMPRS-LS for always challenging us to become not only better scientists, but also better people. Thank you Hans-Jörg, Ingrid, Marta and Maxi! I am proud to be part of this amazing network through which I made friends like Anna, Kerstin, Stephan and especially Geri and Jasmin.

Moreover, I want to thank Jürgen Lassak and Marja Driessen for letting me profit from their experience. You always provided a fresh perspective on science, taking my concerns serious and were there also in the blue days, helping me to get back on track.

Thanks to all my friends, who just accepted delays or short-term cancellations of various engagements due to malfunctioning FACS machines, dying cells or spontaneously extended lab days.

Finally, I want to thank the people who had to suffer almost as much as me - especially during the challenging moments of this PhD. Thanks to my parents for enduring all my moods when I needed someone to listen to my complaints. I appreciate that I could always ask for an open ear and was provided with food and encouragement. Thanks to my partner Peter (B.! ☺), who never complained about short-dated cancellations, cheered me up when I was stressed out and always provided me with emergency demonstrations of his excellent cooking skills, even if requested in the middle of the night.